Engineering of Artificial Bone Tissues

Mohd Riduan Mohamad

B. Biomedical Eng. (Hons.), University of Malaya, 2008
M. Eng. (Biomedical Engineering), University of Malaya, 2011

In partial fulfillment of the requirements for the degree of Doctor of Philosophy (PhD)

2016

University of Strathclyde

Faculty of Engineering

Department of Biomedical Engineering

DECLARATION OF AUTHORS RIGHTS

This thesis is the result of the author‘s original research. It has been composed by the author and has not been previously submitted for examination which has led to the award of a degree.

Signed:

Date:

ACKNOWLEDGMENTS

The author would like to express the deepest gratitude to the following that without their persistent help and counsel, this dissertation would not have been possible:

First to the author's supervisors, Professor Mary Helen Grant and Dr Philip Riches, who were always there with continuous support, guidance, and infinite encouragement throughout this research project.

To the author's beloved family members, his dad, Mr Mohamad, his mum, Mrs Rosani, and his siblings (Hadre, Roslan, Azura, and Azwani) who were always free in giving constant support, morally and financially.

To Mrs Catherine Henderson and Mr Brian Cartlidge, the author's laboratory technicians for their kindness, limitless help, and patience in the laboratories at the Department of Biomedical Engineering.

To Dr Fiona Sillars and Mr Gerry Johnson for their vital assistance and invaluable input with the equipment in the Advanced Materials Research Laboratory (AMRL).

To all the author's friends, who gave their help and motivations in all the possible aspects during the research. And most of all.....

To God, who provided the author enough confidence, strength, good health, and appropriate knowledge to think about this project. Last but not least to the Majlis Amanah Rakyat (MARA) who helped the author in terms of finance.

THANKS A MILLION...!!!

ABSTRACT

Bone defects caused by trauma and pathological and physiological bone resorption denote a major challenge and have become a global health problem.

Decellularised bone has been proposed in bone tissue engineering studies as a donor scaffold for bone implantation into patients. The aim of a decellularisation approach is to efficiently eliminate all donor cellular material while minimising any adverse effect on the composition, mechanical integrity, and biological activity of the remaining extracellular matrix. In fact, the major aim of this study is to develop an efficient protocol to decellularise and recellularise the xenogenic bone so that it can be used for bone regeneration applications.

The effectiveness of donor cell removal from a tissue is influenced by the origin of the tissue and also the use of specific physical, chemical, and enzymatic methods. In this study, the success of a bovine bone decellularisation using 10 mM Tris, 1 mM EDTA, 0.1 % (v/v) Triton X-100 and 0.5 % (w/v) Trypsin has been established through analytical DNA assays.

This study was further extended to measure the mechanical properties of bone before and after decellularisation. Compression mechanical testing has been applied. Mechanical testing of square-shaped specimens loaded in compression was accomplished using the Bose ElectroForce 3200 to ensure maintenance of mechanical integrity. Likewise, the pore sizes of bone samples were measured before and after decellularisation using the PoreMaster-60 to ensure the scaffolds have an ideal diameter for cells to grow on/into after the decellularisation process.

Further to establish the recellularisation protocol, reseeding using HOS cells was allowed to progress for up to 5 weeks in the presence of an adherent and a nonadherent surface. Several test parameters such as alkaline phosphatase (ALP) activity and DAPI staining for DNA presence were measured. The culture samples were also compared in static and dynamic culture conditions.

After 3 weeks of *in vitro* culture, the reseeded cells and materials in adherence and non-adherence conditions were measured for the MTT reduction, mechanical testing, pore diameter, and human osteocalcin syhthesis by an ELISA kit.

The adherence and proliferation within the scaffolds were then confirmed by the SEM after 21 days post reseeding. The effects of vitamin D_3 on the cell growth were also carried out.

Overall, the findings presented that the decellularised bovine bone scaffolds are capable of supporting cell adherence and proliferation. Moreover, some test parameters after recellularisation have shown the potential use of this bone scaffolds *in vivo*. Taken together, the studies carried out in this project show that this bovine donor bone scaffold could be used to repair bone defects in recipient patients.

CONTENTS PAGE

MECHANICAL PROPERTIES OF BONE SAMPLES

LIST OF FIGURES

LIST OF TABLES

LIST OF EQUATIONS

LIST OF ABBREVIATIONS

2D:	Two-dimensional
3D:	Three-dimensional
α-MEM:	Minimum essential medium α
β-TCP:	β-tricalcium phosphate
ACL:	Anterior cruciate ligament
AFM:	Atomic force microscopy

ALP:	Alkaline phosphatase
AMRL:	Advanced Materials Research Laboratories
ANOVA:	Analysis of variance
ATP:	Adenosine triphosphate
AVAs:	Aortic valve allografts
BCIP:	5-bromo-4-chloro-3-indolyl phosphate
bFGF:	Basic fibroblast growth factor
BG:	Bio Glass
BGP:	Bone gla protein
BHI:	Brain heart infusion
BMC:	Bone mineral content
BMD:	Bone mineral density
BMPs:	Bone morphogenetic proteins
BMSCs:	Bone marrow stromal cells
BP:	Band pass
BSA:	Bovine serum albumin
BSP:	Bone sialoprotein
BTE:	Bone tissue engineering
cAMP:	Cyclic adenosine monophosphate
CC:	Clara cell
CCSP:	Clara cell secretory protein
CD:	Cluster of differentiation
CHAPS:	3-[(3-cholamidopropyl) dimethylammonio]-1-propanesulfonate
CK:	Cytokeratin
CM:	Culture medium
CMFDA:	5-chloromethylfluorescein diacetate
CT:	Calcitonin
Cx43:	Connexin - 43
DAPI:	4', 6-diamidino-2-phenylindole
DMBA:	Dimethylaminobenzaldehyde

DMEM:	Dulbecco's modified eagle medium
DMSO:	Dimethyl sulfoxide
DNA:	Deoxyribonucleic acid
DNase:	Deoxyribonuclease
DPBS:	Dulbecco's phosphate-buffered saline
ECM:	Extracellular matrix
EDTA:	Ethylene diamine tetraacetic acid
EGTA:	Ethylene glycol tetraacetic acid
ELISA:	Enzyme-linked immunosorbent assay
EM:	Emission
ESCs:	Embryonic stem cells
EU:	European Union
EX:	Excitation
FCS:	Fetal calf serum
FDA:	Food and Drug Administration
FR:	Flow rate
GAGs:	Glycosaminoglycans
GCs:	Glucocorticoids
H&E:	Haematoxylin & Eosin
HA or Hap:	Hydroxyapatite
HA:	Hyaluronic Acid
hASCs:	Human adipose-derived stem cells
hESC:	Human embryonic stem cells
hFOB:	Human fetal osteoblastic
HHP:	High hydrostatic pressure
hiPSCs:	Human induced pluripotent stem cells
hMSCs:	Human mesenchymal stem cells
hOB:	Human osteoblast/ Human osteoblast explant cultures
hOB^{col}:	Osteoblast explant culture from collagenease-treated bone
HOb:	Human osteoblast

HOS:	Human osteoblast/ Human osteosarcoma
HUVECs:	Human umbilical vein endothelial cells
IHC:	Immunohistochemistry
keV:	Kiloelectron volt
LDH:	Lactate dehydrogenase
LV:	Left ventricular
MAPK:	Mitogen-activated protein kinase
M-CSF:	Macrophage colony stimulating factor
MC3T3-E1:	Mouse osteoblastic cell line
MHC:	Major histocompatibility complex
MG-63:	Human osteosarcoma
MNF116:	Mouse monoclonal anti-cytokeratin 1 antibody
MSCs:	Mesenchyme stem cells
MTT:	3-(4,5-dimethylthiazol-2-yl)-2,5-diphenyltetrazolium bromide
N:	Newton
NADH:	Nicotinamide adenine dinucleotide
NADPH:	Nicotinamide adenine dinucleotide phosphate
NBT:	Nitroblue tetrazolium
NCPs:	Non-Collagenous Proteins
NEAA:	Non-essential amino acids
NTIRE:	Non-thermal irreversible electroporation
OC:	Osteocalcin
OD:	Optical density
OPG:	Osteoprotegerin
OPHr:	Hydroxyproline
OPN:	Osteopontin
OST:	Osteoblast
P4HB:	Poly 4- hydroxybutyrate
Pa:	Pascal
PAA:	Peracetic acid

PBS:	Phosphate-buffered saline
PCL:	Polycaprolactone
PDLLA:	Poly (D,L-lactic acid)
PEST:	Penicillin/streptomycin
PEUU:	Poly(ester urethane urea)
PG:	Prostaglandin
PGA:	Polyglycolide or Polyglycolic acid
PHAs:	Polyhydroxyalkanoates
PHB:	Poly 3-hydroxybutyrate
PHBHHx:	Copolymers of 3-hydroxybutyrate and 3-hydroxyhexanoate
PHBV:	Copolymers of 3-hydroxybutyrate and 3-hydroxyvalerate
PHO:	Poly 3-hydroxyoctanoate
PI:	Propidium iodide
PICP:	Procollagen type I carboxy-terminal peptide
PLA:	Polylactic acid or Polylactide
pNPP:	P-nitrophenol phosphate
psi:	Per square inch
PTH:	Parathyroid hormone
PTHrP:	Parathyroid hormone-related protein
RANKL:	Receptor activator of nuclear factor kappa-B ligand
RGD:	Arginylglycylaspartic acid
RIA:	Radioimmunoassay
rMSCs:	Rat mesenchymal stem cells
RNA:	Ribonucleic acid
RNase:	Ribonuclease
r.p.m:	revolutions per minute
RT-PCR:	Reverse transcriptase–polymerase chain reaction
SAB:	Sabouraud
Saos-2:	Human osteosarcoma
SB-10:	Sulfobetaine-10

SB-16:	Sulfobetaine-16
SDC:	Sodium deoxycholate
SDS:	Sodium dodecyl sulfate
SEM:	Scanning electron microscope/ Standard error of the mean
sGAG:	Sulfated glycosaminoglycans
SIS:	Small intestine submucosa
SMA:	Smooth Muscle Actin
SP:	Sufactant protein
SPSS:	Statistical package for the social sciences
std.:	Standard deviation
TBS:	Tris buffered saline
TE:	Tissue engineering
TEM:	Transmission electron microscope
TGF:	Transforming growth factor
TGF-β:	Transforming growth factor beta
TMJ:	Temporomandibular joint
TnBP:	Tri (n-butyl) phosphate
TNF:	Tumor necrosis factors
Ttf:	Transcription factor
TUNEL:	Transferase dUTP nick end labeling
U-2 OS:	Human osteosarcoma
US:	United States
USA:	United States of America
VEGF:	Vascular endothelial growth factor
vWF:	Von willebrand factor

Chapter 1

LITERATURE REVIEW

1.1 Introduction

Bone defects caused by trauma and physiological and pathological bone resorption represent a major challenge and have become a global health issue (Arvidson et al., 2011; Wei et al., 2004; Frohlich et al., 2010; Pathak et al., 2012). Every year in the United States (US), bone is used to help heal bone fractures in more than 450,000 graft procedures, and about 2.2 million procedures are carried out worldwide (Vaccaro 2002; Frohlich et al., 2010; Wahl & Czernuszka, 2006). Surprisingly, more than six million bone defects arise in the US every year, and almost one million bone grafting cases are accomplished (Yeatts & Fisher, 2011; Salgado et al., 2004). Furthermore, a study by the Japanese Orthopaedic Association Committee demonstrated that 82.4% (134,782) of tissue grafting from 1985 to 2004 was related to bone grafting (Quan et al, 2014).

A main concern for the United States of America (USA) and European Union (EU) is the socioeconomic results in handling these patients with bone defects, and this concern will probably rise in the next years caused by ageing of people in communities, the fast worldwide population growth and improved life expectancy (Salgado et al., 2004; Frohlich et al., 2010). Moreover, the costs for healing bone and regeneration treatments are expected to reach 3.5 billion by 2017 (Sladkova & Maria de Peppo, 2014).

1.2 Tissue engineering (TE)

The interdisciplinary area of research that employs the methods and principles of engineering and life sciences in relation to the development of biological substitutes for clinical applications that repair, sustain, or enhance tissue function is defined as Tissue Engineering (TE) (Salgado et al., 2004; Pathak et al., 2012; Chen et al., 2012). TE approaches have been used frequently to produce functioning suitable tissues that can be entirely incorporated into host organ systems (Flynn et al., 2006; Patnaik et al., 2013) to reconstruct tissues or organs used for replacing, both physically and/or functionally, organ deficiency, damaged/injured organs, and pathological irregularities (Patnaik et al., 2013; Wang et al., 2013). Consequently, tissue engineering studies have made much progress throughout the past three decades (Patnaik et al., 2013).

TE combines the fields of biology, engineering, chemistry, medicine and biotechnology in order to restore impaired tissues and organs (Patnaik et al., 2013). In addition, it creates a useful tissue replacement *in vitro* by applying biomaterials alone or in combination with cells, and biological factors (Pathak et al., 2012). Generally, there are three important elements for a TE substitute and these are (i) cells (tissue-specific), (ii) scaffold biomaterials (constructed to sustain the cells in a three-dimension environment), and (iii) signals (appropriate tissue specific environment) that lead to specific gene expression and the creation of extracellular matrix (ECM) during tissue development (Cigliano et al., 2012; Wang et al., 2013). Moreover, according to Sourav et al. (2013), there are three approaches that have mainly been applied in tissue engineering and regeneration, and they are (i) to directly implant the

cultured cells, (ii) to regenerate the tissues *in situ* and (iii) to assemble the cells and scaffolds *in vitro* (Patnaik et al., 2013). In addition to approach (iii) are seeding and growing a cell source onto scaffold followed by implanting the cells and scaffold into the injury place. In order to enhance cell proliferation and differentiation on the scaffold, the cells are usually cultured *in vitro* on the constructs before being implanted into the body (Yeatts & Fisher, 2011).

However, TE studies have several challenges in establishing an appropriate scaffold for the growth of cells with the correct phenotypes, providing and supporting sufficient oxygen and nutrients in tissue constructs, deciding ideal engineering environments (such as bioreactors, physical simulations and growth media for specific constructs) and sustaining the durability and adaptability of tissue constructs within hosts (Patnaik et al., 2013).

1.3 Bone tissue engineering (BTE)

Bone tissue engineering (BTE) occupies a multidisciplinary strategy focusing on the principles of cell biology, material science, biomechanics and molecular development in order to assist in repairing the defective tissues beyond the regular healing ability of the bone (Alvarez et al., 2009). From this approach, TE has been used to design artificial bone that mimics the structure of real bone (Nguyen et al., 2012). The purpose of BTE is to regenerate damaged or diseased bones within the body and this can be established by applying biological substitutes or developing implants for bone restoration (Gerhardt et al., 2012, Gleeson et al., 2010;

MarcosCampos et al., 2012; Alvarez et al., 2009; Nguyen et al., 2012; Teixeira et al., 2008).

Its goals are to create an unrestricted amount of feasible tissue substitutes (Sladkova et al. 2014).

A great potential for bone reconstructions lies in engineering anatomically accurate parts of functional human bone after trauma, cancer resections, and congenital defects (Grayson et al., 2010). In conventional methods, bone defects are resolved using bone grafts and synthetic bone filling materials. But, TE methods focus on the tissue regeneration compared to tissue replacement (Miao et al., 2008).

BTE is applied to correct bone defects using three-dimensional (3D) bone graft replacements to heal bone losses (Alvarez et al., 2009; Wahl et al., 2006) and improve bone function (Quan et al., 2014). Bone grafting is a common method in orthopaedic surgery (Quan et al., 2014). Bone grafts have been utilized in the United States for about one half of the 5.2 million musculoskeletal procedures performed every year (Bracey et al., 2014). The success of engineered bone grafts can be assessed mainly by their mechanical behaviour and the capability of cells to form tissue-specific proteins (Grayson et al., 2010). Bone grafts can be categorised as autografts, allografts, and xenografts (Leukers et al., 2005; Alvarez et al., 2009;

Nguyen et al., 2012; Teixeira et al., 2008; Wahl et al., 2006).

1.3.1 Autografts

Autologous bone grafting means that the bone to be used occupied another part of the patient's own body and then was reimplanted into the patient's damaged bone

site. The bone used is usually in the form of trabecular bone (from the patient's iliac crest), or cortical bone (Salgado et al., 2004; Gleeson et al., 2010). In this technique, autologous cells are added within biodegradable material scaffolds, or cultured in bioreactors. Engineered bone tissue is an ideal model for investigating bone development, disease, and remodelling because the environmental parameters can be controlled and adjusted consistently (Marcos-Campos et al., 2012).

Implantation of autologous bone grafts still remains the most popular treatment for skeletal regenerations (Sladkova et al., 2014; Quan et al., 2014) and orthopaedic practice (Bracey et al., 2014) even though many other bone substitute materials have been offered recently. There were approximately 500,000 to 600,000 bone grafting procedures in the US and in total 75% of these bone grafts were allografts (Quan et al., 2014).

For several years, they have been the "gold standard" for substituting large areas of damaged bone. Autografts produce osteogenic cells (important osteoinductive factors) required for the bone regeneration and healing process
(Vaccaro, 2002; Salgado et al., 2004; Gleeson et al., 2010; Marcos-Campos et al., 2012). They attain a lot of success in repairing procedures to provide functional bones (Salgado et al., 2004; Woodard et al., 2007).

In terms of disadvantages, there are important surgical and practical problems related to this method such as:

i) donor site morbidity (Vaccaro, 2002; Salgado et al., 2004; Bracey et al., 2014; Gerhardt et al., 2012; Gleeson et al., 2010; Wei et al., 2004; Marcos-Campos et al., 2012; Woodard et al., 2007; Nguyen et al., 2012;

Frohlich et al., 2010; Quan et al., 2014; Grayson et al., 2010), ii) restricted availability (Salgado et al., 2004; Leukers et al., 2005; Bracey et al., 2014; Gerhardt et al., 2012; Gleeson et al., 2010; Wei et al., 2004; Woodard et al., 2007; Frohlich et al., 2010; Teixeira et al., 2008; Quan et al., 2014), and iii) need clinicians' capability to form appropriate 3D shape (Leukers et al., 2005; Teixeira et al., 2008; Grayson et al., 2008).

Other significant drawbacks are expensive, limited autografts to treat the small defect (Nguyen et al., 2012), difficulty in harvesting (Grayson et al., 2010), and donor site chronic pain (Vaccaro, 2002; Bracey et al., 2014; Gerhardt et al., 2012; Frohlich et al., 2010; Quan et al., 2014).

1.3.2 Allografts

Allograft bone grafts use bone that is retrieved from somebody else's body (Salgado et al., 2004; Gleeson et al., 2010). It is quite common to use allograft bone instead of autograft bone in bone grafting because it has the same osteoconductive properties (Quan et al., 2014). Allografts are very efficient in restoring processes and function of defective bones (Woodard et al., 2007). It becomes the chosen replacement when autologous transplantation is impossible (Vaccaro, 2002; Gerhardt et al., 2012). Allograft can be applied for larger areas of bone damage (Nguyen et al., 2012). Other advantages are readily available, free from any further surgery and no limit to size of graft material (Gleeson et al., 2010).

However, allograft bone has limitations in terms of:

i) disease transmission (Salgado et al., 2004; Leukers et al., 2005; Gleeson et al., 2010; Wei et al., 2004; Woodard et al., 2007; Nguyen et al., 2012; Teixeira et al., 2008; Quan et al., 2014),

ii) immune rejection (Vaccaro, 2002; Salgado et al., 2004; Leukers et al., 2005; Gleeson et al., 2010; Wei et al., 2004; Marcos-Campos et al., 2012; Woodard et al., 2007; Nguyen et al., 2012; Teixeira et al., 2008; Quan et al., 2012),

iii) infection and inflammation and have perceived ethical disadvantages (Nguyen et al., 2012), iv) donor morbidity (Leukers et al., 2005; Gleeson et al., 2010; Woodard et al., 2007; Nguyen et al., 2012; Teixeira et al., 2008), v) lack of osteogenesis (Gerhardt et al., 2012), vi) lack of donor (Gleeson et al., 2010; Quan et al., 2014), and vii) lower integration rate as compared to autografts (Nguyen et al., 2012).

1.3.3 Xenografts

A bone graft retrieved from a donor of one species which is grafted into a recipient of another species is called a xenograft (Salgado et al., 2004; Gleeson et al., 2010). Xenografts (non-human bone) have been used as an alternative to autologous and allogenous bone grafts (Quan et al., 2014). Xenograft is the chosen replacement when autologous transplantation is impossible (Gerhardt et al., 2012). This method is dependent on the use of accelular matrix xenografts (taken commonly from porcine and bovine) as scaffolds which are repopulated with cells from the patient (Cigliano et al., 2012).

Other advantages are readily available, free from any further surgery and limitless size of graft material (Gleeson et al., 2010). Xenograft origins are unlimited and are normally taken from bovine or porcine tissue (Bracey et al., 2014; Quan et al., 2014). Moreover, the morphology and composition of xenogenous cancellous bone are the same as human cancellous bone. Besides, it has osteoconductivity capability (Quan et al., 2014).

On the other hand, xenografts is restricted by the risk of:

i) diseases transmission (Leukers et al., 2005; Gleeson et al., 2010; Woodard et al., 2007; Nguyen et al., 2012; Teixeira et al., 2008; Wahl et al., 2006),

ii) infection and inflammation and have perceived ethical disadvantages (Bracey et al., 2014; Wahl et al., 2006), iii) donor morbidity (Leukres et al., 2005; Gleeson et al., 2010; Woodard et al., 2007; Nguyen et al., 2012; Teixeira et al., 2008), iv) immune response and transplant rejection (Leukers et al., 2005; Gleeson et al., 2010; Wei et al., 2004; Woodard et al., 2007; Nguyen et al., 2012; Teixeira et al., 2008; Quan et al., 2014),

v) lack of osteogenesis (Gerhardt et al., 2012), and vi) physiological function and structure mismatch with the human tissue (Nguyen et al., 2012).

Recently, the use of impacted morselized cancellous allograft has become a popular clinical technique. Cancellous bone (normally from the proximal femur) is morselized and impacted into a cavitary defect with a cemented component. Impacted bone is resorbed, substituted by host bone and incorporated within the cavity. It supports the remodelling and restoration of proximal femoral bone, and gives implant stability (Heiner, 2002; Malkani et al., 2015).

In conclusion, all the bone grafts seem to have pros and cons. In the present study, trabecular bone was retrieved from the bovine tissue and it is intended to be grafted into the human recipient. Several important aspects related with xenografts are those that deal with the disease transmission and immune rejection with donors and recipients. These infectious diseases can be transmitted either in short or long term to the patients. Concerns have also arisen regarding immunogeneic drawbacks associated with the transplanted of foreign donor tissue. An implanted bone tissue from bovine origin might be rejected by the human's immune system. As an alternative to the bone grafting, there are some biomaterials used as bone tissue engineering scaffolds and it has been explained in the following subtopic.

1.3.4 Biomaterials used as bone tissue engineering scaffolds

The choice of the most suitable material to provide a scaffold that can be used in bone tissue engineering uses is very critical towards the development of a tissue engineered creation, since its characteristics will present, to a great extent, the role of the scaffold. Several materials including metals, ceramics, and polymers from either natural or synthetic sources, have been recommended in creating scaffolds for bone tissue engineering (Salgado et al., 2004).

1.3.4.1 Ceramics

Ceramics have been extensively applied in biomedical engineering and bone replacement and regeneration studies. They can be derived naturally or synthetically

from hydroxyapatite (HA) and/or β-tricalcium phosphate (β-TCP). They have been recognized for bone tissue engineering uses because they have superb properties in terms of being osteoconductive and osteoinductive. Many studies have reported that by applying ceramics *in vivo*, either with or without bone marrow cells, excellent findings as regards to bone regeneration can be achieved. But, these materials have several limitations such as brittleness, and poor mechanical stability, which can minimise their application in the regeneration of huge bone defects. Moreover, due to causes that occur *in vivo*, like osteoclastic activity, the degradation rates of ceramics are unpredictable. As other options to the ceramics, there are biodegradable polymers that can be divided in two groups called natural and synthetic (Salgado et al., 2004).

1.3.4.2 Natural biodegradable polymers

Natural biodegradable polymers are retrieved from natural origins, either from vegetable or animal sources. Naturally derived proteins/polymers include collagen, fibrinogen, chitosan, starch, hyaluronic acid (HA), poly (hydroxybutyrate), alginate or fibrin, all of which show basic cell biocompatibility. The additional details on the characteristics of several natural biodegradable polymers are explained in **Table 1.1**. The major benefits of these materials are based on their immunogenic compatibility, the possible bioactive behaviour and the ability to interact with the host's tissue, chemical adaptability, and in numerous cases, almost infinite sources as in starch and chitosan (Salgado et al., 2004). Naturally occurring polymers must not produce a foreign material reaction when transplanted in humans. They give a natural substrate for cellular adhesion, proliferation and differentiation and are regarded as the preferred

substrate for tissue engineering (Seal et al., 2001). However, they are some difficulties with obtaining reproducible physical and mechanical properties (Patnaik et al., 2013; Vacanti et al., 2000).

The problems related with naturally occurring polymers could be avoided by using polyhydroxyalkanoates (PHAs), aliphatic polyesters created by microorganisms under disturbed growth circumstances (Doi et al., 1995). They are mostly biodegradable (through hydrolysis), are greatly biocompatible, and this has made them attractive for uses in tissue engineering (Chen et al., 2005). The combinations among some PHAs can effectively alter material properties and biocompatibility. In fact, PHAs, mainly poly 3-hydroxybutyrate (PHB), copolymers of 3-hydroxybutyrate and 3-hydroxyvalerate (PHBV), poly 4- hydroxybutyrate (P4HB), copolymers of 3-hydroxybutyrate and 3-hydroxyhexanoate (PHBHHx) and poly 3-hydroxyoctanoate (PHO) have revealed propriety for tissue engineering over the past years. They are reviewed and studied by Chen et al., (2005) and Misra et al. (2006).

In bone tissue engineering, PHB is widely used in bone tissue without indication of unwanted chronic inflammatory reaction after transplantation durations up to 12 months (Doyle et al. 1991). Nevertheless, as stated in the literature by Chen at al., (2005); a potential problem of several PHAs is their restricted availability and the time consuming extraction from bacterial cultures that is essential for attaining adequate amounts. Thus, it becomes a challenge to produce huge amounts of several PHAs because of expensive industrial production from the extraction process.

1.3.4.3 Synthetic biodegradable polymers

One of the most frequently employed materials in the biomedical engineering field is synthetic biodegradable polymers. The benefits of using synthetic polymers with excellent processing characteristics is they can be custom-made and manufactured with great precision, duplicated without any significant changes in physical and mechanical properties (for instances; tensile strength, elastic modulus, and degradation rate), surface structure and porosity (Middleton & Tipton, 2000; Patnaik et al., 2013; Salgado et al., 2004; Vacanti et al., 2000). The most widely used synthetic polymers include poly(lactic acid) (PLA), poly(glycolic acid) (PGA), poly(ε-caprolactone) (PCL), polyester (urethane urea) (PEUU), poly(hydroxyalkanoate), poly(α-hydroxyacids), poly(propylene fumarates), poly(carbonates), poly(phosphazenes), and poly(anhydrides) (Patnaik et al., 2013; Salgado et al., 2004). In addition, the particulars on the characteristics of some synthetic biodegradable polymers are described in **Table 1.1**.

Nevertheless, these have some restrictions in terms of undetermined degradation rates and products, and they are often weak in cell compatibility (Salgado et al., 2004; Patnaik et al., 2013). Additionally, they also have limitations in terms of causing persistent inflammatory responses, being worn, not being amenable or accomplished to incorporate with host tissues. In comparison between the two forms of synthetic polymers which are i) bulk biodegradable and ii) surface bioerodible polymers, the previous have demonstrated more potential seeing that one of the necessities of a tissue engineering scaffold is that it has to be substituted by newly created bone tissue *in vivo*. Moreover, among the bulk degradable polymers, amorphous poly (D,L-lactic

acid)(PDLLA) is one of the most famous materials used for scaffold fabrication, as well as in blending with bioactive glasses (Boccaccini et al., 2005), since it can be mixed with biomolecules comprising growth factors (Schmidmaier et al., 2001) and antibiotics (Gollwitzer et al., 2003), to create a locally performing drug-delivery system. It is predicted that a scaffold with a regulated drug-delivery function will stimulate bone reconstruction and reduce inflammatory reaction upon scaffold degeneration.

Table 1.1: Additional details on the source and characteristics of natural and synthetic polymers used for bone tissue engineering applications. Adapted from (Salgado et al., 2004).

Material	Source	Characteristics	References
Collagen	Natural	Poor immune reaction, excellent substrate for cell attachment, and chemotactic, but scaffolds have poor mechanical properties.	Ueda et al., 2002; Sachlos et al., 2003.
Fibrin	Natural	Stimulate cell migration, vascularization, osteoconduction, and normally is used as a carrier to seed the cell on scaffolds.	Hojo et al., 2003; Salgado et al., 2002; Endres et al., 2003.
Chitosan	Natural	Haemostatic, and stimulates osteoconduction and wound healing.	Tolaimate et al., 2003; Zhao et al., 2002; Zhang et al., 2003; Baran et al., 2004.

Starch	Natural	Thermoplastic behaviour, excellent substrate for cell attachment, non-	Salgado et al., 2002; Marques et
		cytotoxic and biocompatible, bone bonding behaviour when strengthened with hydroxyapatite, and scaffolds based on these materials have excellent mechanical properties.	al., 2002; Elvira et al., 2002; Salgado et al., 2004.
Hyaluronic acid (HA)	Natural	Limited immunogenicity, chemotactic, and scaffolds with poor mechanical properties.	Brekke et al., 1998; Liu et al., 1999; Solchaga et al., 1999.
Poly (hydroxybutyrate)	Natural	Natural occurring β-hydroxyacid, sufficient substrate for bone development, but efficacy is restricted due to brittle nature.	Kostopoulos et al., 1994; Chen et al., 2002.

Poly (α-hydroxy acids)	Synthetic	Widely studied aliphatic polyesters, degraded by hydrolysis, acidic byproducts (for example lactic acid, glycolic acid), that pass into the tricarboxylic acid cycle or as an alternative (for example glycolic acid) are secreted in the urine, and it can demonstrate complications regarding cytotoxicity in the nearby area of the implantation site.	Abukawa et al., 2003; Taboas et al., 2003; Almin et al., 2003; Luu et al., 2003.
Poly(εcaprolactone)	Synthetic	Aliphatic polyester, degradation through hydrolysis or bulk erosion,	Washburn et al., 2002; Schantz et
		slow degrading, degradation products combined with the tricarboxylic acid cycle, poor chemical adaptability, and several problems associated with resisting mechanical loads.	al., 2002; Kweon et al., 2003.
Poly(propylene fumarates)	Synthetic	Unsaturated polyester comprised of alternating propylene glycol and fumaric acids, major degradation products are fumaric acid and propylene glycol. Acceptable biological results.	Shun et al., 2002; Shung et al., 2003; Sim et al., 2003; Sin et al., 2003.

Poly(BPA iminocarbonates)	Synthetic	Excellent biocompatibility when implanted in a bone canine chamber model.	Choueka et al., 1996; Ertel et al., 1995.
Poly(anhydrides)	Synthetic	Mostly established as drug delivery carriers, biocompatible, and can help both endosteal and cortical bone regeneration.	Ibim et al., 1998; Uhrich et al., 1998.

1.4 Decellularisation

Regenerative medicine approaches involving decellularised ECM scaffolds are developing fast (Sandmann & Tischer, 2010; Koch et al., 2012; Marcos-Campos et al., 2012; Benders et al., 2012; Ning et al., 2012; Gilbert et al., 2006; Hashimoto et al., 2011).

In tissue engineering, scaffolds derived from decellularised tissue give another option for ECM (Sandmann & Tischer, 2010; Marcos-Campos et al., 2012; He & Callanan, 2013; Hashimoto et al., 2011; Wang et al., 2012) being more close to the biological properties of natural tissue structure (Ning et al., 2012). Biological scaffold material derived from the extracellular matrix has been previously used in reconstructive surgery. In this case, scaffold has been applied for the specific tissue after a decellularisation process (He & Callanan, 2013).

Decellularisation is a method to develop biological scaffolds (templates) which minimise possible adverse immune responses, and support host cell diffusion into the graft (Fini et al., 2012). Basically, this approach segregates the ECM components by

extracting cells from tissues or organs. The process of tissue decellularisation preserves the natural ultrastructure (collagen, elastin etc.) and biochemical content of ECM (Ning et al., 2012; Patnaik et al., 2013). In addition, the accelular scaffolds also usually preserve bioactive molecules such as laminins, fibronection, collagen, and glycoproteins. Bioactive molecules perform roles as signals for numerous growth factors and other proteins/biofactors (cadherins, integrins, etc.), help to create cell-cell communication and cell-ECM communication (Fu et al., 2014; Patnaik et al., 2013; Hashimoto et al., 2011; Kang et al., 2011) and also to determine the character and stability of tissues (Fu et al., 2014). Decellularised ECM tends to keep the differentiated phenotype of subsequently seeded cells (Hashimoto et al., 2011). Taken together, this decellularised scaffold which has a combination of structural and functional proteins can be utilised for many applications in tissue engineering and regeneration (Patnaik et al., 2013).

The aims of the decellularisation method are to successfully eliminate all cellular materials, antigens, cell fragments, chromosome debris, and nuclear content, at the same time preserve the composition, biological activity and mechanical strength of the remaining extracellular matrix as mentioned in **Figure 1.1** (Fu et al., 2014; Gundula et al., 2012; Fini et al., 2012; Pathak et al., 2012; Patnaik et al., 2013; Gilbert et al., 2006; Hashimoto et al., 2011; Choi et al., 2012). Using decellularised tissue where the donor cells (xenogeneic) and antigen molecules are entirely removed so reducing the host immune rejection is one of the main strategies in making such a scaffold (Gundula et al., 2012; Flynn et al., 2006; Sasaki et al., 2009; Choi et al., 2012).

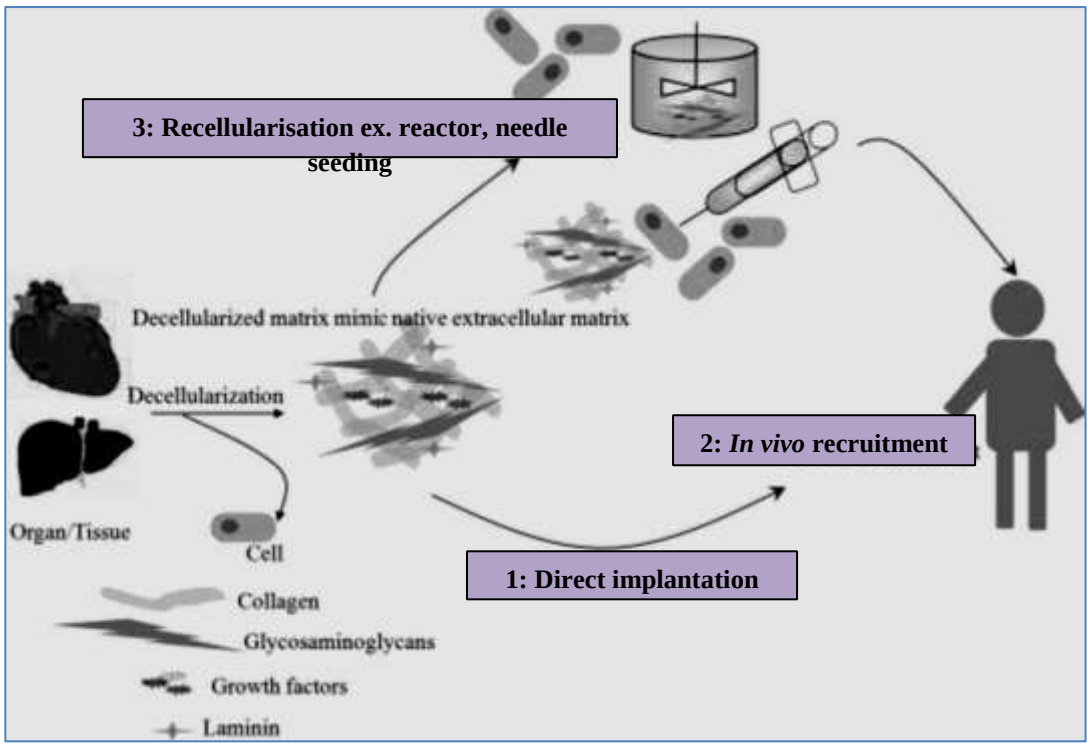

Figure 1.1: The principle of tissue decellularisation. Adapted from (Fu et al., 2014).

The optimal scaffolds must be biodegradable, non-immunogenic, and at the same time provide signals and support (biological, mechanical and structural) for cell proliferation, adhesion, and differentiation (Patnaik et al., 2013). Consequently, the scaffold should provide excellent cell-scaffold interaction that facilitates tissue regeneration and organization, is able to support the recellularisation process on a complex 3D surface, and also maintain a suitable cellular and tissue functionality (Flynn et al., 2006; He & Callanan, 2013; Patnaik et al., 2013). Decellularised scaffold is an ideal substrate to give an optimal cellular microenvironment because it has the similar composition and structure to the natural ECM (Hashimoto et al.,

2011) and it is predicted to encourage regenerative processes (Fu et al., 2014). Furthermore, decellularised scaffolds have been proven to minimise the creation of scar tissue (Flynn et al., 2006) and to act as an efficient 3D vascular network delivering required oxygen and nutrients (He & Callanan, 2013).

The effectiveness of the decellularisation process has been established by histological, biochemical, and immunohistological methods; and biocompatibility of the decellularised scaffold examined using *in vitro* and *in vivo* tests. The biomechanical properties have been evaluated to assess possible clinical application (Kheir et al., 2011). However, the decellularisation approach faces challenges in finding the best protocols to maintain the native properties of ECM for clinical application based on its intended goal because any chosen methods to eliminate cells during decellularisation will change the original three-dimensional structure of the ECM (Fu et al., 2014; Patnaik et al., 2013). Decellularised scaffolds tend to cause inflammation due to foreign body reactions and may also elicit immune rejection
(Patnaik et al., 2013). Such scaffolds should also allow clinically implanted tissues/organs to continually turnover and regenerate further *in vivo*, and this is a major challenge.

1.5 The properties of ECM

Many studies have been published regarding the use of 3D natural ECM from different types of tissues and organs for regenerative medicine and tissue engineering applications (Patnaik et al., 2013; Wang et al., 2013) either in pre-clinical animal studies or in human clinical applications. These studies include blood vessels, heart/cardiac valves, vascular tissues, cardiac tissues, pericardial matrix, porcine meniscus, skeletal muscle, skin, nerves, ligaments, tendons, urinary bladder, small intestine submucosa (SIS) (Wang et al., 2010; Kheir et al., 2011; Benders et al., 2012; He & Callanan, 2013; Patnaik et al., 2013), and liver (Kheir et al., 2011; Fini et al.,

2012; Gilbert et al., 2006). Other successful clinical applications over the last years have been reported in tissue-engineered hearts, arteries, lungs (Wang et al., 2012), cardiovascular, gastrointestinal, breast reconstructive surgery (Benders et al., 2012) and orthopaedic surgery (Kheir et al., 2011; Gilbert et al., 2006). Interestingly, the U.S. Food and Drug Administration (FDA) has approved the experimental use of various decellularised ECM scaffolds for SIS, skin, heart valves and pericardium in both human clinical studies and pre-clinical animal applications (Patnaik et al., 2013).

Fundamentally, the ECM is an ideal natural biological scaffold material that consists of different components such as collagens, laminins, and glycoproteins which act for example as adhesive molecules like integrins (a main group of ECM receptors) and cadherins (Pei et al., 2011). In the body, the ECM is a combination of both structural and practical lipids, proteins, and proteoglycans and in every tissue and organ that combination produces different compositions and physical properties (Fu et al., 2014). Almost all cells exist *in vivo* in an ECM that contains a complex 3D fibrous network to control the many cellular characteristics (Hashimoto et al., 2011). Several growth factors are required for remodelling of new host ECM scaffolds including basic fibroblast growth factor (bFGF), vascular endothelial growth factor (VEGF), and transforming growth factor-beta (TGF-β), and the combinations are different in each organ/tissue (Fini et al., 2012; He & Callanan, 2013).

All the functional molecules of the ECM are arranged in a 3D-structural complex, and are difficult to purify as well as to synthesize (He & Callanan, 2013; Wang et al., 2013). Each tissue contains perfectly matched organ specific ECM so it can be used as a scaffold template for specific organ regeneration (Wang et al., 2013; Hashimoto et al., 2011).

After undergoing decellularisation processes with a variety of agents and approaches, ‘naked’ ECM scaffolds can therefore be created from naturally derived tissues. Different decellularisation techniques involve different degrees of difficulty and duration, and, in fact, the ECM composition and ultrastructure are prone to be disrupted by any technique or agent used, thus these effects should be reduced and minimised (He & Callanan, 2013).

The functional effect of scaffolds that are derived from ECM on cells subsequently seeded on it, is affected by some issues. These include the surface topology of the ECM, the variation of the immune response evoked by the scaffold, the microenvironmental signals applied to the cells (e.g. biomechanical loading) and the preservation of growth factors within the ECM (Benders et al., 2012). The host response to the scaffold material depends on whether there is a species difference between the host and the species providing the source of ECM, the tissue of source, and the processing methods used during the construction of the ECM scaffold. Also it depends on the decellularisation technique, methods of sterilisation and the use of chemical crosslinking mechanisms (Fini et al., 2012; He & Callanan, 2013).

The mechanical integrity of the ECM can be described from both its collagen fibre structural and kinematic architectural characteristics (e.g. fibre size, arrangement and position) (He & Callanan, 2013). The 3D arrangement and hydration level of ECM scaffold, the decellularisation process and the sterilisation protocol affect the biomechanical properties in general. The form and amount of forces applied upon the scaffold, and the degradation rate are factors that might also affect the biomechanical characteristics of ECM scaffolds *in vivo* (Benders et al., 2012). Moreover, usually a combination of growth factors or other functional proteins influence the turnover and

alignment of the collagen fibres to create the 3D structure, biomechanical strength and resilience of a tissue (Gundula et al., 2012; Benders et al., 2012). The load-bearing performances of the preserved structural constituents of the ECM (collagen, proteoglycans, and elastin) can be determined by how elastic the elastin fibres are, the mechanical strength of the collagen fibrils/fibres, and the cushion/hydration/binding role of the proteoglycans (Patnaik et al., 2013).

The use of xenogeneic tissue (for example bovine or porcine tissue) and some kinds of human allogeneic tissue as ECM scaffold biomaterials (He & Callanan, 2013) results in the recognition of xenogeneic and allogeneic cellular antigens by the host and as a result of this, an inflammatory response and immune-mediated rejection of the tissue may occur. However, the ECM components are normally well-preserved among species and are well tolerated by xenogeneic recipients (Benders et al., 2012; Gilbert et al., 2006).

After a suitable animal donor has been chosen, the decellularised scaffold can be either implanted directly or used as composite graft after reseeding with appropriate cells (Pathak et al., 2012). Choi et al. (2012) has reported that decellularised xenogenic ECM gives an appropriate material to human cells (*in vitro*) for adhesion and proliferation and it seems promising to be used as a biocompatible material in tissue reconstruction (*in vivo*). In their studies, they used decellularised porcine ECM derived from adipose tissue and realised that the scaffold had an enormous potential (as xenogeneic substance) in the application of xenograft tissue engineering. It is possible to eliminate cellular antigens from the xenogeneic source as long as the ECM scaffolds are successfully decellularised (Benders et al., 2012). The key element for

transplantation in using xenogeneic tissues is the complete removal of immunogenic antigens (Gundula et al., 2012).

1.5.1 Advantages of natural ECM scaffolds

Some advantages are achieved from the use of a natural scaffold (or ECM) because it:

i. acts like a support, allows constructive remodelling to form the anatomical basis of tissues and provides anchorage for the compounds used as biochemical signals including proteins, proteoglycans, glycosylaminoglycans (GAGs), and growth factors (Benders et al., 2012; Flynn et al., 2006; He &

Callanan, 2013; Ning et al., 2012; Choi et al., 2012), ii. is in a state of dynamic equilibrium (in terms of structural and functional molecules) situated in the neighbouring microenvironment that allows cells to interact with each other and also with the external surroundings. This is called bioinductive properties of ECM that permits the productive remodelling of tissue after implantation (*in vivo*) of ECM scaffolds (Benders et al., 2012; Fini et al., 2012; He & Callanan, 2013). In general, a natural ECM scaffold will provide an ideal environment to cells for proliferation and adhesion

(Pathak et al., 2012), iii. allows tissue homeostasis to occur with a balance of regeneration, and supports tissue biodegradation (Benders et al., 2012), iv. proposes the biophysical and biomechanical properties (Gundula et al., 2012; Sandmann & Tischer, 2010; Benders et al., 2012; Flynn et al., 2006;

Hashimoto et al., 2011),

v. permits cell adhesion, survival, morphogenesis, cell aggregation, proliferation and differentiation, and does not cause adverse immune reactions (Fu et al., 2014; Sandmann & Tischer, 2010; Benders et al., 2012; He & Callanan, 2013; Pathak et al., 2012; Hashimoto et al., 2011; Choi et al., 2012; Wang et al., 2012), vi. can be taken from either human or animal donors (Koch et al., 2012). Due to plentiful availability of allo- or xenogeneic tissues this avoids donor site morbidity caused by autografting (Gundula et al., 2012),

vii. allows a supportive platform for lymphatic vessels, blood vessels and nerves (He & Callanan, 2013; Hashimoto et al., 2011) and has chemotactic factors (which attract and capture cells, and perform supportive functions) that help to capture nutrients from the blood (Sandmann & Tischer, 2010; He & Callanan, 2013), viii. is extensively used to preserve the function and structure of cell, tissue and organ morphogenesis, to promote wound healing (Perniconi et al., 2011; Gundula et al., 2012; Flynn et al., 2006), and to sustain structurally organized substances such as elastin, glycosaminoglycans, collagen, and fibronectin (Patnaik et al., 2013), ix. is produced from the local cells of each tissue and organ in a 3D structure, in a highly specific organization and configuration, and is highly biocompatible because of the production of their own matrix by host cells (Benders et al., 2012; Flynn et al., 2006; He & Callanan, 2013; Hashimoto et al., 2011).

1.6 History and current state of decellularised approach

In one of the first decellularisation protocols, acellular SIS was successfully formed by Badylak et al. in 1995. Moreover, the acellular SIS was applied in repairing shoulder injury, with impressive clinical results (Patnaik et al., 2013). This research continued to utilise acellular SIS in tissue engineering of tendon/ligament, blood vessel, cartilage, abdominal wall, facial restoration, and heart valves. The SIS scaffold studies were then extended applying decellularisation to blood vessel, skin, bladder, esophagus, heart valve, trachea, muscle, artery, and other tissues. The equivalent acellular scaffolds were used in regenerative and tissue engineering applications (Fu et al., 2014; Benders et al., 2012; Patnaik et al., 2013; Wang et al., 2013; Hashimoto et al., 2011). Decellularised acellular matrices were used in similar approaches along with synthetic polymeric scaffolds and naturally-derived polymers/proteins (Patnaik et al., 2013). Successful decellularised ECM based scaffolds were developed for repairing of cartilage and osteochondral defects (osteochondral allografting and mosaicplasty) (Benders et al., 2012), and in creating well-preserved acellular myocardial tissue (Fini et al., 2012) and tendon (Gundula et al., 2012). These scaffolds have great cell proliferation, allowing ingrowth of viable differentiated cells for recellularisation *in vivo* (Gundula et al., 2012; Fini et al., 2012). As described by Gundula et al. (2012), tendon reconstruction really needs robust scaffolds and it seems to the authors that implantation of a natural ECM might be useful and could provide a promising therapeutic method. In their studies, encouraging *in vivo* findings using cell-free ECM (which gave a natural structural, biomechanical and biochemical scaffold for neo-tendon construction) in rabbit models have been carried out. However, cells maintained mostly inhomogeneously allocated in the reseeded ECM and did not align. Thus, they proposed to focus on optimization of tendon ECM decellularization and to

cultivate efficient cell recolonization approaches for determining tendon functionality for future work.

The transplantation of tissue engineered cellular scaffolds has also contributed to functional human organ substitutions. Clinical success in this was announced in 2008 in the Lancet by an International team (Macchiarini et al., 2008). In their studies, they eliminated cells and major histocompatibility complex (MHC) antigens from a human donor trachea, which was then readily inhabited by epithelial cells and mesenchymal stem-cell-derived chondrocytes that had been seeded from cells derived from recipient who was a 30-year old woman with end-stage bronchomalacia. Then this graft was employed to substitute the recipient's left main bronchus. From the outcomes, the graft directly supported the recipient with a functional airway, increased her quality of life, and had a normal condition and mechanical properties for 4 months. Moreover, the patient was free from the risks of rejection, and in addition she was not on immunosuppresive drugs. These results highlighted that patients with chronic clinical disorders can be treated successfully with the combination of autologous cells and suitable biomaterials (Macchiarini et al., 2008). This successful application of autologous cells, adult stem cells, and a decellularised allogeneic scaffold heralded rapid advance in this field, which can potentially revolutionise therapy. The first clinical success in 2008 was rapidly followed up by several other successfully treated patients for a number of tissues, including the liver, kidneys, pancreas, bladder, artery, esophagus, skin, and trachea (Fu et al., 2014).

The decellularisation of whole-organs was another major step taken in tissue engineering (Patnaik et al., 2013). Decellularised whole-organ scaffolds have been prepared for several organs such as kidney, heart, liver, and small bowel. The details

of the life stages of whole-organ decellularisation and the decellularisation protocols employed in the literatures are stated in **Figure 1.2** and **Table 1.2** respectively (He & Callanan, 2013). Several successful studies were reported using decellullarised whole heart such as the creation of acellular whole rat heart that maintained perfusable vascular structure and functional capable acellular valves with strong chamber geometry (Patnaik et al., 2013). Decellularised whole heart that retains the original structure and its microvascular network produces excellent recellularisation (Fu et al., 2014).

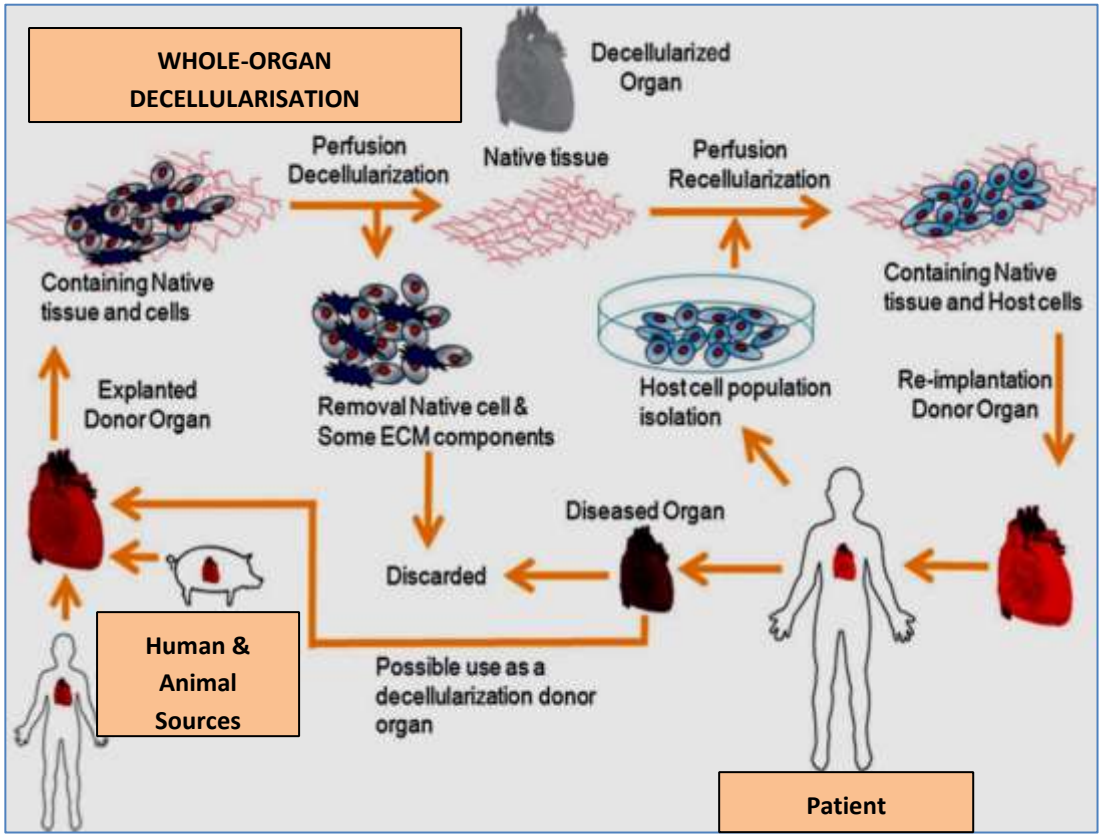

Figure 1.2: The illustrative description of the life stage of whole-organ decellularisation and possible clinical uses. Adapted from (He & Callanan, 2013).

The aim of the present study is to develop an effective protocol for bone scaffolds using decellularisation techniques. In bone tissue engineering, the optimal

scaffold needs to have a 3D microstructure and morphology, a structural template for cells to grow and proliferate, an interconnected porous network with a permeable structure, biochemical configuration, a natural nanoscale structure and hierarchical topography, appropriate mechanical properties, and a microenvironmental surface characteristic that provides biological signals for cells to function, and maintain bone strength (Gerhardt et al., 2012; Kang et al., 2011). Decellularised bone has been well utilised as a scaffold because of its superb osteoinductive and biomechanical characteristics, and its match to the natural bone matrix. It has been previously proven by Marcos-Campos et al. (2012) that using human mesenchymal and embryonic stem cells can produce a functional bone matrix scaffold without using additional growth factors. In this study, decellularised trabecular bone was used and it seems to give an acceptable "biomimetic" scaffold that allows cell attachment, proliferation, differentiation, and re-organization (Correia et al., 2012; Gerhardt et al., 2012; Marcos-Campos et al., 2012; Grayson et al., 2008).

Furthermore, Wang et al., (2012) have proven that decellularised bone matrix scaffolds can be used successfully in restoring chondral defects. The cancellous bone-derived scaffolds from this study gave a suitable platform (in term of surface) for endogenous cell adhesion, migration, and chondrocytic differentiation due to its mechanical properties, porosity, and prolonged slow degradation rate.

Organ	DECELLULARISATION PROTOCOLS		
	Tissue harvesting (Species/strain/age/explanation details)	**Characterization of decellularised scaffold**	**Authors**
Heart	12-week-old Fischer 344 rats Systemic heparinization	Histology + immunofluorescence of ECM-collagen I + III, laminin, fibronectin. Aortic valve-Evans blue perfusion. Scanning electron microscope (SEM)/Transmission electron microscopy (TEM) of ECM architecture. Vascular corrosion resin casting + heterotopic transplantation. Mechanical (stress-strain/tangential modulus) testing.	Ott et al., 2008
Heart	Adult pigs (strain not specific)	Histology + immunohistochemistry (IHC)/ immunofluorescence of ECM4',6-diamidino-2-phenylindole (DAPI), elastin, collagens (I, III, IV), GAGs. Deoxyribonucleic acid (DNA)/GAG/ elastin quantitative assays. SEM of ECM architecture.	Wainwright et al., 2010

		Mechanical (ball burst) testing.	
Lung	12-week-old male Sprague- Dawley rats Systemic heparinization	Histology of ECM-collagen, proteoglycans, elastin . Morphometry and stereology of alveoli. TEM of ECM alveolar architecture. Dynamic lung testing- compliance + vital capacity.	Ott et al., 2010
Lung	3-month-old Fischer 344 rats Intraperitoneal heparin	Histology + immunofluorescence of ECM-elastin, collagen I + IV, laminin, fibronectin. DNA/ collagen/ GAG/ elastin quantitative assays. SEM/TEM of ECM architecture. Micro-CT of vascular + alveolar architecture. Mechanical (stress-strain/ compliance) testing.	Petersen et al., 2010
Lung	Rats (age/ strain not specified)	Immunofluorescence-DAPI, MHC-1 Gel electrophoresis of DNA content.	Cortiella et al., 2010
Lung	2-3-month-old C57BL/6 female mice	Histology + immunofluorescence of ECM-collagen, elastin, DAPI, laminin. Collagen/ GAG/ laminin/ elastin quantitative assays.	Price et al., 2010

		SEM of ECM architecture. Pulmonary function tests.	
Liver	Female adult (150-200 g) Lewis rats	Histology + immunofluorescence of ECM-collagen I + IV, laminin, fibronectin. DNA/ collagen/ GAG quantitative assays. SEM of ECM architecture. Vascular corrosion resin casting.	Uygun et al., 2010
Liver	Adult Fischer 344 rats	Histology + immunofluorescence of ECM-collagen IV, laminin, DAPI.	Shupe et al., 2010
Liver	Male adult (250-300 g) Sprague-Dawley rats Systemic heparinization	Histology + IHC of ECM-collagen IV, laminin, fibronectin, DAPI. Gel electrophoresis of DNA content. SEM/ TEM of ECM architecture. Vascular corrosion resin casting.	Soto-Gutierrez et al., 2011
Liver	Ferret (age/ strain/ gender not specified)	IHC + Western blotting-collagen I/III/IV, laminin, fibronectin. DNA/ collagen/ GAG quantitative assays. SEM of ECM architecture.	Baptista et al., 2011

		Fluoroscopy + confocal microscopy of vasculature.	
Liver	Male adult (250-300 g) Sprague-Dawley rats Systemic heparinization	Histology + IHC of ECM-collagen I + IV, laminin, fibronectin, VEGF. SEM of ECM architecture. Vascular corrosion resin casting.	De Kock et al., 2011
Liver	Yorkshire swine (25-35 kg)	Histology + IHC of ECM-collagen I + IV, laminin, fibronectin. Vascular corrosion resin casting + fluoroscopy.	Barakat et al., 2012
Kidney	Male adult (250-300 g) Sprague-Dawley rats Systemic heparinization	Histology + IHC of ECM-collagen IV, laminin. SEM of ECM architecture.	Ross et al., 2009
Kidney	12-week (180-220 g) Wistar rats	Histology + immunofluorescence of ECM-DAPI. SEM of ECM architecture.	Liu et al., 2009
Liver, Kidney, Pancreas, Small bowel	Ferret liver Pig kidney/ pancreas/ small bowel	Histology. Fluoroscopy of vasculature.	Baptista et al., 2009
Small bowel	Adult (320-350 g) Sprague-	Histology + IHC of ECM-MHC-II, smooth muscle actin (SMA),	Totonelli et al.,

	Dawley rats	vimentin, mouse monoclonal anti-cytokeratin 1 antibody (MNF116). DNA/ collagen/ GAG quantitative assays. SEM/ TEM of ECM architecture, Mechanical testing-stress/strain.	2012
Skeletal muscle	Adult BALB/C mice	Histology + immunofluorescence of ECM-actin, laminin, fibronectin.	Perniconi et al., 2011

Table 1.2: Summary of the decellularisation protocols employed in the literature. Adapted from (He & Callanan, 2013).

1.7 Methodologies in decellularisation approaches

A review of tissue decellularisation approaches and also their effects related to ECM characteristics was published in 2006 (Gilbert et al., 2006). Decellularisation approaches are classified by three main treatments into chemical, enzymatic, and physical methods (Kheir et al., 2011; Fu et al., 2014; Funamoto et al., 2010; Patnaik et al., 2013; Gilbert et al., 2006; Wang et al., 2013). When considering the use of animal-derived tissues as substitute materials, there are many significant issues that require caution. A lot of protocols have been established for removing the antigenicity of the grafts, and determining the biocompatibility *in vitro* and *in vivo* for decellularisation of tissues or organs in the recent two decades. More importantly the graft morphology and structure are conserved, and suitable for many applications such as orthopaedic grafting (Quan et al., 2014). Conventionally, the selected tissue is treated with a chemical or detergent solution, and then followed by mechanical shaking or manually scraping to ease elimination of the cellular components. These treatments are only suitable for the tissues with a few millimetres of thickness (Patnaik et al., 2013). Each chosen approach should consider both elimination of cellular elements, and protection of mechanical integrity, structural, and biochemical behaviour for the tissue functionalities.

1.7.1 Chemicals agents

In general, chemical methods can be used to remove the cellular constituents in biologic tissues or organs and they consist of detergents (ionic, non-ionic, and

zwitterionic), hypotonic and hypertonic solutions, acid and base solutions, alcohols or other solvents (Crapo et al., 2011; Patnaik et al., 2013).

1.7.1.1 Detergents

Among all the treatments, detergents are the most extensively used (Ning et al., 2012; Funamoto et al., 2010; Sasaki et al., 2009). But, these agents appear to damage and detach proteins, lipids, lipoproteins in the ECM, and the elimination of ECM proteins and DNA increases with exposure time, type of tissue, donor age, and differs with organs (Fu et al., 2014; Crapo et al., 2011). As a result, the ECM ultrastructure may be destroyed, affecting collagens, GAG, and growth factors (Fu et al., 2014). Detergents should be washed out because they are usually toxic and sometimes, the subsequent wash-out process will contribute to the denaturation and structural damage of the tissue (Sasaki et al., 2009).

The most widely used ionic detergents are sodium dodecyl sulfate (SDS) (Fu et al., 2014; Sandmann & Tischer, 2010; Patnaik et al., 2013; Gilbert et al., 2006), sodium deoxycholate (SDC) and Triton X-200 (Patnaik et al., 2013; Gilbert et al., 2006). SDS has an anionic hydrophobic ligand that works by concentrating charges on the scaffolds (Patnaik et al., 2013). It is well known that SDS is very efficient at eliminating the cellular constituents from tissue compared with other detergents; indeed it removes cytoplasmic proteins (such as vimentin) entirely. However, SDS has a tendency to break up the native tissue structure as well as the cell membrane, and leads to a reduction in the GAG concentration and damages the collagen integrity (Booth et al., 2012; Kheir et al., 2011; Fu et al., 2014; Gundula et al., 2012; Flynn et

al., 2006; Frohlich et al., 2010; Crapo et al., 2011; Gilbert et al., 2006). Despite this, SDS does not readily eliminate collagen from the tissue (Gilbert et al., 2006). The scaffold seems to remain durable in terms of collagen content after treatment with SDS during the decellularisation process (Booth et al., 2012). At high concentration, it has been revealed to produce significant adverse effects on collagen due to the destructive nature (Kheir et al., 2011; Patnaik et al., 2013). The SDS detergent is suitable for eliminating cells when used at 0.1% concentration, it will completely preserve tissue dimensions, and it does not cause swelling or contraction. In terms of cell proliferation, this can be affected by the use of chemical protocols. When SDS is used for decellularisation, cell proliferation is slightly decreased compared to Tri(n-butyl)phosphate (TnBP) or Triton X-100 (Sandmann & Tischer, 2010). SDS has been used to decellularise several cardiovascular tissues like myocardium, heart valves, and blood vessels (Sasaki et al., 2009; Patnaik et al.,
2013), for dermis or ligament (Sasaki et al., 2009), and tendons or meniscus samples (Sandmann & Tischer, 2010). Additionally, SDS has been reported to be inefficient to decellularise the placenta because of the damage to tissues as well as to the blood vessel network (Flynn et al., 2006).

While ionic detergents seem to be useful in solubilizing both cytoplasmic and nuclear cellular membranes, there were some studies reporting the limitations of SDS treatment as it may denature proteins due to disruption of non-covalent bonds (Elder et al., 2009; Gilbert et al., 2006). On the other hand, SDS treatment will remove ECM growth factors, and calcification entraps the excessive SDS in ECM, and produces imperfect elimination of cellular material and antigens (such as porcine and bovine). As a solution, washing or detoxification with chemicals (Triton X-100 and peracetic

acid) has to be followed after the SDS treatment (Crapo et al., 2011; Patnaik et al., 2013). In some decellularisation studies, SDS treatment is followed by Triton X-100 and this method is well established for acellular matrix (Wang et al., 2013). The most effective method to eliminate intracellular protein (vimentin) and cell nuclei from the anterior cruciate ligament (ACL) is by a combination of the Triton X-100 with SDS. However, this has influenced the GAG and collagen constituents of the extracellular matrix, and as a result the tensile stiffness of ligament is enhanced (Sandmann & Tischer, 2010). Vavken et al. (2009) have stated that the best subsequent cell proliferation with unaffected extracellular matrix could be achieved when treating decellularised tendons with Triton X-100. On the other hand, SDS treated tissue performs the best decellularisation properties (excellent in terms of removing cells) but is less compatible in terms of encouraging proliferation of regenerating reseeded cells (Komlev et al., 2010).

Cellular remnants also can be dissociated efficiently by sodium deoxycholate, however, more disruption to the original tissue architecture may result as compared to SDS. Using sodium deoxycholate alone has not been reported in tissue decellularisation, this causes difficulty to characterise its effect on the ECM (Gilbert et al., 2006).

Meanwhile, the choice of non-ionic detergents in decellularisation processes is based on their minor affects upon tissue geometry. The interactions that occur with non-ionic detergents disrupt lipid-lipid and lipid-protein bonds. However, they leave protein-protein interactions intact, therefore the conformation of proteins in a tissue or organ after non-ionic detergent treatment may be retained. The most extensively studied for decellularisation procedures is Triton X-100 (Fu et al., 2014; Gundula et

al., 2012; Sandmann & Tischer, 2010; Gilbert et al., 2006). Triton X-100 has been used widely for tissue decellularisation including heart valve, liver, blood vessels, pericardium, lungs, ligament, and dermis (Sasaki et al., 2009; Patnaik et al., 2013). The properties of Triton X-100 are solubility in water, very good in cell elimination and helping cellular re-growth, and it is biodegradable. Mostly, Triton X-100 detaches cellular elements from intact ECM and vascular structure (Patnaik et al., 2013). It leaves a superior substrate architecture for re-seeding cells because the decellularised scaffolds are well maintained (Wen et al., 2012). Moreover, Triton X100 is very effective at removing residues from thicker tissues such as valve ducts (Crapo et al., 2011). Nevertheless, some studies have reported ECM disruption such as GAG loss (Fu et al., 2014; Gundula et al., 2012; Patnaik et al., 2013), scaffold contraction (Patnaik et al., 2013), and extraction of laminin and fibronectin components (Fu et al., 2014). In general, non-ionic detergents (like Triton X-100) have a better capability compared to ionic detergents (deoxycholate) for the removal of lipids/ lipid groups from a protein (Crapo et al., 2011). While Triton X-100 treatment can be a potent decellularisation procedure, its ability is related to the type of tissue being decellularised and the other treatments with which it is combined in a specific decellularisation procedure (Gilbert et al., 2006).

The combination of ionic and non-ionic detergent properties is called zwitterionic-based detergents because it has both anionic and cationic properties (Patnaik et al., 2013; Gilbert et al., 2006). Zwitterionic detergents have been used widely for thinner tissues such as lung, and nerve that need gentle treatment (Crapo et al., 2011; Patnaik et al., 2013). As compared to non-ionic detergents, a zwitterionic detergent is more effective to denature proteins (Gilbert at al., 2006). Examples of

zwitterionic detergents are 3-[(3-cholamidopropyl) dimethylammonio]-1propanesulfonate (CHAPS), and sulfobetaine-10 and 16 (SB-10 and SB-16) (Patnaik et al., 2013). CHAPS has been utilised for decellularisation of nerves by combining the treatments. Sodium deoxycholate was added with some zwitterionic detergents, but, an entirely decellularised nerve ECM can be only produced in combination of Triton X-200 and the zwitterionic detergents. The produced results were much better on the architecture of the nerve ECM than the combination of Triton X-100 and sodium deoxycholate treatments (Gilbert et al., 2006).

1.7.1.2 Acid and base solutions

The use of acid and base treatments in decellularisation approaches solubilizes the cytoplasmic constituent of the cells and nuclear material, including removal of nucleic acids such as ribonucleic acid (RNA) and DNA. Cell membranes and intracellular organelles can be disrupted successfully by using acid (acetic acid, hydrochloric acid, sulphuric acid, and peracetic acid (PAA)), and base (sodium hydroxide, calcium hydroxide, and ammonium hydroxide (NH_4OH)). Unfortunately, these chemical reagents will also detach significant molecules like GAGs (from collagenous tissues) and growth factors, denature proteins, and disrupt ECM structure (Fu et al., 2014; Patnaik et al., 2013; Gilbert et al., 2006). Besides, acid and base treatments catalyse hydrolytic degradation of biomolecules. Based on Crapo et al. (2011), acetic acid disrupts and eliminates collagens that could reduce the ECM integrity, but sulfated glycosaminoglycans (sGAG) are not affected. Peracetic acid is

a commonly used sterilisation agent, and also eliminates residual nucleic acids. It causes a minimal effect on the ECM architecture and conformation (Kheir et al., 2011; Crapo et al., 2011).

1.7.1.3 Hypotonic and hypertonic solutions

Generally, hypertonic saline detaches DNA from proteins while hypotonic solutions damage cells via osmotic shock with minimal alteration of matrix molecules and structure. The disruption of the cell membrane via osmotic shock will efficiently lyse the cells within tissues and organs. This technique has been broadly applied together with chemicals to eliminate cellular residues as well as to efficiently lyse the cells (Elder et al., 2009; Kheir et al., 2011; Fu et al., 2014; Crapo et al., 2011; Patnaik et al., 2013; Gilbert et al., 2006). To have an optimal osmotic shock, the tissues are repeatedly immersed in hypertonic and hypotonic solutions for several cycles, but when this method was used for cartilage scaffolds it had disruptive effects on scaffold functional properties (Elder et al., 2009). These protocols are thus unlikely to provide effective scaffolds for tissue engineering of replacement functional organs.

1.7.1.4 Alcohols and acetone

The most effective treatment to decellularise dense tissues is using solvents such as alcohols and acetone. In fact, alcohol (glycerol) and acetone lyse cells by dehydration and eliminate lipids from the tissues during decellularisation (Fu et al.,

2014; Crapo et al., 2011; Patnaik et al., 2013). Acetone and alcohol are tissue preservatives (Fu et al., 2014). In addition, alcohols (isopropanol, ethanol, and methanol) and acetone are more commonly used than lipase to eliminate lipids from tissue and are be able to produce adipose tissue lipid-free (Crapo et al., 2011). Alcohol and acetone have a tendency to disrupt the mechanical properties of architectural proteins and make crosslinks (Fu et al., 2014; Crapo et al., 2011; Patnaik et al., 2013). The formation of acetone crosslinks with ECM creates stiffer scaffolds with altered-mechanical behaviour in comparison to detergent approaches to decellularisation. Other limitations when using alcohol (ethanol and methanol) and acetone for tissue treatment is the destruction they cause to ECM ultrastructure (Crapo et al., 2011). They are therefore not to be recommended for preparation of tissue engineering scaffolds.

1.7.1.5 Tri (n-butyl)phosphate (TnBP)

TnBP is an organic solvent. It is used to inactivate viruses in blood without effecting coagulation activity. Nowadays, TnBP has also been recognised as an encouraging chaotropic agent for decellularisation of dense tissues such as ligament and tendon with only a small effect on the mechanical behaviour of the ECM (Fu et al., 2014; Crapo et al., 2011; Gilbert et al., 2006).

As reported by Fu et al. (2014), TnBP did not produce any adverse effect on the tensile strength of collagen fibers detached from tendon (rat tail) compared with the control group. However, after TnBP treatment on the anterior cruciate ligament, collagen contents were reduced (Fu et al., 2014). The use of Graft jacket ® in irreparable rotator cuff defects for tendon augmentation has been tested in orthopaedic

surgery. Graft jacket ® is an immunologically inert acellular scaffold containing collagen and extracellular proteins, including collagen, elastin, and proteoglycans, and vascular networks. It was successfully used to give supplemental support, protection, and reinforcement of tendon and ligamentous tissue by providing a scaffold for host cell repopulation, revascularization and eventually, transformation to host tissue. Moreover, this approach has triggered further attention in decellularisation of meniscal and tendon samples (Sandmann & Tischer, 2010).

1.7.2 Biological agents

Biological agents are divided into enzymatic and non-enzymatic (chelating agents) treatments (Crapo et al., 2011).

1.7.2.1 Enzymatic treatments

Examples of enzymatic treatments in decellularisation protocols are the application of nucleases, collagenases, trypsin, dispase, lipase, thermolysin, and αgalactosidase. To remove the residues of nucleic acids after cell disruption and the peptide bonds that attach to the ECM, enzymes are used (Fu et al., 2014; Sandmann & Tischer, 2010; Crapo et al., 2011). Enzymes are prone to stay in the tissue and this can produce greater levels of immune response. However, the use of enzymes for a long duration may also eliminate the collagens, fibronectin, GAG, laminin, and elastin, and also disrupt the ECM ultrastructure (Fu et al., 2014). In fact, enzymatic treatments are not effective enough to completely eliminate cells unaided, and also any enzyme

remaining may damage recellularisation and produce an adverse immune response (Crapo et al., 2011).

Nuclease enzymes consist of endonucleases, exonucleases, deoxyribonuclease (DNase), and ribonuclease (RNase). They have been widely used for removing nuclear or genetic material (Patnaik et al., 2013). Endonucleases activate the hydrolysis of the interior bonds of the ribonucleotide or deoxyribonucleotide chains while exonucleases activate the hydrolysis of the terminal bonds of deoxyribonucleotide or ribonucleotide eventually contributing to the degradation of RNA or DNA (Gilbert at al., 2006).

Trypsin has become one of most commonly used proteolytic enzymes for passaging cells in subculture (Fu et al., 2014; Gilbert et al., 2006). It is a serine protease that is frequently used as an enzymatic agent to decellularise tissue (Crapo et al., 2011; Patnaik et al., 2013). Trypsin tends to effectively disrupt collagen and elastin, and to eliminate cells gently, while preserving the GAG constituent. Disruption of the ECM by trypsin may lead to variation in mechanical integrity. The effectiveness of trypsin to eliminate cells and ECM components is time-dependent. A complete decellularisation process with trypsin alone requires several incubations even for thinner tissues (such as valve ducts). Additionally, trypsin can be applied successfully to break tissue ultrastructure and increase penetration of any following decellularisation agents. Thus, the initial stage to decellularise tissue is by exposing to trypsin, mainly to completely eliminate cell nuclei from dense tissues (Crapo et al., 2011). Destruction will occur to ECM when using trypsin at high concentration. At 0.5% w/v, trypsin was reported to break down the elastin structure in aortic valve ducts. Interestingly, the combination of trypsin at low concentration (e.g., 0.01%) and

detergents such as SDS (e.g., 0.1%) has been greatly effective to dissociate cellular components in myocardium decellularisation (Patnaik et al., 2013). However, the combination of trypsin and collagenase causes adverse effects both on the extracellular matrix and the collagen network, so that the reseeding of the decellularised samples and/or the biomechanical effects could be affected (Sandmann & Tischer, 2010).

Another enzymatic agent is collagenase, which has been used during decellularisation for clinical application (Crapo et al., 2011), but gives minimal protection to collagen and ultrastructure of the ECM. Lipase helps in delipidation, however, it seems not effective to eliminate all lipids on its own, without any other agent. Dispase shows greater decellularisation than trypsin after delipidation of dermis, and presented superior cell infiltration in dispase-treated tissue for subcutaneous implantation. The dissociation of cells from thicker tissues such as dermis can be effectively enhanced by combining dispase and trypsin with detergents, and the repetition of protocols with dispase may produce better decellularisation effects (Crapo et al., 2011). Moreover, dispase has been widely used in decellularisation to degrade fibronectin and also collagen IV (Patnaik et al., 2013). The immunogenic cell surface antigen, galactose-α-(1,3)-galactose (Gal epitope), in decellularised xenogeneic tissues can be reduced with α-galactosidase treatment. The immunomodulatory presence of Gal epitope does not adversely influence *in vivo* remodelling of xenogeneic ECM (Crapo et al., 2011).

1.7.2.2 Non-enzymatic treatments

Non-enzymatic chemical treatments consist of chelating agents such as ethylenediaminetetraacetic acid (EDTA) and ethylene glycol tetraacetic acid (EGTA) (Fu et al., 2014; Crapo et al., 2011). EDTA and EGTA have a tendency to bind with ions and metal ions that initiate cells detachment from ECM proteins (Fu et al., 2014; Crapo et al., 2011; Gilbert et al., 2006). Likewise, chelating agents aid dissociation in protein-protein interactions (Crapo et al., 2011). EDTA is the most extensively used agent for decellularisation (Patnaik et al., 2013; Gilbert et al., 2006). It is generally used together with enzymes including trypsin (Crapo et al., 2011; Patnaik et al., 2013; Gilbert et al., 2006) or detergents (Crapo et al., 2011). In addition, the use of protease inhibitors, EDTA (as chelator) and aprotinin (as serine protease inhibitor) during the treatment may avoid digestion of the matrix by the release of endogenous protease (Kheir et al., 2011). Unfortunately, extended exposure to EDTA may decrease the mechanical integrity of scaffolds (Patnaik et al., 2013). Besides, prolonged treatment with trypsin/EDTA has been revealed to reduce the elastin constituent and GAGs over time, which reduces the tensile strength to 50%. Therefore, long term exposure to trypsin/EDTA treatment should be minimised (Fu et al., 2014; Gilbert et al., 2006).

1.7.3 Physical and miscellaneous agents

Physical and miscellaneous agents can be categorised into temperature, force and pressure, and nonthermal permanent electroporation (NTIRE) in decellularisation procedures (Fu et al., 2014; Crapo et al., 2011). Several examples of physical methods are scraping, snap freezing, sonication

(such as ultrasound treatment), direct pressure, pressure gradient, supercritical fluid, and solution agitation (such as rocking, stirring, etc.) which can be carried out to ease decellularisation of tissues (Patnaik et al., 2013; Gilbert et al., 2006).

1.7.3.1 Temperature

The process of freeze-thaw is very effective to lyse cells in tissues and organs. However, subsequent processing is needed to eliminate all of the cell nuclei because membranous and intracellular constituents endure (Fu et al., 2014; Crapo et al., 2011). The treatment of tissue by repetitive freezing and thawing process is called lyophilization. Many studies have been accomplished on tendon allografts applying cryopreservation protocols; however, exposure to ice crystal formation affects the mechanical properties and histological properties (Sandmann & Tischer, 2010).

Multiple freeze-thaw treatments have been practised as part of many decellularisation processes for biologic scaffolds (Fu et al., 2014; Ning et al., 2012; Crapo et al., 2011) including dermis, nerve, tendon, and embryoid bodies (Ning et al., 2012). Multiple freeze-thaw treatments are able to preserve the ECM proteins from tissue (Fu et al., 2014; Crapo et al., 2011), make minimal disruptions of the ECM ultrastructure (Sandmann & Tischer, 2010; Ning et al., 2012; Crapo et al., 2011), and maintain the mechanical integrity (Crapo et al., 2011) for successful tissue replacement. It has been reported that freeze-thaw treatments need to be combined with other treatments to produce more effective results for decellularisation (Fu et al., 2014; Crapo et al., 2011). According to several studies, detergent and nuclease are combined during freeze-thaw treatment to achieve ideal

decellularisation of menisci. While ammonium hydroxide is used as well during freeze-thaw treatment to detach cellular constituents and as the result, the two dimensional culture of this ECM is well retained (Fu et al., 2014).

Another approach that applies temperature is snap freezing, whereby biological tissues are frozen rapidly at a very low temperature such as -80°C. The principle of this treatment is that the fast freezing dissociates the cell membranes because of unavoidable ice crystal creation and increased volume, therefore encouraging cell lysis (Patnaik et al., 2013). Snap freezing has been applied very often in decellularisation of nerve tissue, tendinous and ligamentous tissue. In theory, intracellular ice crystal formation fragments cellular membranes, and induces cell lysis. Destruction of the ECM by ice creation can be avoided by monitoring the amount of temperature change. Freezing is a useful procedure for lysing cells; however it must be continued by the elimination of cellular material from the tissue. These methods are effective, and cause minimal disruption to the three dimensional architecture of the ECM (Gilbert et al., 2006). But, the problem with snap freezing is that the creation of ice crystal will also damage ECM microstructures (Patnaik et al.,
2013).

1.7.3.2 Force and pressure

Cells can be effectively lysed with the use of direct pressure to tissue. Nevertheless, this protocol is only suitable for tissues or organs. The use of mechanical

force is actually to pull off layers of tissue from organ such as urinary bladder and small intestine. All these treatments are effective, producing only minor dissociation to the three-dimensional structure of the ECM in the tissues (Fu et al., 2014; Gilbert et al., 2006).

The combination of mechanical agitation with enzymes, chelating agents, or hypertonic saline can be effectively used to remove cells on the surface of a tissue and organ like small intestine, urinary bladder, skin, and amnion. But, any direct treatment by mechanical agitation tends to give side-effects due to disruption of the fundamental ultrastructure and basement membrane strength (Fu et al., 2014; Crapo et al., 2011). Mechanical agitation and sonication have been carried out simultaneously with chemical treatment to assist in cell lysis and removal of cellular debris, with the use of a magnetic stir plate, a low profile roller, or an orbital shaker. There are no studies which define an ideal magnitude or frequency of sonication for breakup of cells. All in all, the composition, density, and volume of the tissue affect the ideal speed, volume of reagent, and duration of mechanical agitation (Gilbert et al., 2006).

In the treatments of blood vessels and corneal tissues, it is more effective to use hydrostatic pressure instead of detergents or enzymes for detaching cells. However, there is a problem due to the baric creation of ice crystals which may damage ECM ultrastructure. Ice crystal creation can be reduced by raising the temperature during pressure decellularisation (Crapo et al., 2011). This pressure gradient approach was applied to successfully decellularise whole heart (Patnaik et al., 2013).

A novel approach of tissue decellularisation has been introduced over the last few years by applying high-hydrostatic pressure (HHP) technology. Actually, this non-cytotoxic approach has two independent processes. Cells, bacteria, and viruses are

destroyed and inactivated at the first stage by high hydrostatic pressurization. At the second stage, the cellular constituents such as proteins, lipids, and nucleic acids are then dissociated by a washing methodology utilising a culture medium. The effectiveness of this approach has been demonstrated in porcine heart valve, trachea, and corneal tissue (Ning et al., 2012; Funamoto et al., 2010). The HHP treatment is also efficient for xenogenic tissue transplantation because it could eliminate all the cells that lead to xenogenic inflammation. HHP treatment has a sterilizing effect that could damage the lipid membranes of animal cells, and the lipid bilayer membranes of fungi, bacteria, and viruses. The application of pressure above 600 MPa has been established to inactivate viruses and destroy the bacilli, while a pressure of 980 MPa is used to confirm the effect of high sterilisation. The HHP approach has special characteristics including ability to disrupt the cell membranes, short handling time, and consistent processing. A decellularised tissue can then be produced from the washing processing of the treated tissue. More importantly, the decellularised tissue is well preserved in terms of the structural and mechanical integrity by regulating the temperature during pressurization (Sandmann & Tischer, 2010; Funamoto et al., 2010). In a study of cornea decellularised by HHP, biomechanical integrity of decellularised cornea was demonstrated, and the collagen architecture in the corneal stroma was not significantly changed by the HHP handling (Ning et al., 2012).

HHP treatment has also been applied to the bone or bone marrow by Hashimoto et al. (2011). In this study, porcine cortical bone and bone marrow were used. The pressurization rate, temperature, and washing time were optimized. All the components of ECMs in the bone remained after the treatment, and this study confirmed the

proliferation and adhesion of rat mesenchymal stem cells (rMSCs) onto the scaffolds and their osteogenic differentiation (Hashimoto et al., 2011).

In the bone, HHP treatment may produce its effect not only to kill tumor cells but also the normal cells, and destroy the ECM proteins, such as fibronectin, vitronectin, and type-I collagen. The impact of HHP on tissue function and structure are dependent on the temperature, pressure and duration of treatment, conditions of the buffer, and also the characteristics of a protein. For instance, some enzymes are deactivated by HHP, although, the rest may not be influenced by HHP treatment and may not increase biological activity. The biological functions of the ECM proteins, fibronectin, vitronectin, and type-I collagen are not damaged after subjecting to HHP ≤600 MPa for 10 minutes (in room temperature) as reported by Diehl and co-workers (2005).

1.7.3.3 Non-thermal irreversible electroporation (NTIRE)

NTIRE has been recognised as one of the approaches in tissue decellularisation (Fu et al., 2014; Crapo et al., 2011). NTIRE requires the application of microsecond electrical pulses through a tissue and the surrounding cells of that tissue to induce the development of damaging micropores in the cell membrane. This is achieved by the destabilization of the electrical potential through the membrane. Like other approaches, NTIRE also has drawbacks. The major limiting one is that the probe size is too small, thus minimising the area of tissue that can be decellularised (Crapo et al., 2011).

1.7.4 Combinations of various decellularisation methods

Generally, the source of the tissue and the combination of particular physical, chemical, and enzymatic techniques will affect the effectiveness of cell elimination from a tissue. Each method will influence the tissue ultrastructure, biochemical composition, and mechanical properties of the remaining ECM scaffold, which then, influence the host response to the material (Fu et al., 2014; Benders et al., 2012; Fini et al., 2012; Patnaik et al., 2013; Gilbert et al., 2006). To have an ideal decellularisation process, the use of slightest treatment possible is required to produce an acellular material with no disruption upon the functional and structural content of the ECM (Gilbert et al., 2006). Basically, the working principle of the combination of various decellularisation methods comprises of two main steps. The first step is to break all the cells. Then, the second step is to dissociate all the cellular elements from the tissue by chemical treatment (Sandmann & Tischer, 2010).

The decellularisation procedure starts with lysis of the cell membrane (applying physical treatments or ionic solutions), continued by disintegration of cellular constituents from the ECM (applying enzymatic treatments), solubilisation of cytoplasmic and nuclear constituents (applying detergents), and lastly elimination of cellular debris from the tissue. Further, an endonuclease agent can be used to remove pathogenic viruses that place the recipient at major risk. To enhance their efficiency, all those protocols can be brought together with mechanical agitation. After decellularisation, all remaining chemicals must be flushed away to prevent an adverse host tissue response to the chemicals (Fu et al., 2014; Crapo et al., 2011; Gilbert et al., 2006).

The choice of the decellularisation agents is totally dependent upon tissue characteristics including density and thickness, and the expectable clinical use of the decellularised tissue. The optimal approaches for thin tissue like urinary bladder, pericardium, intestine, and amnion are by freezing and thawing, mechanical elimination of unwanted submucosa and muscle, and reasonably short-term exposure to detergents or acids continued by a washing process. Meanwhile thicker tissue layers including dermis must involve more extensive biochemical exposure and prolonged wash cycles. Usually, the addition of lipid solvents such as alcohols is proposed in fatty, amorphous organs and tissues including brain, adipose tissue, and pancreas. The grade of structural and biological preservation of the decellularised tissue (for example ultrastructure, macrostructure, growth factors, matrix and basement membrane proteins) is dependent on the duration of the decellularisation process, particularly for complex tissues and whole organ applications (Fu et al., 2014; Crapo et al., 2011).

All treatments including physical, enzymatic, and chemical can have considerable effects on the mechanical performance, the composition, and host response to biologic scaffolds resultant from the decellularisation of internal tissue and organs. The elimination of GAGs and adhesive proteins from the scaffold has caused slow cell movement during recellularisation of the scaffold and delay in the bioactivity of the scaffold itself. If collagen linkage is disrupted, the mechanical performance and collagen fibre kinematics of the scaffold can be altered, so that the load bearing capability of the scaffold will be affected and the mechanical conditions surrounding the cells will be changed (Gilbert et al., 2006). Chemical and enzymatic agents are excellent at removing cellular residues and xenogeneic epitopes but they are prone to leave cytotoxic agents in the decellularised ECM. In fact in clinical use, biological

scaffold materials comprise a small quantity of fragmented DNA because any combinations of enzymatic and chemical agents are unable to entirely detach cell constituents from a tissue or organ (Choi et al., 2012).

Patnaik et al. (2013) has reported the success of various studies applying the combinations of different decellularisation agents in whole rat heart (utilising fluid perfusion, a combined SDS and Triton-X treatment, and a pressure gradient), intact whole porcine heart (utilising perfusion and pressure gradient protocol), and whole organ liver, intestines, pancreas and kidneys (perfusion of 1% Triton X-100 and 0.1% ammonium hydroxide). In another example, a combination of cryopreservation with a detergent (N-lauroyl sarcosinate)-enzyme (benzoase) approach was carried out in acellular arterial scaffolds which were then suitable for proliferation and cellular growth, and allowed for calcification These achievements have demonstrated great upcoming innovative strategies in decellularisation approaches (Patnaik et al., 2013). While Ning et al. (2012) has found that the success of decellularisation in tendon/ligament tissues has been accomplished by treating with detergent (such as SDS) and/or enzymes. The decellularised tendon was well retained in terms of the mechanical integrity and matrix structure in comparison to the natural tendon (Ning et al., 2012). It has been confirmed by Sandmann and Tischer (2010) regarding the use of SDS in tendon and meniscus tissue. By means of *in vitro* tests it has been determined, that tissue treatment with SDS did not affect the biomechanical behaviour, being the strongest cell elimination agent among Triton-X and TnBP, and it removed all cells that could lead to immunological effects (Sandmann & Tischer, 2010). Moreover, a decellularised rat Aortic Valve Allograft (AVA) with less antigenicity and preserved ECM has been established by Meyer et al. (2006) with a combination of

hypotonic and hypertonic buffers, endonucleases, Triton X-100, and washout in Phosphate-buffered saline (PBS) (Meyer et al., 2006).

In conclusion, there is no gold standard protocol yet for decellularisation in a specific tissue and organ. Each of these protocols has advantages and disadvantages that have important implications for the experimental and clinical use of ECM membranes (Fini et al., 2012; Patnaik et al., 2013). Different combinations of methods need to be investigated by the researchers depending on the tissue and organ of interest. The current approaches must be continually improved, and optimized, as well as new protocols constantly explored and further studied using ECM scaffolds for tissue regeneration (Fu et al., 2014; Patnaik et al., 2013).

1.8 Bone micro-anatomy

Bone is a natural compound material and has a 3D structure (Alvarez & Nakajima, 2009). It is one of the toughest tissues in the body and it is the core component of the skeleton (Arvidson et al., 2011). Bone has ability in healing and remodelling processes due to its capacity to self-regenerate (Martins et al., 2010). The functions of bone are to support fleshy structures, house bone marrow in which the blood cells are produced, shield important organs especially those located in the cranial

and thoracic cavities, form a system of levers that is useful in the movement of body (e.g. walking and chewing), and provide a mineral source for homeostasis (Arvidson et al., 2011).

Generally, bone consists of 45-60% minerals, 20-30% matrix, and also 1020% water. The composition of bone is described in **Figure 1.3** below. There are two major parts namely the mineral phase and organic phase. The organic phase is composed of collagen (Type I) and non-collagenous proteins (NCPs), bone cells which consist of osteoblasts (bone forming cells), osteocytes (bone maintaining cells) and osteoclasts (bone destroying cells) (Alvarez & Nakajima, 2009). HA or Hap is the major component of vertebrate bone in the mineral phase. The chemical structure of hydroxyapatite is denoted by the formulae $Ca_{10}[PO_4]_6[OH]_2$, and it appears in small crystallite form (Shuai et al., 2012; Cruz, 2010; Ramay & Zhang, 2003;
Alvarez & Nakajima, 2009; Narbat et al., 2006). HA has good biocompatibility (Shuai et al., 2012; Ramay & Zhang, 2003; Narbat et al., 2006), high osteoconductivity (Ramay & Zhang, 2003; Narbat et al., 2006), high bioactivity
(Narbat et al., 2006) and has good biological and chemical closeness to bony tissues (Ramay & Zhang, 2003). HA is able to produce a direct chemical bond with hard tissue. Porous HA has been used widely in restoring huge defects in bone (Cruz, 2010). However, HA is brittle and has poorer mechanical properties than bone due to its lack of collagen (Cruz, 2010; Narbat et al., 2006).

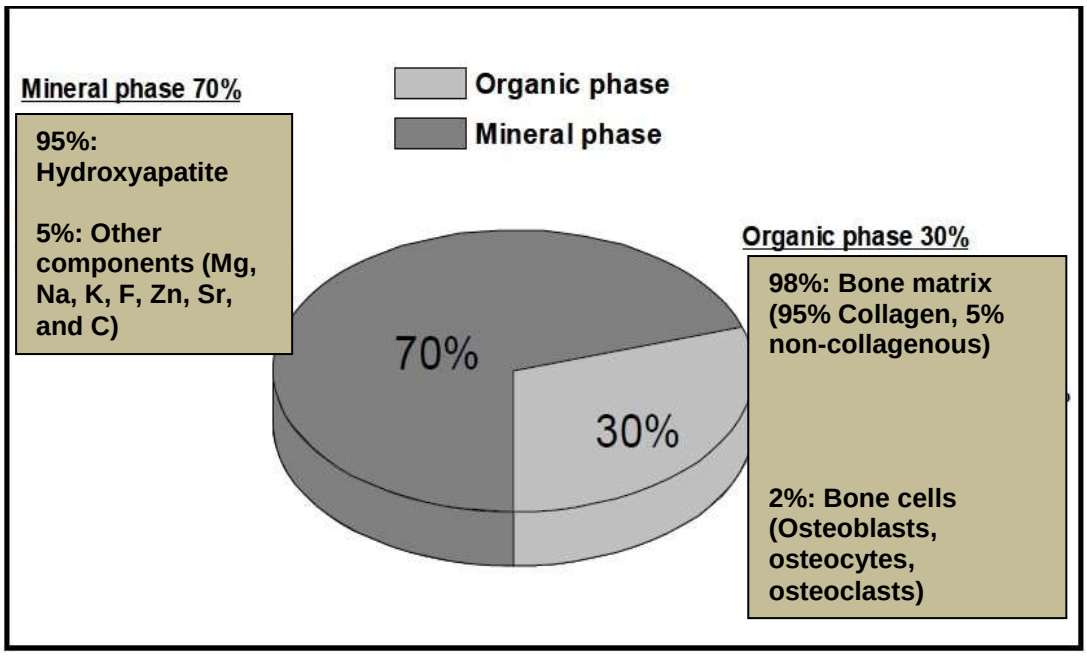

Figure 1.3: Chemical composition of bone tissue. Adapted from (Alvarez & Nakajima, 2009).

The growth of bone is altered in consequence of mechanical stress. In the early phase, the growth process of bones is caused by a level of mechanical stability (Cruz, 2010). Besides, it has low degradation rates and osteoinductive potential (Kim et al., 2003; Narbat et al., 2006). Thus, HA is commonly used as an implantation material in BTE (Shuai et al., 2012), as a bioactive material for conducting the bone to regenerate (Ramay & Zhang, 2003). But, the mechanical performance restriction of HA has been noticed during research. HA is prohibited from being applied in load bearing circumstances because of poor fatigue resistance, low fracture toughness, brittleness, and low tensile strength value (Cruz, 2010).

In the human skeleton, bone tissue is categorized into two major architectural parts such as trabecular (also named cancellous or spongy bone), and also cortical (also so-called compact bone) as shown in **Figure 1.4** (Salgado et al., 2004; Syahrom et al., 2010). The percentages of cortical and trabecular bone of the total skeleton are 80% and 20% respectively. However, these two architectural parts have dissimilar

proportions at several locations in the skeleton (Salgado et al., 2004). Cortical bone can be considered as homogenous and isotropic, whilst trabecular bone (with interconnecting plates and struts) has structural difference rely upon the anatomical site (Syahrom et al., 2010).

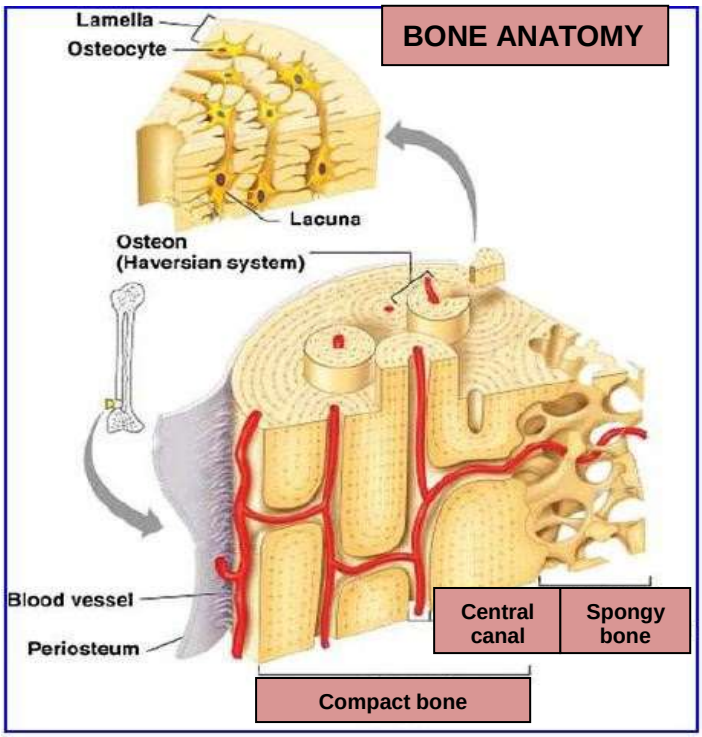

Figure 1.4: The anatomy of bone (Copyright © 2004 Pearson Education, Inc., publishing as Benjamin Cummings). Adapted from Colour images available online at http://www.liebertpub.com/teb.

Cortical bone is nearly solid and is only 10% porous. It is separated according to different subsections such as long bones that consist of femur and tibia, flat bones in the skull, and short bones that are found for example at the wrist and ankle (Salgado et al., 2004). There are functional units in the cortical bone structure, called osteons that contain central haversian canals. On the other hand, there are no osteon units in the trabecular bone due to its extreme porosity (open-spaced structure). This will allow penetration of vasculature at the surface area (Nguyen et al., 2012).

Trabecular bone has a sponge-like form that has numerous sizes of trabeculae of branching bars, rods and plates. Trabecular bone has a greater porosity (50-90%).

This behaviour makes the modulus and ultimate compressive strength of trabecular bone much less compared to the cortical bone. Trabecular bone is normally located in methaphysis of long bones, coated with cortical bone, and also found in the vertebral bodies (Salgado et al., 2004). In addition, it is also found in the skeleton (for example see **Figure 1.5**) (Parkinson & Fazzalari, 2013).

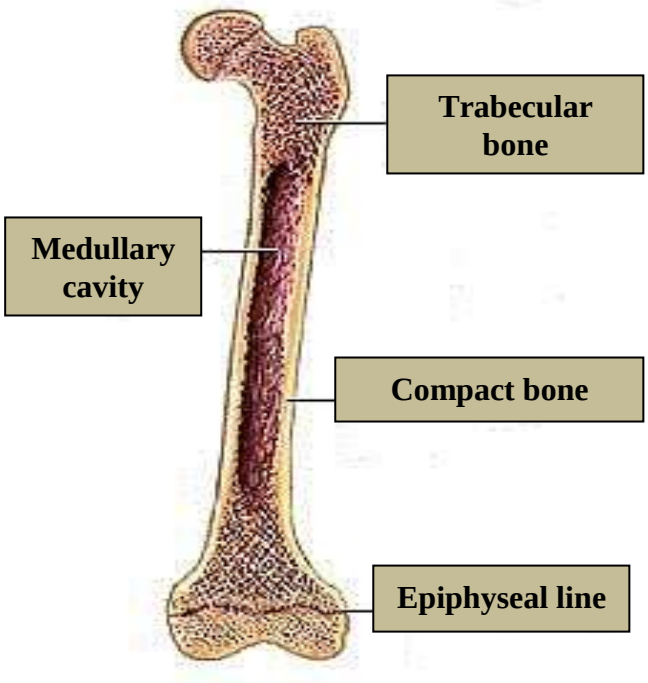

Figure 1.5: Characteristics of long bone. Adapted from http://academic.brooklyn.cuny.edu/physed/yingling/bone/Structure/Cortical/graphics/long-bones.gif.

The construction of trabecular bone is affected by the forces being applied on it and also the vast surface area that contains bone mineral found in the bone tissue marrow. It helps cellular actions in an extremely dynamic environment to eliminate and deposit bone (Parkinson & Fazzalari, 2013). Trabecular bone creates a trabecular network that consists of an intersected rod-like and plate-like structure and the amount of such bone is unequally distributed based on skeletal position. The skeletal positions which are prone to fragility or osteoporotic fractures will have more trabecular bone volume than other positions. The combination of great mineral surface area and the

organisation of the trabecular bone constituents produce a huge substrate that allows cellular interaction to take place (Parkinson & Fazzalari, 2013). Trabecular bone scaffolds also provide great versatility for *in vitro* culture systems and have enabled for example evaluation of the interactions of growth factors and mesenchymal stem cells (MSCs) (Correia et al., 2011).

1.9 Biology of bone tissue: Structure, function, and factors that influence bone cells

Bone is a mineralized connective tissue that contains four categories of cells - osteoblasts, bone lining cells, osteocytes, and osteoclasts (Florencio-Silva et al., 2015). Osteoblast-lineage cells (comprising of osteoblasts, osteocytes and bone lining cells) are involved in bone creation, while bone metabolism is facilitated by osteoclasts (Nakamura, 2007). In the bone remodelling process, mature bone is substituted by fresh bone. This highly complex cycle consists of three stages called induction of bone absorption by osteoclasts, the conversion (or reversal period) from absorption to fresh bone construction, and the bone construction by osteoblasts. Regular bone remodelling is essential for fracture healing and skeleton alteration in response to mechanical stress, and also for calcium homeostasis. However, many bone diseases involve disparity between bone absorption and construction. It has been established that bone cells react to various factors and molecules both *in vivo* and *in vitro.* Hence, the balance between bone construction and absorption is vital and relies on the responses to some local and systemic factors consisting cytokines, hormones, chemokines, and biomechanical input. Additionally, it seems that hormones, cytokines and determinants that control

bone cell activity, including oestrogen, calcitonin, parathyroid hormone, sclerostin, semaphoring, and ephrinB2 have shown an important function in the bone histophysiology, in both normal and pathological circumstances (Florencio-Silva et al., 2015).

1.9.1 Bone cells

Bone is composed of support cells called osteoblasts and osteocytes; remodelling cells called osteoclasts; and non-mineral matrix of collagen and noncollagenous proteins named osteoid, with inorganic mineral salts accumulated inside the matrix (see **Figure 1.6**). The bones go through several processes such as longitudinal and radial development, modelling and remodelling throughout life
(Fogelman et al., 2012).

1.9.1.1 Osteoblasts

Osteoblasts are derived from mesenchymal stem cells (or also known as osteoprogenitor cells) (Clarke, 2008; Fogelman et al., 2012; Nakamura, 2007; Florencio-Silva et al., 2015) of the bone marrow stroma (see **Figure 1.6**) and are liable for the production of bone matrix and following mineralization, the control of osteoclasts (Fogelman et al., 2012; Nakamura, 2007). Osteoblasts are cuboidal cells and usually round in shape. They are found along the bone surface and contribute 4 to 6% of the amount of local bone cells and they are mainly identified for their bone developing role. Osteoblasts form the ultrastructural components of protein and contain rich rough endoplasmic reticulum, Golgi apparatus, and many secretory

vesicles (Nakamura, 2007; Florencio-Silva et al., 2015). They are mononucleated, and have different forms, indicating their level of cellular activity, and align along bone-forming surfaces (Fogelman et al., 2012).

When osteoblasts differentiate, they obtain the capability to release bone matrix (Fogelman et al., 2012). Freshly created bone matrix is calcified directly. Thus, uncalcified matrix, called osteoid, is under the control of active bone creating osteoblasts. The amount of osteoid is directly related to the bone-creating activity of osteoblasts as the more osteoid, the more active bone-creating osteoblasts there are (Nakamura, 2007). Eventually, numerous osteoblasts will be entrapped in their own bone matrix, causing differentiation to osteocytes, which stop producing osteoid. The most plentiful cells in bone are osteocytes. These cells interact with each other and with the environment medium by extending their plasma membrane. Thus, osteocytes are stated to function as mechanosensors, directing osteoclasts (to absorb bone) and osteoblast (to create bone) (Fogelman et al., 2012).

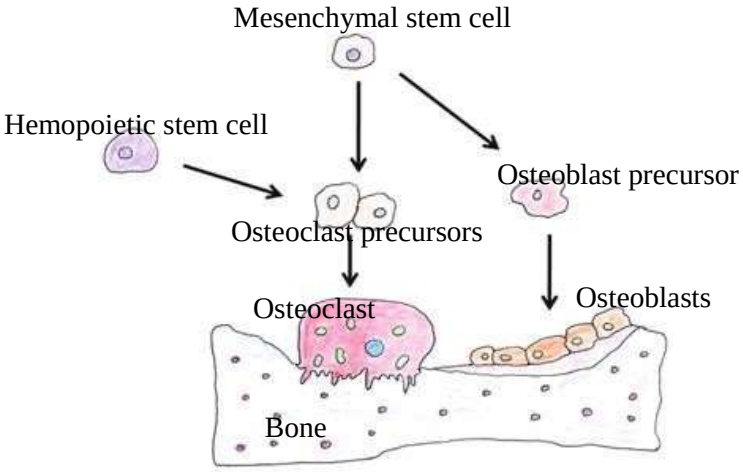

Figure 1.6: Illustration to demonstrate development of osteoblasts and osteoclasts in the creation of bone. Adapted from (Fogelman et al., 2012).

The commitment of mesenchymal stem cells to form cells of the osteoblast lineage needs activation of the Wnt/j3-catenin pathway (Clarke, 2008; Fogelman et al., 2012). Wnts are released by glycoproteins that control a number of different cellular activities including cell fate, proliferation, movement, polarity, endurance, and gene expression. This pathway is crucial in order to differentiate the mature osteoblasts (Fogelman et al., 2012). The Wnt pathway is also required in chondrogenesis and hematopoiesis and may be to provoke or hinder various phases of osteoblast differentiation. Decreased Wnt signalling has been related to osteoporosis (Clarke, 2008; Fogelman et al., 2012).

Osteoblasts act to synthesise cytokines such insulin-like growth factor I and II, TGF-β, and bone morphogenetic proteins (BMPs). These growth factors are then deposited in calcified bone matrix and perform a crucial function in the differentiation of osteoblasts. Hence, bone matrix appears to be a depository site for growth factors, as well as for calcium and phosphates (Nakamura, 2007).

Further, osteoblasts are abundant in alkaline phosphatase, an organic phosphate-splitting enzyme, which has receptors for parathyroid hormone (PTH) and estrogen. The differentiation of osteoblast-lineage cells is controlled by hormones, vitamins and cytokines including $1,25(OH)_2D_3$, oestrogen, and PTH, and cytokines including BMPs. BMPs, including BMP-2, BMP-4, and BMP-7, promote

osteogenesis *in vivo* and *in vitro* (Fogelman et al., 2012; Nakamura, 2007).

Phosphate-containing compounds are broken down by the ALP excreted by osteoblasts, allowing phosphate ions inside the matrix vesicles. Thereafter, the phosphate and calcium ions inside the vesicles nucleate, creating the hydroxyapatite crystals. Certain mature osteoblasts form cytoplasmic processes extending into the

bone matrix and attain the osteocyte processes and at this phase, the mature osteoblasts can either be subjected to apoptosis or grow into osteocytes or bone lining cells (Florencio-Silva et al., 2015).

The proliferation of osteoblasts *in vitro* (analogous to the osteoprogenitor cell *in vivo*) is influenced by the effects of glucocorticoids. Glucocorticoids encourage differentiation of progenitor cells to the osteoblast phenotype. Dexamethasone is a synthetic glucocorticoid, and it enhances the amount of mineralized bone nodules in primary foetal rat calvarial osteoblast cultures, while, TGF is a major mediator of cell growth and differentiation which controls bone matrix creation and revolution *in vivo* (Lian & Stein, 1993).

1.9.1.2 Bone lining cells

After active bone creation, osteoblasts tend to become osteocytes deposited in bone matrix. Others deposit on inactive bone surfaces and are known as bone lining cells (Nakamura, 2007). Bone lining cells are passive flat-shaped osteoblasts that coat the bone surfaces, where neither bone development nor bone metabolism happens. These cells have only a few organelles, and show a thin and flat nuclear form. The secretory activity of bone lining cells is affected by the bone physiological condition, and under certain circumstances these cells can retrieve their secretory activity, expanding their size and maintaining a cuboidal characteristic (FlorencioSilva et al., 2015). These properties indicate that bone lining cells are intimately involved in bone development (Nakamura, 2007).

The purposes of bone lining cells have not been totally discovered, however, these cells inhibit the continuous interaction between osteoclasts and bone matrix, when bone metabolism should not happen, as well as contributing to osteoclast differentiation, by creating osteoprotegerin (OPG) and the receptor activator of nuclear factor kappa-B ligand (RANKL) (Florencio-Silva et al., 2015). Osteoblastlineage cells control bone metabolism through the expression of RANKL and OPG (Nakamura, 2007). Bone remodelling is accomplished by the coordinated organization of osteoblast-lineage cells and osteoclast-lineage cells (Nakamura, 2007). Additionally, the bone lining cells and other bone cells are a vital element of the bone multicellular units (BMU), an anatomical architecture that appears throughout the bone remodelling cycle (Florencio-Silva et al., 2015).

Another important aspect in the differentiation and role of cells is the cell-cell interaction among osteoblast-lineage. Gap junctions in osteoblast-lineage cells mostly consist of connexin 43. Osteoblasts together with bone lining cells and osteocytes are attached by their cell processes via gap junctions. These junctions are required in transporting micromolecules and ions among osteoblast-lineage cells.

Gap junctions are involved in synchronized function of osteoblast-lineage cells enabling them to react to numerous physiological signals (Nakamura, 2007).

1.9.1.3 Osteocytes

In general, osteocytes contribute 90 to 95% (most abundant) of the overall bone cells (Clarke, 2008; Nulend & Burger, 2003; Florencio-Silva et al., 2015). They are plentiful and long-lasting cells, with a lifetime of up to 25 years.

Osteocytes are regarded to be the final differentiation phase of osteoblasts. They are planted in osteocytic lacunae, which are linked by canaliculi containing their cytoplasmic processes. The functions of these canaliculi are to deliver oxygen and nutrients from blood capillary to osteocytes (Clarke, 2008; Nulend & Burger, 2003). The arrangement of planted osteocytes varies depending on the bone type. For example, osteocytes from trabecular bone seem more rounded compared to osteocytes from cortical bones which have an elongated architecture. Osteocytes are determined from MSCs lineage during osteoblast differentiation. There are four identifiable phases that have been suggested in this process -: osteoid-osteocyte, preosteocyte, young osteocyte, and mature osteocyte. A subpopulation of osteoblasts is altered into osteocytes and integrated into the bone matrix at the end of the bone development cycle. The total number of organelles including Golgi apparatus and rough endoplasmic reticulum reduces, while the nucleus-to-cytoplasm ratio rises as a result of the reduction in protein synthesis and excretion (Florencio-Silva et al., 2015).

During mechanical stimulation, osteocytes generate some messengers, for example, adenosine triphosphate (ATP), Ca^{2+}, nitric oxide (NO), and prostaglandin E_2 (PG E_2) and prostaglandin I_2 (PG I_2), which affect the physiology of bone. The mechanosensitive function of osteocytes responds to the environment because of the complex canalicular system, which permits communication among bone cells (Florencio-Silva et al., 2015).

Generally, osteocytes express little ALP (Clarke, 2008; Nulend & Burger, 2003). However, they express osteocalcin, osteonectin, osteopontin, CD44 (a cell attachment receptor for hyaluronate), galectin 3, and also some other bone matrix proteins (that help intercellular attachment and control exchange of mineral in the bone

fluid inside lacunae and the canalicular linkage) (Clarke, 2008; Nulend & Burger, 2003). Moreover, osteocytes are active throughout osteolysis and may perform as phagocytic cells because they have lysosomes (Clarke, 2008). Osteocytes uphold communication with each other and the bone surface through their numerous filipodial cellular processes. They are connected electrically and metabolically via gap junctions formed mainly of connexin 43. The main role of the osteocyteosteoblast/lining cell syncytium is mechanosensation (Clarke, 2008; Fogelman et al., 2012).

The existence of hollow lacunae in elderly bone suggests that osteocytes may suffer apoptosis, possibly due to the destruction of their intercellular gap junctions or cell-matrix communications. Osteocyte apoptosis that relates to the lack of oestrogen or glucocorticoid treatment is adverse to bone structure. Thus to avoid osteoblast and osteocyte apoptosis, bone could be treated with oestrogen and bisphosphonate, or physiologic loading of bone (Clarke, 2008; Fogelman et al., 2012), this is particularly relevant in osteoporosis.

1.9.1.4 Osteoclasts

Osteoclasts are critically differentiated multinucleated massive cells responsible for bone metabolism (Clarke, 2008; Nakamura 2007; Florencio-Silva et al., 2015). The ultrastructures of osteoclasts present many mitochondria, endoplasmic reticulum and a well-established Golgi apparatus. Also they have vesicles, tubular lysosomes, lysosomes and vacuoles. All these morphologies indicate that osteoclasts are strongly implicated in energy and protein synthesis, specifically synthesis of lysosomal enzymes (Nakamura, 2007).

Osteoclasts are formed from mononuclear cells of the hematopoietic stem cell lineage due to the action of various factors such as the macrophage colonystimulating factor (M-CSF), which is excreted by osteoprogenitor mesenchymal cells and osteoblasts, and RANK ligand, which is excreted by osteoblasts, osteocytes, and stromal cells. As a group, these cytokines support the stimulation of transcription factors and also gene expression in osteoclasts. Both RANKL and M-CSF are synthesized mostly from marrow stromal cells and osteoblasts, and is an important determinant for osteoclastogenesis. It is a member of the tumour necrosis factor (TNF) family and is expressed by osteoblasts, osteocytes, and stromal cells. Osteoclast development is activated when RANKL fixes to its receptor RANK in osteoclast precursors. Meanwhile, M-CSF is needed to proliferate, maintain, and differentiate the osteoclast precursors, and osteoclast survival is essential for bone metabolism (Clarke, 2008; Nakamura 2007; Florencio-Silva et al., 2015).

Several bone disorders like osteoporosis, a disease where absorption surpasses creation resulting in deteriorated bone density and susceptibility to bone fractures, may occur due to unusual osteoclast development. Furthermore, several pathological cases such as bone metastases and inflammatory arthritis may involve unusual osteoclast stimulation (Florencio-Silva et al., 2015). **Table 1.3** summarises the characteristics of the major bone cell types.

Type of cell	Structural characteristics	Function
Osteoblasts	Cuboidal in shape, polarized and located, with their precursors, at the bone surface, where they create a fitted layer of cells.	Synthesis and regulation of bone ECM deposition and mineralization. React to mechanical stimuli.
Osteocytes	Stellate shaped. Have fewer organelles than the osteoblasts.	Calcification of the osteoid matrix. Blood-calcium homeostasis. Mechanosensor cells for the bone.

Osteoclasts	Polarized cells. Multinucleated cells.	Bone resorption.

Table 1.3: Summary of bone cell types and respective functions. Adapted from (He & Callanan, 2013).

1.9.1.5 Extracellular bone matrix

In general, calcified bone is comprised of approximately 70% inorganic component, (5-10%) water, and (20-25%) organic matrix. The inorganic component of bone consists mainly of hydroxyapatite (99%). The organic matrix of bone has collagenous proteins (85-95%), mainly type I collagen, and non-collagenous proteins (5-15%) including osteocalcin, osteopontin, osteonectin, fibronectin and bone sialoprotein II, BMPs and growth factors. Also, there are small leucine-rich proteoglycans such as decorin, lumican, biglycan, osteoaderin, and seric proteins.

Osteoblasts are responsible for producing collagen and non-collagenous proteins (Clarke, 2008; Fogelman et al., 2012; Nakamura, 2007; Florencio-Silva et al., 2015).

The inorganic element of bone contains mostly phosphate and calcium ions; but, important numbers of bicarbonate, potassium, citrate, sodium, magnesium, carbonate, barium, zinc, fluoride, and strontium ions also exist. The hydroxyapatite crystals, which are denoted by the chemical formula $Ca_{10}(PO_4)_6(OH)_2$, are composed of calcium and phosphate (Florencio-Silva et al., 2015). The final bone product is a highly structured compound of protein (mainly collagen) and mineral (mainly

hydroxyapatite), that has enough structural strength to support the mechanical roles of the skeleton (Fogelman et al., 2012).

Matrix development is related to expression of ALP and some noncollagenous proteins, consisting of osteocalcin, osteopontin, and bone sialoprotein. These calcium- and phosphate-binding proteins assist in control of degradation of mineral by controlling the number and content of hydroxyapatite crystals created

(Clarke, 2008).

There is a difference in the concentration of bone matrix proteins with variations due to age, disease, nutrition, and anti-osteoporotic treatments, which may lead to defects and rupture of bone. For example, it has been stated that the upsurge in hyaluronic acid production after PTH treatment *in vivo* and *in vitro* is associated with bone absorption, which indicates a connection between hyaluronic acid production and osteoclast activity (Florencio-Silva et al., 2015). Inadequate intake of vitamin D or hyperparathyroidism also reduces the bone mineral content (Fogelman

et al., 2012).

1.9.1.6 Interactions between bone cells and bone matrix

Bone matrix has an important function in controlling the activity of bone cells by the action of adhesion molecules. Integrins are the most common adhesion molecules implicated in the communications between bone matrix and its cells (Florencio-Silva et al., 2015). Cell-matrix communication between osteoblasts and bone matrix proteins, such as type I collagen, non-collagenous proteins, and fibronectin, is vital for the differentiation of osteoblasts (Nakamura, 2007). Integrins identify and bind to the arginyl-glycyl-aspartic acid (RGD) amino acid sequence and

other sequences available in bone matrix proteins such as osteopontin, collagen, fibronectin, and bone sialoprotein. In osteoblasts, the most typical integrins available are $\alpha_1\beta_1$, $\alpha_2\beta_1$, and $\alpha_5\beta_1$. These proteins perform a key role in osteoblast configuration on the bone surface throughout osteoid production (Florencio-Silva et al., 2015). In addition, the communication between β1 integrins (α1β1 and α2β1), and type I collagen plays an important function in the differentiation of osteoblasts through activation of the mitogen-activated protein kinase (MAPK) signalling passageway (Nakamura, 2007).

Again, the communication between osteoclasts and bone matrix is necessary for the role of osteoclasts because bone metabolism results only when osteoclasts fix to mineralized bone surface. Hence, throughout bone metabolism osteoclasts direct $\alpha_v\beta_3$ and $\alpha_2\beta_1$ integrins to communicate with the extracellular matrix. They bind to RGD-containing proteins, including bone sialoprotein and osteopontin, while β_1 integrins fix to collagen fibrils (Florencio-Silva et al., 2015).

Osteocyte-bone matrix communications are needed for the mechanosensitive role of cells, in which signals activated by tissue distortion are developed and augmented. It is still unsure which integrins are involved, however, it has been proposed that β_3 and β_1 integrins are associated with osteocyte-bone matrix communication. In specific, these communications occur between the osteocyte body and the bone matrix of the lacuna wall, and also between the canalicular wall and the osteocyte. To date, bone matrix and integrin-dependent bone cells communications are necessary for bone construction and metabolism (Florencio-Silva et al., 2015).

Mass transport, construct structure and behaviour influence the distribution of mechanical forces, nutrient intake and kinetics of tissue development. The change of

physical stimuli into molecular signals and biological reactions is named mechanotransduction. Bone cells are responsive to mechanical stimuli, and their incorporation and transformation into intracellular signals plays a crucial function in encouraging bone remodelling during the lifetime, and regeneration of bone throughout fracture healing. Mainly, human bone is exposed to two kinds of mechanical stimuli such as strain (initiated by deformation from bending or compression from physical movement and the projected value is less than 2000μ□), and fluid shear stress (as a result of interstitial fluid activity via the lacunae in consequence of loading and the projected values are between 0.8 to 3 Pa) (Sladkova & Maria de Peppo, 2014).

1.9.1.7 Local and systemic factors that regulate bone homeostasis

Osteoblasts contain receptors for several bone active mediators like PTH, parathyroid hormone-related protein (PTHrP), gonadal and adrenal steroids, vitamin D metabolites, and specific cytokines and growth factors. PTH is an 84-amino acid peptide excreted by two pairs of parathyroid glands that are posterior to the thyroid gland. The primary regulatory indication for PTH excretion is serum calcium, which conversely influences PTH excretion. Serum phosphate has an impact on calcium concentration, and environment phosphate directly increases 1,25-D synthesis.
Hence, serum phosphate may either directly and indirectly control PTH expression (Fogelman et al., 2012).

Calcitonin (CT) is a 32-amino acid peptide whose major action is to hinder osteoclast-mediated bone resorption. CT is released by parafollicular C cells of the thyroid and

other neuroendocrine cells. In opposition to PTH, hypercalcemia enhances secretion of CT, whereas hypocalcemia impedes secretion (Fogelman et al., 2012).

Vitamin D appears in humans in an endogenous (as vitamin D_3) and exogenous (as vitamin D_2) structure. The endogenous structure of vitamin D_3 (cholecalciferol) is produced in the skin from the cholesterol metabolite 7dehydrocholesterol, with the help of ultraviolet (UV) radiation from the sun, and it is

absorbed from food. Meanwhile, the exogenous structure of vitamin D_2 (ergocalciferol) is synthesized by ultraviolet irradiation of the plant sterol ergosterol and is accessible via the diet. Both structures of vitamin D need additional metabolism to be biologically active (Fogelman et al., 2012).

The liver produces 25-hydroxyvitamin D and the kidneys then synthesize biologically active 1,25-dihydroxyvitamin D [1,25-$(OH)_2$D]. The serum concentration of 1,25-dihydroxyvitamin D only drops in situations of extreme vitamin D insufficiency. 1,25-dihydroxyvitamin D has significant roles in calcium metabolism as well as increasing the excretion of parathyroid hormone from the parathyroid glands.

It preserves serum calcium and phosphorus mainly by triggering intestinal resorption of calcium and phosphate. Also, serum 1,25-$(OH)_2$D encourages differentiation of osteoblasts and stimulates osteoblast expression of bone-specific ALP, osteonectin, osteocalcin, OPG, and a number of different cytokines. Additionally, serum 1,25-$(OH)_2$D affects proliferation and apoptosis of other skeletal cells like chondrocytes (Clarke, 2008). Oestrogen also shows important functions in bone tissue homeostasis. Bone destruction and osteoporosis are highly related to the reduction in estrogen level (Fogelman et al., 2012; Nakamura, 2007; Florencio-Silva et al., 2015).

1.9.1.8 Bone remodelling process

Bone volume is preserved by the equilibrium between bone resorption and bone creation. Also, these processes maintain the reshaping or substitution of bone throughout development and control healing of trauma including fractures and microdamage. The aggregation of bone microdamage is prohibited by replacing elderly bone with new bone (mechanically tougher to maintain bone integrity), which happens throughout normal activity. Moreover, remodelling reacts to the application of mechanical loading. All in all, the bone remodelling process is crucial in the preservation of bone integrity and mineral homeostasis (Clarke, 2008; Fogelman et al., 2012; Nakamura, 2007). This should not be confused with the reseeding process which involves the process of culturing cells (volume or cell number) *in vitro* on the decellularised bone scaffolds after removing the native cells.

Modelling is the process in which bones alter their whole shape in reaction to physiologic effects or mechanical forces, guiding continual adaptation of the skeleton to the forces that act on it (Clarke, 2008). Bone remodelling starts with an initiation (activation) stage, in which bone is resorbed by osteoclasts, followed by a stage of bone creation by osteoblasts. It is recognized that throughout the bone remodelling phases, there are direct and indirect interactions among bone cells. This process is called the coupling mechanism, in which soluble coupling determinants are produced when osteoclasts absorb bone deposited in bone matrix. Mature osteoclasts excrete

several factors that promote osteoblast differentiation including the secreted signalling molecules Wnt10b, BMP6, and the signalling sphingolipid, sphingosine-1phosphate. As well as osteoclasts and osteoblasts, osteocytes perform important functions throughout the bone remodelling phase (Clarke, 2008; Florencio-Silva et al., 2015). At the end of every bone remodelling series, a fresh osteon is produced.

The remodelling process is basically similar in both cortical and trabecular bone (Clarke, 2008).

1.9.1.9 Markers of bone metabolism

Biochemical indicators of bone metabolism produce vital evidence regarding the state of osseous tissue, and can be generally categorized as expressing either bone creation or bone resorption (Fogelman eta l., 2012).

ALP is one of the indicators for bone creation, and its activity in serum has been used for over 50 years as a commonly used indicator of bone metabolism. But, ALP is not particular to bone, and there is a major difficulty for diagnosis in clinical applications in differentiating between the isoenzymes originating from liver and bone, while the intestinal enzyme may be increased after taking meals and the placental isoenzyme throughout pregnancy. The bone isoenzyme can be differentiated according to sialic acid residues. In fact, approximately half of the amount of serum ALP is extracted from bone and the rest from liver, in normal persons (Fogelman eta l., 2012).

Another indicator for bone development is osteocalcin. Osteocalcin, also called bone gla protein (BGP), is a bone specific protein, which is a particular indicator of

osteoblast activity in different metabolic bone disorders. The production of osteocalcin is reliant upon the activity of active metabolites of vitamin D, specifically 1,25-dihydroxyvitamin D and vitamin K is also needed for its formation.

Measurements of serum osteocalcin by immunoassay show raised levels in situations correlated with raised bone development, for instance, hyperparathyroidism, hyperthyroidism, and bone metastases. Decreased amounts of osteocalcin may indicate slower rates of bone development, for instance in myeloma. Osteocalcin levels may be significantly decreased during treatment with glucocorticosteroids, although in this condition, glucocorticoids particularly restrain osteocalcin production by osteoblasts, while not impairing collagen production or synthesis of

ALP (Fogelman eta l., 2012).

1.10 Research main objectives

Although some main progresses have been proposed in the area of bone regenerative medicine during the years, existing treatments, like bone grafts, still have many drawbacks. Furthermore, even though the material science technology seemed to have a better progress in the area of bone replacement medicine, there is no suitable bone biomaterial revealed and thus huge bone defects/injuries still demonstrate a key challenge in regenerative and orthopaedic surgeons. In this situation, TE has been developing as an effective strategy to the present treatments for bone reconstructive/replacement. Work in TE in recent decades involved the understanding of tissue development and reconstruction, goals to create new functional tissue, whereas what happened in the biomaterial approach was just to embed new spare parts

(Salgado et al., 2004). However, the rational aggregation of a TE strategy for bone regeneration is eventually directed by the clinical status of the patient. A suitable approach is yet to be discovered and it is at the same time urgently required for full recovery for the patients. In fact, a possible solution for these limitations may be in TE, that has a great potential to solve the problems of the present treatments for bone substitution. Thus, this project aims to:

- create porous bovine bone scaffolds as xenografts for bone tissue engineering.
- demonstrate and establish decellularisation protocols to make donor bone scaffold, which could be used to repair bone defects in recipient patients.
- show effective removal of donor bone cells from bovine bone.
- establish a sterilisation procedure for the decellularised bone.
- determine whether the decellularisation process alters the mechanical properties, and porosity of the bone scaffold before and after the treatments.
- obtain efficient re-cellularization with human derived cells.
- test the function of the human derived bone cells residing on the decellularised bovine matrix measure.
- measure the mechanical properties, and porosity of the recellularised tissue.
- determine the morphology of the reseeded human bone cells resident on the matrix.
- decide whether decellularised bovine bone could provide a scaffold for reseeded human bone implants.

Chapter 2

GENERAL MATERIALS AND METHODS

2.1 Introduction

The general materials and methods for this study are described in this chapter. However, any other alterations to the general method are specified in the related chapter. Also, methods particular to each chapter are specified in the methods section of the related chapter.

2.2 Chemical solutions and tissue culture

Unless stated otherwise, all chemicals used in this project were purchased from Sigma – Aldrich Company Ltd., Dorset, UK. Tissue culture media and solutions as 1x Dulbecco's modified eagle's medium (DMEM), penicillin & streptomycin (PEST) (5000 Unit/ml-5000 μg/ml), and non-essential amino acids
(NEAA) were purchased from Biowhittaker ™ Cambrex Bio Science Wokingham Ltd., Berkshire UK. Foetal calf serum was (FCS) supplied by Harlan Sera-lab Ltd., Loughborough, UK. Falkon ®, Becton Dickinson Labware, New Jersey USA was the supplier of Petri dishes. Sabouraud's medium (SAB) which is used to test for fungal contamination and brain heart infusion (BHI), which is used to test for bacterial contamination, were both purchased from Oxoid Ltd., Basinstoke, UK.

2.3 Media and solutions preparation

2.3.1 Sterilization procedures

All cell culture work was carried out under aseptic conditions. Autoclavable apparatus was sterilised by autoclaving for 30 minutes at 120C. Aseptic work was carried out in a laminar-air-flow cabinet maintained by Crowthorne Hi-Tec Service Ltd., Glasgow UK, which was swabbed thoroughly with 70% ethanol prior to and after use. Plastic apparatus was micro-waved for 5 minutes at 800 W. Solutions and culture media were tested routinely for contamination by adding 1-2 ml to 20 ml of BHI and SAB and incubating at 37C for 72 hours. If contamination was present the solutions became turbid, otherwise they remained clear.

2.3.2 Versene (EDTA) in PBS, pH 7.2

Versene (EDTA solution) at 0.02% (w/v) with a pH of 7.2 was prepared by dissolving the following compounds in 0.5 litre of distilled water.

1. 4 g of NaCl.
2. 0.1 g of KCl.
3. 0.5835 g of Na_2HPO_4.
4. 0.1 g of KH_2PO_4.
5. 0.1 g of EDTA.
6. 1.5 ml of Phenol red 0.5% (w/v).

The made up solution was sterilized by autoclaving and stored at room temperature.

2.3.3 Trypsin

Tris buffered saline (TBS) solution with a pH of 7.7 was prepared by dissolving the following compounds in 996.5 ml of distilled water.

1. 8 g of NaCl.
2. 0.1 g of Na_2PO_4.
3. 1 g of D-glucose.
4. 3 g of Tris.
5. 2 ml of 2.25M KCl.
6. 1.5 ml of Phenol red 1% (w/v).

The pH was adjusted to 7.7 at room temperature and the product was sterilized by autoclaving. Trypsin stock solution was made by adding 50 ml of sterile trypsin solution 2.5% (w/v) to 450 ml of TBS. The made up solution was then stored at -20C.

n This product was further diluted to 0.05% (w/v) with 0.02% versene before use.

2.3.4 Dulbecco's modified eagle's medium (DMEM)

Most of the cell lines grown in the laboratory were grown in DMEM. This was purchased as a 1X stock and stored in the cold room. When required, the media from Cambrex was used and the following were added to the 500 ml 1X bottle under sterile conditions.

1. 50 ml sterile FCS.
2. 5 ml sterile PEST.

3. 5 ml NEAA.

Once everything was added to the medium, it was checked to make sure it was not contaminated. To do this 1 ml of the medium was added to both a universal with BHI and SAB broth. These were then placed in the incubator at 37C for 2-3 days, and if they went cloudy the medium was contaminated.

2.3.5 Bone culture medium

The medium used for bone cell culture was DMEM. However, 50 ml were removed from a 500 ml bottle, and the supplements for mineralization were added in the 50 ml as follows (Griensven et al., 2002):

1. 50 μg/ml L-ascorbic acid (Sigma, Deisenhofen, Germany).
2. 10 mM β-glycerophosphate (Sigma, Deisenhofen, Germany).
3. 100 nM dexamethasone (Dex) (Sigma, Deisenhofen,

   Germany).

These were dissolved in 50 ml DMEM, and the solution was then mixed well and filtered (0.22 μm filter). Then, it was added to the rest of 450 ml DMEM bottle (resulting in a 10-fold dilution) and the following additions were also supplemented:

1. 50 ml sterile FCS.
2. 5 ml sterile PEST.
3. 5 ml sterile NEAA.

This complete medium was stored in the cold room at 4°C. Once everything was added to the medium, it was checked to make sure it was not contaminated. To do this 1 ml of the medium was added to 2 universal containers with BHI and SAB

broth. These were then placed in the incubator at 37C for 2-3 days, and if they went cloudy the medium was contaminated, and discarded.

2.4 Cell cultivation

2.4.1 OST 5 osteoblasts

Immortalised neonatal rat osteoblast cells (OST 5) were used in these experiments, and they were thawed from the stock held in liquid nitrogen as required.

2.4.1.1 Procedures

OST 5 was split twice a week at a ratio of 1:10 every 4 days. The growth medium was drained from the flask; the adherent cells were washed twice with versene to remove all traces of serum which hinders the action of the trypsin.

A few ml of 0.05% (w/v) trypsin were added, left to act for about 5 – 7 minutes and observed under the phase contrast microscope (Nikon Corporation Japan). This step is used to detach the adherent cells as trypsin is a protein digestive enzyme. The flask was tapped to help detach the remaining cells. When the cells were in suspension, complete DMEM was added to stop the action of trypsin by the presence of FCS.

The cells were split at the appropriate ratio. Cells intended for seeding were counted by haemocytometer, resuspended in complete DMEM and seeded at 2.5 x 10^4 cells/ cm^2.

OST 5 cells were used in this project to set up ptotocols for reseeding of bone scaffolds, and to develop assays.

2.4.2 Human osteosarcoma (HOS) cell line

When the re-seeding conditions for OST5 were established, immortalised human caucasian osteosarcoma cells were then used in reseeding experiments. The human osteoblastic cells were purchased (Order Number: 87070202) from SigmaAldrich (Dorset, UK). As required, they were thawed and isolated from the stock held in liquid nitrogen. These cells are derived from human osteosarcoma as mentioned by the manufacturer (http://www.phe-culturecollections.org.uk/).

2.4.2.1 Procedures

Usually, HOS cells were subcultured twice a week at a ratio of 1:6 every 4 days when they reached confluency, as described previously for the OST 5 cells in **Section 2.4.1.1.** HOS cells intended for seeding were counted by haemocytometer, resuspended in complete DMEM and seeded at 5 x 10^5 cells/ cm^2 onto the bone scaffolds.

2.5 Statistical methods

Microsoft Excel was used for statistical analysis when a comparison was made directly between two groups of data, in which an unpaired student's t- test was applied. However, a single control group analysis of variance (ANOVA) was chosen for multiple comparisons (more than two variables). Furthermore, repeated measurements

ANOVA were also performed for multiple comparisons using statistical package for the social sciences (SPSS) Statistics 21 (a product of IBM SPSS Inc., Chicago, Illinois, USA) for Windows. The significance level applied for the experiments was 0.05, and a Bonferroni correction was applied to adjust the significance level for multiple comparisons. Confidence intervals were 95%.

Repeated measurements were applied to find groups with significant differences for ANOVA. P-values smaller than ($p<0.05$) were considered significant and all data are presented as mean ± standard error of the mean (SEM).

Chapter 3

DECELLULARISATION APPROACH FOR TRABECULAR

BOVINE BONE

3.1 Introduction

The details regarding decellularisation have been explained in the previous chapter; there is no gold standard protocol for decellularisation in a specific tissue and organ. Effective removal of donor bone cells must be shown, and a standard sterilisation procedure for the decellularised material needs to be established to make a potential donor bone scaffold. With these ideas, this study was conducted to develop, improve and optimize a method for fabrication of donor bone scaffold based on the current strategies.

The success of decellularisation was proven in the literature by applying different histological, biochemical, and immunohistological procedures (Kheir et al., 2011). The effectiveness of the elimination of cellular material from tissues can be carried out using many approaches. The existence of DNA in the specimen is distinguished by staining with DAPI or Hoechst, hematoxylin and eosin (H&E), propidium iodide (PI) and PicoGreen and a-Gal before and after decellularisation
(Benders et al., 2012; Macchiarini et al., 2008; Gilbert et al., 2006; Choi et al., 2012). Biocompatibility tests are also carried out *in vitro* and *in vivo* (Kheir et al., 2011). Moreover, quantitative methods have also been established in detecting the existence of DNA in ECM. The application of DNA probe procedures was used to indicate both the presence of DNA from allografts after implantation and to verify the absence of any DNA in the decellularised tissue (Macchiarini et al., 2008; Gilbert et al., 2006).

While defining what has been eliminated from the decellularised materials, the preservation of required contents of the ECM such as adhesion proteins (laminin and fibronectin), elastic fibres, GAGs, collagens, and growth factors must be verified as those are needed to allow permeation of the matrix by cells of interest either *in vivo* or *in vitro*. The existence and integrity of the structural proteins within the scaffold can be observed from mechanical testing of the ECM once the treatment has been completed (Gilbert et al., 2006). The biomechanical properties of the decellularised tissue or organ were measured to confirm possible clinical function (Kheir et al., 2011). As mentioned by Marcos-Campos et al. (2012), the successful elimination of cellular material is related to the protection of tissue matrix proteins, which allow the production of osteoinductive molecules for regulating cell characteristics. The production of bone-like architectures by this protocol increases the equilibrium Young's modulus and that is associated with the amount of mineral in the scaffolds.

A major factor that could affect the mechanical performance and bioactivity of the scaffold is degradation of the material, and this could be influenced by the decellularisation treatments. These chemical treatments could adjust the ECM scaffold to be more prone to enzymatic degradation *in vivo* which would cause a reduction in the scaffold's durability (Gilbert et al., 2006). Subsequent implantation would result in loss of mechanical integrity due to the rapid degradation of decellularised tissue. The construction of the scaffold is a time-consuming process, and is affected by mechanical loading and rehabilitation activities. For that reason, success or failure may rely upon reasons other than the decellularised tissue itself

(Gundula et al., 2012).

In this chapter we had the following aims to:

(i) compare the sensitivity of two DNA probes for using to detect DNA on decellularised bone.

(ii) optimise decellularisation methods for trabecular bone.

(iii) produce decellularised scaffolds for subsequent recellularisation.

3.2 Materials and methods

3.2.1 The sensitivity of DAPI and PI

In order to choose the best agent for trabecular bone DNA staining, the sensitivity of the stains DAPI and PI was determined and compared in OST 5 cells. OST 5 cells are an immortalised rat osteoblast cell line that was used for this experiment. A standard curve was plotted relating the fluorescence intensity to cell numbers for both agents.

The fluorescence was measured by using a Spectrofluorophotometer (Model number: UV-2401PC) (Shimadzu Corporation, Japan).

3.2.1.1 Procedures

Different numbers of cells were selected for these experiments ranging from 0, $5x10^3$, 10^4, $5x10^4$, 10^5, $2.5x10^5$, $5x10^5$ to $1x10^6$ cells/cm^2, in order to construct a standard curve for fluorescence versus cell number. All the cell samples were added to DMEM and centrifuged (MSE Mistral 2000, England) at 800 rpm for 4 minutes. Then, the medium was discarded from the samples and 1.5 ml Dulbecco's phosphate-buffered saline (DPBS) (Lonza, Inc. Walkersville, USA) added. They were

frozen for an hour at -20C analogous to the storage of the cells on a bone sample which was also stored at the same temperature.

Next, the cells were thawed in the incubator at 37C. They were then stored at -20C. On thawing, the samples were then treated in 1.5 ml PBS (Sigma-Aldrich, Inc. FLUKA) with 0.6 nM DAPI and 30 μM PI independently. The fluorescence was read by the Spectrofluorophotometer after the samples were left for 5 minutes in the dark. The fluorescence were set for DAPI wavelengths [Excitation (EX): 358 nm, Emission (EM): 461 nm] and for PI wavelengths (EX: 535 nm, EM: 617 nm).

3.2.2 The reproducibility of DAPI

The reproducibility of DAPI agent was determined for DNA quantification. The mean and the SEM were determined for each trial.

3.2.2.1 Procedures

The same number of cells ($5x10^5$ cells/cm^2) was selected with 6 repeated measurements. They were centrifuged gently at 800 rpm for 5 minutes, frozen at 80C for an hour, thawed in the incubator at 37 C, then they were treated with 0.6 nM DAPI and the fluorescence read by Spectrofluorophotometer (EX: 358 nm, EM: 461 nm) after being left for 5 minutes in the dark. The experiments were repeated

for three trials.

3.2.3 The specificity of DAPI

The experiment was carried out to determine the specificity of DAPI. The OST 5 cells were measured both in suspension and after being fixed.

3.2.3.1 Procedures

A concentration of OST 5 cells (0.499 ml) and fresh medium (14.5 ml) was made up. The seeding density was $2x10^4$cells/cm^2. This was then cultured in the incubator at 37C overnight. To fix the OST 5 cells, 1.5 ml of 4% buffered formalin was added for 30 minutes after washing them with DPBS. The final concentration used for DAPI was 0.6 nM. The fluorescence was detected using a Spectrofluorophotometer and the stained intracellular DNA was observed under the Zeiss Microscope (Carl Zeiss MicroImaging GmbH, Germany).

For the cells in suspension, the OST 5 cells were frozen at -20C for an hour and thawed in the incubator at 37 C. The same concentration of DAPI (0.6 nM) was added to the OST 5 cells. These freeze and thaw processes were applied as described previously to break up the membrane of the cells. The OST 5 cells were also processed without the DAPI agent. For comparison, the OST 5 cells were also left in the incubator at 37 C with no freeze-thaw process.

3.2.4 Detecting DNA in bone samples after the decellularisation processing

3.2.4.1 Preparation of bone samples

Fresh bovine femur bone was bought from a local abattoir and transported to the lab. The proximal trabecular bone was cut out from the bovine femur bone using a bandsaw. Briefly, the bone was washed under high-velocity streams of water to remove the marrow from the pore spaces, adherent tissues, and fat. This was continued until the cores appear completely white. The trabecular bone was placed on the Titan Bandsaw and Smart Cut Machine and cut into square-shaped specimens (dimension: 7 mm x 7 mm x 2 mm). Bone specimen thickness was (Mean ± SEM, 1.778 ± 0.256 mm, n = 6). Then, all the samples were immersed in 0.5 M NaCl to avoid dehydration. The dried samples were stored in the freezer at -20 C. **Figure 3.1** shows the preparation of the bone pieces.

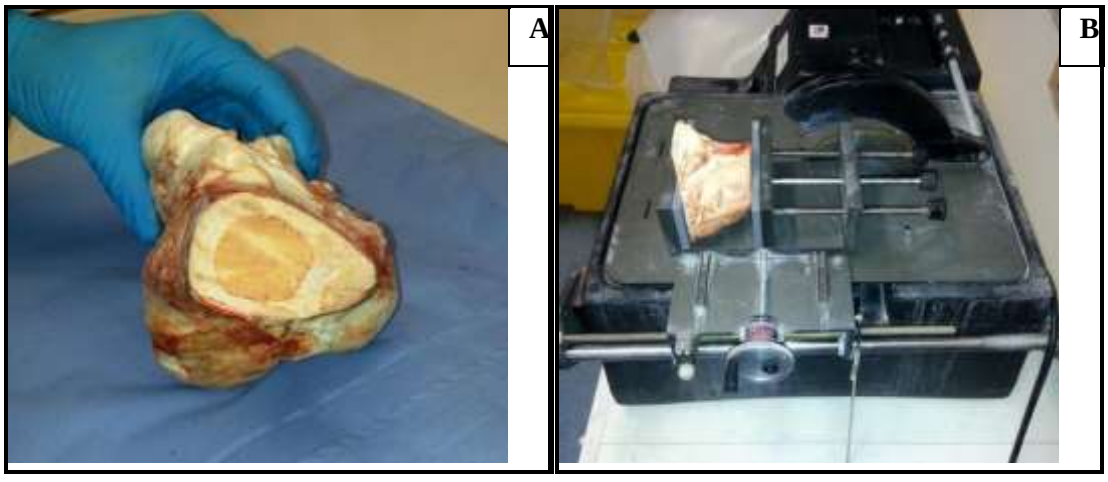

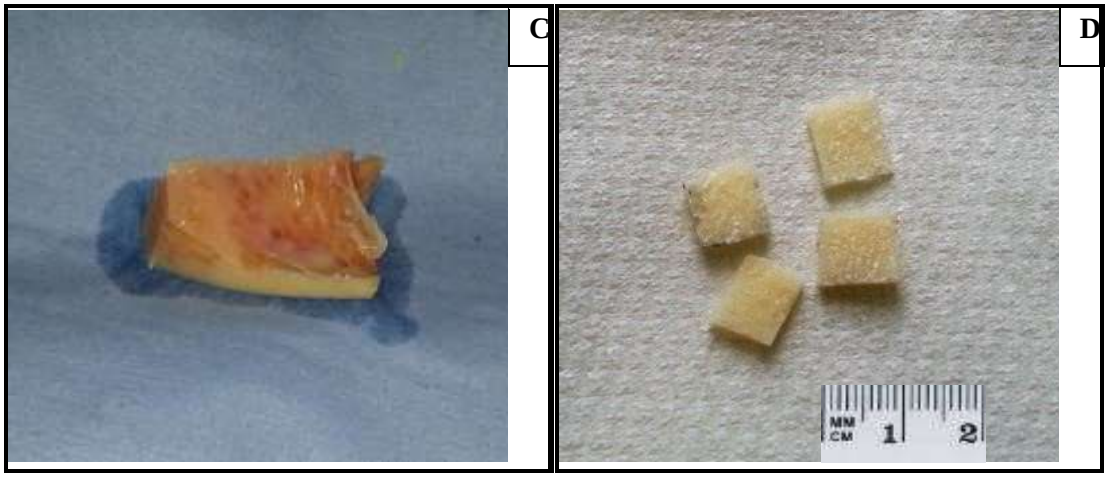

Figure 3.1: A) The bovine femur bone after being cut by a bandsaw. B) The Smart Cut Machine by UKAM Industrial Superhard Tools. C) The bovine trabecular bone extracted from the femur. D) The dimension of bone samples made of bovine trabecular bone.

3.2.4.2 Preparation of the digestion buffer

The digestion buffer prepared for use with the bone samples was 10 mM Tris, 1 mM EDTA and 0.1 % (v/v) Triton X-100, with pH of 7.4. The solution was stored in the cold room at " 4C overnight.

3.2.5 Decellularisation of bone scaffolds

Mostly the experimental protocols were adapted from published studies (Correia et al., 2012; Correia et al., 2011; Marcos-Campos et al., 2012; Frohlich et al., 2010; Grayson et al., 2010; Grayson et al., 2008).

The working concentration used for DAPI was 0.6 nM as before. The DNA of bone samples was detected under the Zeiss Microscope. Bone samples were incubated

with 0.6 nM DAPI after washing them with PBS. Some tests were carried out to identify the decellularisation effect of digestion buffer and 0.5 % (w/v) trypsin on the bone samples as follows:

Sample 1: 1.6 ml digestion buffer and 400 µl of 0.5 % (w/v) trypsin,

Sample 2: 2 ml digestion buffer and bone sample, and

Sample 3: 1.6 ml digestion buffer, 400 µl of 0.5 % (w/v) trypsin and bone sample

The procedures for monitoring the efficiency of decellularisation are shown on **Figure 3.2.** The samples were left in the incubator at 37C. The supernatants of each sample were removed and their fluorescence measured after 10 minutes and then after an overnight incubation. Decellularisation was confirmed by the absence of DNA staining with DAPI on the bone matrix both by eluting any stain from the samples into the supernatant spectrofluorometrically, and by microscopic examination of the bone material itself under the Zeiss Microscope.

3.2.5.1 Stability of the DAPI fluorescence over time

Bone samples were used to measure fluorescence stability of the DAPI over time. The measurements were taken before (at t = 0 hour) and after overnight (at t = 24 hours) incubation by using Spectrofluorophotometer. The wavelength for excitation and emission were set to 358 nm and 461 nm respectively. To confirm the stability of DAPI, the fluorescence of a number of bone samples was measured also after 5 minutes, 10 minutes, 20 minutes, 30 minutes and 60 minutes.

The details of the stability protocols were explained on **Figure 3.2** as bone samples were taken from the freezer (where they were stored at -20 C) and incubated for 2 minutes at 37C. They were washed with 1 ml Phosphate-Buffered Saline (PBS) (pH 7.4) and stirred for 1 minute. Then, the bone samples were treated and stirred for 5 minutes with 3 ml PBS and 0.6 nM DAPI (covered with aluminium foil). Again, the bone samples were washed three times with 1 ml PBS to remove any residual stain and stirred for 1 minute for each wash. Next, three different samples were prepared as follows:

Sample 1: 1.6 ml digestion buffer and 400 µl of 0.5 % (w/v) trypsin,

Sample 2: 2 ml digestion buffer and bone sample, and

Sample 3: 1.6 ml digestion buffer, 400 µl of 0.5 % (w/v) trypsin and bone sample

All the samples were stirred for 5 minutes before the fluorescence of the supernatants was measured on the spectrofluorophotometer (t = 0 hour) in the dark. Next, the samples were left overnight to incubate (t = 24 hours) at 37 C and 5% CO_2. The supernatants were removed and fluorescence measured the next day. The experiments were repeated for six cycles of incubations.

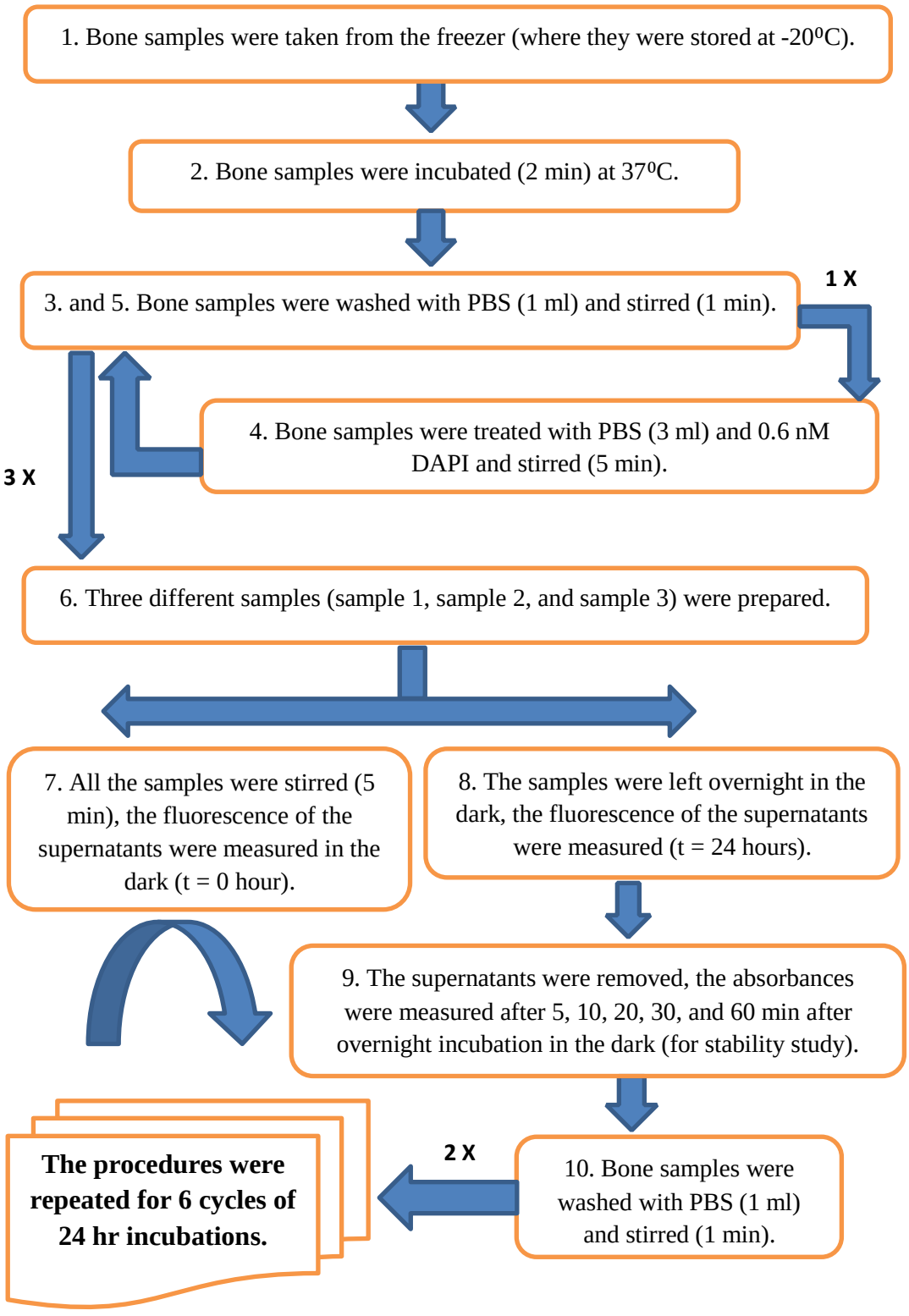

Figure 3.2: The flowchart represents the procedures to measure the efficiency of decellularisation and the stability of the DAPI fluorescence over the time. The protocol above was repeated with sample 1 (3.2 ml digestion buffer and 800 µl of 0.5 % (w/v) trypsin), sample 2 (4 ml digestion buffer and bone sample) and sample 3 (3.2 ml digestion buffer, 800 µl of 0.5 % (w/v) trypsin and bone sample).

3.3 Results and discussions

3.3.1 The sensitivity of DAPI and PI and the reproducibility of DAPI

Generally, the sensitivity of the two DNA stains was measured according to the minimum cell number that could be detected by the Spectrofluorophotometer to produce a stable reading. In the sensitivity experiment, it was shown that the reading for each measurement was much higher for the DAPI agent compared to PI agent. Unpaired student's t-test shows that the measurements were significantly different (*p≤0.05) except for $5x10^4$, $1x10^5$ and $2.5x10^5$ cell numbers (**Figure 3.3**). The minimum number of cells that could be detected by DAPI was $5x10^4$ cells while $2.5x10^5$ cells by PI.

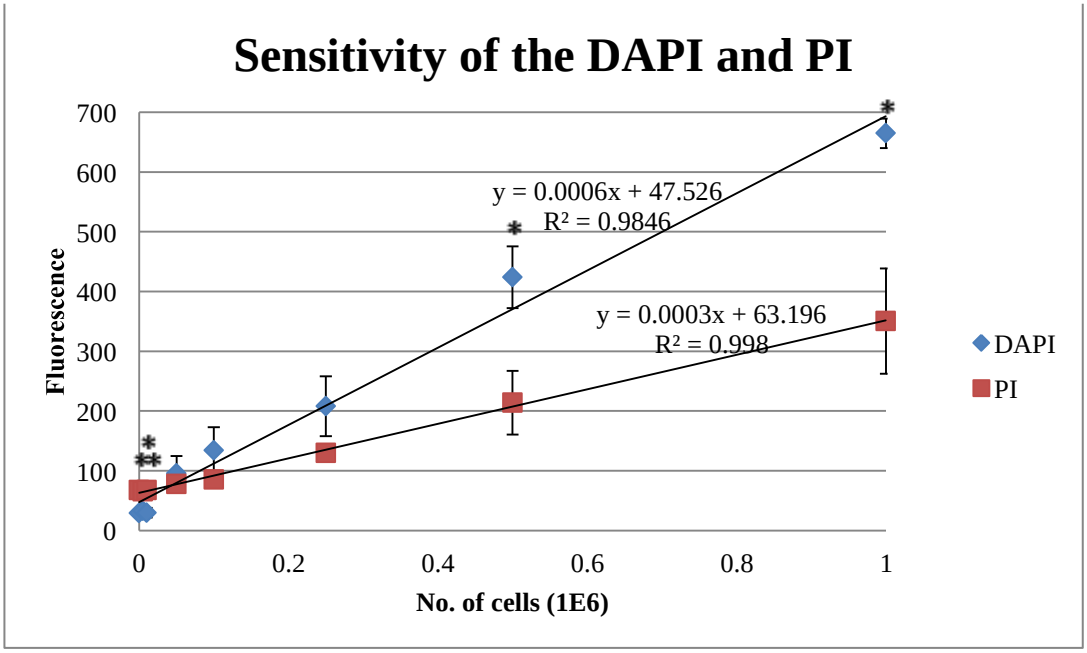

Figure 3.3: Sensitivity of the DAPI and PI staining, *p≤0.05, by unpaired t-test, comparing differences between the stains at the same cell numbers. Results are mean ± SEM, n = 3.

However, the fluorescence measurement was not consistent and reliable at the low cell numbers. This was due to the stains not being sensitive enough to be detected by the Spectrofluorophotometer and might be caused also by any technical error during

the experiment. The fluorescence of both agents has a linear relationship graph with cell number. Different cell numbers acted as the DNA source and the DNA content increased as the number of cells increased. All in all, the DAPI agent was more sensitive to OST 5 cell DNA as compared to the PI agent (**Figure 3.3**).

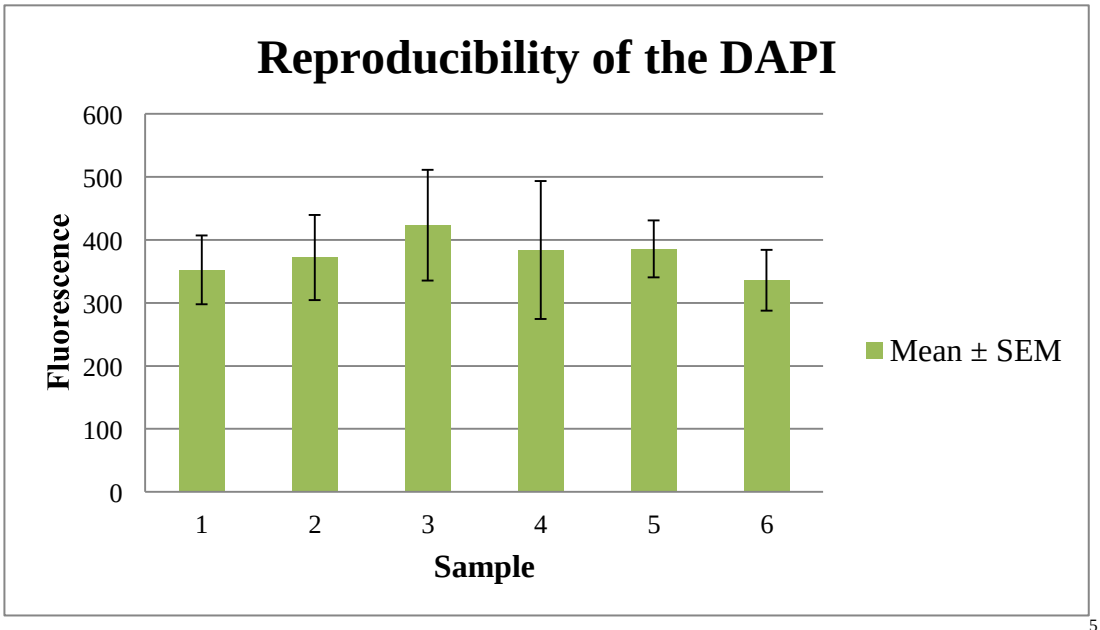

Figure 3.4: Reproducibility of the DAPI for Trial 1, 2 and 3 at the same number of cells (2.5 x 10 cells). Results are mean ± SEM, n = 3.

In the reproducibility experiment, it seemed that the fluorescence measurement for each trial was consistent at the same number of cells. Single control group ANOVA test shows that fluorescence values in all three trials (Trial 1, Trial 2, and Trial 3) were not significantly different ($p>0.05$) (**Figure 3.4**).

At the moment, it has been confirmed that the DAPI agent has a good reproducibility for intra and inter-assay experiment for OST5 cell DNA

3.3.2 The specificity of DAPI

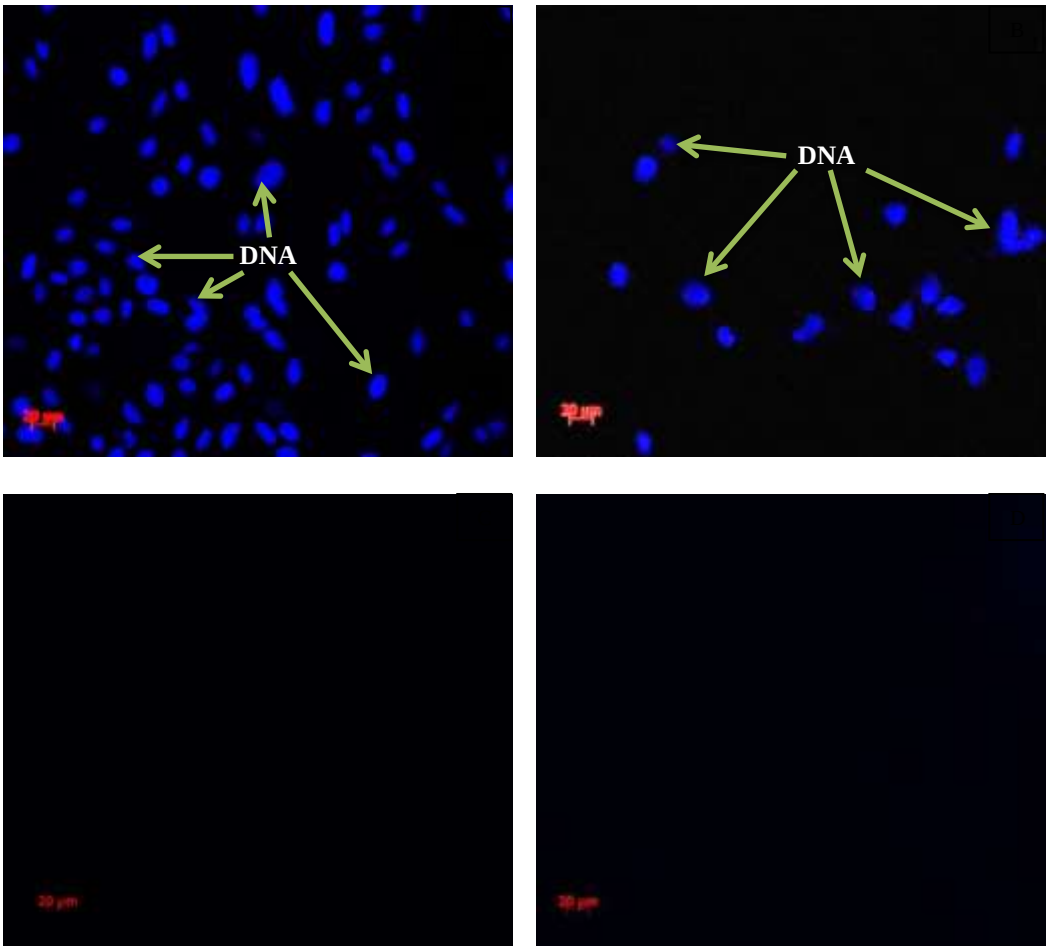

Figure 3. 5: Specificity of DAPI to OST 5 cells **A)** after being fixed with 1.5 ml of 4% buffered formalin in 0.6 nM DAPI agent. **B)** frozen at -20 ₁C with 0.6 nM DAPI agent. **C)** frozen at -20 ₁C without DAPI agent. **D)** after being incubated in 0.6 nM DAPI agent with no freeze-thaw decellularisation processing. All images were taken at the surface.

In the specificity experiment, the DNA could be seen very clearly under the Zeiss Microscope for the OST 5 cells after being fixed (**Figure 3.5 A**) and could be viewed also when the cells were frozen (**Figure 3.5 B).** But, it has been observed that no fluorescent DNA was detected in the OST 5 cells under the Zeiss Microscope when they faced the same freeze and thaw processes without the DAPI agent (**Figure 3.5 C**). The existence of DNA in the specimen can therefore be detected by staining with DAPI (Gilbert et al., 2006; Choi et al., 2012). Fluorescence is generated when the DAPI

attaches to the AT clusters in the minor grove of DNA (Kubista et al., 1987; Gilbert et al., 2006).

Moreover, in the OST 5 cells which had been left in the incubator with no freeze-thaw process, we could not view the DNA even when the cells were treated with DAPI agent (**Figure 3.5 D**); this is because DAPI cannot penetrate the intact membranes. In decellularisation, the most generally used procedures comprise the combination of physical and chemical treatments. The physical treatment usually involves the freezing and thawing process to break up the structure of cells (cell membrane), release cell components, and enable consequent rinsing and elimination of the cell components from the ECM. Thus, the fluorescence will pass through the membrane of the cells to detect the DNA (Fini et al., 2012; Gilbert et al., 2006).

DAPI staining therefore provides a sensitive, specific and reproducible quantification and detection method for DNA on the bone samples after decellularisation, and later after re-seeding cells on these scaffolds.

3.3.3 Detecting DNA in bone samples after decellularisation processing

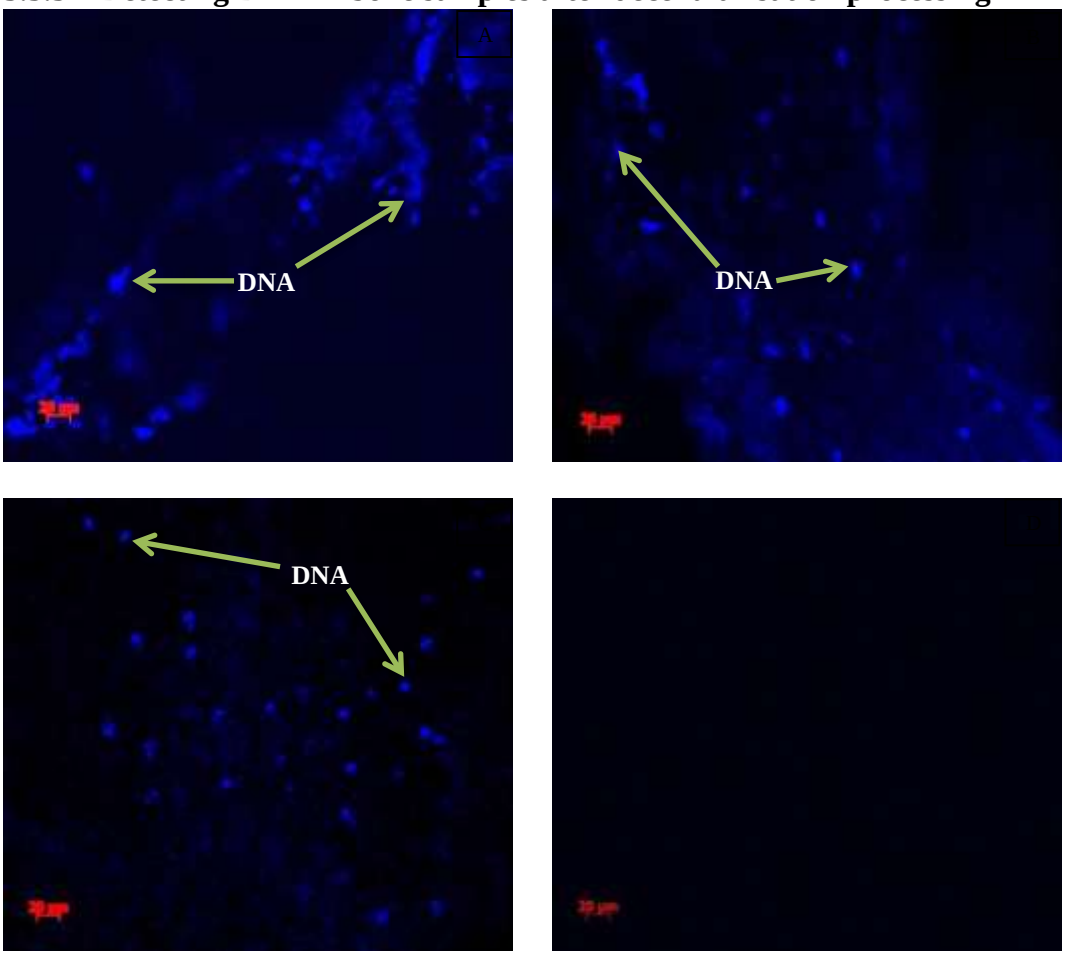

Figure 3.6: Detecting DNA in bone samples after decellularisation processing. Bone sample **A)** tested in 0.6 nM DAPI agent before addition of digestion buffer and 0.5 % (w/v) trypsin. **B)** incubated with 2 ml digestion buffer, and bone sample incubated with combination of 1.6 ml digestion buffer and 400 µl of 0.5 % (w/v) trypsin in 0.6 nM DAPI agents after 10 minutes incubation. **C)** added with 2 ml digestion buffer in 0.6 nM DAPI agent after overnight incubation. **D)** after incubation with 1.6 ml digestion buffer and 400 µl of 0.5 % (w/v) trypsin in 0.6 nM DAPI agent after overnight incubation. All images were taken at the surface.

When detecting DNA in the bone samples, the images were not clearly viewed under the Zeiss Microscope before addition of digestion buffer and trypsin in DAPI because the surfaces of the bone samples were not sufficiently flat and the cells were fixed to each other at different surfaces (**Figure 3.6 A**). The fluorescence measurement for all bone samples were almost the same after 10 minutes incubation because the digestion buffer and trypsin did not digest the bone samples sufficiently in that duration of time. Moreover in confirmation of this, the DNA in the bone cells could still be seen under the Zeiss Microscope after the incubation of 10 minutes for both the bone sample

with digestion buffer and also the bone sample with digestion buffer and trypsin (**Figure 3.6 B**). The treated bone specimens have more than 50% cells left after 10 minutes incubation. Incomplete decellularisation treatment will retain the main cellular elements comprised of osteoblasts, osteocytes, the hematopoietic components and adipocytes on the material (Quan et al., 2014).

In comparison, the amount of fluorescence released from the bone matrix was increased obviously after addition of digestion buffer and trypsin to the bone sample (**Figure 3.7**). The measurement was taken after overnight incubation. This was due to the DNA being extracted from the cells and it would be detected by the Spectrofluorophotometer as fluorescence. Likewise, the fluorescence was read and compared for the bone sample with digestion buffer only, and the bone sample with a combination of digestion buffer and trypsin before and after overnight of incubation. The fluorescence measurement after addition of digestion buffer only to the bone samples was not different from the results after 10 minutes incubation. The DNA in the cells could not be disrupted by the digestion buffer only (**Figure 3.6 C**). No detectable DNA on the bone sample could be seen under the Zeiss Microscope after overnight incubation in digestion buffer and trypsin (**Figure 3.6 D**). This happened because the DNA was removed from the cells by the trypsin. DAPI staining demonstrated that the bone specimens were successfully decellularised because there was no red blood cell residues and bone cells after the treatment. This was also observed by Quan et al., 2014.

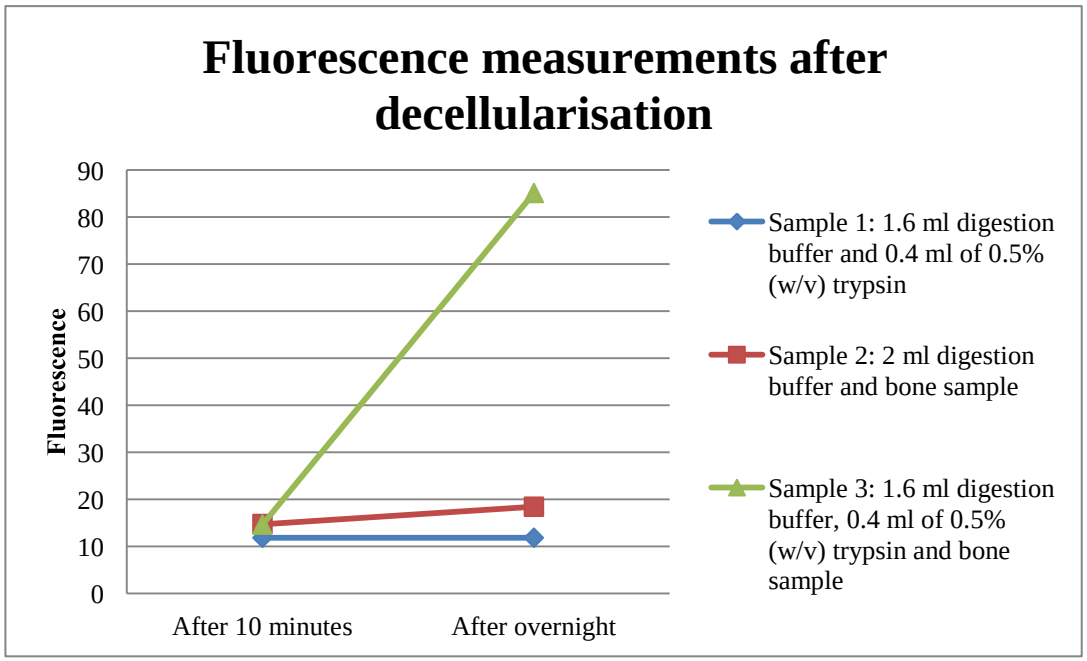

Figure 3.7: The comparisons of fluorescence measurements for the following samples: sample 1) 1.6 ml digestion buffer and 0.4 ml of 0.5 % (w/v) trypsin, sample 2) 2 ml digestion buffer and bone sample, and sample 3) 1.6 ml digestion buffer and 0.4 ml of 0.5 % (w/v) trypsin after 10 minutes and overnight incubation. Results are mean ± SEM, n = 3. (SEM bars are within the symbols).

3.3.4 The release of DAPI staining over time

The fluorescence measurements of DAPI staining were read at t = 0 and t = 24 hours (after each overnight incubation). **Figure 3.8** represents the release of DAPI staining from the bone during several cycles of incubations at t = 0 (before the overnight

incubations). In comparison with bone sample in 2 ml digestion buffer and the buffer (1.6 ml digestion and 400µl of 0.5% (w/v) trypsin), bone sample in 1.6 ml digestion buffer and 400µl of 0.5% (w/v) trypsin has always higher fluorescence.

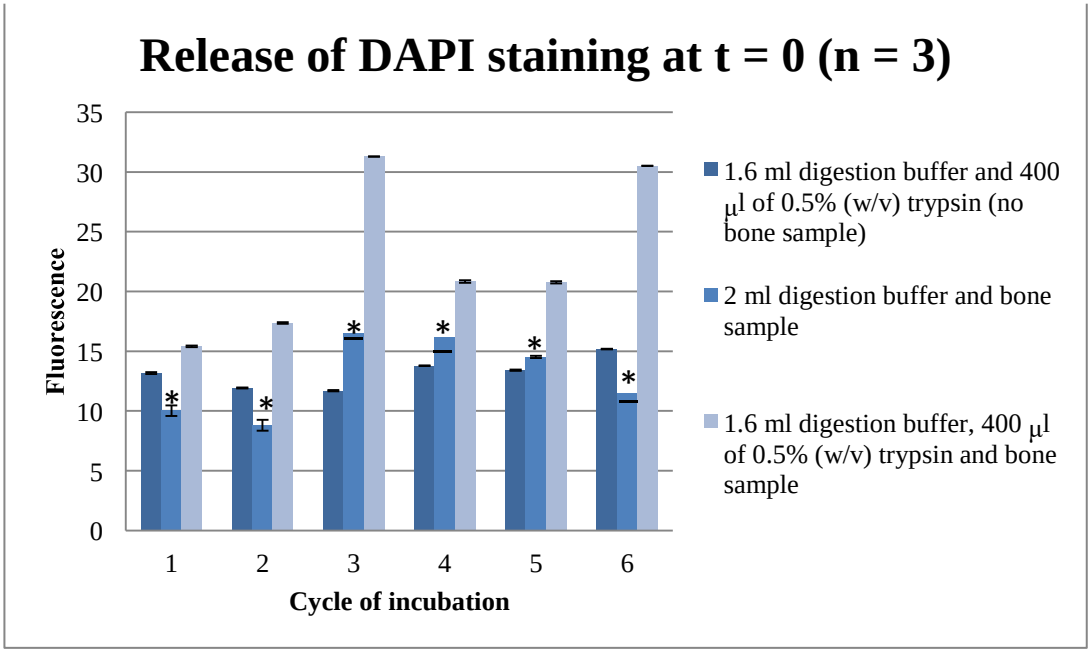

Figure 3.8: The release of DAPI staining from the bone samples at t = 0 for six cycles of incubations in 1.6 ml digestion and 400µl of 0.5% (w/v) trypsin (no bone sample); 2 ml digestion buffer and bone sample; and 1.6 ml digestion, 400µl of 0.5% (w/v) trypsin and bone sample. *p≤0.05 compared to all protocols, by ANOVA. Results are mean ± SEM, n = 3.

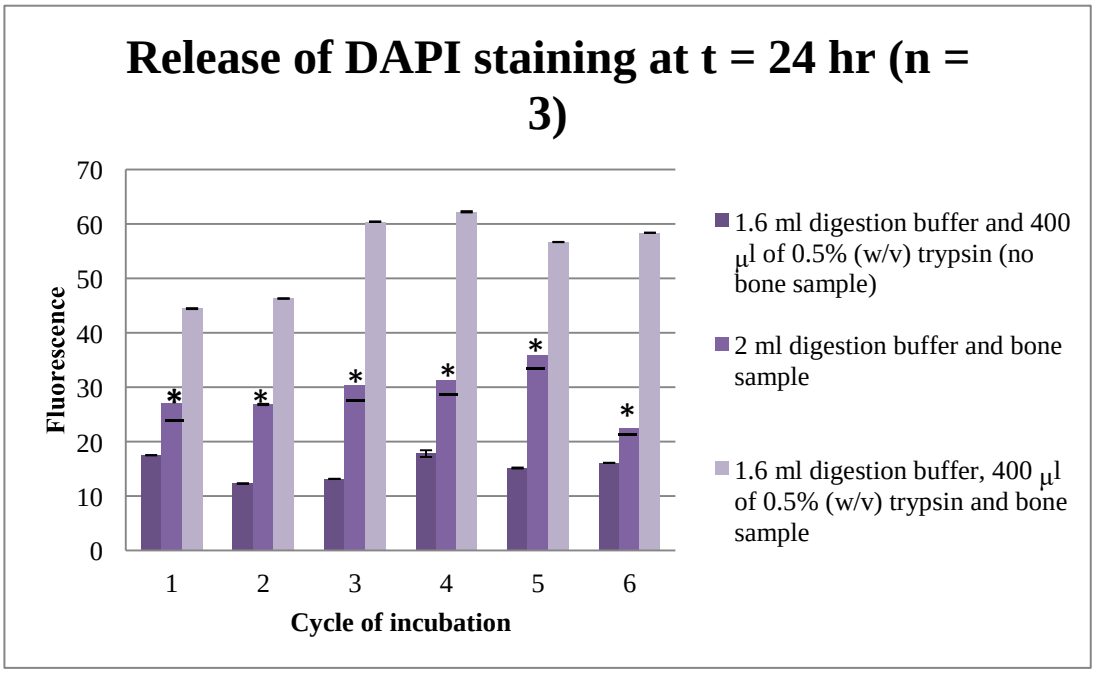

Figure 3.9: The release of DAPI staining from the bone samples at t = 24hr for six cycles of incubations in 1.6 ml digestion and 400µl of 0.5% (w/v) trypsin (no bone sample); 2 ml digestion buffer and bone sample; and 1.6 ml digestion, 400µl of 0.5% (w/v) trypsin and bone sample. *p≤0.05 compared to all protocols, by ANOVA. Results are mean ± SEM, n = 3.

Figure 3.9 shows the release of DNA from the bone after each successive overnight incubation. Release is greatest in the presence of trypsin. Moreover in **Figure 3.9**, the fluorescence measurements seemed to decrease after four cycles of overnight (t = 24 hours) incubations in bone sample with 1.6 ml digestion buffer and 400µl of 0.5% (w/v) trypsin and in the buffer. Meanwhile, the fluorescence has fallen off after five cycles of overnight incubations in bone sample with 2 ml digestion buffer. Taken together, six cycles of incubations were applied for this study to eliminate the donor entities in the scaffold. It was a challenge to completely remove the entire donor entities in these studies albeit there was no DNA observed under the Zeiss Microscope. However, the choice of six cycles of incubations was based on the fact that fluorescence measurements did not increase further after 4 cycles of incubations. Our studies have also demonstrated that the bone specimens were red before undergoing the six cycles of incubation processes due to comprising many types of cells containing blood cells (such as leukocytes, erythrocytes, and bone cells) and bone cells (such as osteocytes, osteoblasts, and osteoclasts). The cancellous bone specimens changed to white indicating that the blood cells were cleaned after decellularisation treatment. At any cycle of incubation time point there was a significant difference among the methods. No further DNA was released from the bone scaffolds when incubated with 4 – 6 cycles of digestion buffer plus 0.5% (w/v) trypsin.

These indicate that the elimination process (the extracted of DAPI from the bone sample) happened very fast in the bone samples incubated in digestion buffer plus trypsin. By using the trypsin as detergent agent, the penetration and extraction of DAPI

staining into the internal structure of the bone samples was helped and then detected as fluorescence by Spectrofluorophotometer.

3.4 Conclusion

These studies have proved that combination of treatments such as chemical, biological, and physical could produce a successful decellularisation protocols. The most effective protocol to decellularise the trabecular bovine bone was with digestion medium plus trypsin incubated overnight for at least six cycles. No further release of DNA took place in the presence of digestion buffer plus trypsin after 4 successive 24 hr incubations. DAPI staining was an effective method to detect the elimination of cells (e.g., DNA) from the bone specimens.

Chapter 4

THE EFFECT OF DECELLULARISATION PROTOCOLS ON MECHANICAL PROPERTIES OF BONE SAMPLES

4.1 Introduction

4.1.1 The mechanical properties of bone

By loading a sample of compact bone in tension (see **Figure 4.1**), the stiffness (Young's modulus) for isotropic materials can be represented as follows:

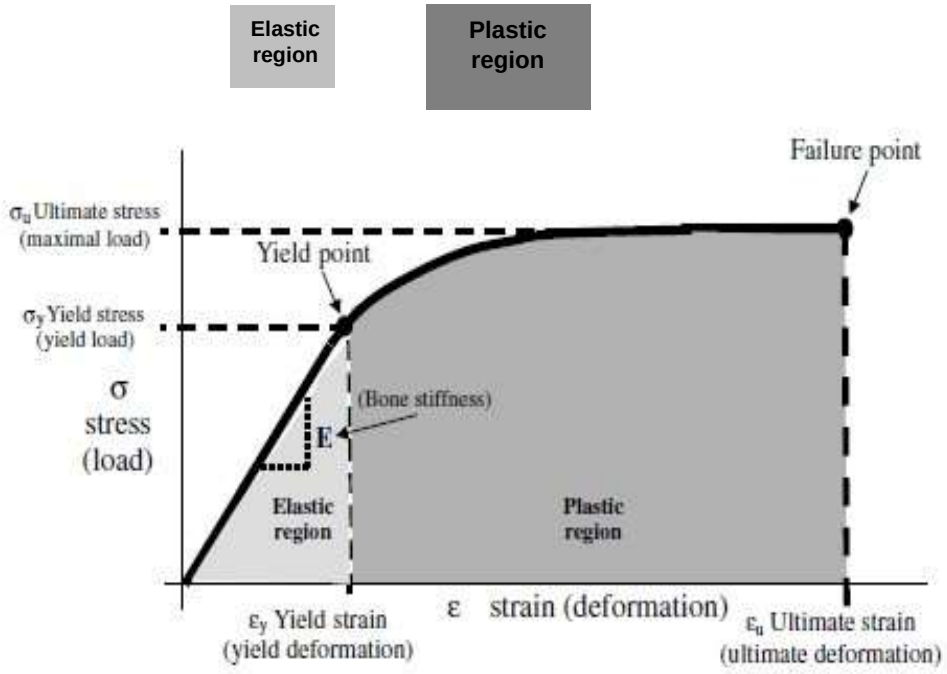

Figure 4.1: The stress-strain curve obtained by loading a sample of compact bone in tension. Adapted from (Sharir et al., 2008).

The mechanical integrity of bone can be characterized in several biomechanical parameters as stated in **Table 4.1**.

Graph	**Parameter**	**Representation**
Loaddisplacement curve	- Slope of elastic region	- The extrinsic stiffness or rigidity of the structure.
	- Ultimate force (Fu)	- General integrity of the bone structure.

	- Work to failure (area under the curve)	- The amount of energy necessary to break the bone.
	- Stiffness	- Closely related to the mineralization of the bone.
	- Ultimate displacement (du)	- Inversely related to the brittleness of the bone.
Stress-strain curve	- Slope (within the elastic region)	- Called Elastic or Young's modulus (E). It measures the intrinsic stiffness of the material.
	- Area	- Measure of the amount of energy needed to cause material failure. This property of a material is called energy absorption or modulus of toughness or just toughness.
	- Ultimate strength	- Maximum stress of the bone. The maximal load it can carry without breaking.
	- Ultimate strain	- Maximum strain of the bone.

	- Yield point (The point where this line intersects the stress-strain curve is arbitrary)	- Separate the elastic strain region and the plastic strain region. - A gradual transition, above which stresses begin to cause permanent damage to the bone structure.
	- Post-yield strains (i.e., strains beyond the yield point)	- Permanent deformations of bone structure caused by slip at cement lines, trabecular microfracture, crack growth, or combinations of these.

Table 4.1: Mechanical integrity of bone characterisation (Turner, 2006).

Porosity is the main factor of the mechanical properties of bone tissue. Porosity is also known as the fraction of the bone volume filled by "voids", such as Haversian canals (in cortical bone) or inter-trabecular marrow spaces (in trabecular bone). It is also called the bone volume fraction. As expected, bone strength and stiffness decreases when the porosity increases. Bone porosity differs extensively; hence the stiffness can be adjusted from nearly zero in scattered trabecular bone to almost 15GPa in cortical bone. In typically solid material, the stiffness decreases quickly with minor changes in porosity. The gradient of the curve is relatively small if the composition of bone is controlled by voids (Martin, 1991).

Another factor is related to mineralization in which it differentiates between the mineral and organic elements of the solid matrix, and is recognized as the mass

fraction of the mineral. The mechanical properties of bone are associated with the grade of mineralization of the bone matrix, obtained from the ratio of residue mass to dry mass (Martin, 1991). Compared to cortical bone, trabecular bone modulus is lower because the material density of trabeculae and the bone mineral content (BMC) are smaller than those found in cortical bone. In fact, the percentage of BMC in cortical and trabecular are 63% and 51%, respectively (Ashman & Rho, 1988). It has been proven by several researchers that bone stiffness (elastic properties) is directly linked (linear or exponential) to its mineralization (Martin, 1991; MarcosCampos et al., 2012; Ashman & Rho, 1988). In scaffolds, the amount of minerals affects the creation of a bone-like architecture (Marcos-Campos et al., 2012). If the mineralization increases, bone stiffness is also increased. Moreover, mineralization is mostly controlled by the rates of bone modelling and remodelling because it takes almost six months to have a complete mineralization for freshly produced bone. Mineralization is also influenced by imperfect calcification of osteoid or of growth cartilage (in children) which causes reduction of mineralization (Martin, 1991).

Meanwhile, variation in the material properties of bone may be explained in relation to its density. Density means the specific gravity of the solid matrix and apparent density, or bulk density means the mass/unit volume of an area of large bone that consists of Haversian canals, marrow spaces, and other voids. Thus, a function of either the porosity or mineralization of the bone material is referred to apparent density (Martin, 1991).

The distribution of the solid matrix in bone is extremely changeable and very different even though two areas may have the same porosity and mineralization. For example in trabecular structure, the placement and arrangement of trabeculae affect the failure stress and elastic modulus of cancellous (trabecular) bone, in addition to the

anisotropy of these changes. In fact, the anisotropy of macroscopically obtained material properties is dependent on the numbers and sizes of trabeculae positioned in dissimilar directions. Besides, both porosity and trabecular positions influence the cancellous bone. The solid matrix of the bone is theoretically assumed as homogeneous and isotropic within single trabeculae. The increase in the ratio of the surface area to bone matrix volume (respective to cortical bone) also affects the strength of trabecular bone. Trabeculae inhabit a small region of the space and anisotropy is controlled by their orientation in cancellous bone (Martin, 1991).

Another determinant which may play a role in the strength of bone is the distribution of collagen fibres which refers to the existence of lamella and the orientation of component collagen fibres in cortical bone. This characteristic of architecture is seemingly governed by extracellular physical processes (called "micromodelling"), as well as cell functions. Tissue strength is affected by the predominant position of the collagen fibres with regard to the mode of loading. For example, transverse fibres assist strength in compression but longitudinal fibres assist strength in tension. However, there are no studies that relate to the collagen fibre orientation characteristics in cancellous bone (Martin, 1991).

4.1.1.1 The mechanical properties of cortical bones

In general, bone tissue consists of a two-phase porous composite material, i.e. the collagen and the mineral. Therefore, the mechanical properties of bone are determined by the quantities, molecular structure and organization of the collagen and mineral components. Collagen is important for the toughness of bone. This constituent

makes the bone less brittle, enabling it to better withstand fracture and to increase work to failure of bone. Collagen has a small effect on both the strength and stiffness of bone, as it mostly promotes its toughness. Meanwhile, the mineral phase is vital for the stiffness and strength of bone. Bones will plastically deform under load if there is inadequate mineralization. However, too much mineral content (or an alteration in the stoichiometry or quality of the mineral) will result in increasing the brittleness of bone. Therefore, both strength and brittleness of the bone are affected by the ratio of mineral to collagen (Turner, 2006).

Due to its ordered microstructure, bone is anisotropic (having different properties in different directions) (Sharir et al., 2008; Syahrom et al., 2010; Alvarez & Nakajima, 2009; Ashman et al., 1987) and due to its water content, bone is also viscoelastic (the relationship between stress and strain being time dependent).

The mechanical properties of the bone can be described through mechanical testing (Syahrom et al., 2010; Ritchie et al., 2008). The evaluation of mechanical performance of whole bones depends on whether experiments are conducted *in vivo* or *in vitro*. The most common test for entire bones is compression or bending (Sharir et al., 2008). Excised samples of bone may be mechanically tested in a variety of ways: e. g. tension, compression, bending or torsion. Indentation testing (micro- or nano-) and ultrasonic techniques are also capable of providing valuable measurements (Alvarez & Nakajima, 2009; Ashman et al., 1987; Goldstein, 1987; Sharir et al., 2008). Irrespective of testing modality, important factors that have a bearing on the mechanical performance are environmental conditions (wet/dry samples or temperature), animal species, age, disease, and bone anatomy (Alvarez &

Nakajima, 2009).

4.1.1.2 The mechanical properties of trabecular bones

Trabecular bone is anatomically located in the vertebral bodies of the axial skeleton and at the end of the long bones of the appendicular skeleton. Maximal strength for minimum mass for the whole skeleton is provided by the complex porous structure. The structure of trabecular bone is reliant on the forces acting upon it. The mechanical properties of trabecular bone are different among individuals due to the loading history, co-morbidities, nutrition, social, and work activities that influence the metabolic rate of bone, independent of direct mechanical stimuli. In fact, the trabecular construction is very changeable due to variations in bone volume fraction (significantly different between males and females due to the variations of trabecular microstructure in clinically related skeletal sites) and the arrangement of trabecular components in space (within skeletal sites and between skeletal sites) (Ashman et al., 1987).

The mechanical properties of cancellous bone are different from cortical bone because of its porous structure, with the porosity being in the range of 75% - 90%. The measurement of the elastic properties of cancellous bone is potentially problematic due to inhomogeneity, porosity, anisotropy (need to determine the mechanical properties in altered directions), and size restrictions (Ashman et al.,

1987)

The microstructure of cancellous bone is anisotropic, highly heterogeneous and affected by skeletal position because of the variation in external mechanical stimuli. Consequently, the mechanical properties will differ based on the level of fitness of the patient in addition to the position from which the bone was taken, and it will also

degenerate due to skeletal diseases such as osteoarthritis and osteoporosis or due to aging (Syahrom et al., 2010).

In order to resist fractures, bone has the ability to adapt to mechanical stresses and external loading situations (Turner, 2006; Lambers et al., 2013) by altering its size and shape (Turner, 2006). It seems that bone remodelling is sufficient to sustain the mechanical integrity of bone. Following a change in stress environment, dynamic bone remodelling rates are increased until the stiffness of bone is sufficient to maintain the new loading state. Once reformed, bone remodelling rates reach an equilibrium, in which the greater bone stiffness and bone volume fraction are conserved (Lambers et al., 2013). Frost (1994), in his review for clinicians of bone's structural adaptations to mechanical usage, summarised Wolff's Law (1892) by stating that "*Every change in the form and function of bone or of their function alone is followed by certain definite changes in their internal architecture, and equally definite alteration in their external conformation, in accordance with mathematical laws.*"

Bone tissue is weakest in tension or shear and strongest in compression (Sharir et al., 2008; Turner, 2006), thus cracks tend to propagate along tension or shear planes within the bone tissue.

4.1.2 Microdamage

Damage in trabecular bone is a regional condition originating from microstructural stress and stress concentrations. Various types of microfracture (**Figure 4.2**) (such as buckling, bending, and shearing) and microdamage (such as

single, parallel, and cross-hatched cracks) are produced from these regional stresses and strains (Moore & Gibson, 2002). Physically, microdamage is caused by falls or other unusual loads that produce localised shear stress above that which the bone can readily absorb without damage (Wang & Niebur, 2006).

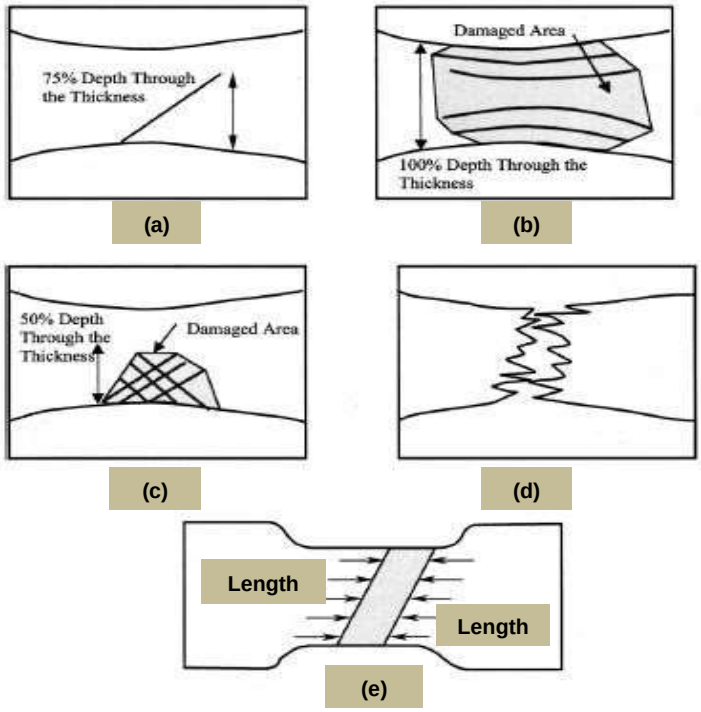

Figure 4.2: Representation of forms of microdamage in trabecular bone (a) single crack (b) parallel cracks (c) cross-hatched cracks (d) whole fracture (e) impaired band across segment. Adapted from (Moore & Gibson, 2002).

During normal loading processes, the key stresses are mainly associated with the major orientation of trabecular bone whereby the stresses are “on axis”. Meanwhile during falls or other unusual loading, the key stresses are “off-axis”. By itself, microdamage created during one fall may exacerbate bone breakability for subsequent falls. The creation of microdamage in trabecular bone happens when the apparent strain surpasses the yield strain during on-axis compressive overloading. Propagation of the microcracks under load further deteriorates bone integrity (Moore & Gibson, 2002). Microcrack propagation is restricted by microstructural

characteristics such as lamella boundaries, which blunt cracks and reduce stress concentrations at crack tips.

In a study of characterisation of microdamage and microstructural of human vertebral cancellous bone *in vivo* by Arlot et al. (2008), and in a study carried out by Burr (2003), it was found that age was directly proportional to microcrack density and diffuses damage. Microcrack density and diffuse damage were linearly and exponentially increased with age in cortical bone (from the femoral and tibial diaphyses) and in trabecular bone (from the femoral head and neck) (Burr, 2003; Arlot et al., 2008). The possible reason might be that the amount and activity of bone cells change with ageing. The existence of osteocyte apoptosis by microdamage in bone might be associated with either direct physical destruction of the cells or the canalicular/lacuna system (which acts to provide them with oxygen and nutrients) or mechanically sensitive signalling pathways (Noble, 2003).

Microdamage produces a deleterious effect on the mechanical characteristics in both cortical and trabecullar tissues in animal and post-mortem studies because it reduces both the elastic modulus and the work to failure (Noble, 2003; Burr, 2003; Wang & Niebur, 2006), reduces bone strength and toughness, increases energy dissipation when bone is impacted, and further, increases the risk of fractures (Noble, 2003; Burr, 2003; Arlot et al., 2008). Importantly, alterations in trabecular bone stiffness in a minor area, localised area may produce huge changes in total bone strength (Wang & Niebur, 2006).

Wang and Niebur (2006) established that the more the shear strain, the greater the microcracks. Microdamage is more simply created and disseminated in

osteoporotic bone than in normal bone. Basically, greater microcrack density was related to lesser volume fraction, rod-like trabeculae and thinner trabeculae.

Microdamage may assemble in trabecular bone impacted in fatigue *in vivo*. No microdamage occurs during loading to strains lower than the yield strain; however, microdamage aggregation starts to lessen the stiffness and strength at loads beyond yield. All microdamage parameters increased with rising maximum compressive strain at greater strains (Moore & Gibson, 2003; Noble, 2003). The continual activities of routine life cause bones to be loaded in fatigue, and this fatigue loading may produce microdamage (Moore & Gibson, 2003; Noble, 2003; Lee at al., 2003). Fatigue-induced microdamage in bone tends to stimulate bone remodelling by initiating osteoclasts to resorb and osteoblasts to form new bone (Noble, 2003; Lee at al., 2003). Thus, bone has a remarkable characteristic which enables it to adapt to the current mechanical requirements of the organism. It is able to self-repair, sense, eliminate, and repair damaged or mechanically deficient volumes of bone (Noble,
2003).

4.1.3 Sterilisation of bone graft materials

After determining the mechanical properties of the bone samples, it was necessary to sterilise the scaffolds prior to using them for re-seeding with human cells. However, the present decontamination and sterilisation methods for bone graft

treatments, that consist of physical, chemical, and combined techniques have unexplained, unavoidable issues, and the topic remains a huge concern (Draenert & Delius, 2007; Haimi et al., 2008). In cancellous bone tissue, the concern of sterilization is really essential due to a high number of adipocytes that can avoid the process of chemical sterilization of the scaffold because of protective barrier creation (Quan et al., 2014). Therefore, allograft bone needs to be defatted (adipocyte removal) before chemical sterilization for a better effect (Haimi et al., 2008; Quan et al., 2014).

Moist heat at 60 to 100°C (usually called boiling) or demineralization do not accomplish complete sterilization and the process reduces the mechanical stability of the bone. But according to Draenert and Delius (2007), steam sterilization (also known as autoclaving) is microbiologically safe. The combination of dehydration and thermal denaturing has been reported to maintain the physiological stiffness of bone grafts and prevent damage by steam sterilisation. Bone tissue collagen type I and its fibrils produce many intra- and intermolecular covalent crosslinks, which can cause thermal denaturing (Draenert & Delius, 2007).

The autoclaving process was carried out for 20 minutes at 121°C and two minutes at 131°C, by Singh et al. (2010). They concluded that this technique can be utilised for reliable and whole sterilisation of total bone specimens. However, after autoclaving, the inductive capacity of bone is devitalised and, its osteoinductivity is decreased with increasing both temperature and time.

Singh et al. (2010) have also reported the effect of heat treatment on the bone mechanical strength. There were significant effects of the different treatment protocols on modulus and strain to failure and compressive stress to failure variables. It has been demonstrated in their study that the stress to failure strength devaluation was 55% (in

autoclaved samples) and 57% (in boiled samples) after treatment with heat at 100°C in the compression testing. However, no significant change in strength was demonstrated after treatment with heat at 60°C (pasteurization). From these outcomes, bone mechanical strength was decreased after treatment with heat above 100°C, but no effect was observed on mechanical strength after treatment with heat at 60°C. Furthermore, there were significant effects in modulus by 66% (in autoclaved samples) and 75% (in boiled samples) (Singh et al., 2010).

Collagen in bone can be affected by heating treatment. Collagen structure did not change with temperatures below 60°C while bone collagen tends to shrink at temperature higher than 80°C. In general, bone collagen deteriorated at 100°C and this will reduce the mechanical strength, while no effect was observed in heat-treated bone at 60°C. In addition, the reduction in the mechanical strength of heat-treated bone at 100°C was obtained in the torsional test compared to the compression test. It is known that bone strength in torsional testing is mainly influenced by the disintegration of collagen, while bone strength against compression is highly reliant on the bone density (Singh et al., 2010).

Usually a gradual reduction in the compressive modulus and strength of bone is influenced by the destruction of the bone microstructure after heating. Likewise, the decrease of strength and stiffness of trabecular bone by autoclaving will enhance the probabilities of early graft failure (Singh et al., 2010). Because of these reports on the susceptibility of bone to heat damage the mechanical properties of the decellularised bone scaffolds were measured before and after autoclaving to check for any heat induced deterioration in mechanical properties.

4.1.4 Porosity

In tissue engineering, a successful scaffold needs to consider the pore structure (Murphy & O'Brien, 2010). A porous extracellular matrix must be permeable with interconnecting pores, essential for placing cells, facilitating cell growth, allowing cell migration, permitting the access of cells and nutrients, and to generally regenerate tissues in 3D (Murphy & O'Brien, 2010; Yang et al., 2001, 2002).

Average pore size is a very important element in tissue engineering. The ratio of surface area to volume of a porous scaffold is basically a function of the density and mean diameter of the pores (Yang et al., 2002). Moreover, pore size is very celltype specific (Burg et al., 2000). The larger pores reduce the cell aggregations that expand along the end of the scaffolds. The specific surface area is obviously reduced and as well as cell attachment, that controls cell proliferation, migration and speed is decreased (Murphy & O'Brien, 2010; Murphy et al., 2010). Moreover, the mechanical properties of the constructs will be affected if the pores are too large because of void volume (Murphy & O'Brien, 2010). Although conversely, the smaller pores minimise the cell migration to the centre of the scaffold, causing the creation of a cellular pellet near the end of the scaffold. The flow of nutrients and elimination of waste are then restricted. As a result, necrotic areas within the scaffold occur. Pore size can affect definite measures like cell adhesion, vascularisation and infiltration in biological scaffolds. Thus, the balance between an ideal pore size (for cell movement) and particular surface characteristics (for cell adhesion) is required and has to be maintained (Murphy & O'Brien, 2010; Murphy et al., 2010).

The ECM delivers signals for cellular activity. The cells attach to their extracellular surroundings via particular ligand-integrin interactions. It has been revealed that cell attachment reduces with increasing pore size (Murphy et al., 2010). The constructs with bigger pores have less available surface area which causes lesser ligand density for early efficient cell adhesion. Cellular behaviour is affected by particular integrin-ligand communications between cells and the ECM. However, all the following activities like migration, proliferation and differentiation around the construct are facilitated by initial cell attachment. The results from Murphy's study have shown that the greatest degree of cell adhesion was created on the scaffolds with the smallest pore size of 96μm (Murphy & O'Brien, 2010; Murphy et al., 2010).

Likewise, the size of interconnecting pores is one of the vital aspects for bone ingrowth and the success of tissue growing into a porous scaffold is largely directed by the diameter of interconnecting pores (Itala et al., 2001). The optimal pore size for bone tissue engineering has been reported differently in the literature. Enlarged surface area (in scaffolds with small pores) may have a positive influence in early cell attachment, however, eventually the enhanced cellular infiltration (in scaffolds with bigger pores) overrides this effect and these later scaffolds might be ideal for bone tissue healing (Murphy et al., 2010). It has been demonstrated by Murphy et al. (2010) that scaffold mean pore size significantly influences cellular behaviour because any small variations in pore size will produce significant effects on cell attachment. In bone tissue engineering applications, scaffolds with mean pore sizes ranging from 20μm to 1500μm have been used. The minimum pore size for significant bone ingrowth is 75-100μm with an ideal range of 100-135μm as

demonstrated in early studies (Hulbert et al., 1970; Klawitter et al., 1976). Also several studies have proposed pore sizes of over 300μm for bone development and vascularisation within scaffolds, while osteochondral ossification can be promoted with pores smaller than 300μm, an average pore size of 325μm seemed ideal for bone tissue engineering. However, earlier studies have suggested a range of average pore sizes from 96 to 150μm to encourage best cell adhesion, and other work has suggested large pores sizes from 300 to 800μm for effective bone growth in bone tissue-engineering (Murphy & O'Brien, 2010; Murphy et al., 2010).

In a study obtained by Itala et al., in 2001, they stated that an ideal pore size for mineralized bone ingrowth is required to be 100-400μm, while the smallest pore size for significant ingrowth of new bone was between 75 and 100μm. The interconnections of the pore sizes larger than 100μm are needed to stimulate mineralized bone. It has been reported that there is no sign of new bone ingrowth under non-load bearing environments in scaffolds with pore sizes ranged from 50-
125μm. However, it is different under load-bearing environments in which the vital pore size for new bone ingrowth is about 140μm or larger (Itala et al., 2001).

Some other material characteristics may affect the osteoblast proliferation such as strain or other mechanical stimuli and surface structure. Cellular proliferation, adhesion, and phenotype can also be influenced by the size of particles, form, and surface roughness. Cells can distinguish very small variations in topography because they are most sensitive to topography, chemistry, and surface energy (Burg et al., 2000).

Optimal pore size is very cell dependent. From experiments regarding the effects of implant pore size on tissue restoration it has been shown that the ideal pore

size for neovascularization is 5μm, for fibroblast ingrowth is 5-15μm, for the ingrowth of hepatocytes is approximately 20μm, for growth of adult mammalian skin is 20-125μm, for culture of bone is 100-350μm, and for osteoid ingrowth is 40-100μm (Yang et al., 2001).

Overall, tissue engineering scaffolds need to have a matrix with various internal interconnected channels or pores of less than 500μm (Yang et al., 2002). In fact, cells are either necrotic or metabolically inactive because of low oxygen tension if they are more than 200μm from a direct blood source. Thus, mass transport is one of the most crucial aspects in tissue engineering. Insufficient nutrition distribution significantly limits the large-scale transplantation of tissue engineered structures currently (Yang et al., 2001).

4.1.4.1 Mercury porosimetry

Mercury porosimetry is a well-established method for the characterization of porous materials (Leon, 1998; Giesche, 2006). It is extensively used as a standard measure of the amount pore volume and pore size distribution in the macro- and mesopore ranges. In principle, mercury porosimetry is relevant for all types of solid materials (Leon, 1998). Using this approach, pore sizes around 500μm down to 3.5nm (Giesche, 2006), and from 0.4mm to less than 4nm (Leon, 1998) can be measured. Furthermore, mercury porosimetry obtains a broad range of data including the amount of pore volume or porosity, the pore size distribution, the skeletal and apparent density, and the specific surface area of a specimen (Giesche, 2006). Additionally, the data from mercury porosimetry can be described in terms of particle

size distributions, permeability, fractal dimension, tortuosity factors, compressibility, and also interprets pore shapes and network effects in any porous solid. In comparison with other pore size approaches recently (such as gas sorption, calorimetry, thermoporometry, etc.), mercury porosimetry is dependent on an easier principle (uses the Washburn equation - **Equation 4.1**), is much quicker (only takes minutes to make a complete pore size distribution compared to hours in gas sorption), and it can measure a very broad range of pore sizes, e.g. huge pores (more than 0.5μm) (Leon, 1998).

However, there are some limitations of mercury porosimetry. It determines the largest entrance close to a pore (refer **Figure 4.3**) and it does not indicate the real size of a pore. Mercury porosimetry is limited and cannot be applied for closed pores analysis because the mercury finds it difficult to penetrate that pore (Giesche, 2006). In addition, the use of mercury porosimetry is limited to calculate the pore volumes or pore sizes distribution only. Regardless of these drawbacks mercury porosimetry still is an enormously helpful analysis method and produces very significant information about the porosimetry of specimens (Leon, 1998).

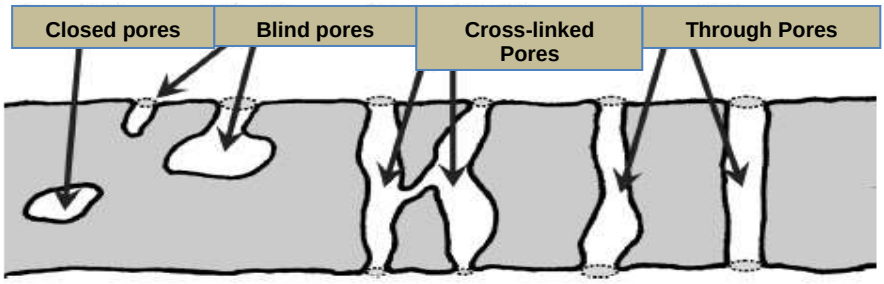

Figure 4.3: Types of pores. Adapted from (Giesche, 2006).

4.1.4.1.1 Theory and fundamental variables

The principle that the structure of porous solids could be defined by imposing a non-wetting liquid to enter their pores was founded by Washburn seventy-six years ago (Leon, 1998). Pore shape is the fundamental theory in mercury porosimetry. The analysis of mercury porosimetry data is conventionally based on the application of the Washburn equation. Basically all porosimeters assume a cylindrical pore geometry and apply the Washburn equation:

$$\Delta P = \frac{2\gamma \cos\theta}{r_{pore}} \quad \text{.....} \quad \textbf{Equation 4.1}$$

The Washburn equation explains the pressure change across the curved mercury edge (r_1 and r_2 define the curvature of that edge) to the equivalent pore size (r_{pore}) applying the surface tension of mercury (γ) and the contact angle (θ) in between the mercury and solid. However, the actual pore shape may be somewhat different as compared to the cylinder pore theory leading to differences between the analysis and reality (Giesche, 2006).

Bone is a porous material and it tends to absorb water or other chemicals. Any impurities should be eliminated during the early evacuation of the specimen.
The formation of artificial pores may also give errors because of filling of the specimen inside the penetrometer cell for example, and the inter-particle voids between (spray-dried) powder granules (Giesche, 2006).

At the low pressure system, the specimen is vacuated in order to eliminate air and remaining moisture or other fluids from the pore system. Then, the specimen is loaded with mercury while the whole system is still under decreased pressure. The penetration of the largest pores or any void spaces in the specimen can be obtained by gradually raising the total pressure. The initial measurement point is commonly recorded at a pressure of 3000 to 4000 Pa (0.5 psi) or higher to push mercury to load the specimen

cell. The specimen cell is then enclosed by hydraulic fluid and pressures of up to 414MPa (60,000 psi) are employed in an isostatic manner. This upper pressure limit is set by safety design margins (Leon, 1998; Giesche, 2006)

4.1.4.1.2 Data interpretation and analysis

Pores size distribution results produced by mercury porosimetry are mainly suitable for relative studies of the same or similar materials. The ultimate precision of the results relies on several theoretical and experimental aspects. Generally, pore size and pore volume data are repeatable within 1% standard deviation; however, interpretation of the results is restricted in three ways. Firstly, mercury porosimetry measures the biggest entrance to a pore instead of the real pore size. Secondly, the minimum pore size which can be occupied with mercury, is affected by the highest pressure that can be reached by the equipment such as 3.5nm diameter at 400MPa estimating a contact angle of 140°C. Lastly, the biggest calculable pore size is influenced by the height of the specimen, which measures a minimum "headpressure". For example, 1cm specimen height is roughly equal to 1mm diameter (Giesche, 2006).

In this chapter information of the following aspects of the decellularised bone scaffolds was obtained:

(i) the Young's modulus before and after freezing, decellularisation, and autoclaving the bone samples – using compression testing.

(ii) the effect of repeated mechanical testing on bone microdamage.

(iii) the porosity of the scaffolds – the range of pore sizes.

(iv) microscopic assessment of the surface of the bone scaffolds after decellularisation by SEM.

4.2 Materials and methods

4.2.1 Mechanical testing of the bones

4.2.1.1 Preparation of bone samples

Refer to the procedures mentioned in **Section 3.2.4.1** and **Section 3.2.5.**

4.2.1.2 Mechanical testing procedures

Compression testing of cuboidal specimens (dimension: 7 mm x 7 mm x 2 mm) was carried out by loading them longitudinally to 400 N compression (8.16 MPa), using a Bose ElectroForce 3200 (Bose Corporation, USA), fitted with a 450 N load cell, at 1 mm/s in a water bath at 37C (see " **Figure 4.4**). Compression was limited to 10 % of the bone sample thickness (2 mm) or to 400N, whichever came first. The orientation of bone samples was marked before the mechanical testing to ensure consistency between measurements (which was important because of trabecular bone's anisotropic properties). Thus orientation was kept constant. Stressstrain graphs were plotted and the Young's modulus, E obtained. Young's modulus is represented as the fraction of stress to strain under elastic area of the stress-strain graph (modulus of elasticity). To do these, the data of displacements (in mm) and load (in N) were extracted from the Bose ElectroForce 3200 software (called

WinTest software) and calculated by using Microsoft Excel. The Young's modulus (when examined under tension) is then determined by the slope of the linear areas of the stress-strain graph.

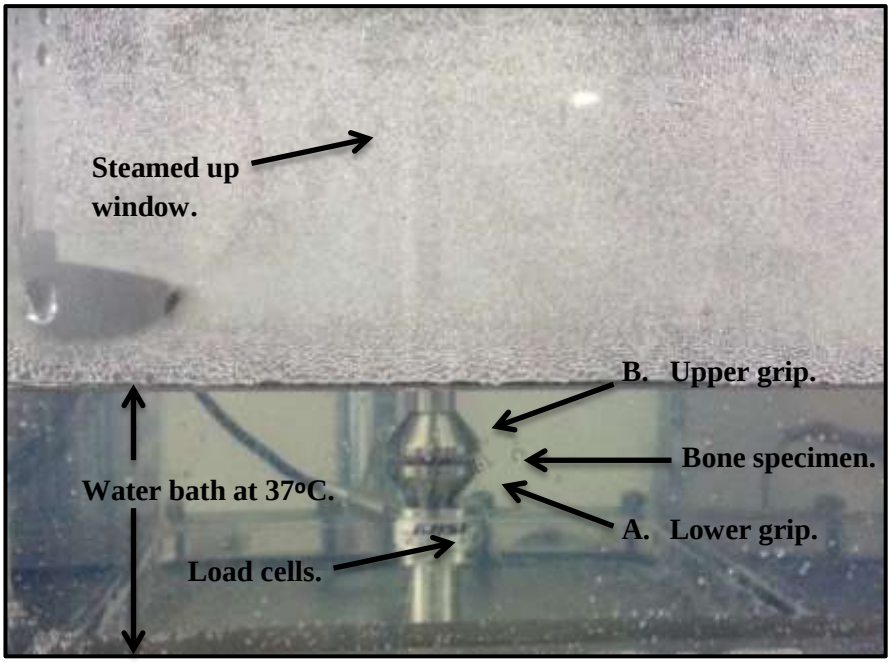

Figure 4.4: Bone specimen under compression test.

4.2.1.3 The Young's modulus of bone before and after freezing

Using the above protocol, six bone samples were tested for both fresh and frozen bones. The mechanical properties of fresh non-frozen bones were tested after keeping them overnight in the cold room at 4°C as explained in **Section 4.2.1.2**. Meanwhile, the frozen samples were stored in the freezer at -20C for up to 4 weeks. After that, the frozen bone samples were incubated at 37C for 2 minutes before measuring the mechanical properties. The mechanical properties of fresh and frozen bone samples were obtained, and compared.

4.2.1.4 The Young's modulus of bone before and after decellularisation

To determine the effect of decellularisation, another six frozen bone samples (stored at - 20C in the freezer for 4 weeks) have undergone the mechanical testing before the decellularisation process. Next, the same bone samples were treated with 0.6 nM DAPI for measurement of fluorescence. Decellularisation was carried out under the following conditions:

Sample 1: Bone samples were treated with 2 ml digestion buffer.

Sample 2: Bone samples were treated with 1.6 ml digestion buffer and 400 µl of 0.5 % (w/v) trypsin.

Six cycles of overnight incubations were carried out at 37°C under 5% CO_2/ air as described in **Section 3.2.5**. Decellularisation was monitored by treated the samples with DAPI as before. A comparison of mechanical properties in bone samples before and after decellularisation process was then obtained.

4.2.1.5 The effect of autoclaving on the Young's modulus of bone samples

Before decellularised bone could be used to prepare grafts they would have to be sterilised. This experiment was carried out to determine the effect of autoclaving on mechanical properties of the bone.

4.2.1.5.1 Preparation of decellularised bone scaffolds

Refer to the procedures mentioned in **Section 3.2.4.1** and **Section 3.2.5.**

4.2.1.5.2 Sterilisation process by autoclaving

Sterile saline 0.9% was prepared from 0.9 g of sodium chloride (NaCl) and 100 ml distilled water. The combination was filtered (0.22 μm filter) in the clean room. Next, bone samples that had undergone six cycles of incubations in 1.6 ml digestion buffer and 400 μl of 0.5 % (w/v) trypsin were placed in glass bottles that were filled with 5 ml of sterile saline and were autoclaved using the Classic Media Portable Steam Sterilizer (Prestige Medical Limited, England). The machine applied a set cycle of 121C for 22 minutes. The mechanical testing protocol was used before and after autoclaving process as stated in **Section 4.2.1.2**.

To make sure the samples were sterile, bone samples were added to both a 20 ml universal of BHI and SAB broth. BHI and SAB were used to detect the growth of bacteria and fungus respectively. These were then left in the incubator for 10 days at 37°C, and if they went cloudy the sterility test had failed and the samples were contaminated.

4.2.1.6 Scanning electron microscopy (SEM)

4.2.1.6.1 Procedures

Frozen bone samples were removed from the freezer (stored at -20C) and incubated for 5 minutes at 37C. Then, they were immersed in 0.5M NaCl (electrolyte) to avoid dehydration. SEM was carried out using the TM-1000 Table top SEM unit (Hitachi, Japan) with up to 1200x magnification and 15keV accelerating voltage. All bone specimens were imaged at different magnifications including 300x,

1000x and 1500x. Images were visually compared in term of structures and obvious defects in bone specimens before and after the
decellularisation process.

4.2.1.7 Porosity measurement

4.2.1.7.1 Preparation of bone samples

In this experiment, the bone samples were obtained from different protocols including:

i) **Sample 1**: Fresh bone samples (before undergoing six cycles of the decellularisation incubation process). ii) **Sample 2**: Frozen bone samples (before undergoing six cycles of the decellularisation incubation process).

iii) **Sample 3**: Bone samples were treated with 2 ml digestion buffer (after undergoing six cycles of the decellularisation incubation process).

iv) **Sample 4**: Bone samples were treated with 1.6 ml digestion buffer and 400µl of 0.5 % (w/v) trypsin (after undergoing six cycles of the decellularisation incubation process).

There were 3 different samples used for each protocol in order to enable statistical comparisons. Decellularised bones to be used for this experiment were prepared as explained in **Section 3.2.4.1** and **Section 3.2.5.**

4.2.1.7.2 Procedures

The porosity and pore size distribution of bone samples were measured before and after decellularisation using the PoreMaster-60 (Quantachrome Instruments, Florida, USA) in the Advanced Materials Research Laboratories (AMRL) at the James Weir Building with the help of Dr Fiona Sillars. The machine is able to determine the pore volumes in the range of about 1000 to 0.0035μm (35Å) diameter. Bone samples were placed in the cell assembly for low pressure measurements as shown in **Figure 4.5**.

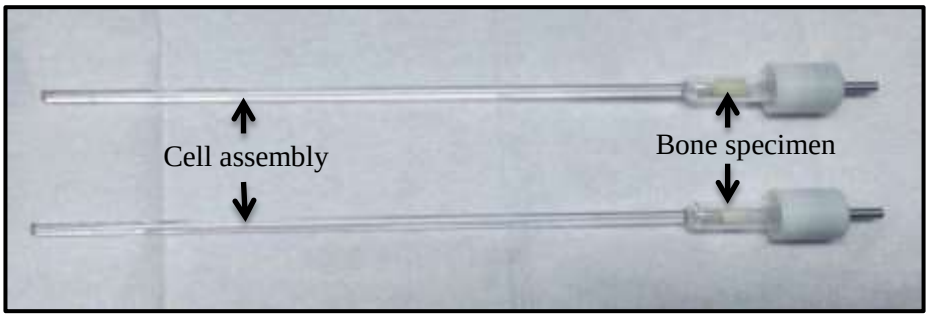

Figure 4.5: PoreMaster long sample cell assembly for low pressure measurements.

4.3 Results and discussions

Several test parameters have been measured in these studies to assess the Young's modulus before and after freezing, decellularisation, and autoclaving. In addition, porosity measurements, SEM images and microdamage aspects of the bone samples were also obtained.

4.3.1 The Young's modulus of bone before and after freezing

The effect of freezing on the Young's modulus of frozen bone samples was compared to fresh bone samples as shown on **Figure 4.6**.

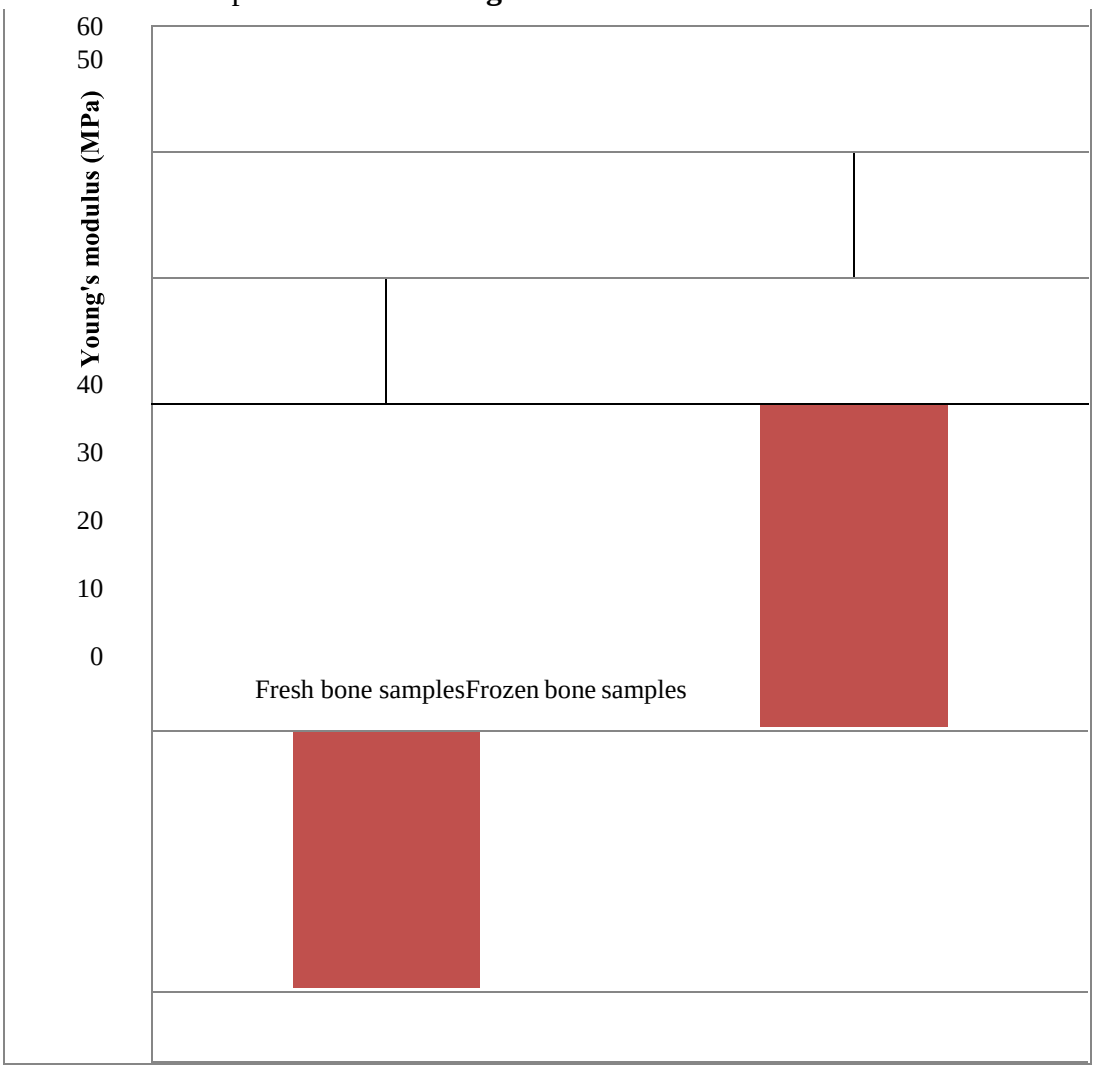

Figure 4.6: The effect of freezing on the Young's modulus of frozen bone samples compared to fresh bone samples. Results are mean ± SEM, n = 6. p>0.05 compared between fresh and frozen, by unpaired t-test.

In most studies, the bone was decellularised in fresh condition. For instance in a study by Quan et al., (2014), fresh porcine spine bones were decellularised within 24 hours after being harvested from a slaughter house. The samples were cleaned and rinsed in Tris-NaCl solution for one hour. The demineralised bone blocks were decellularised in acetone (for 17 hours) or chloroform/ methanol solution (for 6 hours), then rinsed in distilled water (for 12 hours) at room temperature. While Pathak et al., 2012 decellularised buffalo femur bone within 2 to 3 hours of slaughtering from the local slaughterhouse. Decellularisation of the bovine trabecular bone graft by Correia et al. (2011), Correia et al. (2012), Frohlich et al. (2010), Grayson et al. (2008), Grayson eta al. (2010), Marcos-Campos et al. (2012) were also carried out in fresh condition. Freezing the bone samples obtained from the abattoir did not affect the Young's modulus in the experiments reported here. In the experiments reported in this thesis all decellularisation was carried out in frozen bone samples. Soto-Gutierrez et al., (2011) reported that freezing tissues prior to decellularisation protocols aided cell lysis, and so this protocol would add to the efficiency of the decellularisation procedure.

4.3.2 The Young's modulus of bone before and after decellularisation, and after autoclaving

After the decellularisation protocols had been established, the effects of Young's modulus of bone samples before and after decellularisation process were carried out (**Figure 4.7**).

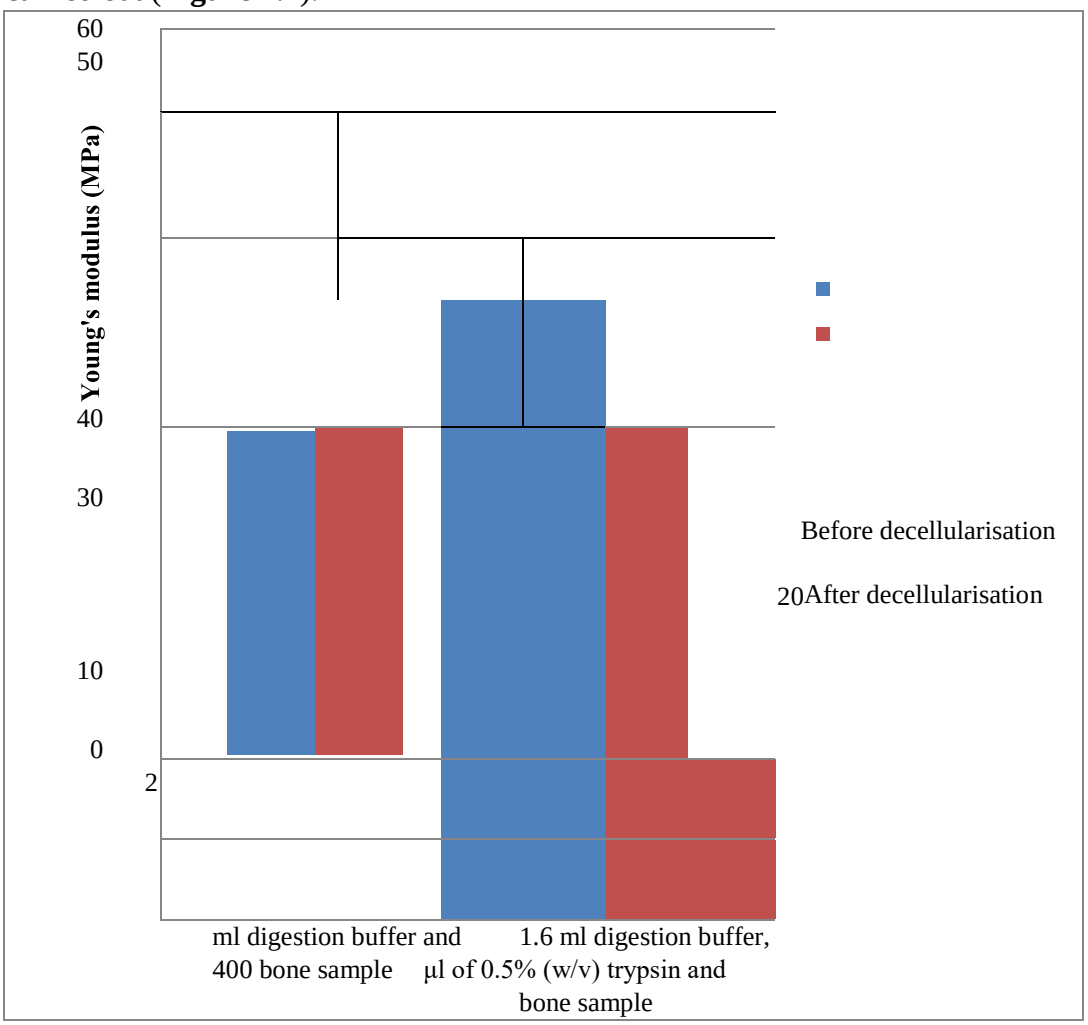

Figure 4.7: Young's modulus before and after six cycles of incubations with protocol A and B. Results are the mean ± SEM of n = 6. p>0.05 compared with the control (before decellularisation), by ANOVA for repeated measures.

In the preparation of bone samples for reseeding after decellularisation, a sterilised scaffold is required. To achieve this condition, all the bone samples were autoclaved at 121C for 22 minutes using the Classic Media Portable Steam Sterilizer (Prestige Medical Limited, England). The Young's modulus of bone samples were measured and then compared before and after autoclaving (**Figure 4.8**).

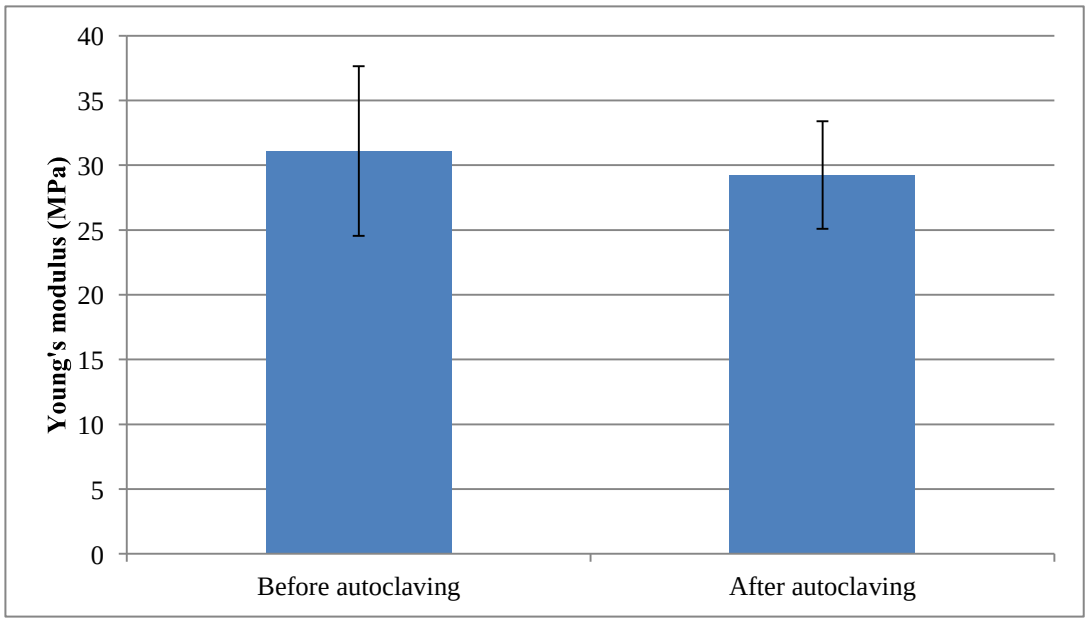

Figure 4.8: Young's modulus of bone samples before and after the autoclaving process. Results are the mean ± SEM of n = 6. p>0.05 compared with the control (before autoclaving), by ANOVA for repeated measures.

From the mechanical testing experiment, there were no significant differences in the Young's modulus between fresh and frozen bone samples (**Figure 4.6**), before and after decellularisation either with 2 ml digestion buffer or with 1.6 ml digestion buffer and 400 µl of 0.5 % (w/v) trypsin (**Figure 4.7**), and before and after autoclaving process (**Figure 4.8**). However, the stiffness of the frozen bone samples was slightly higher compared to the fresh bone samples. Storage procedures have been reported to affect the bone specimen's stiffness and strength (Goldstein, 1987). It was reported by Agbadua et al., 2011 that the impacts of thermal cycling on a material which is subjected to a temperature gradient cannot be underestimated. During this process it

expands differentially and thermal stresses are developed. The thermal cycling process involves the alternate heating and cooling of a material causing molecular reorganization which tightens or improves the granular structure of the material throughout, releasing stresses and creating it denser and more uniform thus reducing defects or imperfections. Moreover, the tighter structure also increases the energy conductivity and heat distribution characteristics of the material. However, according to Syahrom et al., 2010, thermal cycling can be reduced when drying and storing the samples in the freezer at -20°C.

There are some factors that influence the mechanical properties of the bone. The stiffness in an anisotropic material like trabecular bone depends on the mode and rate of loading and its geometry (Sharir et al., 2008; Martin, 1991; Holtrop, 1975). Greater loads in bone tissue can be achieved in the longitudinal direction and a smaller amount of load measured over the bone surface respectively. This is because the bone is used to accepting loads in the longitudinal direction and it becomes more durable (Holtrop, 1975). The force applied to the bone is dissimilar from the intrinsic strength because the ultimate load will differ according to bone size (Turner, 2006; Goldstein, 1987) as the bone samples used in the experiment were not exactly the same dimensions. Differences are also caused by the direction of applied load (Martin, 1991). The vast difference in the modulus and strength of the bone also may be caused by a function of anatomic position, storage procedures, conditions of testing, and loading direction (Goldstein, 1987).

As stated above, the bone samples used in the experiment were not exactly the same dimensions and also some variation was caused by the direction of applied load. Some of the previous papers have regarded the size and shape of the samples. The most

commonly used shape was cylindrical, followed by block or square shape. The sizes ranged from 1.75 mm to 25 mm (diameter) and 2 mm to 20 mm (thickness) for cylindrical-shaped (Syahrom et al., 2010; Correia et al., 2012; Marcos-Campos et al., 2012; Frohlich et al., 2010; Pathak et al., 2012; Grayson et al., 2010; Grayson et al., 2008) while block-shaped was 4 mm (width) x 4 mm (length) x 3 mm (thickness) (Quan et al., 2014).

In this study, bone samples were physically cut into square shapes (small blocks) with dimensions of 7 mm (width) x 7 mm (length) x 2 mm (thickness). The possibility to damage or break the samples during testing is less in this square shape as opposed to cylindrical shape. In fact, the use of 400N of compression force to the samples did not break any of the samples. Several strength tests have been measured in bone biomechanics studies including bending, compression, torsion and tension. But in this research, the compression test has been applied because the transplanted bone is commonly subjected to many such loads *in vivo* (Singh et al., 2010). The common test for entire bones is compression or bending (Sharir et al., 2008). Bone tissue is weakest in tension or shear and strongest in compression (Sharir et al., 2008; Turner, 2006).

In general, the Young's moduli of tested bone samples in our studies were determined from 20 MPa to 50 MPa. Compared to the previous study carried out by Ashman & Rho (1988) on the measurement of trabecular bone material, the mean trabecular modulus of three human and one bovine distal femur, was 13.0 ± 1.47 GPa and 10.9 ± 1.57 GPa, respectively. Meanwhile, as mentioned in **Table 4.6**, Hutmacher et al., (2007), Wilson et al., (1993), and Yang et al., (2001) stated that the Young's modulus of human cancellous bone was 0.02 – 0.5 GPa. Moreover, Orgaard

and Linde (1991) found that the average of Young's modulus was 689 MPa (by the extensometer method) and 871 MPa (by the optical method). The experiments were carried out in non-destructive uniaxial compression to 0.8% strain rectangular samples (human cancellous bones). In addition, Goldstein (1987) has reported in his reviews that the Young's modulus of human trabecular bone (proximal femur) applying unixial compressive stress was obtained from 20.68 MPa to 965 MPa (Schoenfeld et al., 1974) and from 1 to 9.8 GPa (Martens et al., 1983). Overall, the achieved values for the Young's modulus in our studies were much lower. This might be due to the non-parallel surface of bone specimens causing uneven load distribution during mechanical testing. Also, a parallax error could occur when measuring the bone specimens because ruler lacks precision. The measurements were often far less accurate compared to other measuring tools such as calipers (vernier or digital), micrometers, and protractor.

Parkinson and Fazzalari (2013) reported that the architecture of trabecular bone is reliant on the loads acting upon it and each individual bone has a different loading history. Moreover, the large mineral surface of the bone marrow enables cellular interaction in terms of eliminating or depositing bone in an extremely dynamic environment. Other reasons that trabecular bone structure alters include comorbidities, nutrition, social activities and work activities that disturb bone metabolism, independent of direct mechanical stimuli. The positive correlation between bone mineral density (BMD) and stiffness and strength is discussed by Turner (2006), however there is a contrary relationship between ultimate strain and bone stiffness (or Young's modulus). It seems that mechanical properties of the bone are generally affected by the molecular structure, quantities, and arrangement of the two-phase porous composite constituents of bone; collagen and the mineral. The toughness of

bone is conferred by the collagen. Meanwhile, the strength and stiffness are conferred by the mineral. But, the effects of too much mineral component are brittleness and destruction of the bone. Thus, the ratio of mineral to collagen is vital for both stiffness and strength of the bone (Turner, 2006). It has been proven that the elastic properties of bone are directly proportional to its mineralisation (Ashman & Rho, 1988). In the present experiments, there appears to be adequate mineralisation because the bones did not plastically deform under the applied load of 400 N.

Meanwhile, the mechanical properties of trabecular bone are mostly controlled by the trabecular architecture, collagen fibre organization and fatigue. Trabeculae occupy a minor area in trabecular bone; however, its direction and arrangement will affect the elastic modulus and failure stress. Moreover, the sizes and relative numbers located in various directions can be predicted to influence the anisotropy of the macroscopically determined material behaviour. On the other hand, the organization of collagen fibres is measured by the presence of lamella and the direction of the collagen fibre component. Different modes of loading will produce different effects as the longitudinal fibres and transverse fibres encourage strength in tension and compression accordingly (Martin, 1991).

In the present study, the applied compression force did not cause fractures in the bone. The bone samples have great toughness because they could resist fracture, and have high strength because they could resist plastic deformation (Ritchie et al., 2008). Interestingly, *in vivo*, in order to resist fractures, bone has the ability to adapt to mechanical stresses and external loading situations by altering its size and shape (Turner, 2006; Lambers et al., 2013). There was no evidence that application of a compression force of our samples caused any change in sample size and shape (see

Table 4.2 and **Table 4.3**).

4.3.3 The effect of repeated measurements on mechanical testing in bone samples

In every mechanical testing experiment, the samples were tested three times. To determine the effect of these 3 trials on the Young's modulus (stiffness) of bone samples, the measurements were analysed and shown on **Figure 4.9 A, B,** and **C.**

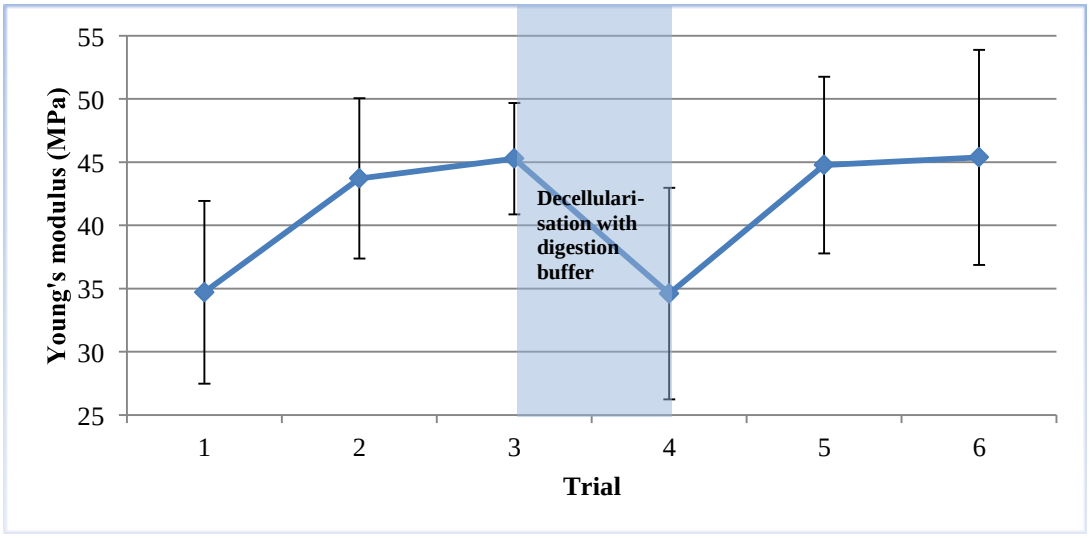

Figure 4.9: A) The effect of number of trials on Young's modulus in bone samples with 2 ml digestion buffer before and after decellularisation. Trial 1, 2, and 3 were before decellularisation while trial 4, 5, and 6 were after decellularisation. $p>0.05$, by ANOVA (one-way repeated measures). Results are the mean ± SEM of n = 6.

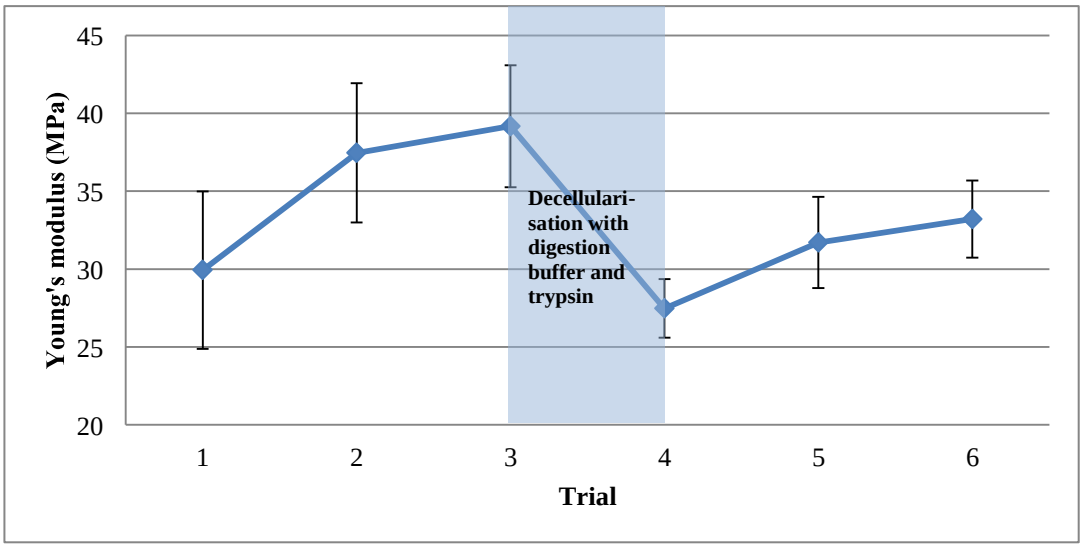

Figure 4.9: B) The effect of number of trials on Young's modulus in bone samples with 1.6 ml digestion buffer and 400 µl of 0.5 % (w/v) trypsin before and after decellularisation. Trial 1, 2, and 3 were before decellularisation while trial 4, 5, and 6 were after decellularisation. $p>0.05$, by ANOVA (one-way repeated measures). Results are the mean ± SEM of n = 6.

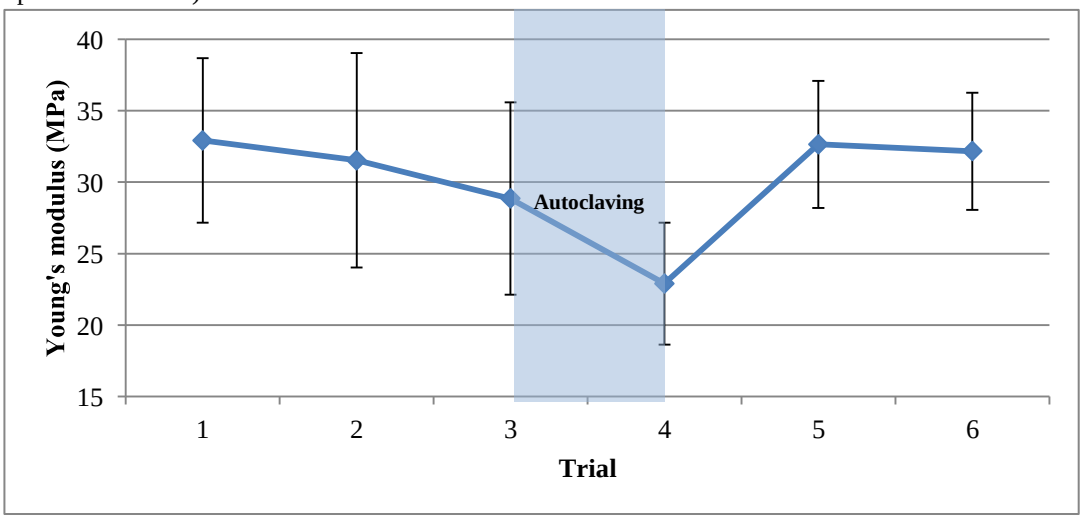

Figure 4.9: C) The effect of number of trials on Young's modulus before and after autoclaving process. Trial 1, 2, and 3 were before autoclaving while trial 4, 5, and 6 were after autoclaving.
$p>0.05$, by ANOVA (one-way repeated measures). Results are the mean ± SEM of n = 6.

It was found that the Young's modulus (stiffness) was gradually increased from one trial to another (trial 1, 2, and 3) before decellularisation either with 2 ml digestion buffer samples (**Figure 4.9 A**), or 1.6 ml digestion buffer and 400 µl of 0.5 % (w/v) trypsin samples (**Figure 4.9 B**). The continual trials and loading may have caused microdamage and local damage in the bone specimens (Moore & Gibson, 2003). Thus, these damage accumulations reduced the elasticity (stiffness) of the bone and have

increased density due to crushing of trabeculae. During loading situation in bone tissue, the energy is absorbed by the bone and is then released as damage assembles or when the bone cracks/fractures. Bone produces numerous cracks if exposed to high energy trauma because the energy assembles very fast and needs to be released (Turner, 2006). However, the stiffness was suddenly decreased after decellularisation (from trial 3 to trial 4). After the decellularisation, the same bone samples were tested for mechanical testing and the problem was found when relocating the samples on the load cells. The increase in stiffness might be due to the deformation instead of compression force when creating parallel specimens.

Moreover, the similar pattern of graphs were found from trial 4 to trial 5 (increased dramatically) and from trial 5 to trial 6 (increased steadily) in both protocols (**Figure 4.9 A** and **Figure 4.9 B**). Meanwhile in **Figure 4.9 C**, the stiffness was decreased slowly from trial 1 to trial 4. Again, the accumulation of microdamages reduces the stiffness of the bone samples before and after autoclaving. However, the stiffness seemed to be increased from trial 4 to trial 5 and it finally decreased slightly after trial 5. As discussed, the stiffness of bone is affected by the inorganic content (mineral) and does not relate much on the temperature and pressure applied during autoclaving.

In addition, further upsurges in load are commonly needed to sustain the plastic flow and an increment in displacement is called work-hardening or strainhardening. This phenomenon will take place with the increase of stress under plastic deformation. The bone becomes harder and stronger due to the dislocation of crystal structure of the material in the bone. The more dislocation in the material (materials become pinned and tangled with limited movement) the more strength in the bone. These moving dislocations will depend on the types of interactions that have occurred. Normally,

there is no obvious change in the microstructure of the distorted material. However, there must be some changes in elastic modulus due to the effect of work-hardening (Bouvier et al., 2005).

On the other hand, there were no significant differences in the bone samples either with 2 ml digestion buffer or with 1.6 ml digestion buffer and 400 µl of 0.5 % (w/v) trypsin, and before and after autoclaving process from the statistical analysis. To sum up, the Young's modulus (stiffness) was not affected by the protocols of using fresh or frozen bone samples, before and after decellularisation processes in digestion buffer with or without trypsin, and before or after the autoclaving process.

4.3.4 Microdamage

Another factor that affects the material properties of the bones as stated by Martin (1991) is the amount of microdamage. It is mainly caused by the loading history of bone specimens and also rate of turnover. This phenomenon is called "fatigue microdamage" and it changes the elastic modulus. It is known that bone mass is decreased when the mechanical loading is reduced, while bone mass is increased when the mechanical demand is raised. Hence, variations in the micromechanical environment are expected to cause variations in bone remodelling effects as well (Lambers et al., 2013). It is important to enhance the micro-architecture of the trabecular bone network against load-bearing in order to prevent any changeability in microstructure within the skeletal system (Parkinson & Fazzalari, 2013). A number of investigations have been carried out in this study to identify the possibilities of microdamage. In the present study, firstly, the samples were inspected visually after

measurements. The results have also shown that there were no variations in terms of dimensions (thickness) in all bone samples before and after the mechanical testing (**Table 4.2** and **Table 4.3**).

Sample	Thickness of fresh bone samples (mm)		Thickness of frozen bone samples (mm)	
	Before mechanical testing	After mechanical testing	Before mechanical testing	After mechanical testing
1	1.5	1.5	1.5	1.5
2	2.0	2.0	2.0	2.0
3	2.0	2.0	2.0	2.0
4	2.0	2.0	2.0	2.0
5	2.0	2.0	2.0	2.0
6	1.5	1.5	1.5	1.5

Table 4.2: The comparisons of bone thickness of fresh and frozen bone samples before and after mechanical testing.

Sample	Thickness of bone specimens with 2ml digestion buffer (mm)		Thickness of bone specimens with 1.6ml digestion buffer and 0.4ml trypsin (mm)	
	Before mechanical testing	After mechanical testing	Before mechanical testing	After mechanical testing
1	2.0	2.0	1.5	1.5
2	2.0	2.0	1.5	1.5
3	2.0	2.0	2.0	2.0
4	2.0	2.0	1.5	1.5
5	1.5	1.5	2.0	2.0
6	1.5	1.5	1.5	1.5

Table 4.3: The comparisons of bone thickness before and after decellularisation in samples with 2 ml digestion buffer, and 1.6 ml digestion buffer, 400µl of 0.5% (w/v) trypsin.

The use of bovine trabecular bone in this study means it is difficult to extrapolate specific findings from bovine to human as the former is usually denser than

human trabecular bone, especially osteoporotic human bone. Hence, the quantity of damage in human trabecular bone could only be estimated to be similar to that in bovine trabecular bone (Moore & Gibson, 2002).

As comparison, on the average an adult male cow weighs between 1,200 pounds (544 kg) and 1,800 pounds (817 kg), and adult females 1,100 pounds (499 kg) and 1,500 pounds (680 kg) from the same species such as Angus, Jersey, and Hereford (http://www.farmsanctuary.org/wp-content/uploads/2012/06/Animal-CareCattle.pdf). However, the average weight of an adult human is 137 pounds (62 kg) according to a league table of the world's 'fattest' nations from the London School of Hygiene & Tropical Medicine (http://www.telegraph.co.uk/news/earth/earthnews/9345086/The-worlds-fattest-countries-how-do-you-compare.html).

In bovine trabecular bone, microdamage has been represented in the uniaxial compression test. The displacements of a sample are expressed as the result of the displacement and the length of the sample for uniaxial loading (Singh et al., 2010). Microdamage variables were predicted to increase with the increase of compressive strain and with the decrease of normalized modulus during compressive fatigue loading in a study by Moore, 2003. However, microdamage was detected in bovine trabecular bone samples under compressive fatigue after the samples had been subjected to yield strain. From this it may be concluded that damage in bone is dependent on strain instead of stress (Moore & Gibson, 2003). All in all, it was proven that the applied force of 400N did not physically damage the bone, and did not cause variation to the dimensions of bone specimens during compression tests.

Another investigation was carried out to detect the microdamage in bone specimens by examining the specimens using the TM-1000 table top SEM. The bone

specimens were observed in different positions with different magnifications - x300, x1000 and x1500. This microdamage phenomenon might be caused by the repetitive trials. However, there was no damage or deformation of the local trabeculae in the internal buckling observed before or after the measurements.

The complex structures in the tissue (**Figure 4.10, Figure 4.11,** and **Figure 4.12**) could still be observed even after decellularisation of cells from the bone tissues (Benders et al., 2012; Gilbert at al., 2006). Furthermore, this approach is limited because only the macroscopic features of bone rather than microscopic features (trabecular or osteonal structure) can be seen, so it is not possible to detect the microdamage.

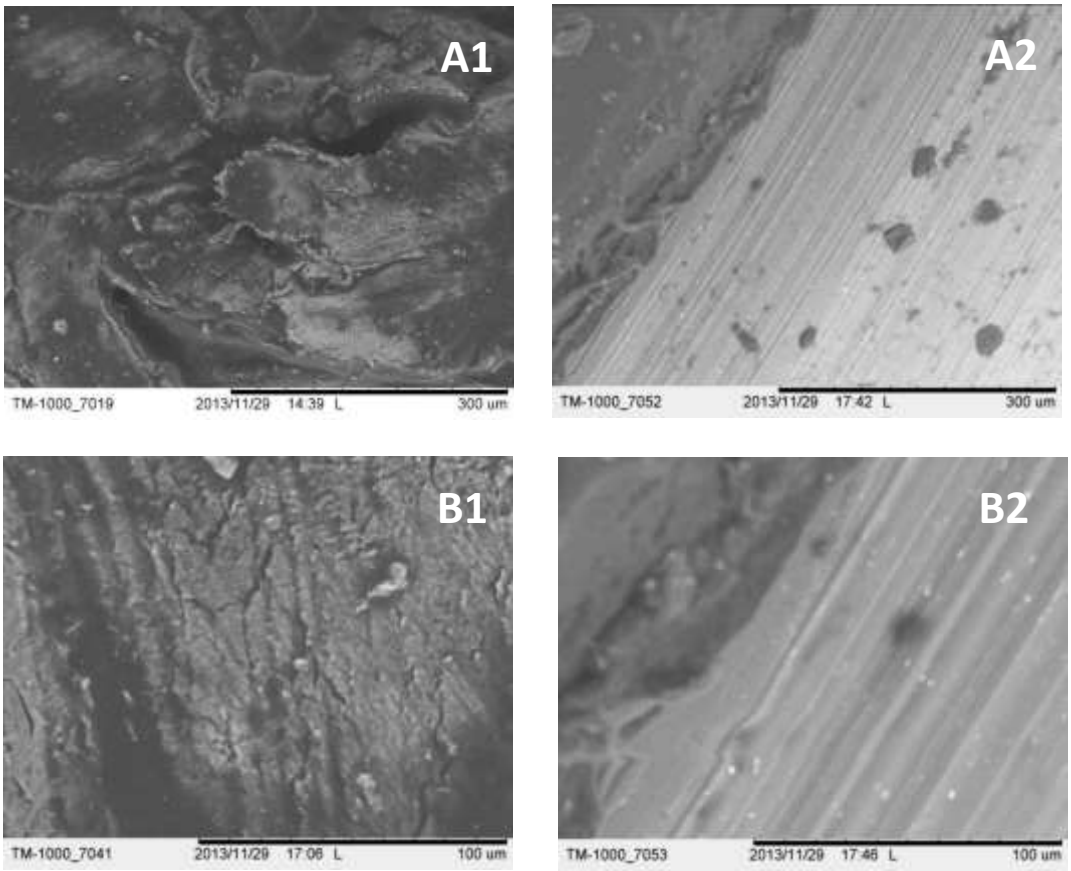

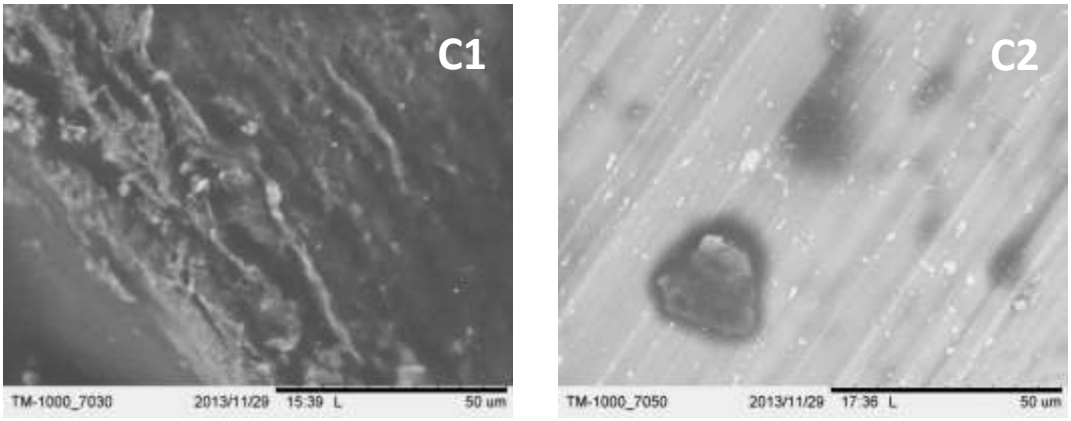

Figure 4.10: The SEM images of bone samples taken before the decellularisation process (control bone samples). SEM images : A1-A2) x300, scale bar = 300µm, B1-B2) x1000, scale bar = 100µm, and C1-C2) x1500, scale bar = 50µm.

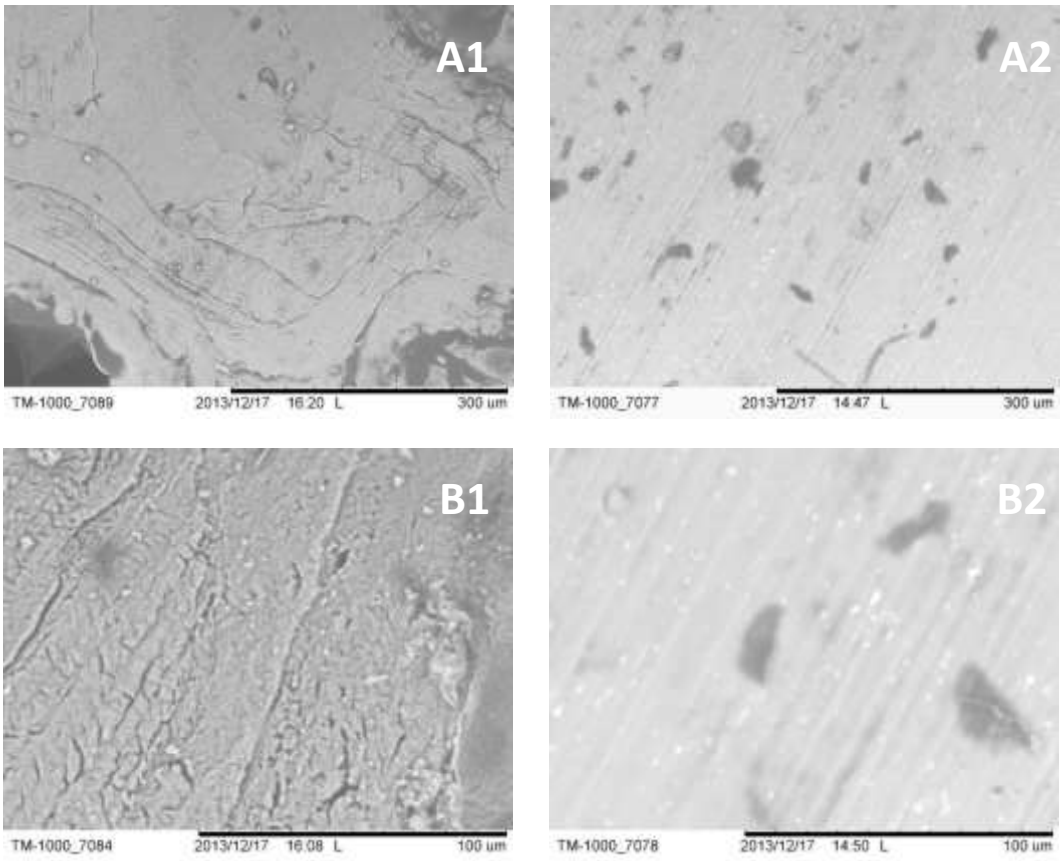

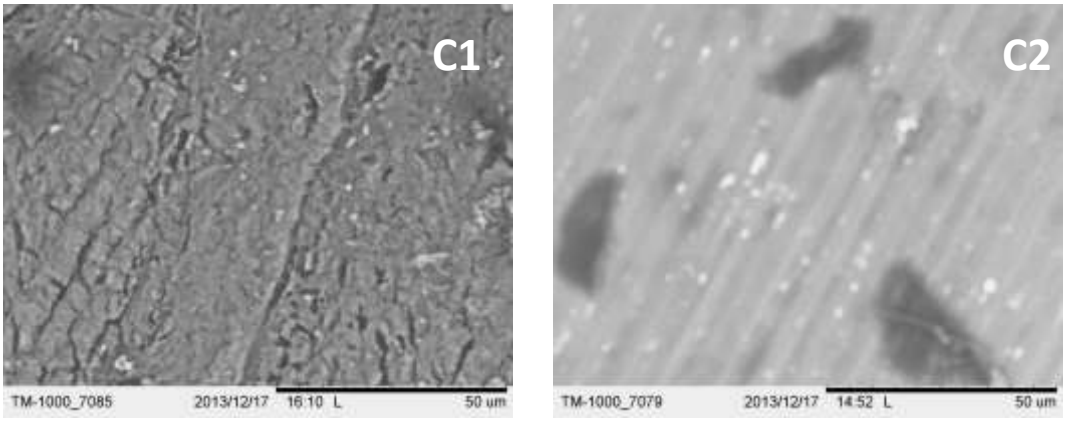

Figure 4.11: The SEM images of bone samples taken after decellularisation process with 2 ml digestion buffer. SEM images : A1-A2) x300, scale bar = 300µm, B1-B2) x1000, scale bar = 100µm, and C1-C2) x1500, scale bar = 50µm.

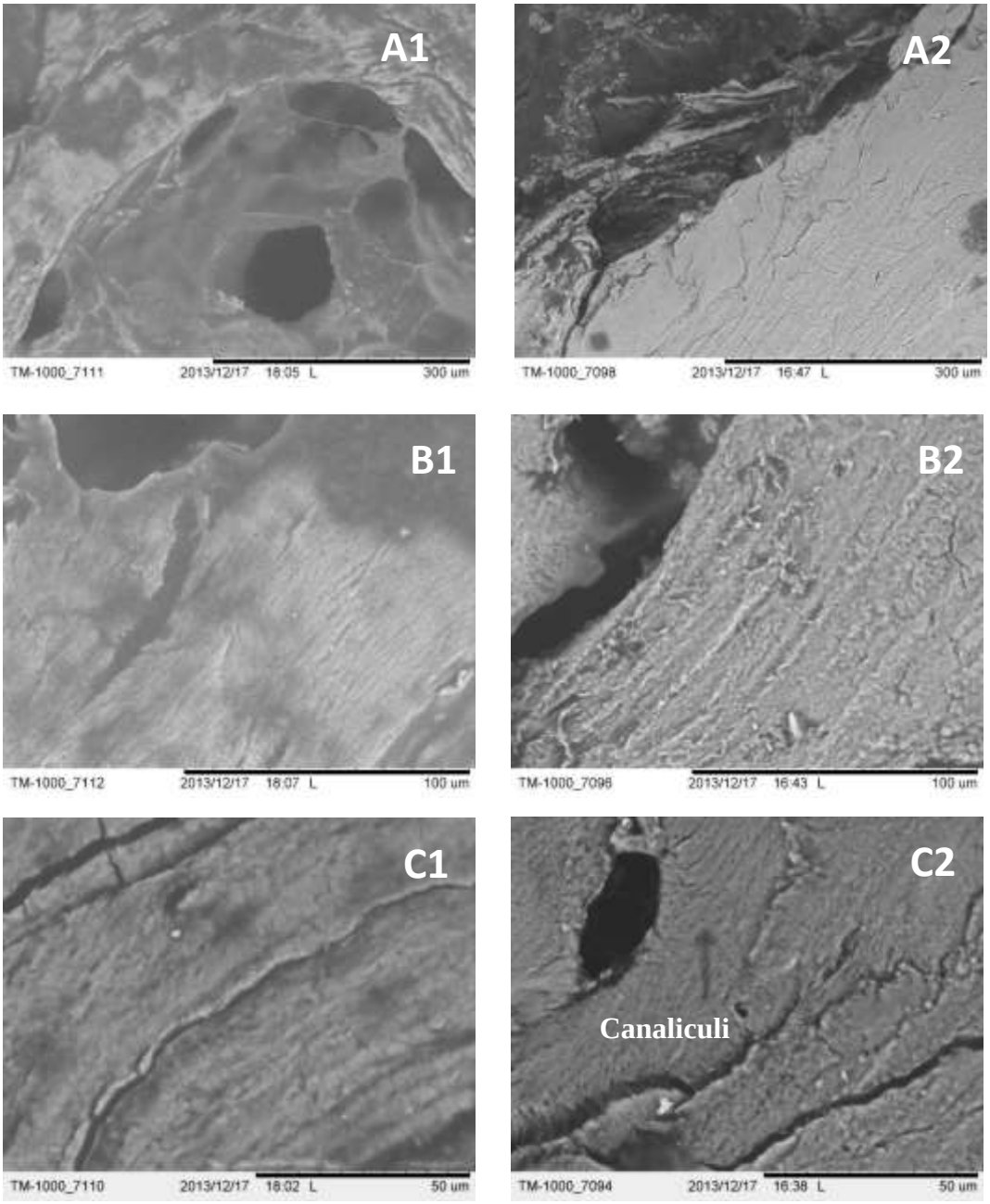

Figure 4.12: The SEM images of bone samples taken after decellularisation process with 1.6 ml digestion buffer and 0.4 ml trypsin. SEM images : A1-A2) x300, scale bar = 300µm, B1-B2) x1000, scale bar = 100µm, and C1-C2) x1500, scale bar = 50µm.

The investigation analysed the complete stress-strain curves during the mechanical testing. Generally, the calculation of Young's modulus (E) values (in MPa) of bone samples were derived from the files generated by the Bose ElectroForce 3200 software (called WinTest software) that consists of displacement (in mm) and load (in N). The values for stress (σ) were calculated by dividing the load or force (F) over the original cross sectional area (A) of the square-shaped bone sample (which was the width of the bone sample times the length). Meanwhile, the strain (ε) value was calculated by dividing the extension (δ) data (also from the Bose ElectroForce 3200 software) over the original length or sample thickness (L) of the exposed part of the bone sample after attaching the flat grips, which was 2 mm.

From the experiments, the stress-strain graphs primarily showed a linear relationship (regression) between the stress and the strain under the elastic region when the bone samples were incrementally loaded. Young's modulus was obtained from the slope of the linear region of the stress-strain curve (Sharir et al., 2008; Turner, 2006; Singh et al., 2010; Wendlova, 2008). The bone samples were compressed freely in wet conditions at a ramp velocity of 1 mm/sec to 10% thickness and maintained in that position for 10 seconds. The Young's modulus was determined from the equilibrium forces evaluated at 10% strain (Sharir et al., 2008; Correia et al., 2012). The steeper the slope, the higher the Young's modulus (also the stiffer the bone) (Sharir et al., 2008). Young's modulus (or stiffness, E) for all the different bone samples were not the same and all bone samples followed Hooke's Law which indicates that the load was directly proportional to extension of the bone sample as long as the elastic limit was not exceeded by this load (Sharir et al., 2008; Wendlova, 2008).

In other words, the plotted graphs described that there were no plastic deformation (permanent deformation). The stress-strain curves tended to present apparent hysteresis loops without residual strain during compression which performs elastic properties of bone (**Figure 4.17 A** and **Figure 4.17 B**), although the size and shape of the loops were different for all the tested specimens.

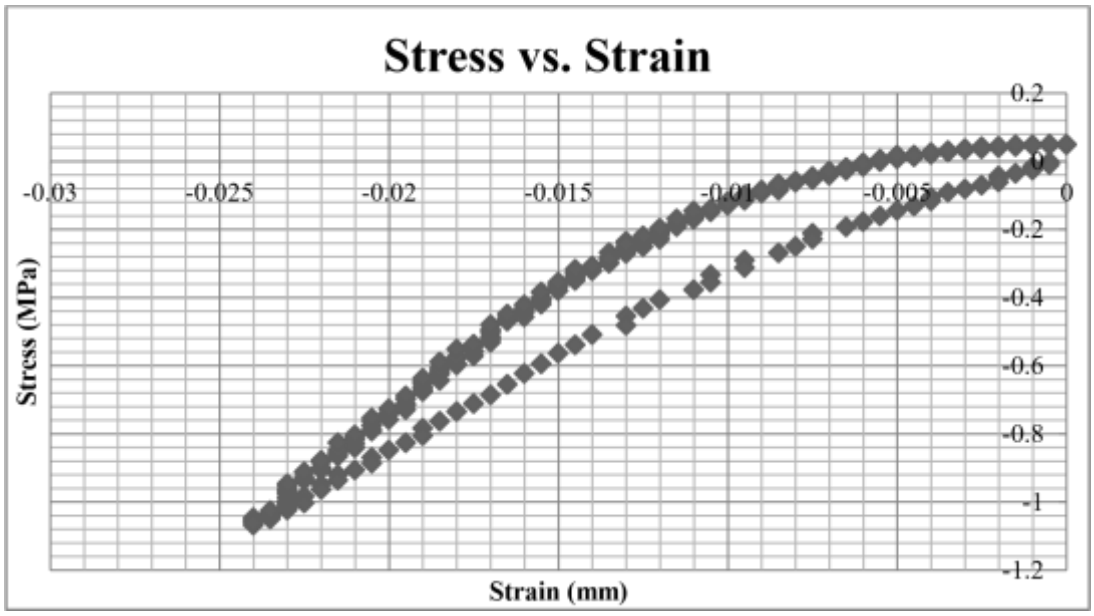

Figure 4.13: A) Stress-strain curves for bovine trabecular bone in compression. Specimen 1 was unloaded to zero strain.

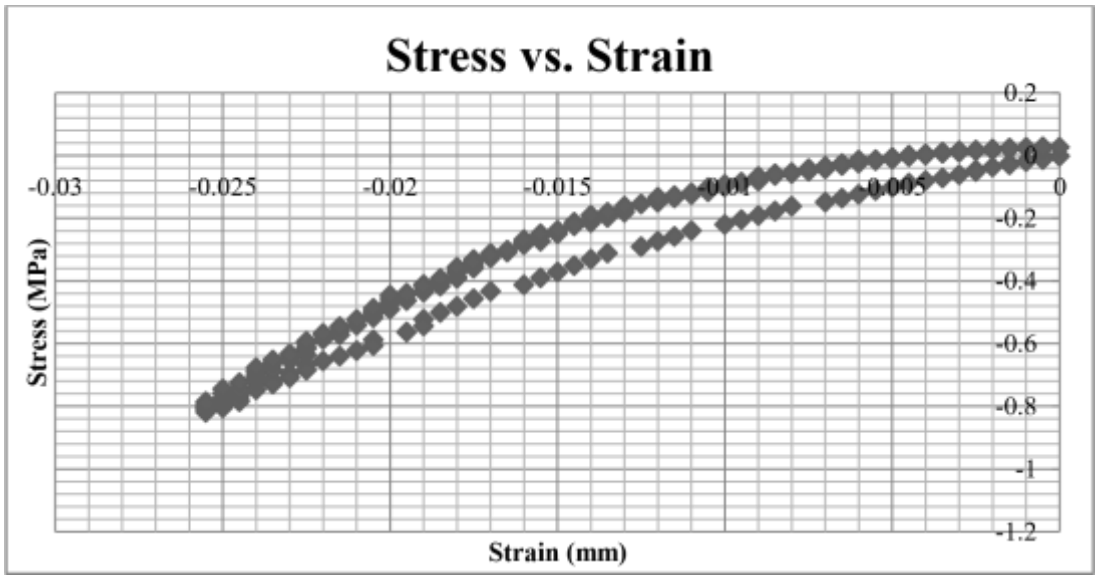

Figure 4.13: B) Stress-strain curves for bovine trabecular bone in compression. Specimen 2 was unloaded to zero strain.

Moreover, the highest stress was achieved before unloading. But, the graphs have not shown a toe region even though it seemed linear. The "toe" region is defined as the initial rapid elongation with negligible force increase (as indicated in **Figure 4.14**). There is a large nonlinear area displaced in the "elastic" area where the curve initiates to reach a straight line (Knudson, 2006). This could happen due to variation in the surface of bone sample (e.g., is it parallel or non-parallel?). The sizes and dimensions of total bone samples were not exactly similar. To minimise nonparallel surfaces and prevent further damage, the bone samples were supported during the cutting process (Moore & Gibson, 2003).

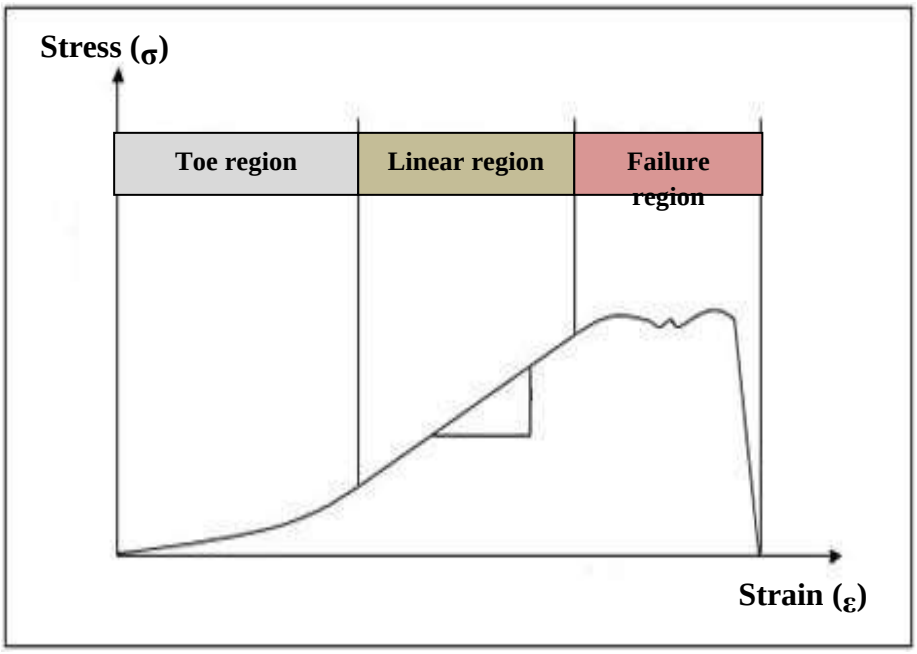

Figure 4.14: Stress-strain curve of biological tissue. Adapted from http://www. uweb.engr. washington.edu/research/tutorials/mechproperties.html.

There were a number of drawbacks in the present study. The small number of samples used in the experiment has affected the accuracy of the results. It was hard to make statistically significant decisions from these data. Six samples were used for each test group. Many more samples would be required for an equivalent fatigue

analysis. In fact, Moore & Gibson (2002, 2003) suggest that more than twenty-five samples would be needed in every test group to attain statistical significance.

4.3.5 Porosity measurements

Concerning the pore size diameter of fresh and frozen bone samples before decellularisation and the effect of decellularisation (pre and post) on the pore size diameter, several tests were carried out and compared as mentioned on **Table 4.4** and **Table 4.5**.

Protocols	Mean ± SEM (µm)
Before decellularisation in fresh bone	219.19 ± 0.44
Before decellularisation in frozen bone	211.35 ± 4.88

Table 4.4: The pore size diameter of fresh and frozen (control) bone samples before decellularisation. Results are the mean ± SEM of n = 3. $p>0.05$, compared between fresh and frozen by unpaired t-test.

Protocols	Mean ± SEM (µm)
Before decellularisation in frozen bone	211.35 ± 4.88
After decellularisation in 2 ml digestion buffer	212.44 ± 11.26
After decellularisation in 1.6 ml digestion buffer and 0.4 ml trypsin	223.28 ± 3.10

Table 4.5: The pore size diameter of frozen (control) bone samples before decellularisation and after decellularisation with 2 ml digestion buffer, and 1.6 ml digestion buffer and 0.4 ml of 0.5 % (w/v) trypsin. Results are the mean ± SEM of n = 3. $p>0.05$ compared with the control (frozen), by ANOVA for repeated measures.

In the porosity experiment, the actual pore size diameter for bone formation and growth were taken during an intrusion process (increasing pressure) for the whole area of each specimen by the mercury porosimeter (PoreMaster). The bone samples used for this experiment were independent as they were different from each other and the fact that different bone samples have a different anatomy and structure of trabecular bone must be accepted. In fact, two sections of bone having the same porosity and

mineralization may still have rather dissimilar material properties due to variation in the organization of the solid matrix (Quan et al., 2014).

In **Table 4.4**, the pore size diameter of frozen bones were not significantly different from the fresh bones ($p>0.05$, using the Student's t-test). The pore size diameter in fresh bone samples (219.19 ± 0.44 μm) was slightly greater than measured in frozen bone (211.35 ± 4.88 μm). There were also small standard errors of means found in fresh bone.

The effects of the decellularisation protocols (2 ml digestion buffer or 1.6 ml digestion buffer and 0.4 ml of 0.5 % (w/v) trypsin) on the pore diameters before and after six cycles of digestions were compared ($p>0.05$, using the ANOVA for repeated measures). It was found that there was no effect of decellularisation protocols with 2 ml digestion buffer or 1.6 ml digestion buffer and 0.4 ml of 0.5 % (w/v) trypsin on the pores size diameter before and after the process as shown in **Table 4.5**. Overall, the range of pore size diameters measured for these samples was from 211.35 μm to 223.28 μm.

Generally, the mean pore diameter (200 - 900 μm) seemed to be very appropriate for the growth of osteoblast cells based on existing literature studies (Itala et al., 2001; Murphy & O'Brien, 2010; Maquet & Jerome, 1997; Murphy et al., 2010; Salgado et al., 2004; Burg et al., 2000; Yang et al., 2001). Local changes in trabecular anatomy, orientation and density, in addition to mineral density difference may define anisotropy of bone specimens (Benders et al., 2012; Gilbert et al., 2006). To be used for reseeding process, an ideal pore structure needs to be considered in which there should be interconnections in order for cell migration, nutrient movement and growth to occur freely. Murphy et al., (2010) have reported a significant effect of mean

pore size on mouse osteoblastic cell line (MC3T3-E1) cell attachment in different pore sizes. Scaffolds with the biggest mean pore size of 325 μm enabled the greatest percentage of cell adhesion with about 62% of cells remaining adhered and feasible 24 hr and 48 hr after seeding. Cell adhesion rose to a peak with more than 45% of MC3T3-E1 cells remaining adhered to scaffold with an average pore size of 120 μm within the smaller range of pore sizes (85 μm to 190 μm). However, no significant variation was observed in cell attachment between intermediate scaffolds of 85 μm, 164 μm and 190 μm. Limited migration of cells, and minimised diffusion of nutrients into tissue and elimination of waste is the result if pores are too small, while there is a restricted specific surface area for cells to adhere to if pores are too large (Murphy et al., 2010).

Ideally, the mechanical properties of the decellularised should match those of living bone. Poor mechanical strength of porous scaffolds may not be appropriate for the healing of load-bearing tissues in many clinical applications. Mechanical properties of the surrounding environment of the scaffold should be considered once employed in an *in vivo* system depending upon the application. Other than giving proper support in the early phases of healing, the long-term accomplishment of the bone scaffold will rely on the effectiveness of graded load transfer required in the later phases of the remodelling process. The mechanical properties of the two types (such as cortical and trabecular bone) for human are shown in **Table 4.6**. Greatly porous structures with interconnected pores may cause low mechanical properties
(Martins et al., 2010).

Type of bone	Compressive strength (MPa)	Young's modulus (GPa)

Trabecular	2 - 12	0.02 – 0.5
Cortical	100 - 230	2 – 30

Table 4.6: Mechanical properties of the human trabecular and cortical bone (Hutmacher et al., 2007; Yang et al., 2001; Wilson et al., 1993).

In general, the material of all bones has similar constituents including mineral, carbonated hydroxyapatite, the structural protein, type I collagen, noncollagenous proteins and water. Bone is also a graded material and it may differ in terms of composition, architecture, and mechanical properties from one region to another. For instance, at the osteonal level, variations in the level of mineralisation result within osteons. This is because of the inner (which are newer) lamellae are originally less mineralised than the outer lamellae. But, they become more mineralised as they get nearer to the blood supply. Besides, the outer line of an osteon is regarded to be surrounded by very little collagen. Also, the interstitial lamellae (leftovers of old osteons) are more greatly mineralised compared to the osteons. This graded structure adversely influences the mechanical properties of bone, and may result in crack propagation. At a different level, the porosity of bone is increased at the transition between cortical and cancellous bone (from the periosteal to the endosteal surface) as both are also graded (Sharir et al., 2008).

Martin (1991) has determined the material properties of bone based on either compositional or organizational factors. In terms of compositional factors, there are porosity (which differentiate between voids and solid matrix in whole bone) and mineralisation (which differentiate between the mineral and organic constituents of the compact matrix) factors. Bone will decrease in both stiffness and strength with rising porosity. A structure with many voids will reduce the gradient of the graph (a

hypothetical plot of the relationship between porosity, p and the elastic modulus, E, of bulk bone). The degree of mineralization (stated as the ratio of ash mass to dry mass) of the bone matrix also plays an important role in the mechanical properties of bone. It has been revealed in many papers that the stiffness of bone rises in a linear or exponential manner with rising mineralization (Burstein et al., 1975; Currey, 1969a,b; Martin, 1991; Schaftler & Burr, 1988).

In addition, an increase of scaffold density would be expected to improve the mechanical properties of the scaffolds as reported by Marcos-Campos et al., 2012. The compressive elastic moduli were 15 ± 4 MPa (low-density), 45 ± 7.7 MPa (medium density), and 55 ± 3.3 MPa (high density). On the other hand, an increase of scaffold density could reduce the bone scaffold porosity with 88.3 ± 1% (lowdensity), 80.4 ± 1.7% (medium-density) and 70.4 ± 1.5% (high density) (MarcosCampos et al., 2012). The distribution of the solid matrix in bone is extremely changeable and can be very different even though two areas have the same porosity and mineralization (Martin, 1991).

4.4 Conclusion

It is clear that the mechanical properties of bone were not statistically affected by using the fresh and frozen bone samples, by the decellularisation process either with 2 ml digestion buffer or with 1.6 ml digestion buffer and 400 µl of 0.5 % (w/v) trypsin, or by the autoclaving process. Moreover, the estimated marginal means of stiffness were not influenced by using fresh or frozen bone samples, by the decellularisation process in digestion buffer with or without trypsin, or by the autoclaving process. However, the stiffness of bone specimens after the mechanical testing was trial dependent. Furthermore, the pore size diameter of control frozen bones were not significantly different from the fresh bones, and also there was no effect of decellularisation protocols with 2 ml digestion buffer or 1.6 ml digestion buffer and 0.4 ml of 0.5 % (w/v) trypsin on the pores size diameters. Not surprisingly, the mean of pore diameter from this study seemed to be very appropriate for the growth of osteoblasts. These findings have supported many previous studies regarding the mean pore diameter.

Chapter 5

THE DEVELOPMENT OF BONE SCAFFOLDS AFTER

RESEEDING

5.1 Introduction

Recellularisation involves the development of a scaffold or matrix to support cell attachment and differentiation. The scaffolds can be natural (such as collagen, alginate, ECM) or synthetic (such as polymeric, ceramic). Moreover, steady degradation of the matrix and its substitution by patient-derived new ECM are considered vital. Meanwhile, provision of a controlled environment is required to let the cells proliferate and differentiate into a tissue structure. Both physical and chemical properties of the environment are essential, and the stimulation of tissue by both chemical and mechanical information has to be regulated.

Theoretically, the ECM has a complicated combination of structural and functional molecules, which are normally formed in a unique, tissue-specific 3D ultrastructure and are perfectly suitable for the tissue or organ from which the ECM is chosen. It is possible that the particular composition and ultrastructural arrangement of the constituent molecules will differ depending on the source of tissue or organ from which the ECM scaffold is produced, because the ECM is created by the local cell populations. Consequently, a template for organ regeneration is very specific to the source of ECM e.g. ECM derived from liver may be the ideal

ECM substrate for hepatocytes (Wang et al., 2013).

As discussed, a successful decellularisation scaffold is achieved when it effectively removes cellular constituents, maintaining the extracellular matrix and the native tissue ultrastructure (e.g. pore size arrangements), enabling proliferation, cell adhesion, and movement of new cells into the construct (Quan et al., 2014).

In addition, the useful scaffold materials created from decellularised ECM could be stimulated by living cells before implantation with reference to the theory that the ECM is able to lead the differentiation of the seeded cells (Fu et al., 2014). To use the naturally created organ morphology, ultrastructure, and architecture from the original organs or tissues seemed to be more straightforward (for example, acellular heart valves), although it might be very complex (for example, whole-heart scaffolds), as acellular templates and frameworks (Patnaik et al., 2013). There should be no intact cells or nuclei left while collagen, intact ECM organization, and elastic fibres should remain after decellularisation of tissues (Wang et al., 2013).

Several fruitful recellularisation protocols in the literature have been reported. Song and co-workers (2013) stated that cadaveric kidneys can be decellularized and reseeded with epithelial and endothelial cells. Then, they can be developed to useful kidney scaffolds *in vitro*, and grafted into the orthotopic site to give excretory role *in vivo*. Moreover, Soto-Gutierrez et al., (2011) engineered functional liver tissue from decellularised xenogeneic liver. Three dissimilar approaches - direct parenchymal injection, multistep infusion, or continuous perfusion were performed reseed the liver tissue. From their findings, the recellularised liver matrix with the multistep infusion of hepatocytes presented approximately 90% cell engraftment and also assisted liverspecific functional abilities of the reseeded cells, including albumin creation, cytochrome p450 activity, and urea formation.

Frohlich and colleagues (2010) have reported on bone scaffolds generated *in vitro* by employing human adipose-derived stem cells (hASCs) on decellularised bone scaffolds in perfusion bioreactors (with medium perfusion). The reseeded hASCs on decellularised bone scaffolds used the structural and mechanical surrounding for

osteogenic differentiation and proliferation. Their studies have shown that the production of compact and functional bone tissue constructs can be achieved by the hASCs, decellularised bone scaffold, perfusion culture, and osteogenic additions. Corriea et al., (2011, 2012) also cultured hASCs on decellularised trabecular bone for 7 weeks in osteogenic culture to demonstrate the impacts of scaffold structure and biomechanical properties in stem cell differentiation towards osteogenic cells. The findings from their studies have also been used to improve silk scaffolds (a promising biodegradable biopolymer) in bone TE applications.

A study of TE strategy for generating *in vitro* a fully bone condyle consisting functional cells and well-constructed bone matrix has been carried out by Grayson et al., (2010). In their studies, hMSCs were reseeded to produce bone on a decellularized bone scaffold that had the specific geometry of the

temporomandibular joint (TMJ). This protocol seemed to have potential for solving a serious difficulty *in vitro* seeding of functional bone constructs of complicated geometries and also to give patient-specific bone constructs for craniofacial and orthopaedic regenerations again using adult stem cells.

Moreover, Quan and co-workers (2014) cultured umbilical cord bloodderived cells on the decellularised porcine bone to obtain an efficient protocol for xenogenic bone decellularisation and cell seeding for bone reconstruction. The attachment and proliferation of cells on accellular cancellous bone were confirmed by MTT and SEM after 5 weeks of culturing *in vitro* culture. The acellular bone scaffolds were implanted *in vivo* and did not cause an immune response. The findings from their studies proved that acellular bone scaffolds could support cell attachment and proliferation *in vivo*, without evoking an immune response.

The aim of this thesis was to use a demanding approach to eliminate all the cellular material from cores extracted from the trabecular areas of bovine bone, with the purpose of obtaining biological, degradable constructs, which are osteoinductive and may be reseeded with human cells to tissue engineer bone grafts for the clinical treatment of load-bearing body regions (Grayson et al., 2008). The key success factors in the recellularization processes are to accomplish a homogeneous cell distribution and to attain adequate cell survival (Gundula et al., 2012). **Table 5.1** shows some of the key recellularisation protocols used for different organs and tissues, and the methods used to characterise function of the new organ constructs.

Organ	RECELLULARISATION PROTOCOLS		
	Culture conditions	**Characterization of organ construct and functionality**	**Authors**
Heart	Culture medium (CM) perfused at atrial flow rate (FR) 20 mL/min, coronary FR 6 mL/min. 37ıı C 5% CO_2 incubator. Duration of culture: 4-8 days	Histology (engraftment) + immunofluorescence- Terminal deoxynucleotidyl transferase dUTP nick end labeling (TUNEL), α-actin, MHC, von Willebrand Factor (vWF), and connexin-43 (Cx43). TEM of ultra-architecture. Perfusion with 5-chloromethylfluorescein diacetate (CMFDA) to demonstarte endothelialization. Left ventricular (LV) pressure monitoring + live video to demonstrate contractile activity.	Ott et al., 2008
Heart	37ıı C 5% CO_2 incubator. Duration of culture: 4 days	Immunofluorescence-α-actin + β-tubulin to identify cardiomyocytes.	Wainwright et al., 2010
Lung	CM perfused at 10-15 mm Hg pressure with negative pressure ventilation. 37ıı C 5% CO_2 incubator. Duration of culture: 5-9 days	Histology (engraftment) + immunofluorescence-caveolin-1, T1α, Thyroid transcription factor-1 (Ttf-1), vimentin, pro-surfactant protein C (pro-SPC). TEM of ultra-architecture. Immunoblotting- SP-A, SP-C. Morphometry + stereology of lung architecture. *In vitro* function testing-blood gas values, dynamic lung function tests. Orthotopic transplantation into syngeneic male rats-fluoroscopy and live video, blood gas values.	Ott et al., 2010
Lung	CM perfused at 1-5 mL/min	Histology (engraftment, TUNEL) + immunofluorescence-cluster of differentiation 31	Petersen et

	with negative pressure ventilation at 1 breath/min. 37ıı C 5% CO_2 incubator. Duration of culture: 4-8 days	(CD-31), Clara cell secretory protein (CCSP), pro-SPC, aquaporin-5, α-actin, Cy-14. TEM of ultra-architecture. Stress-strain + compliance testing. Orthotopic transplantation into syngeneic male Fischer 344 rats + blood gas values tested to demonstrate gas exchange.	al., 2010
Lung	CM circulated by pump action at speed of 2 rpm. 37 ıı C 5% CO_2 incubator. Duration of culture: 14-21 days	Immunofluorescence-DAPI, live/dead staining, TUNEL, cytokeratin 18, CD31, proSPC, laminin, collagen IV.	Cortiella et al., 2010
Lung	Mechanical ventilation at 180 breaths/ min (300 μL volume). 37ıı C 5% CO_2 incubator. Duration of culture: 7 days	Immunofluorescence-DAPI, cytokeratin 18, CD31, pro-SPC, aquaporin-5, CCSP, CD45, CD11b, vimentin.	Price et al., 2010
Lung	CM perfused at 1-5 mL/min with negative pressure ventilation at 1 breath/min. 37ıı C 5% CO_2 incubator. Duration of culture: 7-10 days	Histology + IHC-TTF-1, pro-SPC, Clara cell 10 (CC10), CD31, vimentin Morphometry + stereology of lung architecture. *In vitro* function testing-blood gas values, dynamic lung function tests. Orthotopic transplantation into syngeneic male rats up to 14 days-fluoroscopy and live video, blood gas values.	Song et al., 2011
Liver	Perfusion FR not stated.	Histology (engraftment) + immunofluorescence-TUNEL, albumin, G6pc, Ugt1a.	Uygun et al.,

	37 C 5% CO_2 incubator. Duration of culture: 1-5 days	Lactate dehydrogenase (LDH) release quantification. Urea + albumin synthesis quantification. Reverse transcription polymerase chain reaction (RT-PCR) of drug metabolism enzymes. Heterotopic transplantation into syngeneic rats + fresh blood perfusion model to test viability and hepatocyte function.	2010
Liver	-	Histology	Shupe et al., 2010
Liver	Perfusion FR 2 mL/min. 37 C 5% CO_2 incubator. Duration of culture: 7 days	Histology (engraftment) + immunofluorescence-DAPI, albumin, Ki-67. Albumin synthesis/ cytochrome activity/ ammonia metabolism quantification assays.	Soto-Gutierrez et al., 2011
Liver	Perfusion FR 3 mL/min for seeding 16 h; Perfusion FR 0.5 mL/min 37 C 5% CO_2 incubator. Duration of culture: 7 days	Histology + immunofluorescence-TUNEL, Ki-67. Urea/ albumin/ prostacylin synthesis quantification. Platelet deposition studies.	Baptista et al., 2011
Liver	Perfusion FR 90 mL/min. 37 C 5% CO_2 incubator. Duration of culture: 3-13 days	Histology + IHC- cytokeratin 18 (CK-18), CK-19, α-fetoprotein (AFP), Cytochrome P450 3A4 (CYP3A4), TUNEL, Ki-67. Urea/ albumin/ lactate synthesis quantification. Orthotopic transplantation-histology.	Barakat et al., 2011
Kidney	Sections of seeded graft	Histology (engraftment + morphology) + IHC-pancytokeratin, Pax-2, Kidney-	Ross et al.,

	cultured for 3-10 days. 37ıı C 5% CO_2 incubator. Perfusion of whole organ at 120/80 mm Hg for 6-10 days.	specific cadherin (Ksp-cadherin), Ki-67 RT-PCR of Pax-2 + Ksp-cadherin expression	2009
Liver, **Kidney,** **Pancreas, Small bowel**	Perfusion FR 6 mL/min. 37ºC 5% CO_2 incubator. Duration of culture: 7 days	Histology IHC-albumin, vWF, Ki-67	Baptista et al., 2009

Table 5.1: Summary of the recellularisation protocols employed in the literature. Adapted from (He & Callanan, 2013).

5.1.1 Recellularisation, cell density, and distribution of oxygen and nutrients

There are a number of challenges found in recellularisation of acellular scaffolds. The main difficulty is to attain accurate, homogeneous reseeding with correct cell densities and cell phenotypes. The characteristics of pores in the acellular scaffolds, affect both reseeding efficiency and permeability. These include pore size, arrangement, shape, interconnections, and mechanical support. For instance, cell infiltration is frequently a challenge in solid ECM structures (less pores), because most reseeding appears in the peripheral area (surface and subsurface) such that the ends of pores get blocked and they become enclosed over time. Likewise, cell infiltration into the middle of the scaffold (limited transfer of oxygen and nutrients) is hard to accomplish in enormous volume scaffolds (whole-organ) even with quite large size pores (such as acellular myocardial scaffolds) (Patnaik et al., 2013).

The development of recellularised bone scaffolds could be increased by effective cell-seeding and hence create a promising clinical impact for bone tissue engineering (Hasegawa et al., 2010). Cell-seeding density is identified to affect the behaviour and functionality of engineered tissues. The inadequate delivery of nutrients and oxygen into the middle areas of the constructs is one of the drawbacks in the development of tissue-engineered bone grafts (Grayson et al., 2008). In previous research, the result of changing the density of cells seeded into scaffolds was studied for different cell types (cartilage, bone, and cardiac tissues) and biomaterials (Hasegawa et al., 2010; Grayson et al., 2008). The result of greater seeding densities depended on the type of tissue and also the culture conditions. For instance, high seeding densities of chondrocytes in agarose gels improved mechanical properties,

however, these gels lacked sensitivity to mechanical stimulation (Grayson et al., 2008). In addition, Hasegawa and co-workers have reported that greater cell viability and osteogenic differentiation is dependent on the density of the cells. This is because of bone marrow stromal cells (BMSCs)/β-TCP composites that have enough numbers of cells allowed an enhanced environment in order to generate bone both *in vivo* and *in vivo* (Hasegawa et al., 2010). Meanwhile, the possibility of cell aggregates obstructing vessels and creating dense polylayers were increased after raising the cell density during reseeding. Thus, restricted mass transfer causes hypoxia and risks formation of a necrotic core (Fu et al., 2014).

However, the flow rate of medium perfusion is an important parameter. The higher perfusion rates produce greater nutrient transport; allow more constant tissue formation and assists maintenance of greater cell densities inside the scaffolds (Grayson et al., 2008). Low flow rates may be applied to minimise the shear stress on the cells during the reseeding process (Fu et al., 2014).

Basically, interconnected pores are vital for effective reseeding and recellularisation, also for controlling the microstructural, mechanical, and possibly nanostructural structures in the cell environment. During tissue remodelling, porosity of the scaffolds decreases because the new ECM may remove or destroy pores, eventually decreasing movement capability of the cells and nutrient absorptivity. Accordingly, cell proliferation rate may reduce and the majority of cells may die in the middle of the tissue scaffold. However, in thin tissues for example, aortic valve leaflets, cells in the middle of the tissue scaffolds might still get adequate nutrients and oxygen through diffusion because they are so thin (~500μm). Revascularization is critical to deliver nutrients and oxygen to reseeded cells far inside tissue constructs in

enormous volume tissues like whole-heart and whole-liver. Revascularization is essential not only for nutrient and oxygen delivery into deep tissues, but also for the functional incorporation of the implant with the host. Thus, there is a large focus on the challenge of vascularization of big-volume organs or tissues (Patnaik et al., 2013).

In addition, many factors influencing cell adhesion, proliferation and differentiation have been reported, and previous studies have already mentioned the pore size needed for effective development of bone cells in constructs for clinical applications (Mayr-Wohlfart et al., 2001; Quan et al., 2014). Other than structural configuration, the surface behaviour of the materials e.g. micro- and macro- pore size, the chemical organization of the materials, an interconnected network of pores and the solubility of the material appears to have a vital effect on the targeted cells (Mayr-Wohlfart et al., 2001). The character of the cells is determined to a large extent by the presence of unique proteins on the surfaces of the constructs after the decellularisation treatment. For the purposes of bone healing and cell adhesion, these types of ECM protein are needed (Quan et al., 2014).

The quantity and quality of cells that are essential to be provided to numerous regions/subsystems of the organ scaffolds is another main difficulty in the recellularisation of the acellular constructs. There are difficulties in cultivating cells into thick, collagenous structures (for example acellular heart valves), distributing the exact types of cells to the correct subsystem (for example in the whole-heart application, endothelial cells for vasculature structure and cardiomyocytes for heart wall constructs), and accurately monitoring cell distribution and tissue renewal (Patnaik et al., 2013).

The use of naturally derived ECM constructs inhabited with definite kinds of cells is an encouraging method for clinical treatment. Numerous engineered tissues have been implanted into patients including trachea, cardiac patches, and bladder. But, the progress of crucial more complex organs is somewhat less advanced because of the necessity to create a complicated vascular network inside the engineered dense organ (Patnaik et al., 2013).

5.1.2 Static vs. dynamic cell-seeding

Several approaches have been carried out in reseeding constructs such as static and dynamic cell-seeding approaches (Fu et al., 2014). The dynamic cell seeding approach seems more practical and productive compared to static approach (Fu et al., 2014). It is crucial to have a uniform allocation of bone-creating cells within tissue-engineered constructs for *in vivo* osteogenesis in the bone tissue engineering (Schliephake et al., 2009). As reported by Schliephake, dynamic culturing and seeding of human mesenchymal stem cells has presented more homogenously located cells and extracellular matrix proteins in perfusion bioreactor systems rather than static seeding. Furthermore, the manner and biochemical activity of seeded cells can be influenced by alterations in the seeding approaches themselves (Schliephake et al., 2009). Some alternative seeding approaches have been established to overcome the cell density limitations in the middle construct region. These include electrostatic, vacuum (low pressure), magnetic, dynamic, and centrifugal seeding (Fu et al., 2014; Schliephake et al., 2009).

In conclusion, the type of cell culturing and seeding is related to the organization, and the material of the constructs that are used for *in vitro* tissue seeding. The culture conditions have been revealed to be more significant than the type of seeding regarding the quantity of cells and the arrangement of cell location on constructs (Schliephake et al., 2009).

5.1.3 Cells for recellularisation

The interconnected actions of several cell types are required in the process of bone development, restoration and healing. Numerous cell types have been cultured in studying osteoblast cell biology, such as primary cells from various species, immortalised, malignant cell lines, and induced osteoblasts from pluripotent stem cells. However, the application of these osteoblast types and sources demonstrate pros and cons (Czekanska et al., 2012).

The cells can be derived from several choices such as primary cells, cryopreserved cells, cell lines (continuously proliferated and kept in liquid nitrogen), immortalised cell lines, and stem cells (either adult or embryonic). For every cell type, the culture conditions are different. However, in culture cells require a substrate or medium that provides the necessary nutrients, hormones, growth factors, gases (include O_2 and CO_2) and a physio-chemical environment that controls the pH, temperature, and osmotic pressure.

5.1.3.1 Primary cells

Primary cells are isolated directly from tissues. Isolation is carried out either by perfusion of the organ with a protease enzyme, or by explant culture. Regarding the primary osteoblast cells, primary human cells have advantages in terms of no interspecies extrapolation and they are applicable for clinical research. But, these cells have heterogeneous phenotype, restricted availability, extended isolation protocol, and a cell phenotype related to donor influences. Tissue for isolating primary mouse or rat cells can be simply accessible, there is the possibility to regulate the choice of donor-animals, and cell removal can be achieved from all bones in the skeleton. However, primary cells have some disadvantages including interspecies variations, and genomic and cell phenotype variations (Czekanska et al., 2012). Several limitations are also noticed in terms of the availability of tissue from which to isolate them. Some tissues can be easily sampled, but for others sampling would be too invasive. Tissues like liver and pancreas will lose their viability and function very quickly after death. Thus, cadaveric tissue cannot be used. Furthermore, division of adult tissue cells in culture is also restricted causing difficulties in creating a bank of cells. Normal adult cells will divide in culture only a limited number of times, before losing their capability to proliferate, which is known as senescence (a genetically determined event). Such cell lines are known as finite. Lastly, primary cells lose the signals that are needed to maintain their specialised functions when they are removed from their natural environment (Sun et al., 2011).

5.1.3.2 Cell lines

When a finite cell line becomes altered and is able to divide indefinitely, it is called a continuous cell line. Cell lines can be sub-cultured when the culture is confluent,

stored in liquid nitrogen, and can be readily transported around the world for commercialization. In terms of advantages of using cell lines in regenerative medicine, they are readily available on demand, and there are an unlimited number of cells, which are easily stored frozen and in culture. However, most cell lines are dedifferentiated. Hence, they have low organ-specific functions (Sun et al., 2011).

The most frequently employed cell lines are MC3T3-E1, human fetal osteoblastic (hFOB), human osteosarcoma (MG-63), human osteosarcoma (Saos-2) and human osteosarcoma (U-2 OS). In the present study, human osteosarcoma (HOS) cell lines have been used. To date, osteosarcoma cell lines are accessible in unrestricted number without ethical approval and the outcomes seem trustworthy and reproducible, while primary cells have clear attractions regarding the cells being closer to the *in vivo* position, and thus, having more preclinical and clinical relevancy. However, current species variations in experimental work impede extrapolation to human clinical disease and treatment results (Czekanska et al., 2012), and primary human adult cells are difficult to access, grow only slowly and show limited life-time in culture.

5.1.3.2.1 Human cell lines

In our study, a human osteosarcoma cell line was used (HOS TE85) for the *in vitro* cellular response. It was derived from a sarcoma of a 13 year old female Caucasian (McAllister et al., 1971).

In fact, HOS TE85 cells have not been employed frequently regardless of their greater basal expression of alkaline phosphatase (ALP). They have been formerly used in several experiments to determine the effects of oestrogen (Komm et al., 1988) and also to localize oestrogen and androgen receptors (Benz et al., 1991; Komm et al., 1988). Moreover, HOS TE85 cells have been reported in some studies regarding the isolation and purification of insulin-like growth factor (IGF) connecting proteins (Hasager et al., 1991; Lempert et al., 1991; Mohan & Baylink 1991).

A study concerning the comparisons of two commonly used osteosarcoma cell lines called MG-63 and HOS TE85, with human bone derived cells in terms of growth, differentiated cell function, integral expression and adhesive profiles has been reported by Clover and Gowen (1994). HOS cells exhibited greater activities of ALP than MG-63 cells under basal environments. However, at present only MG-63 is known to demonstrate the improved enzyme activity resulting from 1,25dihydroxyvitamin D_3 ($1,25(OH)_2D_3$) treatment, which is representative of bone derived cells. Moreover, osteocalcin could not be identified in supernatants from any cells under basal environments. On the other hand, amounts formed by MG-63 cells after being supplemented with $1,25(OH)_2D_3$ were equivalent with those of

osteoblast-like cells. Also, serum-free cell assays showed that the cell types attached to collagen I, fibronectin, and laminin. Greatest attachment of osteosarcoma cell lines and human bone derived cells was found after 2 hours and the same extracellular matrix protein coating concentrations were needed by all cell types to produce ideal binding. Greatest attachment to fibronectin and collagen I was detected at 0.1–0.5 $\mu g/cm^2$ while greatest attachment to laminin was detected at 5–10 $\mu g/cm^2$. Taken together, these findings show that MG-63 and TE85 HOS osteosarcoma cell lines are

in vitro models for determining cell attachment and integrin subunit expression. Proliferation and ALP activity were also measured in both MG-63 and HOS TE85 cells (Clover & Gowen, 1994).

5.1.3.3 Immortalisation

Immortalisation involves overriding the growth control (or senescence) of cells causing them to divide continuously, and can be achieved by several means. They can be isolated from a malignant tumour (e.g. HeLa cells; Hep G2 cells; Jurkat cells), occur spontaneously (e.g. 3T3 fibroblast cells which developed from a spontaneous transformation in embryonic mouse tissue), or be obtained by insertion of viral DNA into the cell genome (e.g. most widely used is simian virus SV40 DNA), stabilisation of telomeres (by artificial expression of telomerase which inhibits the breakdown of telomeres at the ends of chromosomes), and hybridoma technology (where an antibody producing B cell is fused with a myeloma cell to produce an immortal source of antibodies) (Sun et al., 2011).

In general, the advantages of immortalised cell lines are unrestricted number of cells without the need for isolation, easy to sustain, and relative phenotypic stability. However, several papers describe phenotypic heterogeneity developing among cell lines, which is associated with extended passaging of cells (Czekanska et al., 2012).

This approach certainly produces an immortal source of cells, but if the cells have been transformed then their function is almost always compromised. There is also the risk from many of these cell lines that if you have interfered with growth regulation, and may have used an oncogenic protein, they could cause tumours (Sun

et al., 2011).

5.1.3.4 Embryonic stem cells, induced pluripotent stem cells and human mesenchymal stem cells

The perfect practical progenitor population as an origin of cells has not yet been recognized for tissue engineering towards clinical application. The use of stem cells has become another alternative. There are several sources of stem cells. Firstly, they can be obtained from embryonic stem cells (i.e. derived from the inner cell mass of the blastocyst). Also stem cells is extracted from foetal tissue, which have unknown plasticity. Secondly, they can be obtained from adult stem cells including mesenchymal cells, which are acquired from bone marrow and adipose tissue. Finally, stem cells can be derived from induced pluripotent stem cells that are generated by reprogramming of adult somatic cells to cells with embryonic stem cell characteristics. This was first achieved in 2006 by Takahashi and Yamanaka with mouse and with human fibroblasts in 2007 (Takahashi et al., 2007). In bone engineering research, human mesenchymal stem cells (hMSCs) have been

extensively used and promising findings in preclinical bone restoration obtained.

Human embryonic stem cells (hESCs) and human induced pluripotent cells (hiPSCs) have practically unrestricted potential and are capable of differentiating into all kinds of specialized cells contained in the human body e. g. cells from the vascular systems. There are an expanding number of scientific papers currently representing the probable use of pluripotent stem cells for bone engineering *in vitro* and *in vivo*. However, the scope of pluripotent stem cells is still at an early stage, and the

employment of hESCs and hiPSCs for regenerative medicine studies requires more rigid technical procedures and regulatory rules compared to hMSCs (Sladkova & Maria de Peppo, 2014).

As a promising supply of cells, xenogeneic cells may be employed to treat problems in treating organ deterioration. Moreover, the accessibility of donors is not an issue in the xenotransplantation of cells. Different cell supplies derived from fetal cells, pig cells, induced pluripotent stem cells, and embryonic stem cells (ESCs), are being studied as a novel model for future approaches to numerous incurable diseases (Fu et al., 2014).

5.1.4 Choice of medium for re-seeding cells

A number of elementary medium types can be used for osteoblast cells, such as DMEM, DMEM/F12 or alpha minimum essential medium (α-MEM). These are supplemented with chemicals to encourage osteoblast functions. The most broadly employed supplements are dexamethasone, β-glycerophosphate, $1,25(OH)_2D_3$, and ascorbic acid (Czekanska et al., 2012).

The response and molecular outcomes of $1,25(OH)_2D_3$ are still not well explained. Continual supplementation of $1,25(OH)_2D_3$ to proliferate rat osteoblasts seemed to obstruct osteocalcin secretion and nodule growth, while intense supplementation of $1,25(OH)_2D_3$ after proliferation promoted ALP, osteocalcin production and type I collagen. Moreover, $1,25(OH)_2D_3$ has been also revealed to stimulate mineralisation through expansion of the development of matrix vesicles (Czekanska et al., 2012).

Ascorbic acid is essential for the differentiation of mesenchyme-derived connective tissue including bone (Pradel et al., 2008). Specifically, the culture conditions for matrix mineralisation of Saos-2 (human osteosarcoma) are 50 μg/mL ascorbic acid and 0-10 mM glycerol-2-phosphate (Czekanska et al., 2012).

The treatment of cultures with phosphate substrates for matrix mineralisation has been extensively discussed. Addition of 10 mM β-glycerophosphate effects mineral deposition and development of ectopic mineralisation. The interaction between cells and extracellular surroundings requires integrins, transmembrane proteins communicating with the cytoskeleton and the ECM. These intercommunications are vital for cell proliferation, migration, and differentiation. Moreover, integrins can work together with growth factor receptors (Czekanska et al., 2012). It is important to attain enough numbers of cells for tissue reconstruction into cell based therapeutic strategies. The determination of cell differentiation can be carried out with tests such as ALP activity and histochemistry, and osteocalcin measurement by the enzyme-linked immunosorbent assay (ELISA) (Pradel et al., 2008).

Cell two-dimensional (2D)-monolayer culture has been the approach used to retain osteoblast cells for a long time *in vitro*. But it is crucial to establish a cell system that mimics to the natural environment of cells. The choice of a 3D-model for the scaffold on which to grow osteoblastic cells in this study is essential to a better understanding of the physiological and regenerative methods to be used.

5.1.5 Characterisation of bone cells

The identification of bone cells is very important for an understanding of bone tissue engineering.

5.1.5.1 Identification of the osteoblast cultures

Several studies have been carried out to determine *in vitro* the appropriate conditions for the preservation of phenotypically representative osteoblast populations (Griensven et al., 2002).

Osteoblast differentiation is a complicated process controlled by several endocrine, paracrine and autocrine factors. The current study proved the osteoblast character of human osteoblast (HOS) cultures by observing the production of a mineralised matrix *in vitro* after being triggered with β-glycerophosphate (Griensven et al., 2002). Human osteoblast-like cell lines have been employed in bone tissue engineering as standards to study primary osteoblast function and they are frequently applied to examine development, protein expression, and the effects of growth factors and cytokines. In many respects osteoblast-like cell lines were found to be very similar to primary osteoblasts. Furthermore, osteoblast-like cell lines were established for studying integrin expression, the development of osteocalcin expression, and cell adhesion. However, osteoblast-like cells may not represent primary cells in terms of ALP expression (Lindsay et al., 2012).

There have been many reviews on biochemical indicators of osteoblast differentiation. Osteoblast outputs such as type I collagen, osteocalcin, and ALP activity have been studied particularly regarding osteoblast differentiation and bone development. The differentiation progression of the osteoblastic cell phenotype has

been categorized into three successive stages called proliferation, extracellular matrix maturation, and mineralization (Yamanouchi et al., 1997). In addition, cell adhesion is necessary for cell movement and tissue integrity *in vivo* and *in vitro*. The physical contact and interaction of a cell with the scaffold could be demonstrated by immunohistochemistry measuring the presence of several adhesion markers including actin, vinculin, talin, and α-actinin (https://www.cellmigration.org/topics/adhesion). This would be an interesting further study of the decellularised scaffolds.

5.1.6 Summary

The scaffolds are just one step towards the renewal of functional and viable bone tissues. The optimal reseeding of the scaffold with cells has not yet been established (Fu et al., 2014). Thus, the studies of the structural, molecular, and functional biology of bone tissue are crucial for the well understanding that enables us to obtain the efficient recellularisation with human derived cells onto the decellularised bone scaffolds. The aims of this chapter were to:

(i) re-seed the decellularised bone scaffolds with human osteosarcoma cell line HOS, and characterise the cell growth rate and viability during culture.

(ii) measure parameters of osteoblast cell function in the cultures – ALP activity and osteocalcin secretion.

(iii) distribution of re-seeded cells on the scaffolds was detected by visualising formation of an insoluble product of the ALP activity, and of the insoluble product of MTT reduction.

(iv) mechanical testing, SEM analyses and porosity measurements of the re-seeded bone matrix were also carried out.

5.2 Materials and methods

Following decellularisation and sterilisation of the bone, the aim was to reseed the pieces of bone with human osteosarcoma HOS cells. In this section the rat osteoblast cell line, OST 5, was used again in order to develop the methods for measuring cell viability and function.

5.2.1 Cell cultivation

5.2.1.1 Culturing HOS cells and the OST5 cells on coverslips

Briefly, HOS and OST5 cells were allowed to grow and reach confluence up to 3 days in the large flasks (75 cm^2) in a humidified atmosphere of 5% CO_2 at 37C as described in **Chapter 2**, **Section 2.4.1.1** and **2.4.2.1**. The cells were then transferred to adherent 24-well plates in an amount of 10^5 cells per well. Cells were grown on coverslips placed in the bottom of these wells. After reaching confluence, the coverslips were collected and used for the different analyses as follows:

Type of cell	Test (n = number of sample)			
	ALP (pNPP)	**ALP (BCIP/NBT)**	**DAPI**	**MTT**
HOS	n = 2	6	2	2
OST5	2	6	2	2

Table 5.2: Analyses carried out to characterise the cultured HOS and OST5 cells. ALP: an assay to measure the cell function. DAPI: a staining agent to determine the number of nuclei, and MTT: a colorimetric assay to assess cell metabolic activity and cell number. The details about these tests are explained in the following sections. Abbreviations: p-nitrophenol phosphate (pNPP), 5-bromo-4chloro-3-indolyl phosphate/Nitroblue tetrazolium (BCIP/NBT).

The 24-well plate was kept in the incubator at 37C and 5% CO_2 for two days.

5.2.1.2 Culturing HOS cells in 24 well plates with an adherent surface

To allow growth of HOS onto the decellularised bovine bone specimens, the prepared bone samples were transferred into a 24-well plate made of adherent polystyrene (Fisher Scientific, Leicestershire, UK). Prior to adding cells, the bone samples were washed with 1 ml DPBS and soaked with 1 ml cell growth medium for 30 minutes. Cells were seeded at a density of $5x10^5$ cells/ well in a 25 µl volume (suspended in growth medium). The cell suspension (25 µl) was gently dropped onto the bone in the well using a sterile pipette tip. Cells were incubated in a 5% CO_2 humidified incubator at 37C for 30 minutes to let the cells attach to the bone. Medium was not added to the well during this time. In the meantime, this 24-well plate was wrapped in wet tissues to avoid dryness and dehydration. This preincubation for

30 min without medium allowed good contact to be made between bone samples and HOS cells which will increase the possibilities of cell adhesion and growth.

Following this period of time, 1 ml of complete DMEM growth medium was added to each bone sample in the wells. The 3D cell cultures were left undisturbed at 37C, in an atmosphere of 5% CO_2 before the first medium change at 3 days, thus allowing cells to adhere to the surface of bone and to infiltrate into the pore structure.

Cells formed a subconfluent layer on and within the scaffold. The supernatant in the wells was removed after 72 hours. The bone samples were then transferred to a new adherent well-plate, and also the bone samples were flipped over to encourage the cells to grow into the scaffold more homogenously. The medium was changed and then renewed every 2-3 days, which was extended for up to 5 weeks.

5.2.1.3 Culturing HOS cells in 24 well plates with a non-adherent surface

To try and increase the extent of cells adhering and seeding on the bone, the bone pieces were also placed onto non-adherent polystyrene 24-well dishes instead of adherent dishes (Fisher Scientific, Leicestershire, UK). The experiments used prepared bone samples in two conditions - static and dynamic culture environments. All the methods were repeated as mentioned in **Section 5.2.1.2** using non-adherent 24-well plates. The extent of recellularisation was compared under static and dynamic culture conditions. The later was achieved using a roller incubator (GyroRocker Incubator S170, Keison Products, England, UK) set at 15 rpm to effect dynamic conditions. Meanwhile the temperature and CO_2 were also set to 37°C and 5% respectively. This experiment was then repeated using further bone pieces to

effectively compare adherent and non-adherent well plates in term of re-seeding efficiency.

5.2.2 Parameters of cell function measured in cultures

5.2.2.1 ALP activity – dephosphorylation of p-nitrophenol phosphate

ALP catalyzes the hydrolysis of phosphate esters in alkaline buffer (BioVision, Inc.). The activity of ALP by this method was measured by the dephosphorylation of pNPP to form the yellow soluble product p-nitrophenol.

5.2.2.1.1 Preparation of ALP (pNPP) assay buffer

A final volume of 1 litre of 0.1M glycine buffer was prepared after dissolving 7.51g of glycine, 0.203g of $MgCl_2$ and 0.136g of $ZnCl_2$ in distilled water. The pH of solution was checked to 10.4 with 5M NaOH. The buffer was stored in the cold room at 4C.

5.2.2.1.2 Activity of ALP (pNPP) in HOS and OST5 cells

Firstly, 0.012g of para-nitrophenol phosphate was well mixed in 12 ml ALP buffer to make up a 2.7 mM pNPP substrate. The medium from 24-well plate was removed and the plate washed with 1 ml D-PBS. 1 ml pNPP substrate was then added to each well. The absorbance was measured immediately (blank) for both HOS and OST5 cells at 405 nm. The measurements were then taken at varying time points (0, 5, 10, 15, 20, and 30 minutes) to record the enzyme reaction by the formation of the yellow product, p-nitrophenol. The enzyme activity was measured using extinction coefficient of p-nitrophenol of 18.75 $mM^{-1}cm^{-1}$.

5.2.2.1.3 Activity of ALP in bone samples

Using a similar method, ALP activity was measured for up to 21 days with re-seeded bone samples. Reseeded bone samples were washed with 1 ml D-PBS, moved to a bijou container by using sterile forceps, and 1.5 ml pNPP substrate added. The absorbance was measured immediately at 405 nm, and with time as described in **Section 5.2.2.1.2**.

5.2.2.1.4 Calibration of the ALP activity in terms of cell number (OST5 and HOS cells)

HOS and OST5 cells were cultured 3 days in the incubator at 37°C and 5% CO_2. They were then counted and centrifuged at 800 rpm for 5 minutes. The medium was discarded and only the pellets left. Another 7 ml of medium was added to the pellets, the mixture shaken and again the cells were counted. The number of cells

ranged from 0 cells to $2x10^6$ cells. The number of cells for the standard curve was achieved as follows:

No. of cells ($cells/cm^2$)	OST5		HOS	
	Volume of cells (µl)	Volume of medium (µl)	Volume of cells (µl)	Volume of medium (µl)
0	0.00	7000.00	0.00	7000.00
1×10^3	0.93	6999.07	3.00	6997.00
2.5×10^3	2.33	6999.67	8.00	6992.00
5×10^3	4.67	6995.33	15.90	6984.10
1×10^4	9.30	6990.70	31.80	6968.20
5×10^4	46.67	6953.33	159.00	6841.00
1×10^5	93.33	6906.67	318.00	6682.00
2.5×10^5	233.33	6766.67	795.00	6205.00
5×10^5	466.67	6533.33	1591.00	5409.00
7.5×10^5	700.00	6300.00	2386.00	4614.00
1×10^6	933.33	6066.67	3182.00	3818.00
2×10^6	1867.00	5133.00	6364.00	636.00

Table 5.3: The number of cells used to construct a standard curve of HOS and OST5 cells.

The different cell number samples were incubated in duplicate (plate 1 and plate 2). All the well plates were left in the incubator overnight at 37C and 5% CO_2. After culturing the OST5 and HOS cells overnight, the medium from the 24-well plates was removed and the plate washed with 1 ml D-PBS. Then, 1.5 ml pNPP substrate was then added to each well. The absorbance was measured immediately for well plates (both OST5 and HOS cells) at 405 nm by using a spectrophotometer. The measurements were then taken at varying time points (every 10 minutes for 1 hour)

generating a linear reaction after 20 minutes. The absorbance was plotted against cell number, to obtain a standard curve of activity against cell number.

5.2.2.2 ALP activity (BCIP/NBT assay)

HOS cells and OST5 cells and bone samples were also tested for ALP activity by Bio-Rad's AP-based colorimetric kit (AP Conjugate Substrate Kit, BioRad), following the manufacturer's guidelines. This experiment is based on BCIP/NBT (5-bromo-4-chloro-3-indolyl phosphate/nitroblue tetrazolium), which reacts with the alkaline phosphatase to generate an insoluble colour precipitate for detection (Bio-Rad). This insoluble product of the ALP reaction could then be used to examine the distribution of functional cells on the scaffolds.

5.2.2.2.1 Preparation of ALP - BCIP/NBT assay

5 ml NBT/ BCIP solution was made up from 0.2 ml carbonate buffer in 4.8 ml distilled water. 50 µl AP Color Reagent A (Bio-Rad) and 50 µl AP Color Reagent B (Bio-Rad) were added dissolved into the NBT/BCIP solution.

5.2.2.2.2 ALP activity (BCIP/NBT assay) in HOS and OST5 cells

To start with, the medium was removed from the well plate containing either cultured HOS or OST5 cells. 0.5 ml NBT/BCIP solution was added to each well plate and was left for 30 minutes. The change in colour was observed visually as coloured

spots of precipitated product and captured using a mobile phone camera (Galaxy Note 2, Samsung, Korea). This method was used to detect the distribution of cells on the bone scaffolds.

5.2.2.3 MTT activity

Viability in terms of intracellular metabolic activity, and cell integrity of cultured HOS cells, OST5 cells and re-seeded HOS cells on bone samples were measured by MTT (3-[4,5-dimethylthiazol-2-yl]-2,5-diphenyl tetrazolium bromide; Sigma-Aldrich, St Louis, MO, USA) reduction.

5.2.2.3.1 Preparation of the MTT assay

To make up 10mM solution of MTT, 0.4143 g MTT was dissolved in 100 ml PBS and the pH was checked to 6.75. The solution was filtered through a 0.22μ filter in the clean room and this solution was stored for use for up to 2 weeks at 4°C (in the cold room).

5.2.2.3.2 MTT reduction in HOS and OST5 cells

Firstly, the medium from both cultured HOS and OST5 cells was removed from the well plate and 200 µl MTT solution was added to each well. The well plate was incubated at 37°C and 5% CO_2 for 4 hours. Unreacted MTT solution was removed as much as possible from the well plate. Cells were not washed at this satge to avoid loss of cells. 1 ml dimethyl sulfoxide (DMSO) was added to dissolve the formazan product in the cells and it was mixed to an even colour. Finally, the absorbance was measured at 540 nm by the spectrophotometer.

5.2.2.3.3 MTT reduction in bone samples

For this experiment the reseeded bone samples were placed in bijou containers. The cultured bone samples to be assessed (cells grown after 3rd, 4th and 5th week) were transferred to a bijou container. 1 ml MTT solution was added into the bone samples to access the proliferation of cells and the bijou containers with lose lids left for 4 hours in the incubator at 37C and 5% CO_2. The cells on the bone samples were observed visually and images of the distribution of the blue stained colonies of cells captured using a mobile phone camera (Galaxy Note 2, Samsung, Korea). The bone sample was washed three times with 1 ml PBS. To dissolve the formazan product, the bone sample was treated with 2 ml DMSO and well-mixed to an even colour with gentle shaking. The absorbance was measured by spectrophotometer at 540 nm. This method was applied for all bone samples seeded in adherent and non-adherent well plates.

5.2.2.3.4 Calibration of the MTT assay in terms of cell number (OST5 and

HOS cells)

All the procedures to culture the HOS and OST5 cells, and to set up the number (from 0 to $2x10^6$ cells) of OST5 and HOS cells for the standard curve were followed as mentioned in **Section 5.2.2.1.4.**

After culturing the OST5 and HOS cells overnight, the medium from 24-well plates were removed. 1 ml MTT solution was added then to each well and incubated at 37C and 5% CO_2 for 4 hours. After that, the MTT solution was carefully removed from the plates. Each plate received 2 ml DMSO which was pipetted up and down and well-mixed to an even colour. The solubilized stain was removed from the plates, and the absorbance was measured at 540 nm using the spectrophotometer. The fluorescence intensity was plotted against cell number to obtain a standard curve.

5.2.2.4 Total cell protein measurement (Lowry assay)

The Lowry protein assay is a biochemical assay to obtain the amount of protein in a solution and it is performed by a colour change of the sample solution correspondingly to protein concentration, which can then be analysed using colorimetric methods. The original protocols of Lowry and co-workers were modified in this study (Lowry et al., 1951).

5.2.2.4.1 Preparation of solutions

There were two solutions called solution A and solution B. Solution A was made up from 98 ml 2% Na_2CO_3, 1 ml 1% $CuSO_4$ and 1 ml 2% NaKtartrate, while solution B was made up from Folin's reagent and d.H_2O. In general, 2 ml Folin was diluted in 6 ml d.H_2O (1 in 4 dilution). Solution B is unstable at alkaline pH. Therefore, it must be quickly mixed into the assay solution.

5.2.2.4.2 Preparation of samples

Refer to the procedures mentioned in **Section 3.2.4.1** and **Section 3.2.5.**

5.2.2.4.3 Procedures

The bone samples were taken from the freezer where they had been stored at -80°C, thawed and then washed with 1 ml DPBS. They were left and solubilised overnight in 0.5 ml 0.5M NaOH at 37°C and 5% CO_2. All the bone samples from day 0 (control), day 7, day 10, day 15, day 21, day 28, and day 35 after reseeding were measured. The test tubes for standards were set up as follows:

Protein concentration (µg/ml)						
Volume	**0**	**25**	**50**	**100**	**150**	**200**
BSA (ml)	0.000	0.125	0.250	0.500	0.750	1.000
0.5M NaOH (ml)	1.000	0.875	0.750	0.500	0.250	0.000

Table 5.4: The protein concentration applied to construct the standard curve of protein measurements. Abbreviation: Bovine serum albumin (BSA).

Meanwhile, the test tubes for bone samples were set up from 25µl bone samples diluted in 975µl 0.5M NaOH [1:40 dilution].

To the test tubes for standards and bone samples were added 5 ml solution A. These were mixed and left for 10 minutes. After that, 0.5 ml solution B was added and well-mixed immediately. They were left for 30 to 90 minutes. The absorbance was read at 725 nm against a water blank.

5.2.2.5 DAPI test

A common nuclear and chromosome counterstain, DAPI produces blue fluorescence upon binding to AT regions of DNA (https://www.thermofisher.com/order/catalog/product/D3571). To confirm that the reseeded human cells were successfully attached to the bone samples, DAPI staining of DNA was determined.

5.2.2.5.1 Preparation of DAPI solution

The working concentration used for DAPI was 0.6 nM. The DAPI solution for this experiment was prepared from 50µg/ml DAPI stock solution. For HOS and OST5 cells 10µl DAPI (50µg/ml) was dissolved in 5000µl PBS meanwhile, for bone samples 5µl DAPI (50µg/ml) was dissolved in 2500µl PBS to make the DAPI solution. All the DAPI solutions were kept in the dark.

5.2.2.5.2 DAPI staining of HOS and OST5 cells

To see the images under the Zeiss Microscope, HOS and OST5 cells cultured on glass coverslips (diameter = 16 mm) in 24-well plates were washed with 1 ml DPBS. For 20 minutes, the cells were fixed in 0.5 ml formalin solution (neutral

buffered 10%). After that, the cells were washed again three times with 1 ml PBS for each wash. The HOS and OST5 cells were stained with 400µl DAPI solution for 2 – 3 minutes in the dark before washing again with 1 ml PBS. The washing process was repeated 3 times and at last, some PBS was added and the samples viewed under the Zeiss Microscope (x20 wet lens, EX: 365 nm, EM: Band Pass (BP) filter 445/50 nm).

5.2.2.5.3 DAPI staining of bone samples

The medium was removed from bone samples in a 24-well plate and they were washed with 1 ml D-PBS. One of the bone samples was moved to a bijou container. 0.5 ml formalin solution (neutral buffered 10%) was first added to fix the cells and it was left for about 20 minutes. The bone sample was then washed three times with PBS (1 ml PBS/ each wash), and stained with 400 µl DAPI solution for 3 minutes in the dark. The washing process was repeated 3 times after staining. Bone samples were transferred to petri-dishes and some PBS was added. The images of DNA were seen under the Zeiss Microscope, under the same conditions as **Section 5.2.2.5.2.**

5.2.2.5.4 Calibration of the DAPI staining in terms of cell number (OST5 and HOS cells)

All the procedures to culture the HOS and OST5 cells, and to set up the number (from 0 to $2x10^6$ cells) of OST5 and HOS cells for the standard curve were followed as mentioned in **Section 5.2.2.1.4.**

The different cell number samples were transferred into test tubes in duplicate. All the test tubes were centrifuged (MSE Mistral 2000, England) at 800 rpm for 5 minutes. The medium was then discarded from the sample tubes and 1.5 ml

DPBS added. They were frozen for an hour at -80C. After that, the cells were thawed in the incubator at 37C. The samples were then treated in 3µl 0.6nM DAPI. Finally, the fluorescence was read by the spectrofluorophotometer after the samples were left for 5 minutes in the dark. The fluorescence was set for DAPI (EX: 358 nm, EM: 461 nm). The fluorescence intensity was plotted against cell number to obtain a standard curve.

5.2.2.6 Picric Sirius red staining test

The Sirius red stain has been used to evaluate collagen in cardiac tissue, lung, and cell culture for many years since 1979. The dye from Sirius red stain will attach to the [Gly-x-y] triple-helix structure present in all collagen I fibres (Kliment et al., 2011). This stain was used to find out if the decellularised bone scaffold retained collagen, or whether the scaffold should be collagen coated to encourage cell adhesion.

5.2.2.6.1 Preparation of picric Sirius red staining assay solutions

There are 75 ml picric acid (saturated), 25 ml 40% formaldehyde, and 5 ml glacial acetic acid in a bottle of Bouin's solution. Meanwhile, picric Sirius red solution was 0.2 g Direct Red 80 (Sigma-Aldrich 365548) saturated in 200 ml aqueous picric acid.

5.2.2.6.2 Bone samples

Firstly, a cultured bone sample (cells grown for 21 days) was washed with 1 ml PBS. 0.5 ml of Bouin's solution was used to fix the cells for 20 minutes. Again, the bone sample was washed two times with PBS. After that, 500µl picric Sirius red stain was added and samples left for 1 hour with gentle shaking. The bone sample was then washed with 5 ml of 0.01M hydrochloric **(**HCl) acid. All the liquid was removed and the samples visualized. The images were taken using a mobile phone camera (Galaxy Note 2, Samsung, Korea).

5.2.2.7 Osteocalcin measurement by ELISA

In this study, osteocalcin was measured using ELISA kits (KAQ1381, Life Technologies). These kits are an enzyme-linked immunosorbent assay, and contain all the required reagents.

5.2.2.7.1 Preparation of reagents

Standards and controls: 1 ml distilled water was added for all controls that come as part of the ELISA kit. They were allowed to dissolve and inverted to mix.

Working anti-OST-HRP conjugate: 240 µl of the concentrated anti-OST-HRP conjugate was added into 12 ml conjugate buffer.

Washing solution: 500 ml d. H_2O was added to 2.5 ml wash solution (200x).

5.2.2.7.2 Preparation of samples

Refer to the procedures mentioned in **Section 3.2.4.1** and **Section 3.2.5.**

5.2.2.7.3 Procedures

The decellularised bone samples were reseeded with cells (in adherent and non-adherent well plates) and incubated with 10 μM 1,25-Dihydroxyvitamin D_3 in serum free medium 72 hours prior to the time points. The measurements were taken on day 7, 10, 15, 21, 28 and 35. The supernatants were then removed and stored at 80 nC for osteocalcin assay.

Firstly, 25μl of each standard, control, and unknown sample was added into the appropriate wells. Then, 100μl of working anti-OST-HRP conjugate was added into all wells. The plates were covered with a plate cover and incubated for 2 hours at room temperature. After that, wells were aspirated and washed 3X with wash buffer (400μl/well for 30 sec). The plate was then dried. To continue, 100μl of chromogen solution was added into each well within 15 minutes after the washing process. The plates were left and incubated for 30 minutes in the dark at the room temperature. Next, 100μl of stop solution was added into each well. The side of the plate was tapped gently to mix (change of colour from blue to yellow). Finally, the plate was read at 450nm by Multiskan Ascent 96/384 Plate Reader (MTX Lab Systems, Inc.), and the unknown sample concentrations calculated from the standard curve.

5.2.2.8 Mechanical testing

The mechanical testing was carried out to obtain the effects of recellularisation on mechanical properties of the bone samples in adherent and nonadherent plates.

5.2.2.8.1 Preparation of bone samples

Refer to the procedures mentioned in **Section 3.2.4.1** and **Section 3.2.5.**

5.2.2.8.2 Procedures

Bone samples were re-seeded for up to 21 days in adherent and non-adherent plates. Mechanical testing was carried out based on the previous methods in **Chapter 4, Section 4.2.1.2.** The mechanical testing of bone samples were measured before and after recellularisation. There were three (3) different samples used for adherent and non-adherent plates in order to enable statistical comparisons.

5.2.2.9 Porosity measurements

The porosity measurements were again carried out to obtain the effects of recellularisation on pore sizes of the bone samples in adherent and non-adherent plates.

5.2.2.9.1 Preparation of bone samples

Refer to the procedures mentioned in **Section 3.2.4.1** and **Section 3.2.5.**

5.2.2.9.2 Procedures

Using a similar method explained in **Chapter 4**, **Section 4.2.1.7.2**, porosity measurements were measured for up to 21 days with re-seeded bone samples in adherent and non-adherent plates. The porosity diameter of bone samples were measured before and after recellularisation. Also, there were three (3) different samples used for each type of culture plate.

5.2.2.10 Atomic force microscopy (AFM)

AFM applies an ultrasharp mechanical probe to investigate various surfaces, which permits 3D surface imaging. Nowadays, AFM has been applied to bone tissue by several authors, primarily in bovine bones (trabecular and cortical parts) (Milovanovic et al., 2013).

5.2.2.10.1 Preparation of bone samples

Refer to the procedures mentioned in **Section 3.2.4.1** and **Section 3.2.5.**

5.2.2.10.2 Procedures

Re-seeded bone samples (after 35 days) were used for this experiment. The samples (n = 3) were transferred to test tubes. Then, they were washed with DPBS once. Cells were fixed with 10% formaldehyde solution for 30 minutes. The processes were continued by washing the bone samples with PBS three times (1ml/ wash). The bone samples were next washed with d.H_2O. At last, the bone samples were rinsed and dried overnight in the fume hood.

AFM (MFP-3D, Asylum Research, Oxford Instruments) was used to observe surface morphology, microstructure, and micro-mechanical properties of bovine trabecular bones with the help of Mr Milovan Cardona. To locate an area suitable for AFM imaging, each dried sample was placed horizontally on the sample disk, and the external trabecular surface was imaged. In this experiment, both height (topography) and phase images were concurrently attained by standard AFM tapping mode using the AR iDrive Probes (Model: BL-TR800PB). The magnification scales were chosen at 1μm x 1μm, 4μm x 4μm, 10μm x 10μm and 80μm x 80μm.

5.2.2.11 Scanning electron microscope (SEM)

During SEM (Nanoscience Instruments), the electrons in the beam interact with the bone sample, creating numerous signals that can be employed to achieve information about the surface configuration and topography. The images were obtained in the AMRL at the James Weir Building with the help of Mr Gerry Johnson. The protocols for SEM were adapted from several studies (Correia et al.,

2012; Frohlich et al., 2010; Grayson et al., 2010; Grayson et al., 2008).

5.2.2.11.1 Preparation of sodium cacodylate buffer

A 0.1M sodium cacodylate buffer was made of 2.14 g sodium cacodylate in 80 ml d.H_2O. The solution was adjusted to pH 7.2, and d.H_2O was added to make 100 ml solution.

5.2.2.11.2 Preparation of 2.5% glutaraldehyde

A 2.5% glutaraldehyde was made of 0.7 ml of 25% glutaraldehyde solution in 6.3 ml of 0.1M sodium cacodylate solution. All the protocols were carried out in the fume hood.

5.2.2.11.3 Preparation of bone samples

Refer to the procedures mentioned in **Section 3.2.4.1** and **Section 3.2.5.**

5.2.2.11.4 Procedures

After 21 days of reseeding, bone samples (n = 6) were washed with PBS. Then, they were fixed in 2.5% glutaraldehyde for 2 hours. Tissue constructs were then washed in 0.1M sodium cacodylate buffer. Next, tissue constructs were put in tubes and 1ml of 0.1M sodium cacodylate buffer added. Finally, bone samples were freeze-dried in liquid isopentane immersed into liquid nitrogen and dried in a sublimation chamber at

5kPa to preserve the microstructure of bone pore size. This process was carried out in the laboratory at the Civil and Environmental Engineering

Department and it was facilitated by a postgraduate student, Miss Bruna De Carvalho Faria Lima Lopes. All the bone samples were placed in a freeze dryer (ScanVac CoolSafe Freeze Drying, LaboGene) overnight. The samples were then sealed and packed under vacuum as shown in **Figure 5.1**.

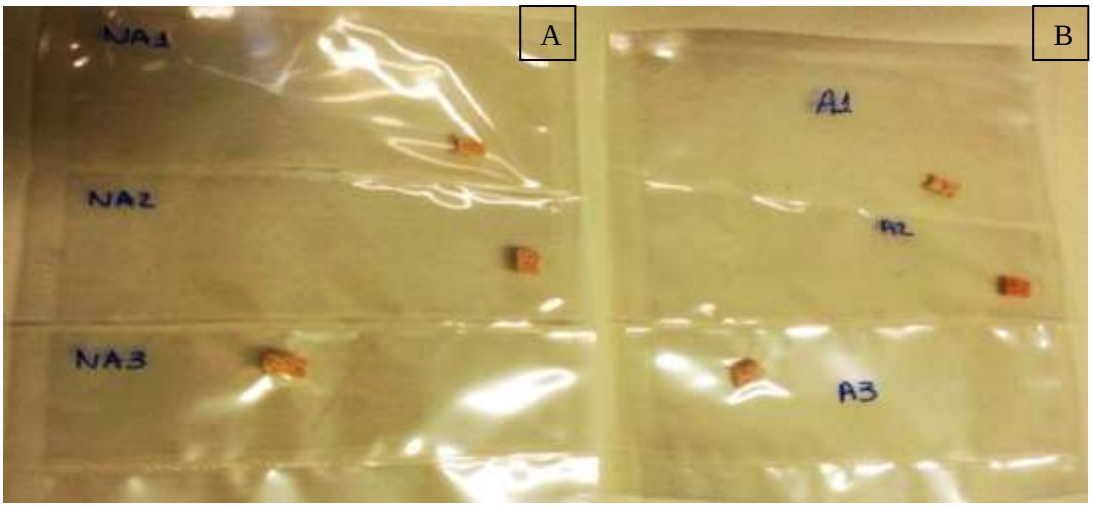

Figure 5.1: A) Non-adherent **B)** Adherent bone samples were sealed and packed under vacuum after overnight freeze-drying.

Before imaging, freeze-dried bone samples were fixed (glued) (**Figure 5.2**) to the metal surface for coating with gold. Again, the process was carried out in the AMRL with the help of Mr Gerry Johnston. The process of coating took approximately 20 minutes using the S150 Sputter Coater (Edwards, High Vacuum

Co. International, USA).

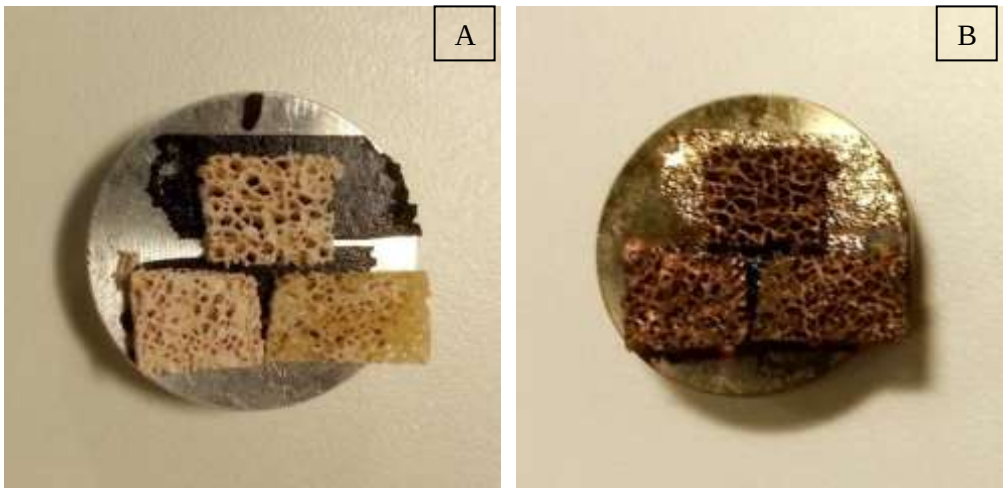

Figure 5.2: The placements of bone samples on the metal surface **A)** before and **B)** after coating with gold.

Finally, the inner and outer regions of coated tissue constructs were imaged under the Scanning Electron Microscope (Hitachi SU 6600 SEM, Japan).

5.3 Results and discussions

5.3.1 Effects of initial seeding density on development of tissue-engineered bone

An appropriate and effective cell-seeding may increase *in vitro* and *in vivo* bone development (Hasegawa et al., 2010). In this study, the employed seeding density was $5x10^5$cells/well. This range was applied based on the some literature on development of tissue-engineered bone. In several studies the initial seeding densities ranged from $5x10^4$cells/well to $60x10^6$cells/well (Holy et al., 2000; Hasegawa et al., 2010; Yamanouchi et al., 1997; Griensven et al., 2002; Schliephake et al., 2009; Grayson et al., 2008). It is important to note that increasing seeding density does not always improve recellularisation of tissue engineered constructs.

A study on the effects of initial seeding density and fluid perfusion rate on formation of tissue-engineered bone has been carried out by Grayson and colleagues. There was no significant effect on the characteristics of tissue-engineered bone when increasing seeding density from $3x10^6$cells/mL to $60x10^6$cells/mL. However, the ultimate cell numbers, cell dissemination in the scaffolds, and the total bone protein and mineral content were improved when increasing the perfusion rate from 100 μms^{-1} to 400 μms^{-1} (exterior velocities through scaffolds). To conclude, these results propose that the rate of medium perfusion during seeding in a bioreactor has an important influence on the behaviour of engineered bone, but the initial seeding density does not (Grayson et al., 2008). In addition, enhancement of cell seeding density throughout reseeding in liver raises the chance of cells accumulating and obstructing vessels and creating thick polylayers of cells. This may cause restriction

in oxygen and nutrient mass transfer, and as a result hypoxia and increase the extent of necrosis in the core of the tissue (Fu et al., 2014).

Information published in the paper by Grayson and co-workers shows that there was no improvement in bone development from $1x10^6$cells/mL to $10x10^6$cells/mL seeding density for tissue engineered bone. However, uniform cell dispersion (that promotes tissue formation) in the constructs was improved at greater seeding densities. Taking all the papers together, early seeding density may affect cellular formation in the developing bone graft, however, it does not seem to increase ultimate bone formation or cellular composition.

Furthermore, the choice of seeding density in our study is also supported by a finding from Holy and co-workers. In their studies, the early seeding densities used were from 0.5 to $10x10^6$cells/cm^3 in culturing the 3D bone constructs. They have reported that the development of tissue was not dependent on the initial cell-seeding density after six weeks of reseeding, whether it was $1.0x10^6$ or $6.0x10^6$cells /cm^3. In their work, the early cell seeding density did not considerably influence tissue development, and reducing seeding density only postponed the creation of mineralized tissue (Holy et al., 2000).

In conclusion, a cell density of $5x10^5$cells/cm^3 was used in our study and was acceptable and practical to allow us to examine the result of the reseeding period on bone tissue development *in vitro*.

5.3.2 Parameters of cell function measured in cultures

5.3.2.1 Sensitivity of ALP activity, MTT reduction and DAPI staining

In order to monitor the success of a recellularisation procedure, a method is required to quantify the number of living functional cells on the scaffolds. To quantify the cells, the sensitivity of three parameters, ALP activity, MTT reduction and DAPI staining was compared in two types of osteoblast cell lines, OST5 and HOS cells, to determine which assay had the lowest limit of detection in terms of cell number.

The relationship between ALP activity, MTT reduction and DAPI staining and cell numbers in the two cell lines is shown in **Figures 5.3 A**, **5.3 B**, **5.4** and **5.5** below, and the lowest limit of detection in terms of cell number for the three assays in each cell line is shown on **Table 5.5**.

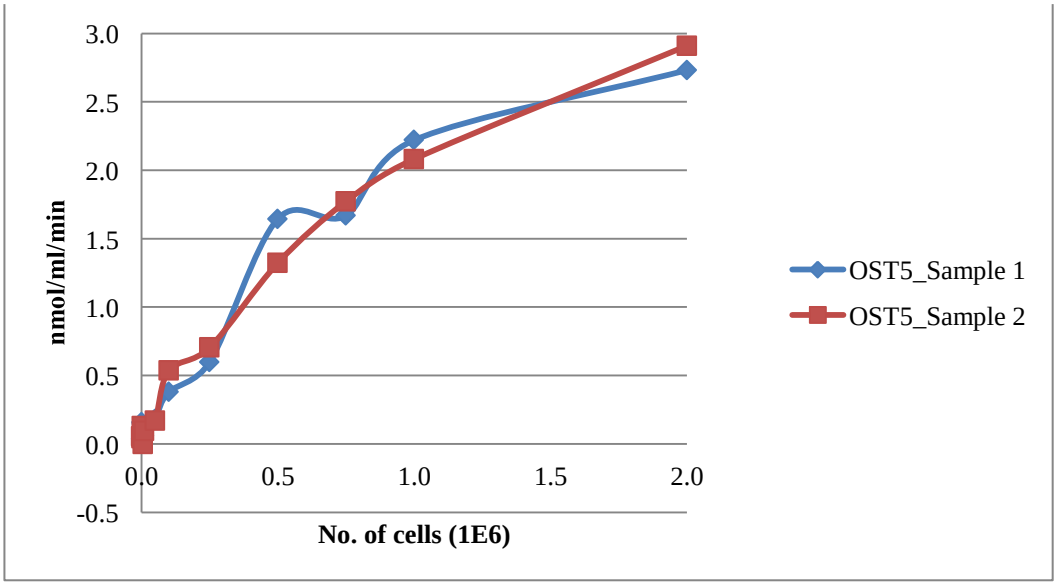

Figure 5.3: A) ALP activity of OST5 cells.

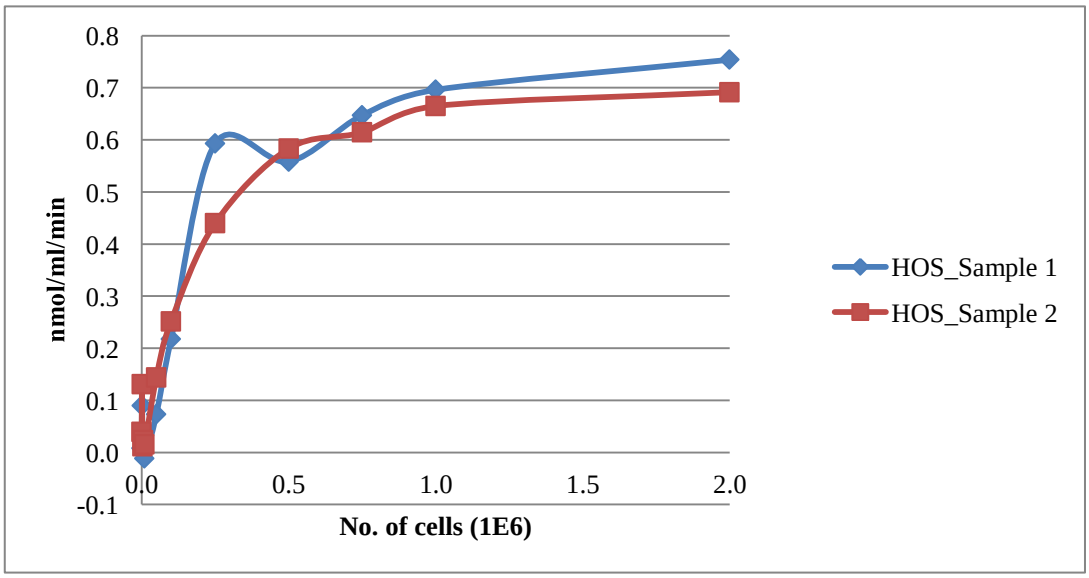

Figure 5.3: B) ALP activity of HOS cells.

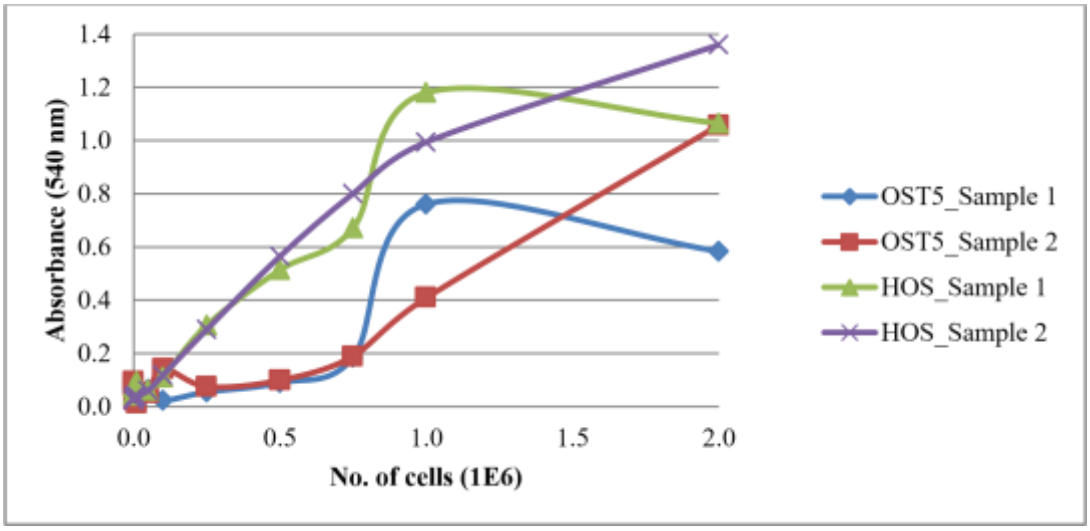

Figure 5.4: MTT reduction of OST5 and HOS cells.

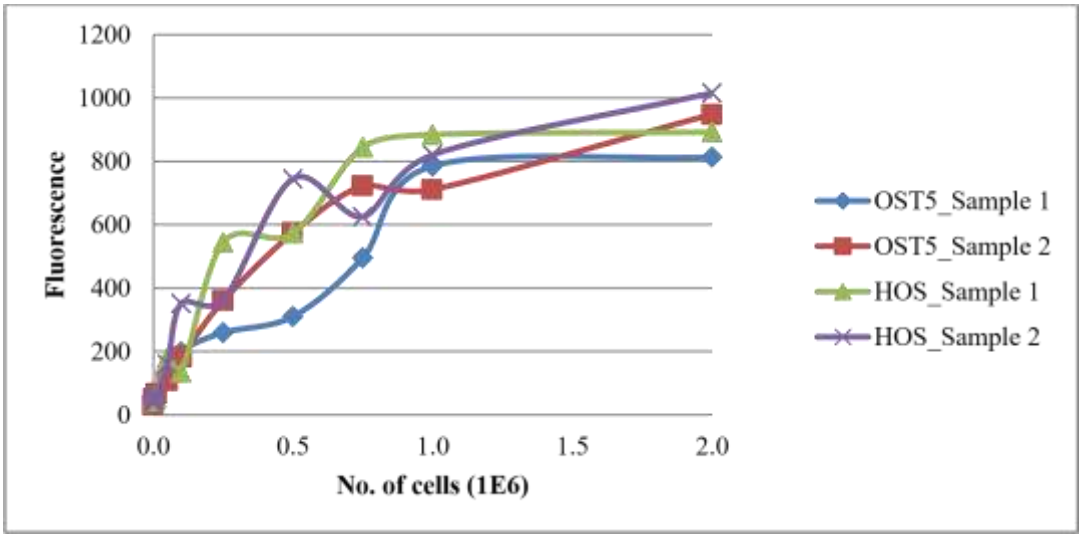

Figure 5.5: DAPI staining of OST5 and HOS cells.

Test parameter	No. of cells per well	
	OST 5	HOS
ALP activity	1.0×10^5	1.0×10^5
MTT reduction	5.0×10^5	2.5×10^5
DAPI staining	5.0×10^4	5.0×10^4

Table 5.5: The lowest limit of detection in terms of cell number for the three assays (ALP activity, MTT reduction, and DAPI staining, in OST5 and HOS cells.

Overall, the most sensitive test parameter was the DAPI staining. In HOS cells, the minimum cell number that could be detected in DAPI staining was $5x10^4$ cells/well as compared to ALP activity ($1.0x10^5$ cells/well) and MTT reduction ($2.5x10^5$ cells/well). Meanwhile, in OST5 cells the minimum cell numbers that could be detected in DAPI staining was $5x10^4$ cells/well as compared to ALP activity ($1.0x10^5$ cells/well) and MTT reduction ($5x10^5$ cells/well).

The sensitivity**: DAPI staining > ALP activity > MTT reduction**

Taken together, DAPI staining was more sensitive than ALP activity and ALP activity was more sensitive than MTT reduction. Hence, DAPI staining was the best parameter to quantify cell number in term of sensivity than ALP activity and MTT reduction. The parameter is also the most appropriate as it does not vary dependent on metabolic activity or differentiation of the osteoblasts.

5.3.2.2 ALP activity - pNPP and (BCIP/NBT) assays

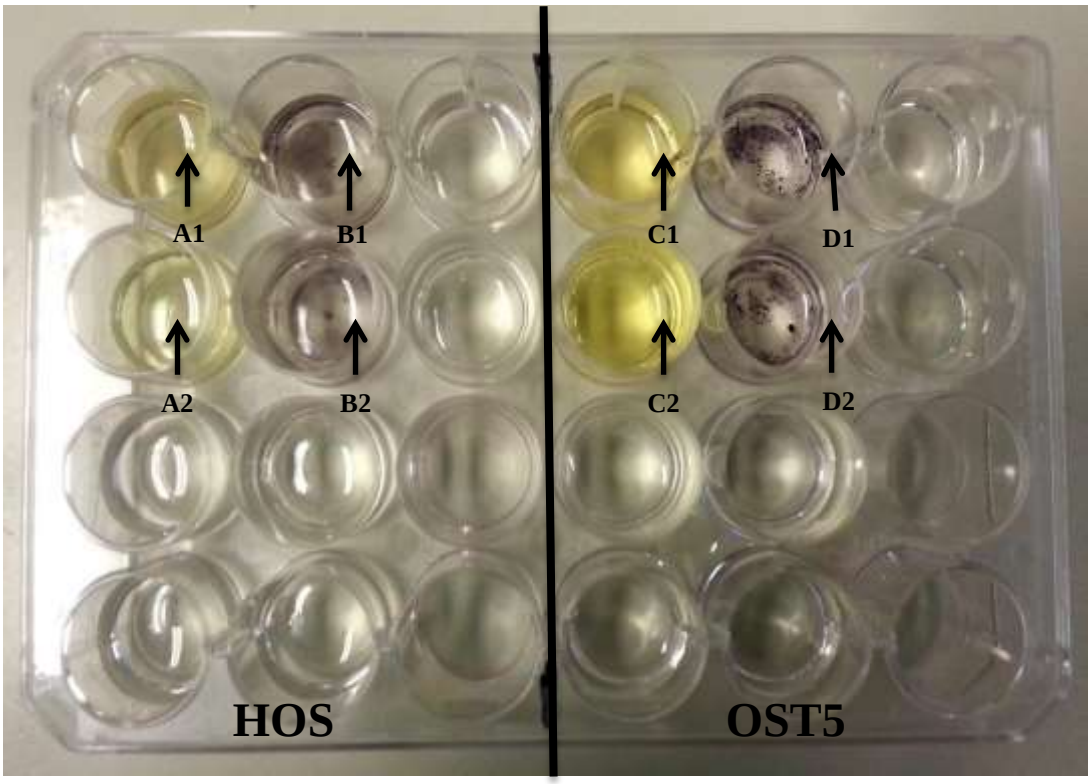

Figure 5.6: Image of ALP pNPP (yellow) and BCIP/NBT (purple) activity of HOS and OST5 cells. A1 and A2 represent ALP (pNPP) in HOS cells, B1 and B2 represent ALP (BCIP/NBT) in HOS cells, C1 and C2 represent ALP (pNPP) in OST5 cells, and D1 and D2 represent ALP (BCIP/NBT) in OST5 cells.

ALP is the most common established biochemical marker for osteoblast activity. The ALP activity test was carried out using two different substrates, which yield a soluble or an insoluble product. From the observations shown on **Figure 5.6** with BCIP/NBT as substrate, ALP catalysed formation of a dark purple insoluble product, and with pNPP as substrate, a yellow soluble ALP product was formed in both cell lines. Greater formation of the coloured product indicates the osteoblast activity was higher in OST5 compared to HOS. To characterise distribution of osteoblasts through the decellularised scaffolds the

BCIP/NBT assay was used.

5.3.2.3 ALP activity of HOS cells

5.3.2.3.1 Effect of static vs. dynamic conditions in adherent and non-adherent plates on the number of HOS cells successfully re-seeded

In bone samples where the cells were cultured in the present of either an adherent or non-adherent surface the ALP activities were compared. The experiment compares the effect of shaking and rotating environment on the number of cells successfully re-seeded. To carry out this experiment decellularised bone samples were incubated with HOS cells sitting in either adherent or non-adherent polystyrene 24-well plates.

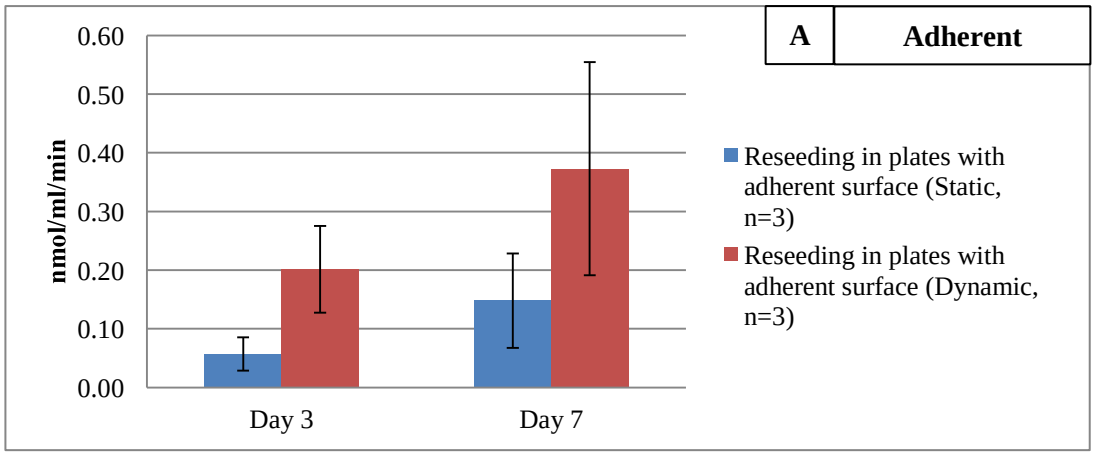

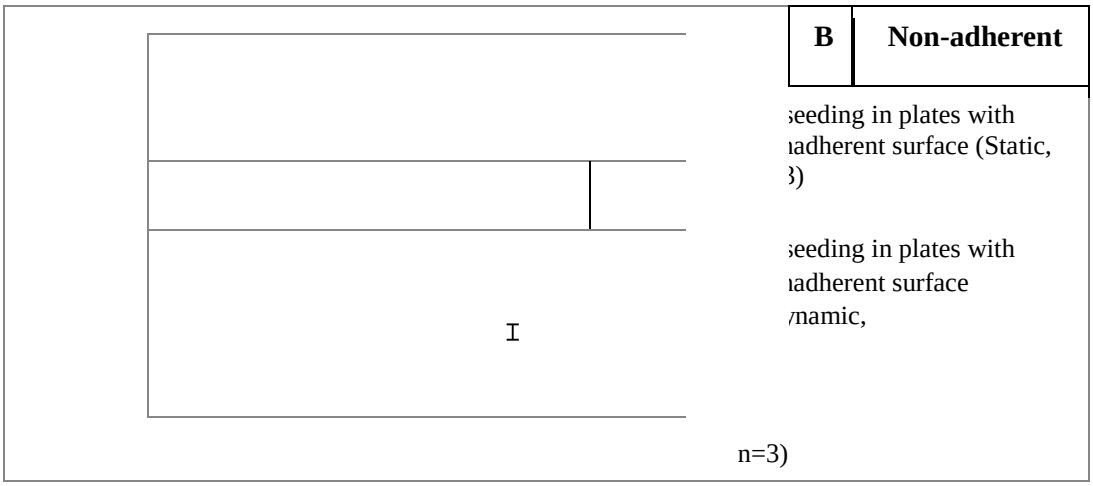

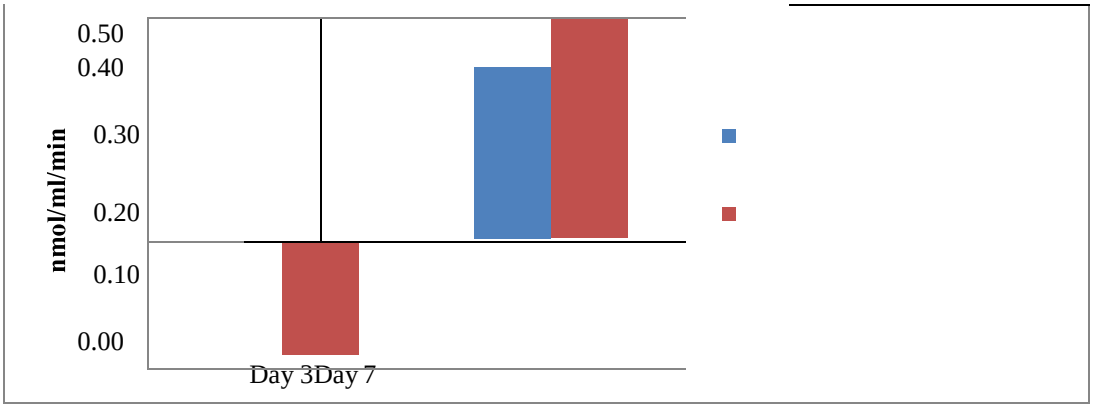

Figure 5.7: ALP activity of HOS cells reseeded (at 5 x 10^5 cells per cm^2) onto decellularised bone in static and dynamic environment on day 3 and day 7 in **A)** adherent and **B)** non-adherent surface. Static (n=3) and dynamic (n=3). Results are the mean ± SEM. p>0.05, comparison between static and dynamic at the same time point in adherent and non-dherent plates by unpaired t-test.

The results were shown on **Figure 5.7 A)** and **B)** and it seems that there was no significant difference between static and dynamic conditions in both adherent and non-adherent surfaces. ALP activity seems gradually increased from Day 3 to Day 7 particularly in non-adherent plates under static conditions. The activities in dynamic conditions were always slightly higher. A dynamic environment has been stated to increase the activity of ALP and promote more evenly distributed cells and greater formation of extracellular matrix proteins as compared to a static environment (Schliephake et al., 2009).

By applying dynamic technique in our studies, the cells were delivered at high concentration at 15 rpm into the vascular perfusion tract of the bone for reseeding *in vitro*. Furthermore, this allowed the cells to move directly via the vascular branch into the construct and parenchyma, and this approach has been broadly applied by many researchers in recellularisation of the blood vessels of lungs, liver, and heart (Fu et al., 2014). Moreover, in spinner flasks, dynamic seeding has been reported to enhance the ALP activity compared to static environments. Also, cultured bone marrow stromal cells in flow perfusion bioreactors have enhanced mineralized matrix by improving fluid shear forces (Schliephake et al., 2009).

Yeatts and Fisher (2011) have also reported that spinner flasks enhanced the activity of the early osteoblastic indicator ALP, late osteoblastic indicator osteocalcin (OC), and calcium deposition to a greater extent than static environment. In this research, they cultured hMSCs for 5 weeks onto collagen constructs in spinner flasks. They found that bone was developed only in the exterior 0.5 to 1.0 mm of 11mm-diameter constructs. Moreover, the constructs had interconnected pores and the thickness was only 1.5 mm. However, the diffusion depth of transfer seemed to be restricted to 1.0 mm or less in spinner flasks. Also, the stem cell differentiation in this study was affected by the pore size either in static culture or spinner flask culture. Dynamic conditions offer extra variables that can influence osteogenic differentiation as compared to static conditions. Generally, spinner flasks can also expose cells at the surface of scaffolds to shear stress. This shear stress could also help in encouraging osteogenic differentiation (as indicated by greater ALP). However, the shear stress on cells during the reseeding process can be reduced by lowering flow rates (Fu et al., 2014). In addition, cells cultured onto constructs with smaller pore size are exposed to greater wall shear stresses that could encourage differentiation (Sladkova & de Peppo, 2014).

Interestingly as reported by Sladkova and de Peppo (2014), scaffolds cultured under dynamic environments showed increased cell proliferation, osteogenic differentiation and mechanical properties as compared to controls (static environment). The cells cultured under dynamic conditions also contained enhanced expression of bone-specific genes, deposition of mineralized matrix, ALP activity and development of bone-like structures. Likewise, the results from their study also

revealed that dynamic cultures were related to enhanced proliferation, uniform cell dispersion and osteogenic differentiation.

Static environment is the traditional approach to culture bone grafts in the laboratory. However, a static environment is not ideal for culturing centimeter-sized bone grafts due to limited nutrient supply and restricted elimination of metabolic waste. In fact, transport appears to be only through diffusion. This is not adequate to help cell survival and proliferation throughout the centre of large cell/scaffold constructs, causing limited tissue development and necrosis. In addition, a static environment does not permit delivery of biophysical stimuli that is important for functional reconstruction (Sladkova & de Peppo, 2014).

Taken together, dynamic seeding produced greater seeding capabilities in most culture environments. Dynamic culture also mimics the environment *in vivo* better, but it requires further study on how to translate this dynamic environment to implanted scaffolds in a clinical situation. To apply the dynamic conditions (by Gyro-Rocker) in this *in vitro* study required a well-controlled roller incubator at 37°C and 5% CO_2, but space was limited on the Gryo-Rocker in the laboratory. Therefore, the remaining *in vitro* experiments in this thesis used static conditions due to the minimal space available in the roller incubator. A lot of well-plates were used to measure different tests at the same time. Thus, it was not practical to use dynamic conditions.

5.3.2.3.2 ALP activity in cells cultured on adherent and non-adherent plates under static conditions for up to 21 days

The results for the comparisons of ALP activity when reseeding in plates with adherent and non-adherent surface are explained in **Figure 5.8.** From the observations shown, there was no significant difference except at Day 10 between adherent and non-adherent surfaces in terms of ALP activity of the cells grown from Day 3 to Day 21. In adherent surfaces, ALP activity appears steadily increased from Day 3 to Day 21. Meanwhile in non-adherent surfaces, ALP activity seems slowly increased from Day 7 to Day 15. However, it increased drastically from Day 3 to Day 7 and after Day 15. The standard mean errors were high on Day 7 and Day 21 in adherent surfaces caused by one rogue sample which had died and was inactive.

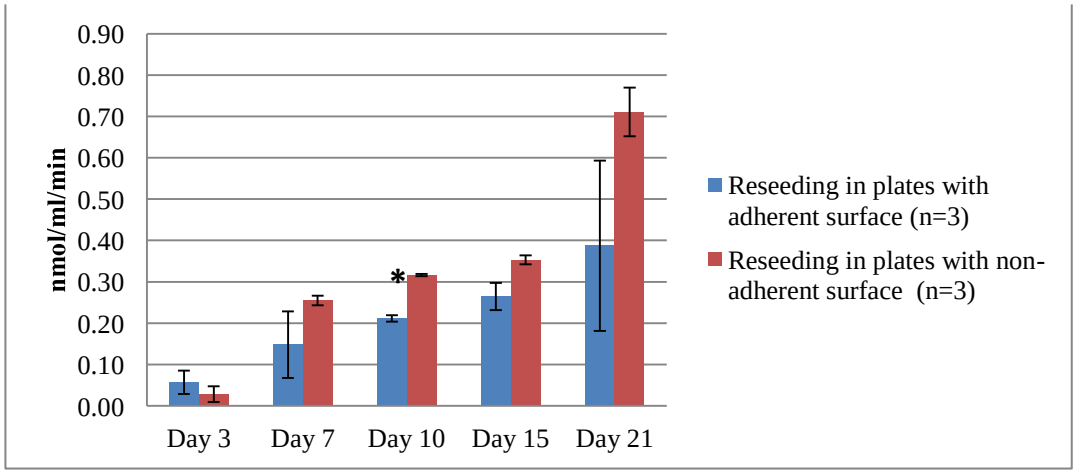

Figure 5.8: ALP activity of HOS cells reseeded (at 5 x 10^5 cells per cm^2) onto bone in adherent and non-adherent surface for 3 weeks. Day 3, 7, 10, 15, and 21. n=3 +/- SEM, *p≤0.05, comparison between adherent and non-dherent plates at the same time point by unpaired t-test.

In vivo and *in vitro*, the differentiation of cultured osteoblasts occurs in three stages; these are cell proliferation, matrix maturation, and matrix mineralization. All these stages are attended by the expression of many genes. Some extracellular matrix proteins like procollagen I, fibronectin, and TGF-β can be identified throughout proliferation. An indicator (marker) to detect the initial state of osteoblast differentiation is ALP. ALP is related to organic bone matrix production before the mineralization. The matrix maturation stage is described by maximal expression of ALP. Meanwhile at the early phase of matrix mineralization, genes for proteins such as osteocalcin (OC), bone sialoprotein (BSP), and osteopontin (OPN) are expressed and when mineralization is accomplished, calcium deposition can be seen using appropriate staining techniques. Osteocalcin is indicated by mature osteoblasts in relation with matrix mineralization (Kostenuik et al., 1997).

As compared to a control medium, cell differentiation in osteogenic medium enhanced ALP activity and calcium deposition (Sladkova & de Peppo, 2014). Matrix maturation and mineralization are also improved by culturing the cells to entire

confluency and by supplementing particular osteogenic additives *in vitro* (Kostenuik et al., 1997). Several vital elements were applied in osteogenic medium including Lascorbic acid, dexamethasone, β-glycerophosphate and L-glutamine to promote and support bone cell differentiation.

In our study, the bone cells were cultured with added β-glycerophosphate to encourage bone matrix mineralization. The process by which β-glycerophosphate generates mineralization is closely related to the ALP activity of bone cell cultures (Chung et al., 1992). Theoretically, β-glycerophosphate is a protein phosphate inhibitor that acts as a phosphate group donor in matrix mineralization. Through an alkaline phosphate-related mechanism, the use of 10 mM β-glycerophosphate is able to stimulate calcification of cultured vascular smooth cells (https://www.caymanchem.com/pdfs/14405.pdf).

50μg/ml ascorbic acid was also used to activate an optimum increase in differentiation (Pradel et al., 2008). As discussed in **Section 5.1.4**, ascorbic acid was supplemented to the cell culture media for the hydroxylation of proline and lysine in collagen and that is required for an appropriate collagenous extracellular matrix synthesis. The production of collagen indicates osteoblast differentiation (Czekanska et al., 2012; Pradel et al., 2008). Ascorbic acid is also essential for the differentiation of mesenchyme-derived connective tissue cells into bone (Pradel et al., 2008). The use of ascorbic acid in osteoblast cell culture has been reported to increase collagen and ALP gene expression, cell proliferation and protein production (Czekanska et al., 2012). The suggested concentration of ascorbic acid for osteoblast cell cultures to promote an ideal increase in differentiation is 50μg/mL (Czekanska et al., 2012; Pradel et al., 2008).

Ideally when the cells reached confluency, the cells will keep differentiating in continuous culture, and ALP activity will also increase with time. To enhance differentiation and *in vitro* mineralization of the osteoblastic cells, 100 nM dexamethasone was added. In a study by Yamanouchi and colleagues (1997), it has been shown that the use of dexamethasone could stimulate the mineralization of the human osteoblastic cells in monolayer cultures. Treatment with 10^{-8} to 10^{-6} M dexamethasone in a dose-dependent manner increased the ALP activity of the cells cultured in their study for 6 days. Moreover, the ALP activity of the cells exposed to 10^{-7} M dexamethasone for 9 days was 1.4-fold greater than that of the cells exposed to the same dose for the first 3 days. Also, it seemed that biochemical markers of osteoblastic differentiation (ALP activity, excretion of procollagen type I carboxyterminal peptide (PICP) and osteocalcin) were increased in the cells treated with dexamethasone at 10^{-7} M for 5 days. So far, characteristics of osteoblasts including

increased ALP activity, raised intracellular cyclic adenosine monophosphate (cAMP) level in response to PG E_2 and PTH, and excretion of osteocalcin and type I collagen, have been shown to respond to dexamethasone. Interestingly, dexamethasone has also been proven to encourage osteoblastic differentiation in bone marrow stromal cells (Yamanouchi et al., 1997).

5.3.2.3.3 Effect of vitamin D3 on ALP activity of cells seeded on decellularised bone in adherent and non-adherent surface plates

The ALP activity of HOS cells reseeded onto bone in adherent and nonadherent surface without the addition of vitamin D3 were earlier reported in **Figure 5.8**. The measurements were taken from Day 3 to Day 21 in which, there was no significant difference on the ALP activity of samples in adherent and non-adherent surfaces from Day 3 to Day 21 except at Day 10. The ALP activity steadily increased from Day 3 to Day 21 in adherent surface. But in non-adherent surfaces, ALP activity seems slowly increased from Day 7 to Day 15 and then increased drastically from Day 3 to Day 7 and after Day 15.

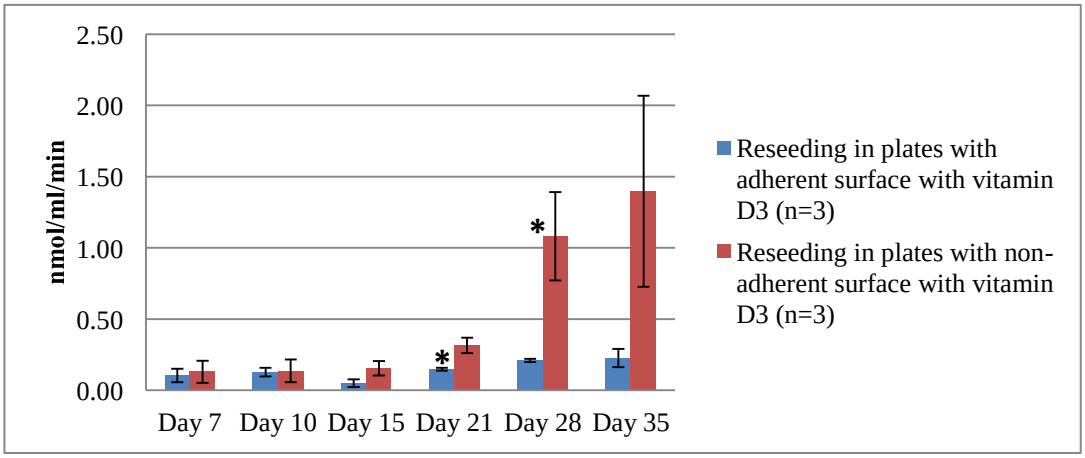

Figure 5.9: ALP activity of HOS cells reseeded (at 5 x 10^5 cells per cm^2) onto decellularised bone in adherent and non-adherent surface from 1st week to 5th week. Day 7, 10, 15, 21, 28 and 35. The cells were added with 10 µM vitamin D3 in FCS-free medium 72 hours prior to the time point. n=3 +/- SEM, *p≤0.05, comparison between adherent and non-dherent plates at the same time point by unpaired t-test.

The use of serum-free medium was to chemically control culture environments *in vitro*. The effect of vitamin D3 on the ALP activity of HOS cells reseeded onto bone in adherent and non-adherent surface is shown in **Figure 5.9**. 10µM $1,25(OH)_2D_3$ was added into the culture in FCS-free medium 72 hours prior to the time point in this study. From the interpretations, there were significant differences at Day 21 and Day 28 between adherent and non-adherent surfaces when vitamin D3 was added. The ALP

activity remained unchanged in adherent surface with the same duration of culture. However, the ALP activity in non-adherent surface was highly affected by vitamin D3 after 21 days of reseeding. The standard mean errors were high on Day 28 and Day 35 in non-adherent surfaces because of one rogue sample which had died and was inactive.

Table 5.6 shows a comparison of the ALP activities in the presence and absence of $1,25(OH)_2D_3$ extracting the data from **Figure 5.8** and **Figure 5.9** for comparison.

Table 5.6: A comparison of ALP activities in the presence and absence of $1,25(OH)_2D_3$ treatment of cells. Results are the mean ± SEM values of n=3, **$p \leq 0.05$, comparison between cells treated and untreated with vitamin at the same conditions by unpaired t-test. Black asterisks refer to adherent cultures, red asterisks refer to non-adherent cultures.

Day	Minus $1,25(OH)_2D_3$		Plus $1,25(OH)_2D_3$	
	Adherent	Non-adherent	Adherent	Non-adherent
10	0.211 ± 0.008	0.317 ± 0.003	0.126 ± 0.030	0.136 ± 0.079
15	0.265 ± 0.033*	0.353 ± 0.011*	0.050 ± 0.027*	0.154 ± 0.050*
21	0.387 ± 0.206	0.711 ± 0.059*	0.147 ± 0.010	0.315 ± 0.055*

In comparison, it is shown on **Table 5.6** that ALP activities in bone samples treated with $1,25(OH)_2D_3$ were lower at any time points (at day 10, 15 and 21), but there were significant differences between treated and untreated bone samples in adherent cultures (on day 15) and non-adherent cultures (on days 15 and 21). Vitamin D3 reduced the ALP activity of HOS in a study by Clover and Gowen (1994). The cells were treated with 10^{-8} M vitamin D3 for 72 hours, and the cells were trypsinized and assessed for ALP activity. They found that ALP activity (μmol ρ-nitrophenol/μg

DNA/ hour) was reduced from 0.113 ± 0.007 (control-without vitamin D3, $p<0.001$) to 0.102 ± 0.015 (with vitamin D3, $p<0.001$).

To understand the effect of vitamin D metabolites on bone is complicated by species variations, variations in reaction of bone and cartilage cells in accordance with their states of differentiation, and variations regarding the vitamin D metabolite being investigated. For instance, $1,25(OH)_2D$ treated in the initial phase of osteoblast cultures restricted the expression of collagen I and alkaline phosphatase. However, when $1,25(OH)_2D$ was added to more differentiated cultures, it promoted their expression. On top of its function in stimulating bone development, $1,25(OH)_2D$ stimulates bone resorption by enhancing the amount and activity of osteoclasts (Bikle, 2012).

In literature using nonhuman cells, $1,25(OH)_2D_3$ has been revealed to enhance ALP activity in rat osteogenic sarcoma cells, however, to reduce the activity of enzyme in mouse osteoblasts. Vitamin D_3 metabolites are expected to perform a significant function in bone mineralization and, in fact, it has multiple, generally biphasic impacts on the role of osteoblasts. It acts to enhance the total number of osteoblasts and their cell size *in vivo*. Impacts of this metabolite on ALP activity clearly depend on the condition of the cell. In poor density rat osteosarcoma cell cultures with poor ALP activity, $1,25(OH)_2$ vitamin D3 promotes production. In contrast, in high density cultures with high ALP activity, $1,25(OH)_2$ vitamin D3 inhibits production. Restriction of cell development in high population densities at $1,25(OH)_2D_3$ concentrations higher than 10^{-9} M has been reported. Meanwhile in cultured human bone cells, $1,25(OH)_2$ vitamin D3 promoted ALP and at the same time hinders proliferation. Further in organ cultures of bone, $1,25(OH)_2$ vitamin D3 restricts collagen production, and reduces

collagen production in several osteoblastic cell lines, corresponding to number of receptors for the hormone. In human cells *in vitro* it enhances collagen production in parallel with ALP activity and proliferative activity (Mulkins et al., 1983). Moreover, Manolagas and co-workers (1981) showed that if calcium concentration is altered in the cellular microenvironment this could affect ALP. They found that the effect of $1,25(OH)_2D_3$ was increased in the presence of enhanced calcium levels.

5.3.2.4 MTT reduction

The sensitivity of the MTT assay is affected by the type of cell, the technique employed for solubilizing the formazan crystals, as well as the metabolic state of the cells (Edmondson et al., 1988). The principle of the assay involves the reduction of the MTT in metabolically active cells. The yellow tetrazolium salt MTT is reduced to an insoluble purple formazan substance due to the activity of dehydrogenase enzymes in viable cells, using reducing equivalents like nicotinamide adenine dinucleotide (NADH) and nicotinamide adenine dinucleotide phosphate (NADPH) (Edmondson et al., 1988; Grayson et al., 2010; Quan et al., 2014). The purple crystals of the formazan product have poor aqueous solubility. DMSO is a common solubilisation agent employed in many studies, readily dissolving the product (Edmondson et al., 1988; Grayson et al., 2010). The range of wavelength to obtain the concentration of the product colour is between 550 to 620 nm (Grayson et al., 2010).

In the MTT reduction experiments, HOS and OST5 (after being cultured overnight) were first stained with MTT solution for 4 hours in well plate to compare the differences. The OST5 cells have higher MTT reduction activity compared to

HOS cells (**Figure 5.10**).

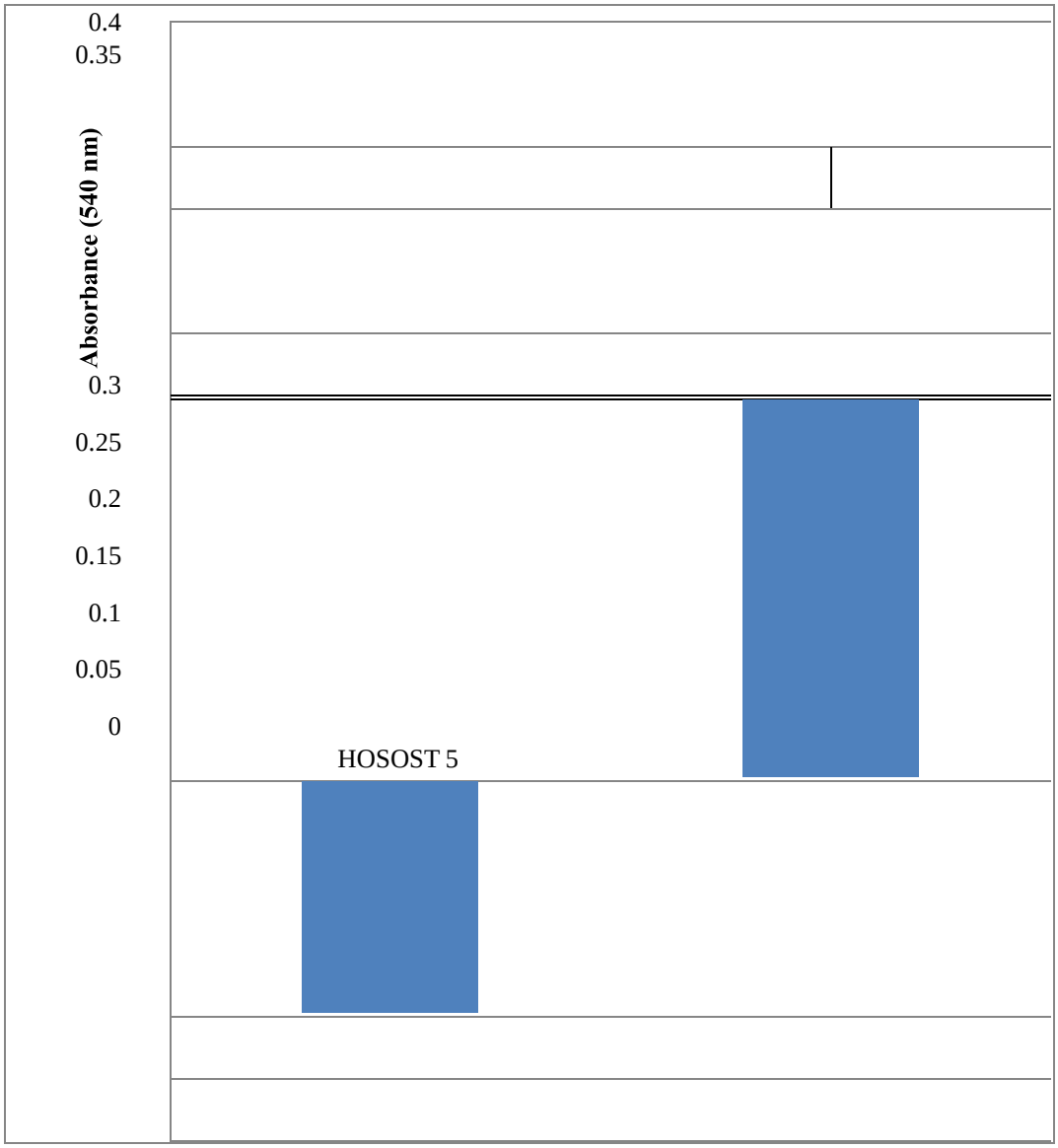

Figure 5.10: MTT reduction of HOS and OST5 cells. Results are the mean ± range, n = 2.

MTT reduction for culture bone samples were measured at day 21, day 28 and day 35. The measurements were carried out in different surface plates (adherent and non-adherent plate) to compare the rate of MTT reduction. After 4 hours of staining in MTT solution, the colour of bone cultures has altered to the dark purple. It can be seen very clearly in some areas on the bone samples indicating the reseeded cells. The cells were not growing uniformly on the bone samples, and it is difficult to ascertain

by examining these images whether proliferation increased over time in adherent and non-adherent surfaces (**Figure 5.11, Figure 5.12** and **Figure 5.13*)***.

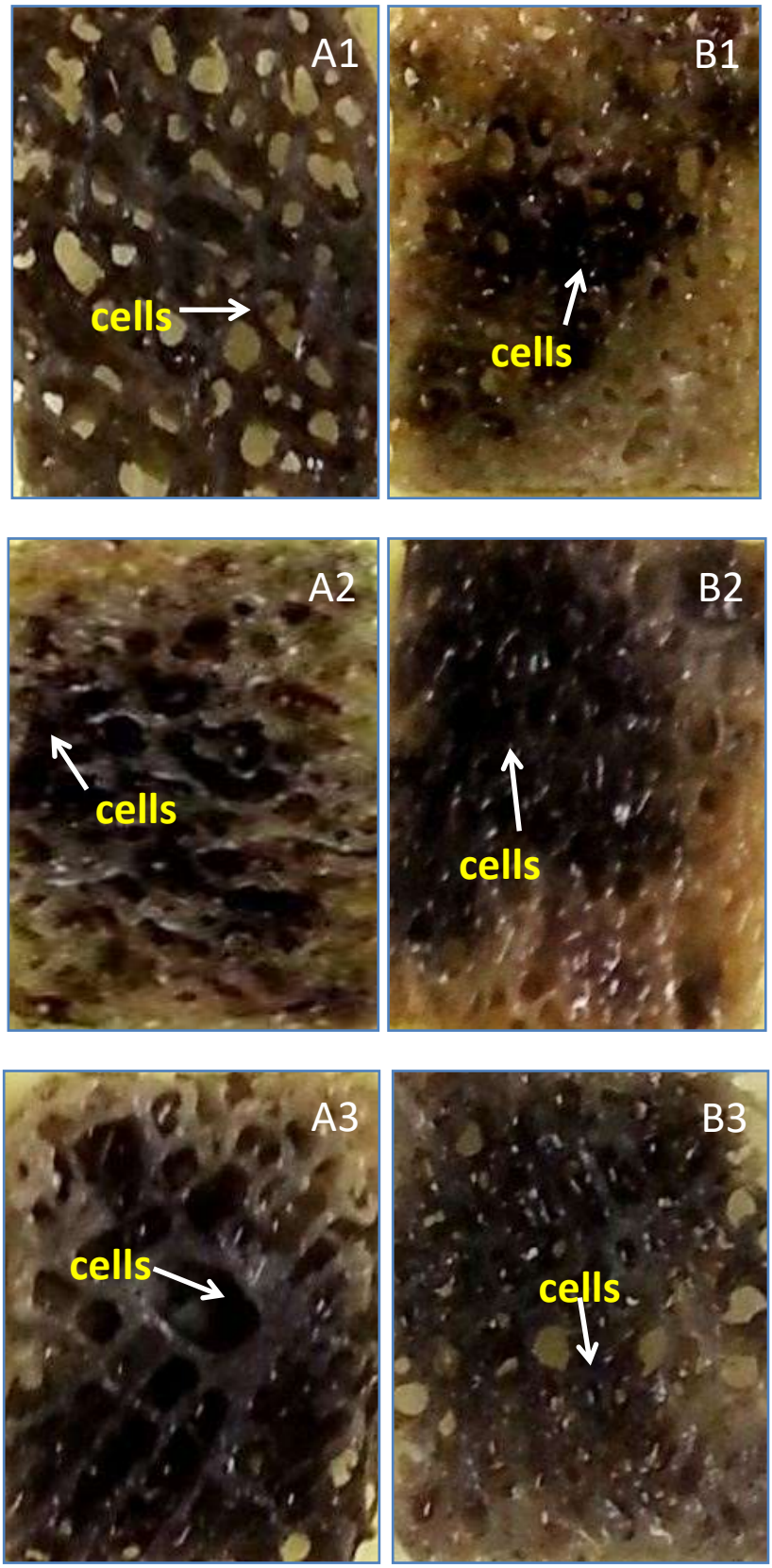

Figure 5.1 1: The images of MTT reduction after being stained with MTT solution for 4 hours in -

reseeded bone samples at day 21 in adherent (A1, A2, A3) and non adherent plate (B1, B2, B3).

-

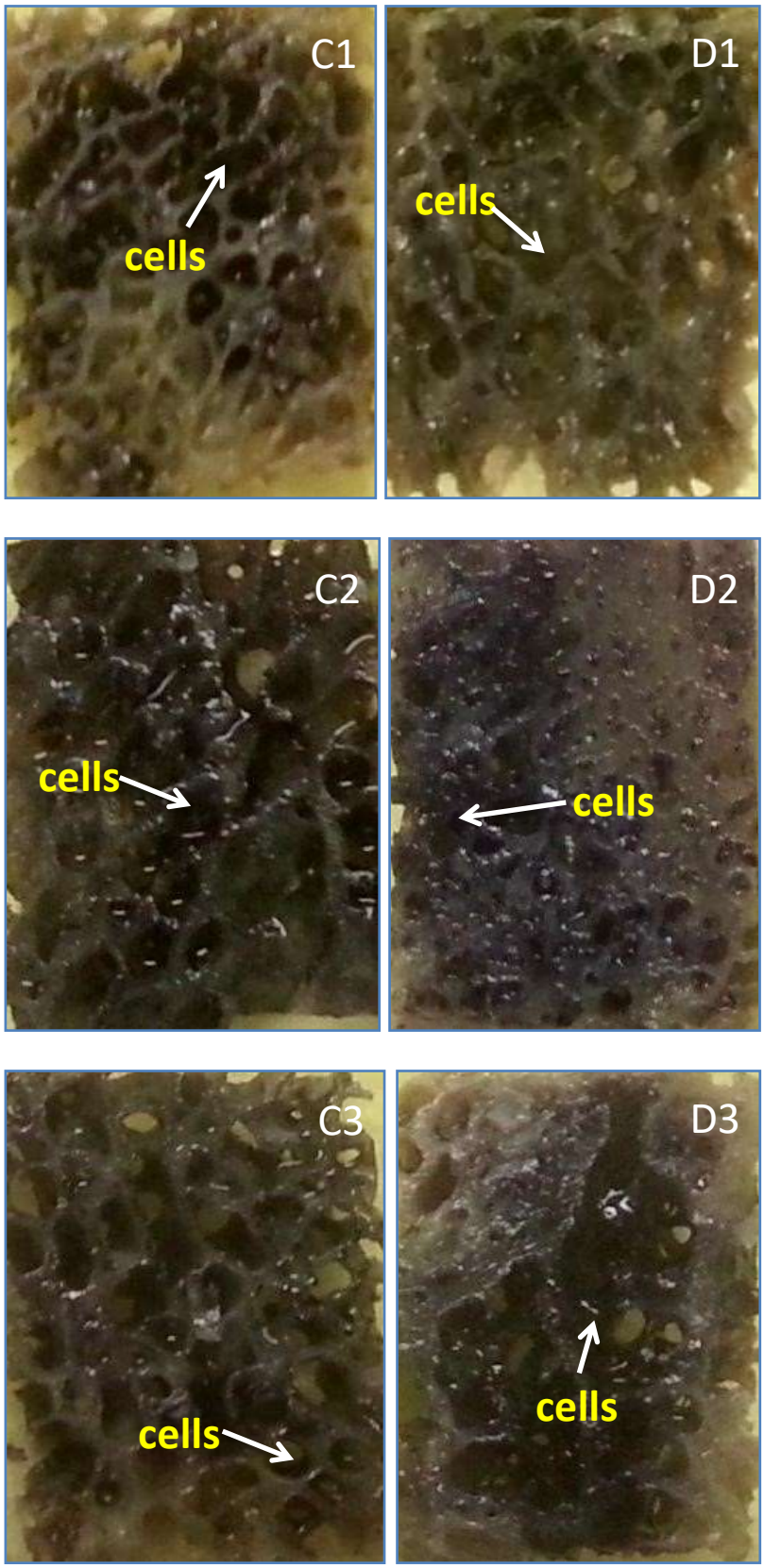

Figure 5.1 2: The images of MTT reduction after being stained with MTT solution for 4 hours in -

reseeded bone samples at day 28 in adherent (C1, C2, C3) and non adherent plate (D1, D2, D3).

-

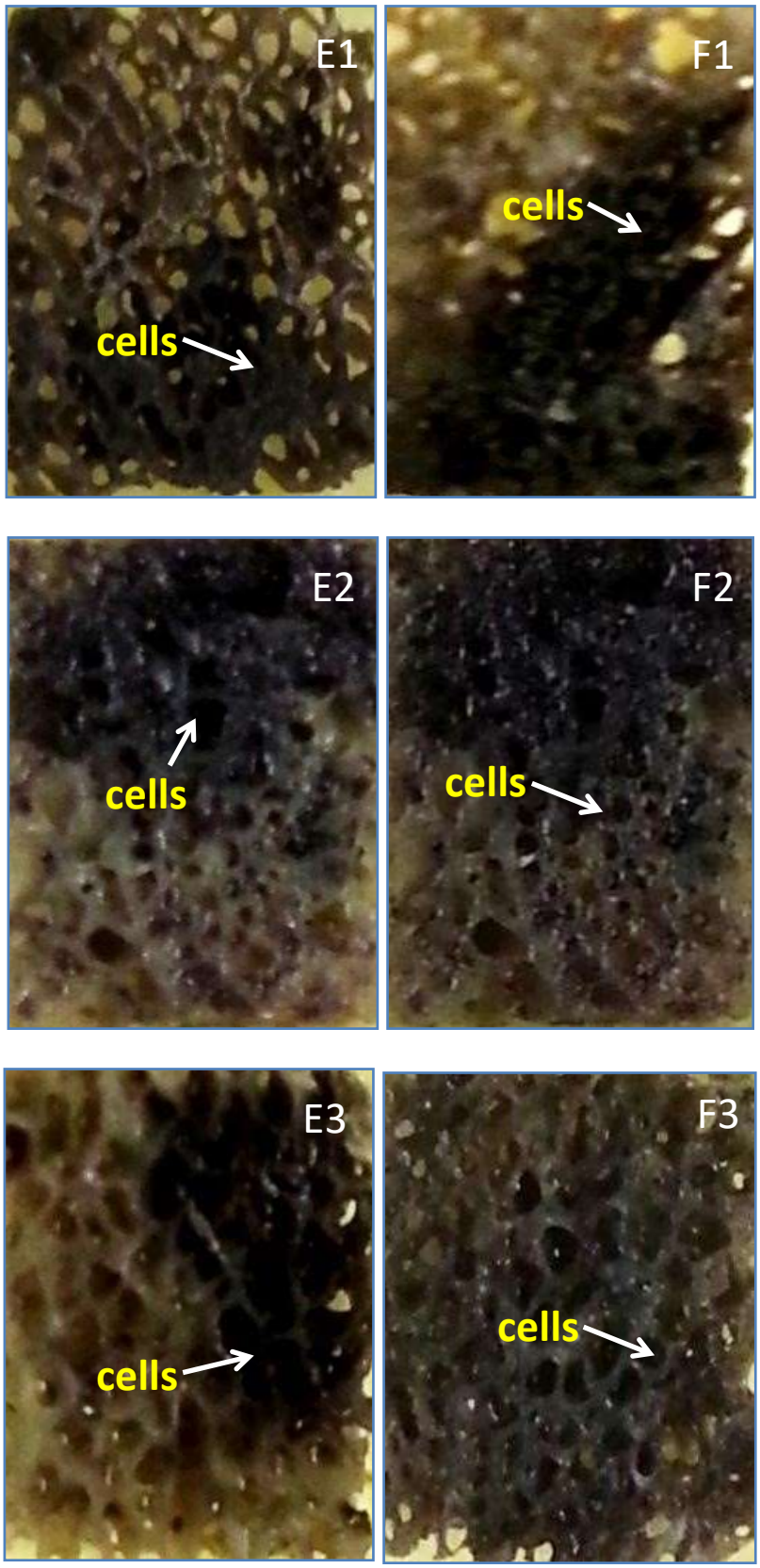

Figure 5.13: The images of MTT reduction after being stained with MTT solution for 4 hours in -

reseeded bone samples at day 35 in adherent (E1, E2, E3) and non adherent plate (F1, F2, F3).

-

The absorbance generated by MTT reduction was quantified by absorbance at 540 nm within minutes by spectrophotometric means. The representative data in **Figure 5.14** present the proliferation rate obtained in adherent and non-adherent plates. The Y axis showing optical density (OD) of the formazan product indicates rising cell numbers. The results of MTT assay for cell proliferation in the decellularised bone scaffold after periods of 21, 28, and 35 days are shown.

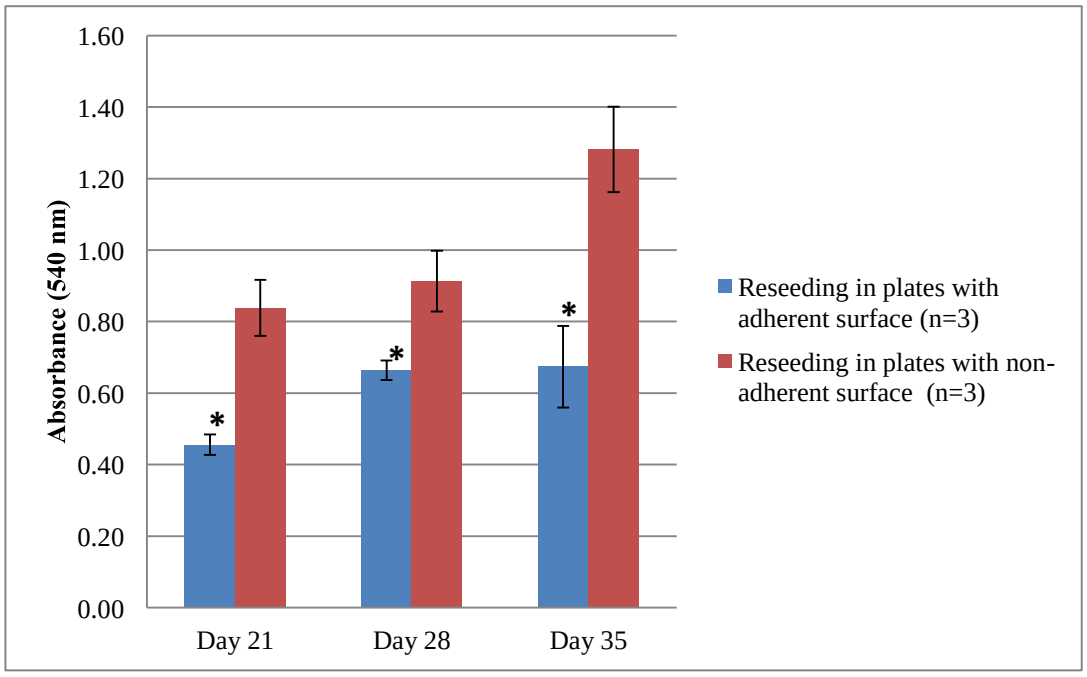

Figure 5.14: MTT reduction of HOS cells growing on bone (seeded at 5 x 10^5 cells per cm^2) in adherent and non-adherent surface from week 3 to week 5. n = 3 +/- SEM, *p≤0.05, by unpaired t-test.

There were significant differences (statistical significance) between reseeding in plates with adherent surface and reseeding in plates with non-adherent surface at day 21, day 28 and day 35. In non-adherent plates, the cell number increased slightly from day 21 to day 28, and then it increased sharply from day 28 to day 35. Meanwhile in adherent plates, the cell number increased abruptly from day 21 to day 28, but the proliferation slowed down from day 28 to day 35. There was always higher absorbance in non-adherent plates compared to adherent plates at any time points.

These results revealed that after 21 days seeding on the bone scaffold, the cells managed to attach and proliferate on the scaffold. To support this, human bone marrow stromal cells were shown to proliferate on allogenous trabecular bone; cell numbers enhanced after 12 days reseeding (Quan et al., 2014). A higher MTT absorbance indicates an increase in cell numbers or in metabolic rate. A decrease in cell numbers might be caused by necrosis or apoptosis (Edmondson et al., 1988).

A standard curve for HOS cell numbers was plotted and mentioned in **Section 5.2.2.3.4** to determine the linear relationship between cell number and formazan production. The graph below (**Figure 5.15**) was constructed from the range of 0 to $1x10^6$cells/well to expand the linear relationship.

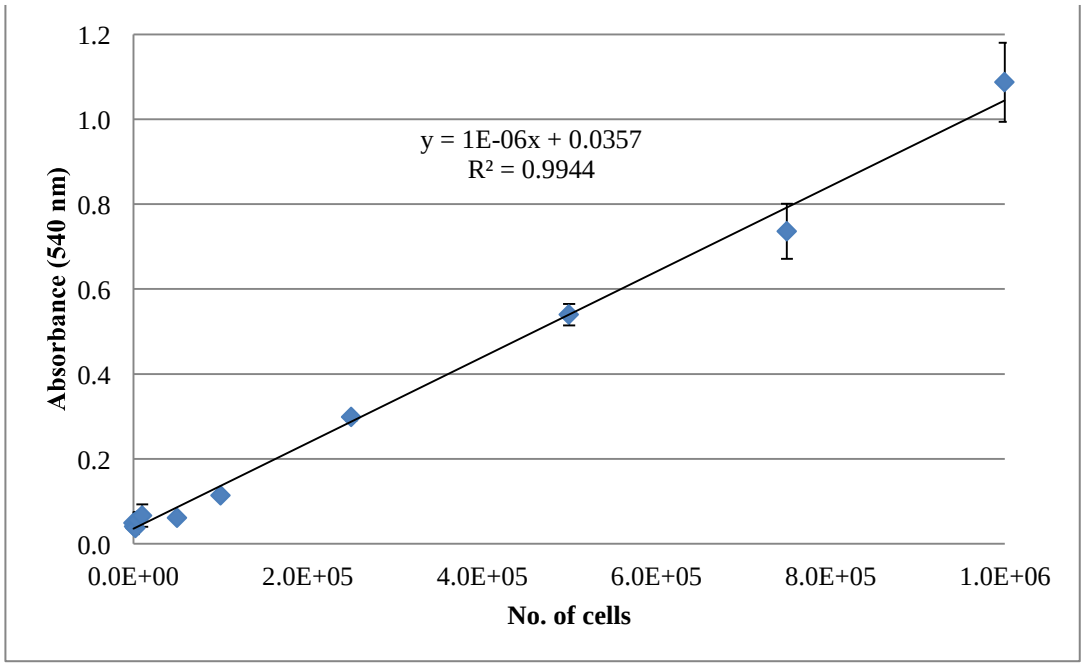

Figure 5.15: Standard curve of MTT reduction of HOS cells. Results are the mean ± range, n = 2.

From this calibration curve the number of viable cells on the scaffolds on each time point can be estimated as shown in the **Table 5.7** below:

Days	Total cells estimation	
	Adherent surface	Non-adherent
21	$4.524x10^5$	$8.023x10^5$
28	$6.283x10^5$	$8.773x10^5$
35	$6.383x10^5$	$> 1.246x10^6$ (out of range)

Table 5.7: The total cells estimation of HOS cells in adherent and non-adherent cultures after 21, 28 and 35 days of reseeding by applying the standard curve of MTT reduction.

The culture medium tended to change the colour from red to yellow after 10 days post-seeding. At the early stage of reseeding, the culture medium was changed every 4 days. But, it was changed every 2 days after 10 days of reseeding. The environment becomes acidic (pH is reduced) if the colour turns to yellow. The medium changes colour because of the increased number of cells, yielding metabolic products which are acidic.

5.3.2.5 Protein measurement

The total protein concentrations contained 10μM vitamin D3 treated HOS cells after 7, 10, 15, 21, 28 and 35 days of reseeding in adherent and non-adherent well plates are shown in **Figure 5.17** and **Figure 5.18**, respectively.

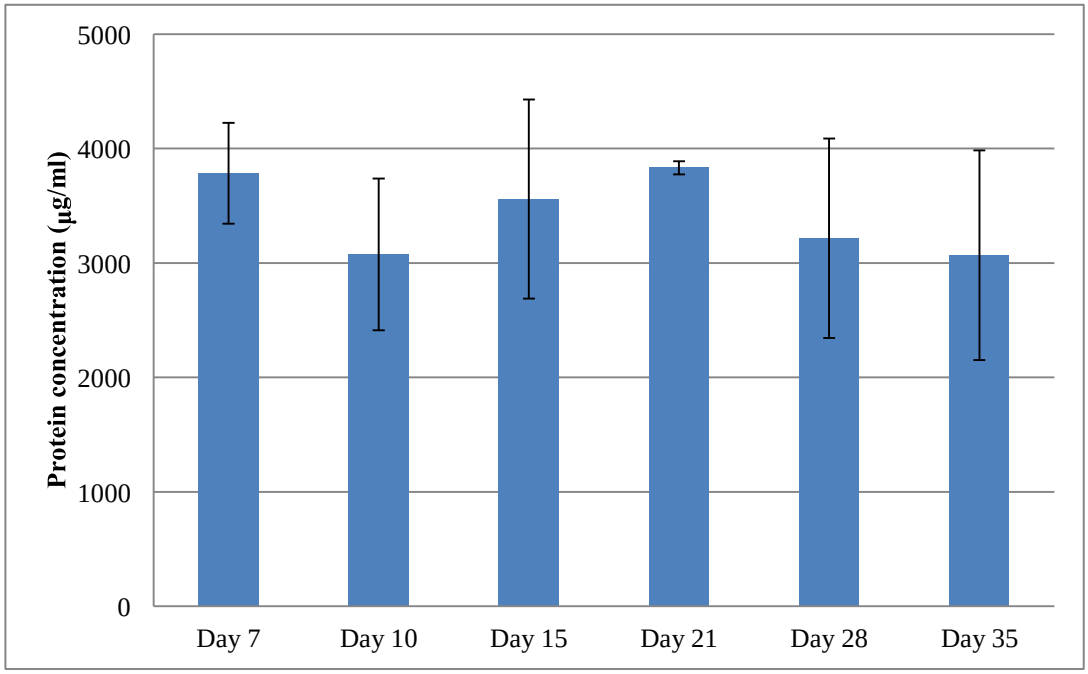

Figure 5.16: Protein concentration in HOS cells after 7, 10, 15, 21, 28 and 35 days of reseeding in adherent well plates by Lowry Assay. Cultures all contained vitamin D3 (10μM). Results are the mean ± SEM of n = 3. $p>0.05$ compared with the sample at Day 7, by ANOVA (repeated measures).

As demonstrated in **Figure 5.16** (adherent well plate), when comparing from control sample at day 7, there was no significant difference in protein concentration at any time points. Overall, the concentration of protein from day 7 to day 35 was within 3000 to 4000 μg/ml. These values are very high, and mask any increases in cell numbers.

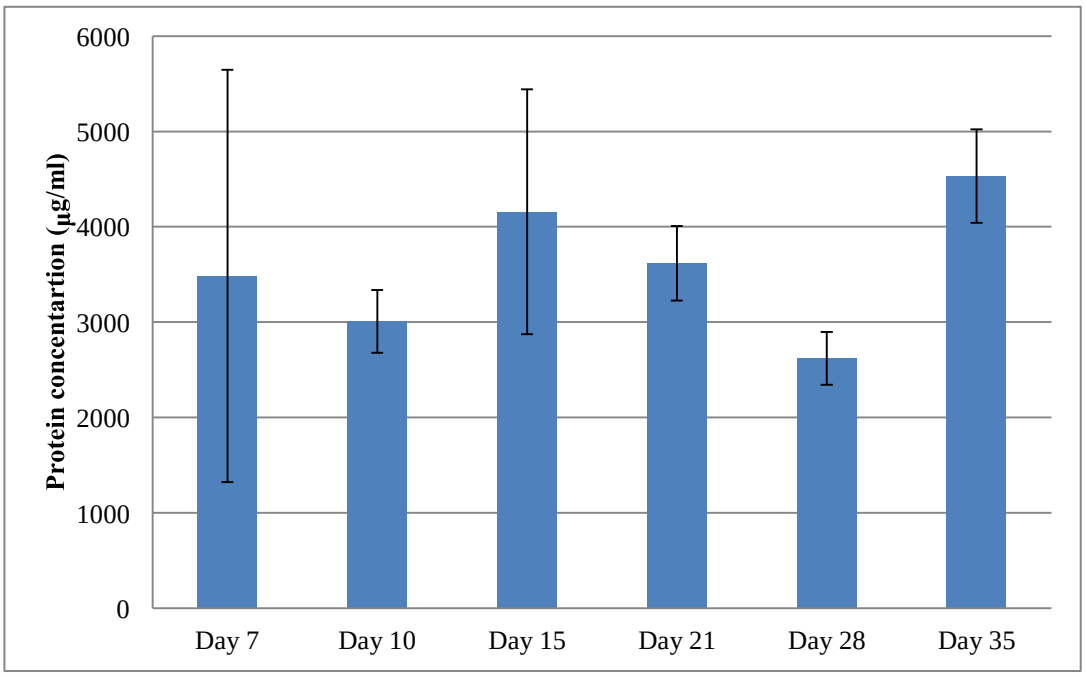

Figure 5.17: Protein concentration in HOS cells after 7, 10, 15, 21, 28 and 35 days of reseeding in non-adherent well plates by Lowry Assay. Cultures all contained vitamin D3 (10µM). Results are the mean ± SEM of n = 3. $p>0.05$ compared with the sample at Day 7, by ANOVA (repeated measures).

In **Figure 5.17** (non-adherent well plate), there were no significant differences at any time points when comparing from control sample at day 7. The concentration of protein from day 7 to day 35 in non-adherent plates was within 2000 to 5000 µg/ml. Again the cell protein values are very high and mask the growth of the cells over the 35 day period.

5.3.2.5.1 The comparison of the Lowry assay and the MTT assay in

quantifying cells numbers

Cell number is one of the important measures of the success of recellularisation. In our study, the attached cells on the decellularised bone scaffolds after 21 days of reseeding were quantified by two different assays such as by Lowry assay of protein content and MTT reduction. Both parameters were compared in terms of the efficacy and practicability to our study as below.

The Lowry assay (Protein by Folin Reaction) (Lowry et al., 1951) has been used widely to determine the total protein (Dulekgurgen, 2004). However, there are some limitations of the Lowry assay method. Firstly, the assay is based on an amino acid specific reaction (Dulekgurgen, 2004). In fact, the Lowry assay is sensitive to differences in the amount of tyrosine and tryptophan predominantly (Dulekgurgen, 2004; Lowry et al., 1951). As stated in **Section 5.2.2.4.2**, bone samples used in the experiment have been incubated in digestion buffer that consists of 10mM Tris, 1mM EDTA and 0.1% (v/v) Triton X-100, and 0.5% (w/v) Trypsin. Indeed, the Lowry assay is easily interfered with many buffer substances including detergents, carbohydrates, glycerol, Tricine, EDTA, Tris, potassium compounds, disulfide compounds, sulfhydryl compounds, most phenols, uric acid, guanine, xanthine, magnesium, and calcium. Besides, the Lowry assay is pH dependent and the colour is unstable. It is sensitive to pH variations, and the pH of assay must be sustained at 10 to 10.5. Likewise, different proteins produce different reactions with the reagents of the Lowry assay and the total color differs with dissimilar proteins (Lowry et al., 1951).

The MTT assay is a commonly accepted method to measure cell proliferation (Jaszczyszyn & Gasiorowski, 2008; Riss, 2014). Nevertheless, there are several weaknesses associated with using the MTT assay. MTT reduction relies on activities of intracellular reductases (enzymes). NADH and NADPH are required for most MTT reduction. The enzymes are found not only in the mitochondria, but also the cytoplasm and linked with membranes in the lysosome/endosome chamber and the plasma membrane. Furthermore, the MTT assay sensitivity differs among cell types, and it is based on the metabolic activity. Under ideal conditions, tetrazolium reduction assays can detect 200 to 1000 cells per well. The rate of tetrazolium reductions indicates the general metabolic activity or the rate of glycolytic NADH creation, not the cell numbers. In addition, the rate of MTT reduction can alter with culture conditions (e.g., pH and glucose amount of medium) and the physiological state of the cells. Another limitation is chemical interference (Riss, 2014).

In these experiments, bone medium was supplemented with ascorbic acid to help bone formation. However, the MTT assay is affected by chemicals, and enzymatic reduction of MTT occurs with chemicals such as ascorbic acid, vitamin A, and sulfhydryl groups. In terms of toxicity, MTT reagent has cytotoxic effects. The cells can be damaged or even killed when adding the reagent to evaluate cell viability. MTT has been stated to be toxic to eukaryotic cells (Riss, 2014). Also, the sensitivity of the MTT assay is affected by the type of cell, the technique employed for solubilizing the formazan crystals, as well as the metabolic state (Edmondson et al., 1988). The MTT assay needs additional solvent to solubilize the productformazan crystals. The solubilization solution destroys cell structure and enzymatic activity. The use of

DMSO has improved the solubilization process but, numerous organic solvents will somewhat alter the absorbance maximum of the formazan product (Riss, 2014).

Nevertheless, the MTT assay is more accurate than Lowry assay. In the MTT assay, it needs enzymes, cofactors, and living cells to react. Meanwhile in the Lowry assay, the reaction is dependent on the amount of tyrosine and tryptophan. In the studies, bone samples were incubated in 0.5 ml of 0.5M NaOH at 37C to digest samples for Lowry assay overnight. The cells from bone samples were assumed been entirely dissolved in 0.5M NaOH. Obviously, the effectiveness of this protocol was unclear, although the alkaline digestion buffers were cloudy indicating successful digestion, but not necessarily complete digestion.

During the MTT assay we are likewise assuming that the MTT solution reaches all the cells within the bone matrix and enables us to account for all of them.

Both the Lowry assay and the MTT have limitations in this respect. Meanwhile, the Lowry assay had a high background and it was thought to be due to serum proteins because bone was conditioned with medium containing 10% FCS for approximately 30 minutes before seeding cells. Also, the Lowry assay can detect any proteins without specificity. The measured proteins in the high background values measured in the study were assumed not to be collagen because collagen is made up mainly of three amino acids - glycine, proline, and hydroxyproline. Glycine is the main amino acid that can be detected by Lowry assay and it is likely that much of the high background is due to absorption of serum proteins onto the bone during the conditioning stage. This is the main limitation of quantitation of cell numbers by total protein, and this method cannot be regarded as accurate, or recommended for future work.

5.3.2.6 DAPI staining

Reseeded bone samples were stained for DNA content in 0.6 nM DAPI and observed under the Zeiss microscope as described in **Section 5.2.2.5.3**. In adherent surface conditions, the cells started to grow on the bone samples after day 3. The cells also tended to outgrow from the bone samples and stick to the 24-well plate (adherent surface). The cells on the non-flat surface of the bone were really difficult to see under the microscope. Cells spread over a large area of the bone samples after 10 days and formed subconfluent cell layers. Cell growth could be seen for both sides of the bone under the microscope (**Figure 5.18 A, B, C, D,** and **E**).

The DNA images also could be seen after 10 days in non-adherent surface (**Figure 5.18 F, G, H, I,** and ***J)***. Like in adherent plate conditions, there was a slow increment in cell numbers after 3 days, then cells also spread over large area of the bone samples after 10 days creating subconfluent cell layers. Cell growth could also be seen for both sides of the bone in these cultures.

The medium altered in colour (from pink to orange) within 3 days of reseeding in both surfaces (showing the large number of cells). When the medium was initially changed, the possibility to lose the suspension cells from cultures in non-adherent surface to the waste medium was higher. It was difficult for the floating cells to attach to the area of bone and they probably died in suspension. The same loss of cells probably happened in adherent surfaces when the bone samples were transferred to a new adherent well plate on day 3. Taken together, the cells growth was restricted by surface area in adherent surface while in non-adherent surface, the cells growth was restricted by concentration of cells in the medium (suspension).

Agitation (i.e., rotating or shaking) was needed for sufficient gas exchange in nonadherent surface.

However, it was a mistake in our study because we did not quantify the amount of DAPI staining from the attached cells during re-cellularisation because as described on **Table 5.5**, the lowest limit of detection in terms of cell number was by DAPI staining and that parameter could be good quantification of cell numbers. In this study, the cell numbers were only quantified by MTT reduction after recellularisation.

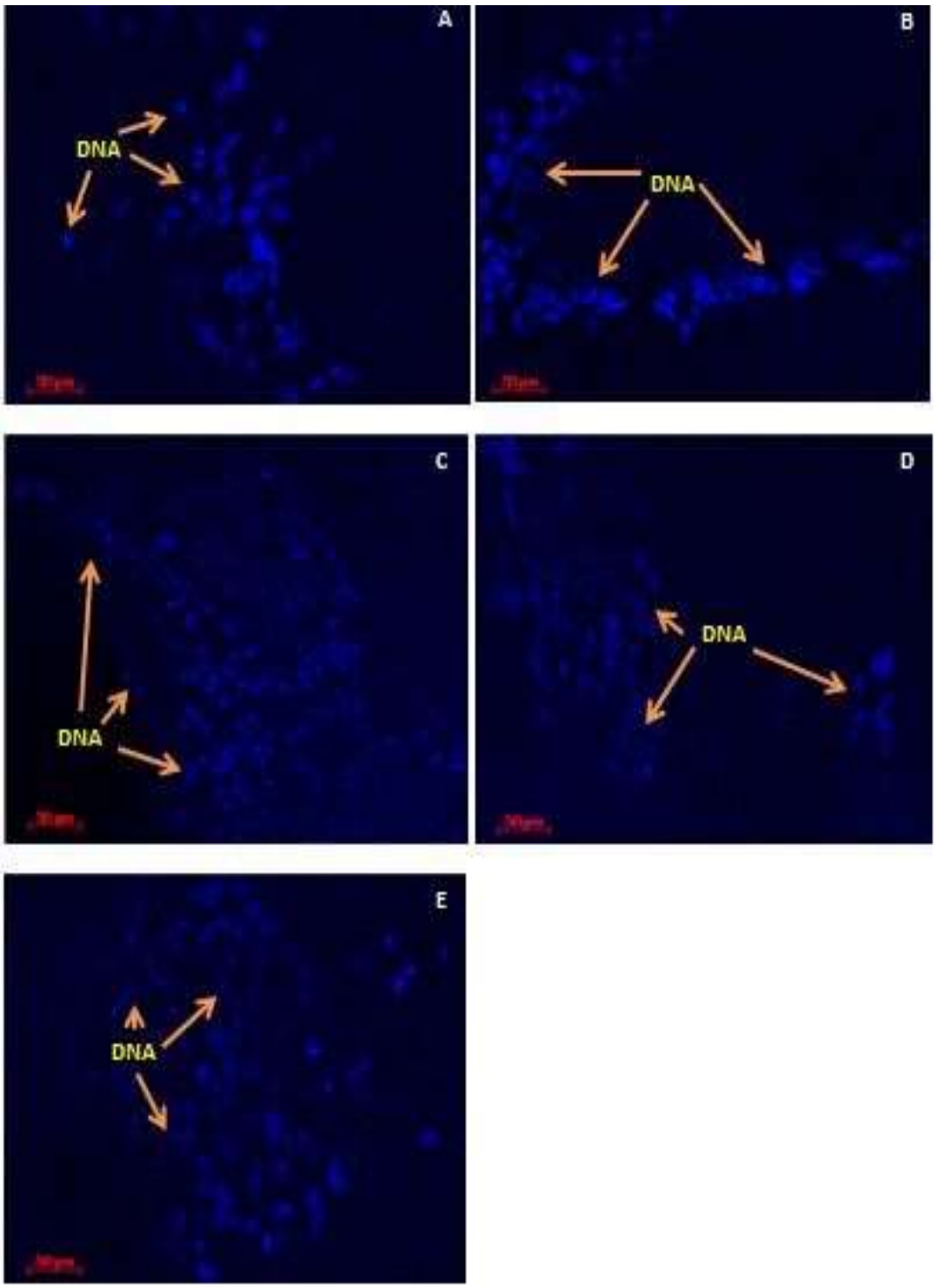

Figure 5.18: HOS cells were reseeded (at 5 x 10^5 cells per cm^2) onto bone. Bone samples were stained in 400µl of 0.6nM DAPI after **A)** 3 days, **B)** 7 days, **C)** 10 days, **D)** 15 days and **E)** 21 days. Cells seeded in plates with an adherent surfaces.

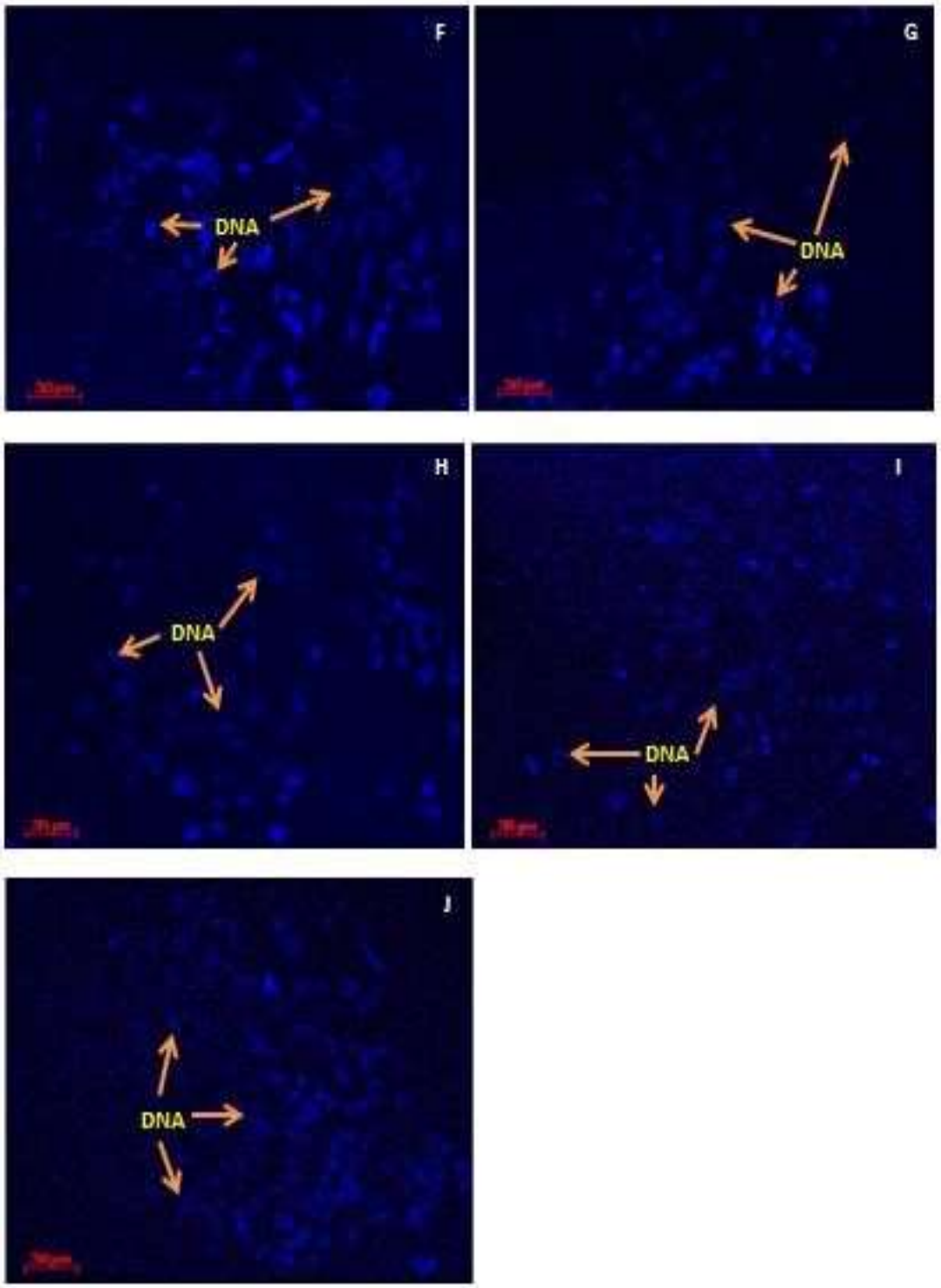

Figure 5.18: HOS cells were reseeded (at 5 x 10^5 cells per cm^2) onto bone. Bone samples were stained in 400µl of 0.6nM DAPI after **F)** 3 days, **G)** 7 days, **H)** 10 days, **I)** 15 days and **J)** 21 days. Cells seeded in plates with non-adherent surfaces.

5.3.2.7 Picric Sirius red stain test

One of the major elements of extracellular matrix in all tissues is collagen. It is a fibrous protein synthesized by fibroblasts and accounts for about one third of the overall proteins in the body. Basically, the collagen molecule has three polypeptide chains that comprise three key amino acids - glycine, proline and hydroxyproline (OHPr) (Taskiran et al., 1999). From all of these, the major component of collagen is 4-Hydroxyproline accounting for approximately 13.5% of its amino acid constitution (Kliment et al., 2011).

A common approach of collagen evaluation is reliant on the quantitation of OHPr that accounts for about 13.5% of the collagen molecule. To accomplish this, OHPr is oxidised to form pryrrole and pryrrole 2 carboxylic acid and this reacts with p-dimethylaminobenzaldehyde (DMBA) to form a red product that is evaluated spectrophotometrically at 550 nm (Taskiran et al., 1999).

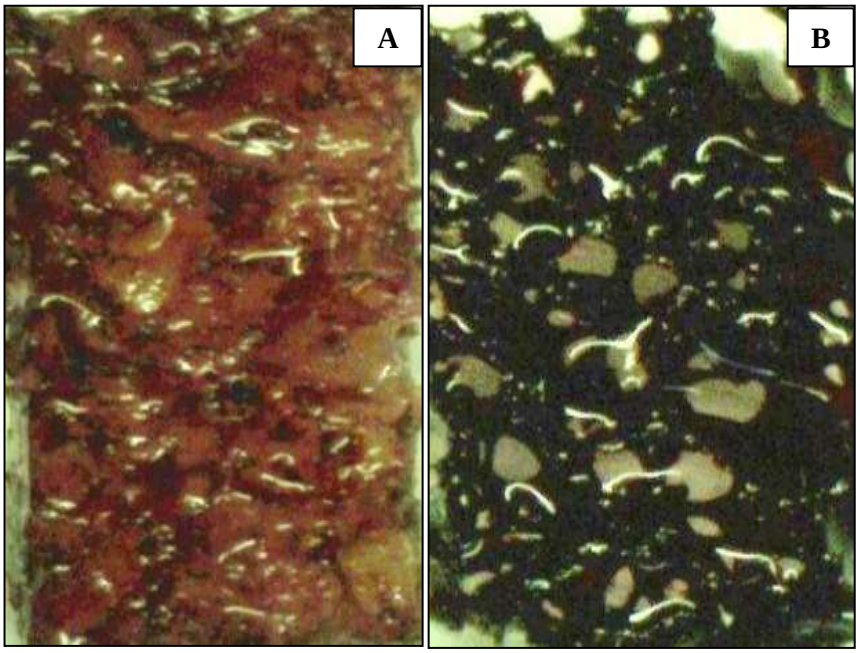

Figure 5.19: Picric Sirius red stain. Bone before decellularisation **(A)** was slightly reddish, whereas the decellularised sample **(B)** showed vast extracellular collagen deposits, stained in dark orange-red.

Tests were carried out before decellularisation, and in decellularised bone to determine whether the decellularisation process removed the collagen. In this study, the presence of collagen was demonstrated by picric Sirius red staining test. The results have shown (**Figure 5.19**) that both type of bone samples (before and after decellularised) stained in picric Sirius red assay. Sirius red is a strong anionic dye that stains collagen by reacting through its sulphonic acid groups. Walsh et al. have stated that Sirius red detects several collagen types such as Types I, III, IV and V; and produced the same calibration curves for every collagen type (Walsh et al., 1992). However, in this study, the measured collagen was assumed to be type I collagen because bone protein consists of 85% to 90% collagenous proteins, in which it is mainly type I collagen (Clarke, 2008).

In conclusion, this method of detecting collagen confirmed that the decellularisation process did not remove the collagen from the bone tissue. It could not be used to detect collagen formation by the human cells. To do this, a human specific collagen antibody would have been necessary. Since the collagen remained in place on the decellularised tissue, collagen coating of the scaffold was not expected to induce any increase in cell adhesion to the decellularised scaffold. However, there is a possibility that the collagen was denatured in some way by the decellularisation process, and its adhesive properties and receptors may have been damaged.

5.3.2.8 The measurement of osteocalcin by ELISA

5.3.2.8.1 The principle of immunological methods for the analysis of protein

Immunological methods for analysing proteins take benefit of the specificity of antibodies for their target antigens. Immunological methods start with the production of antibodies to a specific antigen. An antibody called an immunoglobulin, Ig (also a protein), is produced by an animal in reaction to the existence of an unfamiliar substance, called antigen. Antibodies have particular and high affinity for the antigens that evoked their production. The useful antigens can be proteins, polysaccharides, and nucleic acids. An antibody identifies a particular group or cluster of molecules on the target molecule called an antigenic factor or epitope. Overall, immunological methods rely on the capability to produce antibodies to a particular antigen (Berg et al., 2006), and are highly specific.

5.3.2.8.2 Proteins can be detected and quantified by using an enzyme-linked immunosorbent assay

As stated, antibodies can be employed as ideally specific analytic reagents to measure the total amount of a protein or other antigen and one method using this interaction is called ELISA. This technique employs an enzyme that reacts with a colourless substrate to form a coloured product. In fact, the enzyme is covalently connected to a particular antibody that identifies a target antigen. The antibodyenzyme complex will attach if the antigen is available, and the enzyme will react with an added substrate forming a coloured product. Therefore, the existence of the coloured product

designates the presence of the antigen. Furthermore, an enzymelinked immunosorbent assay, which is fast and appropriate, can identify less than a nanogram (10^{-9} g) of an antigen. ELISA can be accomplished with either polyclonal or monoclonal antibodies; however, the application of monoclonal antibodies produces more-reliable and specific results. There are two types of ELISA such as indirect and direct (sandwich) ELISA (Berg et al., 2006).

There are two well established methods to measure the presence of an antigen with great sensitivity in an *in vitro* assay - Radioimmunoassay (RIA) and ELISA. In fact, RIA is an assay that is dependent on the measurement of radioactivity related with immune complexes. In any specific experiment, the label may be on either antigen or the antibody (http://www.microbiologybook.org/mobile/m.immuno7.htm). RIA has been the first immunoassay method established to measure nanomolar and picomolar concentrations of hormones in biological solutions (http://www.antibodies-online.com/resources/17/1215/Radioimmunoassay+RIA/). Meanwhile, ELISA is dependent on the measurement of an enzymatic reaction related with immune complexes. In any specific assay, the enzyme may be bound to either the antigen or the antibody (http://www.microbiologybook.org/mobile/m.
immuno-7.htm).

5.3.2.8.3 Analysis of osteogenic differentiation *in vitro*

In this study, a standard curve (optical density vs. human osteocalcin) was constructed. From this graph (**Figure 5.20**), human osteocalcin concentration in the bone samples were determined.

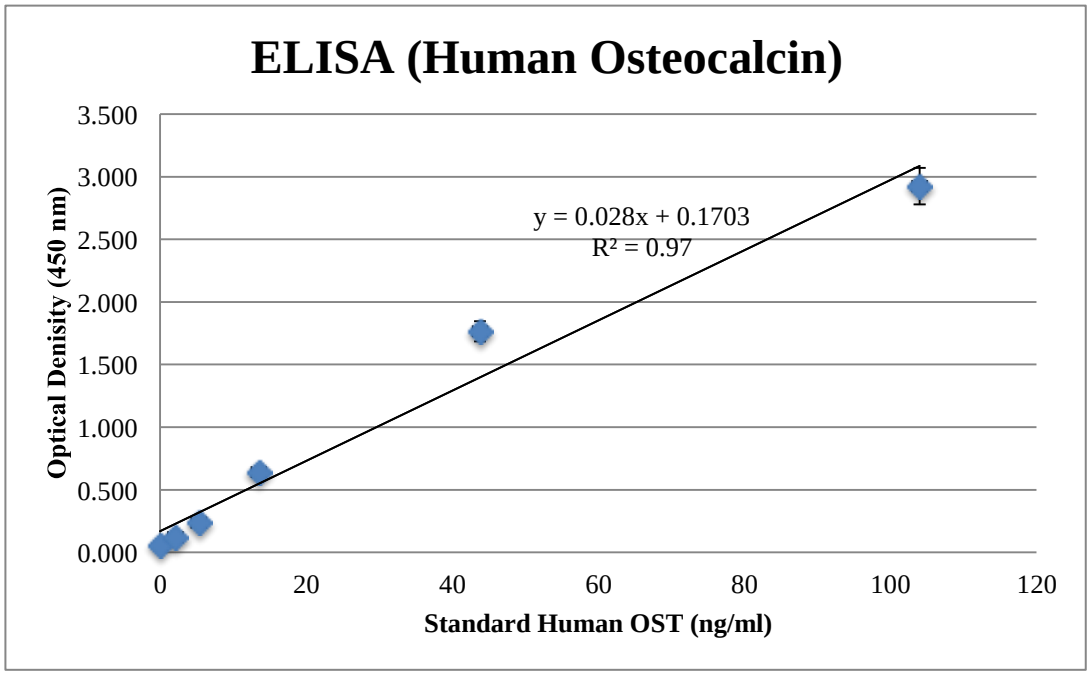

Figure 5.20: Standard curve of human osteocalcin production over the optical density. Results are the mean ± range of n = 2.

Osteogenic differentiation by HOS cells in bone samples was assessed by detection of the late osteogenic marker, osteocalcin. Separate bone samples were reseeded and cultured in adherent and non-adherent surfaces. HOS-produced osteocalcin in the medium was measured in the samples using the osteocalcin ELISA Kit (Invitrogen, KAQ1381) according to manufacturer's instructions. Representative data for the secreted osteocalcin in the presence of vitamin D3 treatment in HOS cells after 7, 10, 15, 21, 28, and 35 days of reseeding for both adherent and nonadherent well plate by ELISA are shown in **Figure 5.21**.

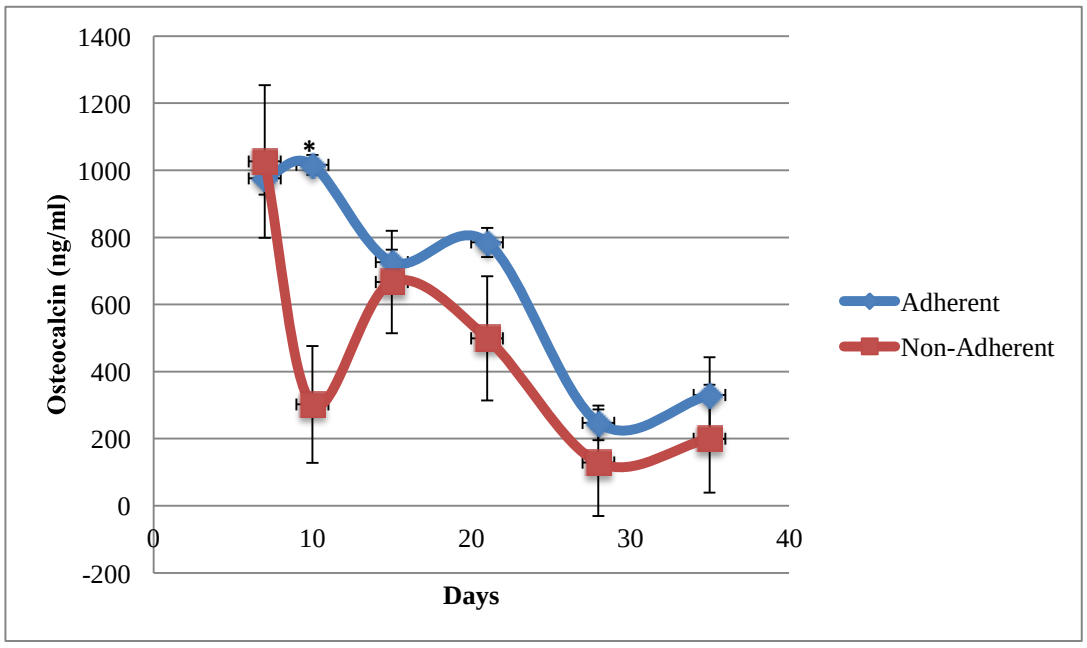

Figure 5.21: Secreted osteocalcin in HOS cells after 7, 10, 15, 21, 28 and 35 days of reseeding decellularised bone pieces in both adherent and non-adherent well plates by ELISA. Cultures all contained vitamin D3 (10μM). Results are the mean ± SEM of n = 3. $p \leq 0.05$ from control at Day 7, by ANOVA (repeated measures), at all time points under both conditions, and $*p \leq 0.05$ comparing adherent and non-adherent well plates, by unpaired t-test.

From the observations, the osteocalcin concentration (ng/ml) in cells grown on decellularised bone on an adherent surface increased slowly from day 7 to 10, day 15 to 21, and also day 28 to 35. But, it dropped gradually from day 10 to 15, and dropped drastically from day 21 to 28. Meanwhile in the non-adherent surface, the osteocalcin concentration decreased suddenly from day 7 to 10, and reduced dramatically from day 15 to 28. However, some increases were shown from day 10 to 15, as well as day 28 to 35. Moreover, in comparisons between adherent and nonadherent surface, the osteocalcin concentration was significantly different at day 10.

No significant differences were assessed at the rest of time points statistically.

Day	OSTEOCALCIN Average ± SEM [ng/1E6 cells]		MTT Average ± SEM [1E6 cells]	
	Reseeding in plates with adherent surface, n=3	Reseeding in plates with non-adherent surface, n=3	Reseeding in plates with adherent surface, n=3	Reseeding in plates with non-adherent surface, n=3
21	1869.6 ± 103.3	622.0 ± 230.5	0.420 ± 0.028	0.803 ± 0.079
28	393.6 ± 81.9	146.8 ± 181.1	0.628± 0.027	0.877 ± 0.085
35	517.4 ± 176.7	160.4 ± 129.0	0.638 ± 0.114	1.246 ± 0.120

Table 5.8: Osteocalcin secretion per million cells [ng/1E6 cells] by ELISA and cell numbers by MTT reduction in HOS cells after 21, 28 and 35 days of reseeding for both adherent and non-adherent well plate. Results are the mean ± SEM of n = 3.

Furthermore, the osteocalcin formation was correlated to the number of osteoblasts present on each scaffold [ng/1E6 cells] after 21, 28 and 35 days of reseeding for both adherent and non-adherent well plate. The results are shown on **Table 5.8.** Also, the number of cells carried out by MTT reduction are shown on the same table as comparisons. According to the results, both adherent and non-adherent samples showed a decrease in osteocalcin secretion per cells from day 21 to 28. The values of osteocalcin secretion per million cells at any time point were always higher in plates with an adherent surface.

Osteocalcin or BGP is the main non-collagenous protein of bone matrix. It is generated in the bone by osteoblasts. After formation, it is partly integrated in the bone matrix and the remainder can be found in the blood circulation. Circulating concentrations of osteocalcin in normal individuals (18 years or order) are approximately 9 - 42 ng/mL (University of Michigan Health Services, 2012).

According to Delmas et al., (2000), osteoblasts generate osteocalcin and combine it into the bone matrix. Throughout bone resorption, osteocalcin is transmitted into the circulation from the matrix. Thus, it is indicated as a bone turnover marker instead of a bone production marker. The circulating levels of osteocalcin have been revealed to indicate the rate of bone production and osteoblast differentiation (http://www.thermofisher.com/order/catalog/product/KAQ1381?ICID=search-product).

Osteocalcin is regulated by PTH among other determinants. The cAMPdependent protein kinase pathway has an crucial function in PTH signalling and determination of osteocalcin expression. Actually, osteocalcin can be found in two different forms called carboxylated and undercarboxylated. Carboxylated osteocalcin has great affinity for the hydroxyapatite crystals and it will remain bound in bone matrix throughout its mineralization. In this form osteocalcin fixes with great affinity to hydroxyapatite crystals and controls bone crystal development. In contrast, undercarboxylated osteocalcin has poor affinity for bone mineral (Sila-Asna et al., 2007).

In our study, it was well-explained (see **Section 5.2.2.7.3**) that the decellularised bone samples either in adherent or non-adherent plates were reseeded with cells and incubated with 1,25-dihydroxyvitamin D_3 in serum free medium 72 hours (Jonsson et al., 1999; Marti'nez et al., 2001) prior to the time points. The findings from a study by Marti'nez et al. (2001) on knee and hip human osteoblast (hOB) cell cultures found that the variations in the reaction of osteocalcin to 1028 mol/L $1,25(OH)_2D_3$ in osteoblastic (hOB) cells from human trabecular bone was reliant on donor age (secreted osteocalcin was greater in hOB cells from the younger donors, than with

those from older donors) and skeletal source. Meanwhile, Jonsson and co-workers (1999) have reported that basal production of osteocalcin was lowto-undetectable among three types of cells - bone stroma cell culture (BMSC), human osteoblast explant cultures (hOB), and osteoblast explant culture from collagenease-treated bone (hOB^{col}). They found that osteocalcin (ρg/1000 cells) were 147 ± 32 (BMSC), 336 ± 60 (hOB) and 356 ± 66 (hOB^{col}).

However, no osteocalcin could be identified in supernants from vitamin D3 treated HOS cells in a study by Clover and Gowen (1994). As reported by the authors, the HOS cells were treated with 10^{-8} M vitamin D3 for 72 hours, and the supernants were removed and stored at -20C for osteocalcin assay. They did not find any osteocalcin (ng/ml) for both control and vitamin D3 treated in HOS cells (0 ng/ml). As a conclusion, they stated that HOS cells were not suitable for studying the synthesis of osteocalcin by osteoblasts.

The synthesis of osteocalcin is reliant upon the existence of active metabolites of vitamin D (1,25-dihydroxyvitamin D). Vitamin D controls the expression of many bone proteins, especially osteocalcin. It encourages the transcription of osteocalcin, as well as having bidirectional impacts on type I collagen and ALP gene transcription. Moreover, the treatment of bone samples with vitamin D seems to stimulate the mineralization of osteoid and results in bone resorption by mature osteoclasts. However, this impact is not direct and requires cell employment and communication with osteoblasts and the synthesis of monocytic precursors to osteoclasts (Fogelman et al., 2012).

As discussed in **Section 5.3.2.3.3**, $1,25(OH)_2$ vitamin D_3 decreased ALP activity in the cultured human cells. The ALP activity decreased particularly between

days 10 to 21 (see **Figure 5.8**, **5.9** and **Table 5.6**). As the ALP activity decreased, the osteocalcin secretion per million cells also decreased (after 21 days of reseeding) and this is shown on **Figure 5.21** and **Table 5.8**. At the initial stage of cell ingrowth, osteoblasts do commonly express ALP rather than osteocalcin. However, osteocytes (mature cells) do express osteocalcin, galectin 3, and CD44, a cell attachment receptor for hyaluronate, and also some other bone matrix proteins (Clarke, 2008). It appears from the data on $1,25(OH)_2D_3$ exposure that osteoblasts differentiation into osteocytes does not parallel cell proliferation. And although the cell numbers increase on the decellularised matrices, most remain as osteoblasts – resulting in a decrease in osteocalcin secretion per million cells.

5.3.2.9 Mechanical testing

5.3.2.9.1 The effects of mechanical testing before and after recellularisation

Based on the representative data in **Figure 5.22**, when reseeding onto the adherent surface, the stiffness after recellularisation was slightly lower compared to before recellularisation. In contrast, the stiffness after recellularisation was slightly higher than before recellularisation when reseeding onto the non-adherent surface. However, statistically no significant differences were found before and after recellularisation either in adherent or non-adherent surface after 21 days of reseeding. To sum up, the stiffness of bone samples were not affected by the recellularisation. The evaluations were extended to obtain the effects of repeated measurements on mechanical testing in bone samples.

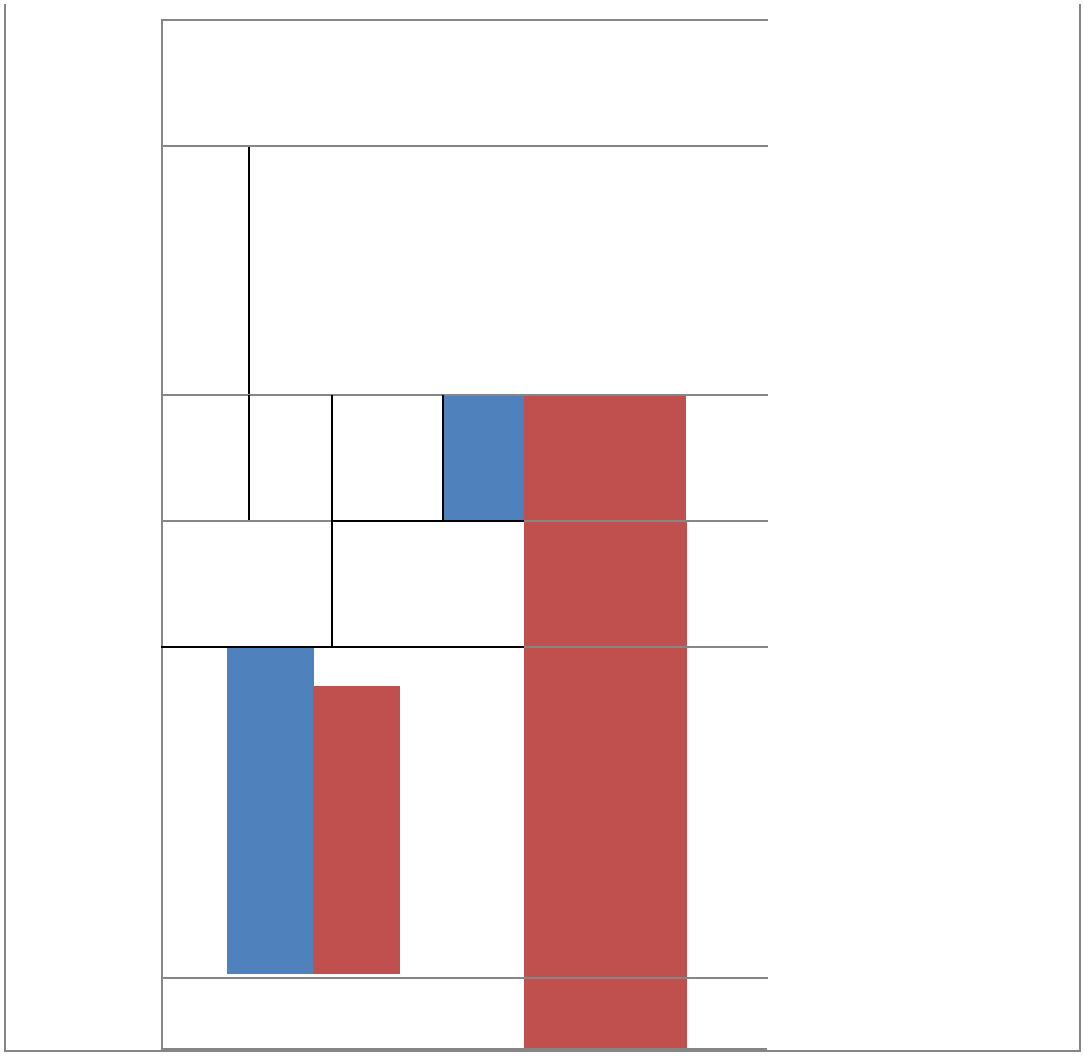

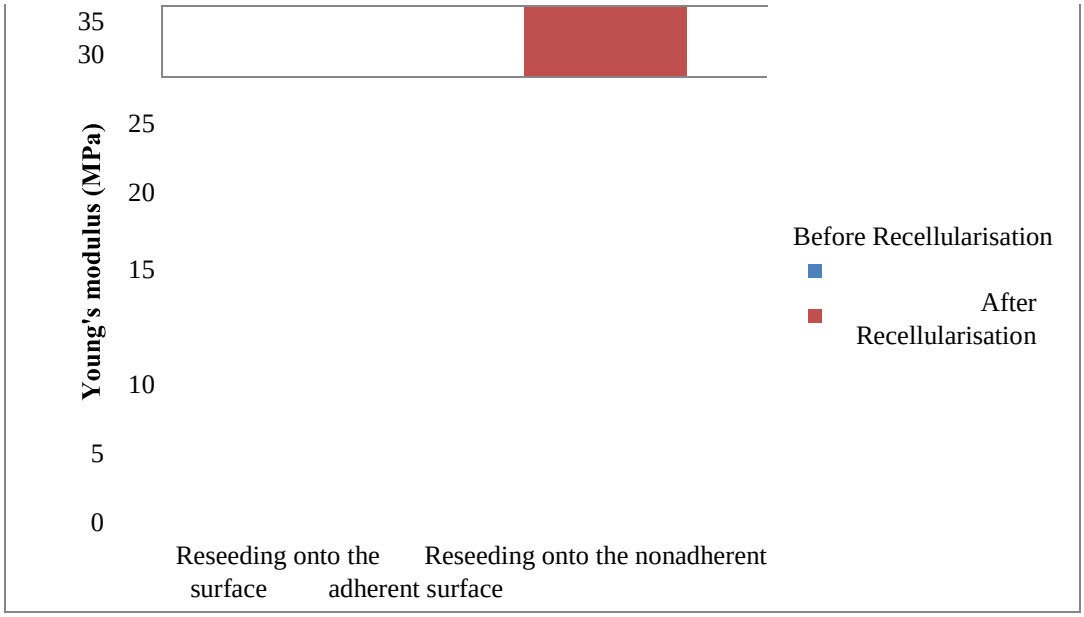

Figure 5.22: Young's modulus of bone samples before and after reseeding onto the adherent and nonadherent surfaces. Results are the mean ± SEM of n = 6. p>0.05 compared with the control (before recellularisation), by ANOVA for repeated measures.

5.3.2.9.2 The effects of repeated measurements on mechanical testing in bone samples

As discussed in **Section 4.3.3**, the repeated trials could affect the mechanical testing of bone samples before and after decellularisation. As well in this section, the effects of trials on mechanical testing were measured before and after 21 days of reseeding in adherent and non-adherent surfaces

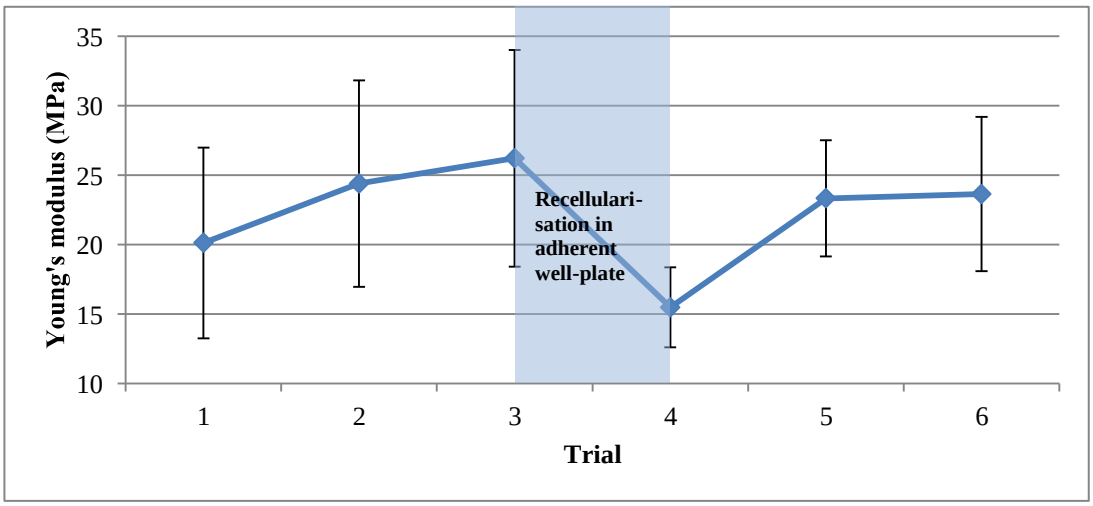

Figure 5.23: A) The effect of number of trials on Young's modulus in bone samples before and after recellularisation in adherent plate. Trial 1, 2, and 3 were before recellularisation while trial 4, 5, and 6 were after recellularisation. $p>0.05$, by ANOVA (one-way repeated measures). Results are the mean ± SEM of n = 6.

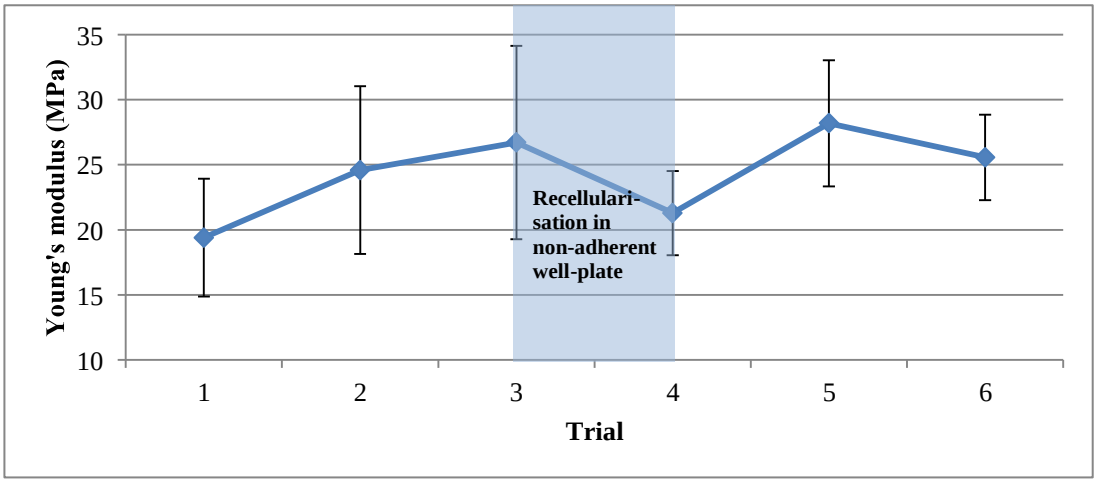

Figure 5.23: B) The effect of number of trials on Young's modulus in bone samples before and after recellularisation in non-adherent plate. Trial 1, 2, and 3 were before recellularisation while trial 4, 5, and 6 were after recellularisation. $p>0.05$, by ANOVA (one-way repeated measures). Results are the mean ± SEM of n = 6.

Again, we revealed that the (Young's modulus) stiffness was gradually increased from one trial to another (trial 1, 2, and 3) before recellularisation whether in adherent (**Figure 5.23 A**) or non-adherent (**Figure 5.23 B**). But, the stiffness was suddenly decreased after the recellularisation process (from trial 3 to trial 4) in both protocols. Furthermore, the same pattern of graphs were observed from trial 4 to trial 5 in bone samples reseeded in adherent and non-adherent plates as they increased dramatically. However from trial 5 to trial 6, the stiffness was unchanged in the

adherent plate and slightly decreased in non-adherent plate. From the statistical analysis, there were no significant differences in the bone samples either reseeded in adherent or non-adherent plates before and after recellularisation.

In conclusion, the stiffness was not affected by the recellularisation protocols of using adherent or non-adherent surfaces before and after recellularisation. However more significantly, the stiffness of bone samples after the mechanical testing was influenced by number of trials as discussed in **Chapter 4**, **Section 4.3.3**.

5.3.2.10 Porosity measurements

Protocols	Mean ± SEM (µm)
Before decellularisation in frozen bone (Control)	211.35 ± 4.88
After decellularisation in 1.6 ml digestion buffer and 0.4 ml trypsin	223.28 ± 3.10
After recellularisation in adherent plate	236.46 ± 9.65
After recellularisation in non-adherent plate	267.58 ± 3.56

Table 5.9: The pore size diameter of bone samples before (control) and after decellularisation, and after 21 days of recellularisation in adherent and non-adherent plate. Results are the mean ± SEM of n = 3. $p>0.05$ compared with the control (ANOVA for repeated measures).

Another crucial aspect was the porosity before and after recellularisation. The data shown in **Table 5.9** show that there were no significant differences ($p>0.05$ compared with the control, ANOVA for repeated measures) before (after decellularisation in 1.6 ml digestion buffer and 0.4 ml trypsin) and after recellularisation in adherent or non-adherent plates.

Nevertheless, the pore size diameter in recellularised bone samples in adherent (236.46 ± 9.65 μm) and in non-adherent (267.58 ± 3.56 μm) surfaces seemed slightly increased as compared to control (223.28 ± 3.10 μm) after 21 days of re-seeding. Every sample used in the porosity measurements was different, and the dimensions were not exactly the same.

According to Yeatts et al., (2011), cells growing on smaller pore size scaffolds differentiated quicker (because ALP activity was enhanced) than those on bigger pores. But in our study, the ALP activity was higher in cells growing in nonadherent conditions that have bigger pore diameters. However, the pore sizes in the non-adherent conditions were not significantly bigger.

However, some previous studies have supported our results. Research has been carried out by Vissers and colleagues on the effect of pore size in controlling mesenchymal stem cells reactions to Bioglass (BG)-loaded composite scaffolds. In their studies, comparisons were made among scaffolds with three pore diameters - 125-300 μm, 300-500 μm and 500-850 μm. Their findings demonstrated that scaffolds with 500-850 μm pores contained more DNA, an expression of greater cell numbers, than other conditions at all time points. Moreover, MSCs cultured on large pore scaffolds

(500-850 μm) performed significantly greater ALP activity at all time points, indicating increased osteogenic potential. Meanwhile in terms of mineral deposition, larger pores enhanced mineral deposition, as measured by the percentage of mineral formed in each scaffold. Scaffolds with the biggest pore diameters (500850 μm) contained about 3-times more mineral than scaffolds with intermediate pore diameters (300-500 μm) and more than 41-times more mineral than scaffolds with the smallest pore diameter (125-300 μm). Taken together, large pore composite scaffolds increase cell proliferation, osteogenic differention, and mineral deposition (Vissers et al., 2015). In our study, the increased pore size after recellularisation in non-adherent surface has also increased ALP activity compared to adherent surface (as discussed in **Section 5.3.2.3.2**), although this effect was not statistically
significant.

Another study has been conducted by Murphy and co-workers regarding the effect of mean pore size on cell attachment, proliferation and migration in collagen glycosaminoglycan scaffolds for tissue engineering. Osteoblast attachment and early phase proliferation up to 7 days after seeding were observed the mean pore sizes ranged from 85 μm – 325 μm. The findings showed that scaffolds with the biggest mean pore size of 325 μm enabled the greatest percentage of cell adhesion with almost 62% of cells adhering and remaining viable 24 hours and 48 hours after seeding. Besides, cell migration to the centre of the scaffold was better with the bigger mean pore size. The cells in scaffolds with a mean pore size of 325 μm had moved away from the surface and started to colonise the centre of the scaffold post 7 days incubation. With regards to proliferation and migration, the total number of cells was significantly greater in 325 μm pore size after 7 days seeding. Scaffolds with the bigger

pore size (325 μm) enabled a greater rate of scaffold infiltration with a more even cell distribution (Murphy et al., 2010). Pores with a big size would assist vascular development supporting appropriate conditions for cell infiltration (Quan et al., 2014). In our study, the increased pore size after recellularisation in nonadherent surface has also increased number of cells (proven by MTT reduction test) compared to adherent surface (as discussed in **Section 5.3.2.4**).

In conclusion, the pore diameter was not significantly affected by the recellularisation process either on adherent or non-adherent surfaces. However, the scaffold mean pore size significantly influences cellular activity and variations in pore size can have major impacts of cellular activity as shown in the literature. Overall, the enhanced surface area produced by scaffolds with small pores may have a useful impact in early cell attachment, however, eventually the better cellular infiltration produced by scaffolds with bigger pores outweighs that (Murphy et al., 2010).

5.3.2.11 Atomic force microscopy (AFM)

In this study, AFM has been used to detect the growth of HOS cells after 5 weeks of reseeding onto the bone. AFM is able to characterize nanomaterials and permits tremendous spatial resolution (Milovanovic et al., 2013), to determine the ultrastructure and nanomechanical properties of bone (Thurner et al., 2007), and to observe the 3D topographical characterization of materials (Xu et al., 2003).

However, from the observations (**Figure 5.24 A, B, C** and **D**), the use of AFM did not allow us to see the images of HOS cells. The scale was too small because the largest area that could be covered by the AFM machine was only 90 μm x 90 μm. Indeed, it required a long time to measure all the area on the samples. Although, we have tried to find the best images from different scales such as 1 x 1 μm^2, 4 x 4 μm^2, 10 x 10 μm^2, and 80 x 80 μm^2. Furthermore, because the sample's structure was not entirely flat **(Figure 5.25 A, B, C** and **D**), the cantilever could not detect the surface easily and could not go deep. Overall, the images seen under AFM were unclear and the reseeded HOS cells could not be viewed as the size of HOS cells are ~20μm. The best scale to see an image of HOS cells is 80 x 80 μm^2, and no
cells were detected on the areas visualised.

On the other hand, AFM has been employed extensively to analyze bone's structure (for instance collagen fibril diameters, collagen ultrastructure, and hydroxyapatite crystal sizes) (Wallace, 2012; Thurner et al., 2007). However, since piezo actuators have a restricted range in the z-direction, which is the axis for specimens topographies, and the extreme topology of cancellous bone, the probe twisted during imaging destroying the tip or impairing the image, i.e. the probe tended to interact with the surface at an angle (Wallace, 2012). Thus despite significant attempts, ultimately AFM images did not provide any useful information (see **Figures 5.24 – 5.25**). All that can be discerned is that the surface of the bone is too uneven for AFM to succeed.

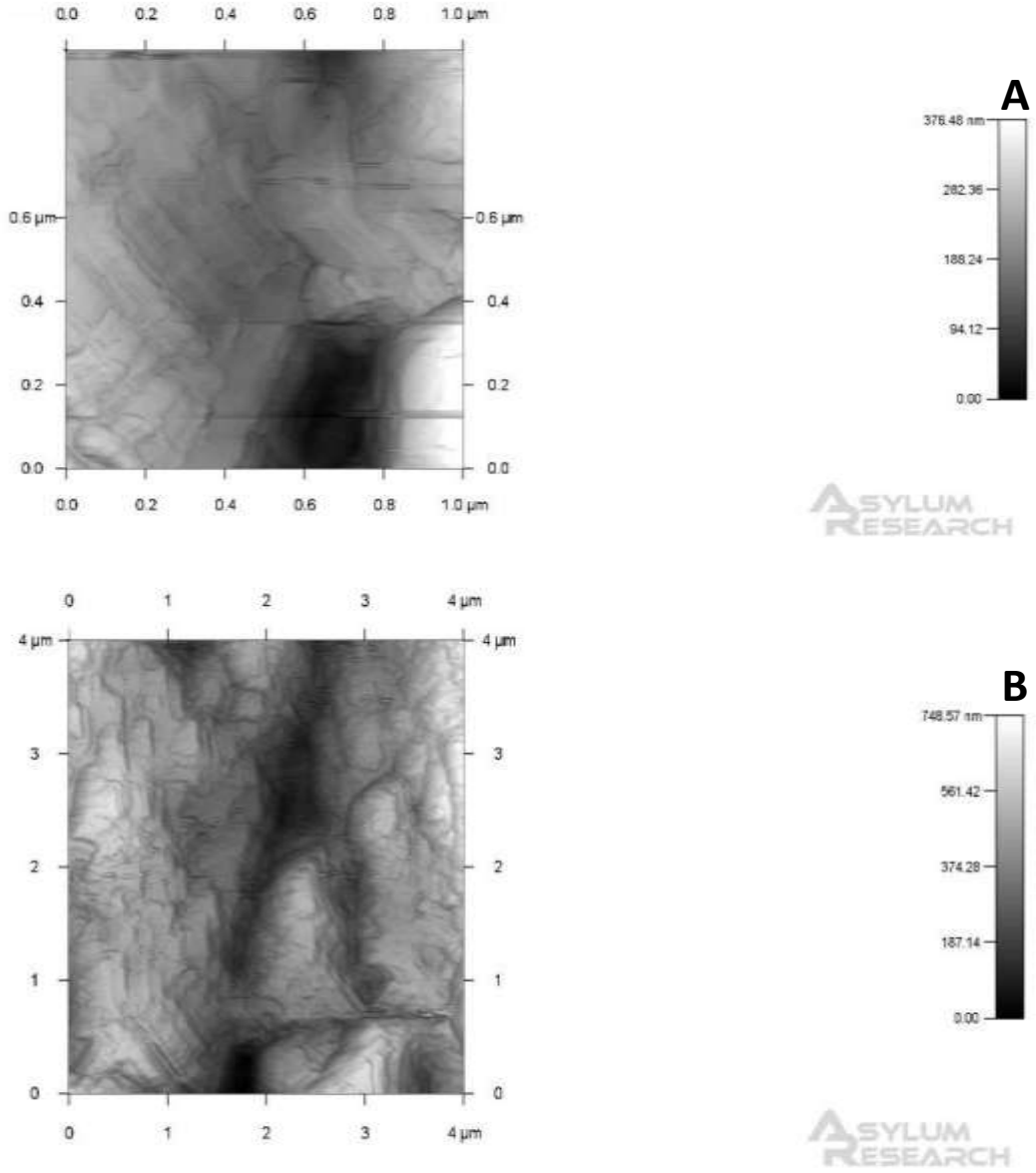

Figure 5.24: AFM topography images showing the external trabecular bone surface after 5 weeks of reseeding process. Scale bars are shown in the images: **A)** 1x1 μm^2 and **B)** 4x4 μm^2.

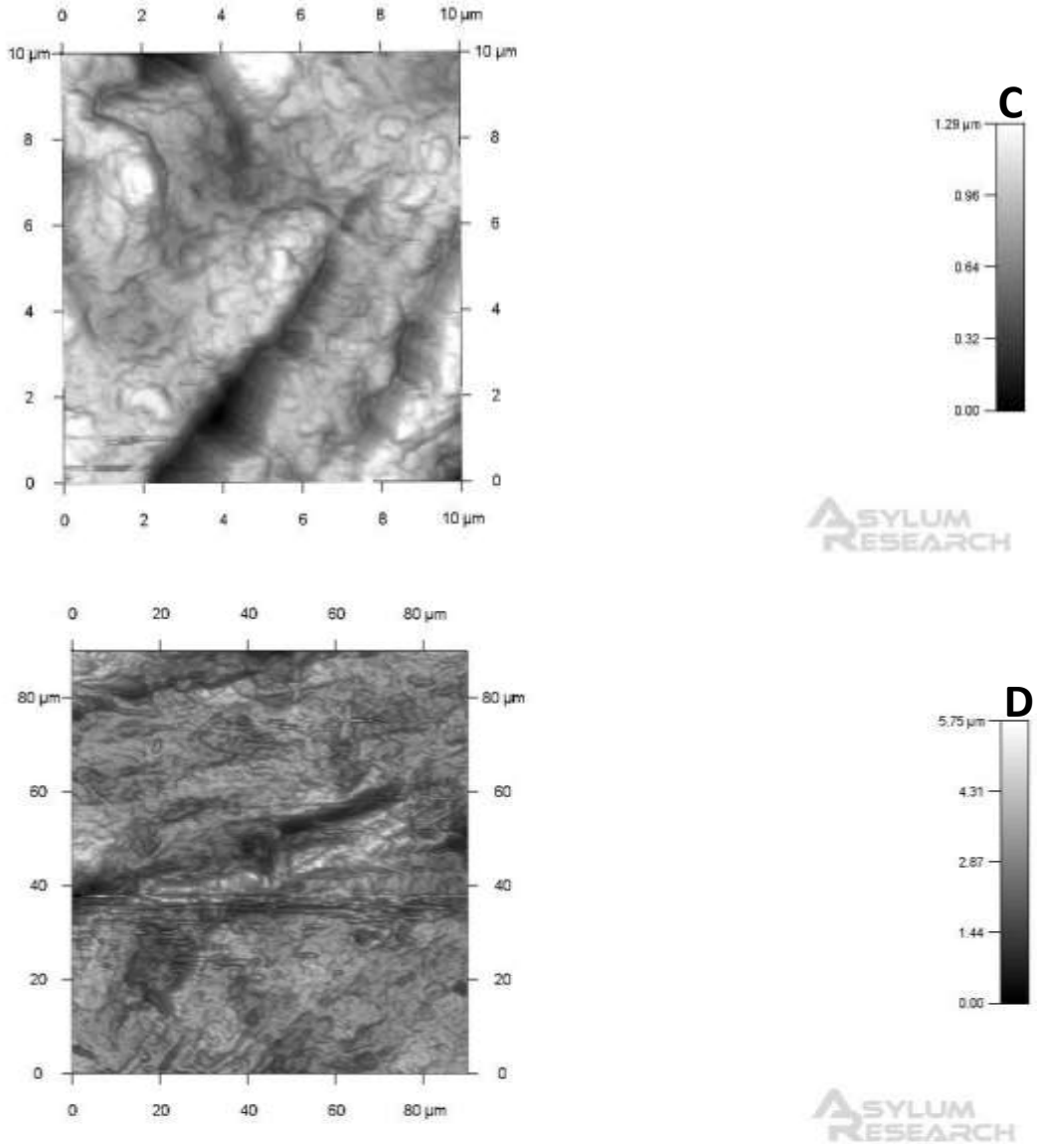

Figure 5.24: AFM topography images showing the external trabecular bone surface after 5 weeks of reseeding process. Scale bars are shown in the images: **C)** 10x10 μm^2, and **D)** 80x80 μm^2.

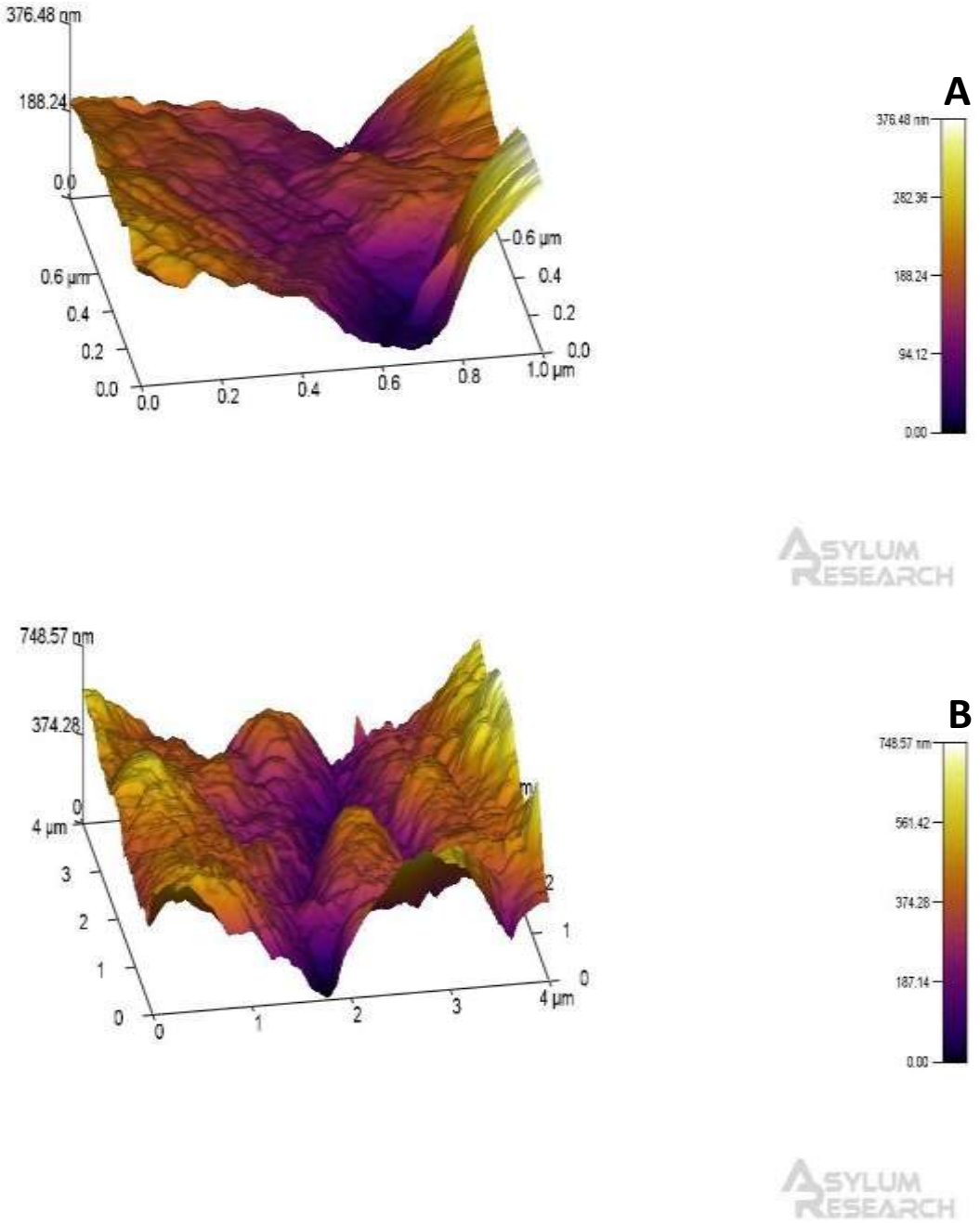

Figure 5.25: Overview of AFM analysis topography showing the external trabecular bone surface after 5 weeks of reseeding process. Scale bars are shown the images: **A)** 1x1 μm^2 and **B)** 4x4 μm^2.

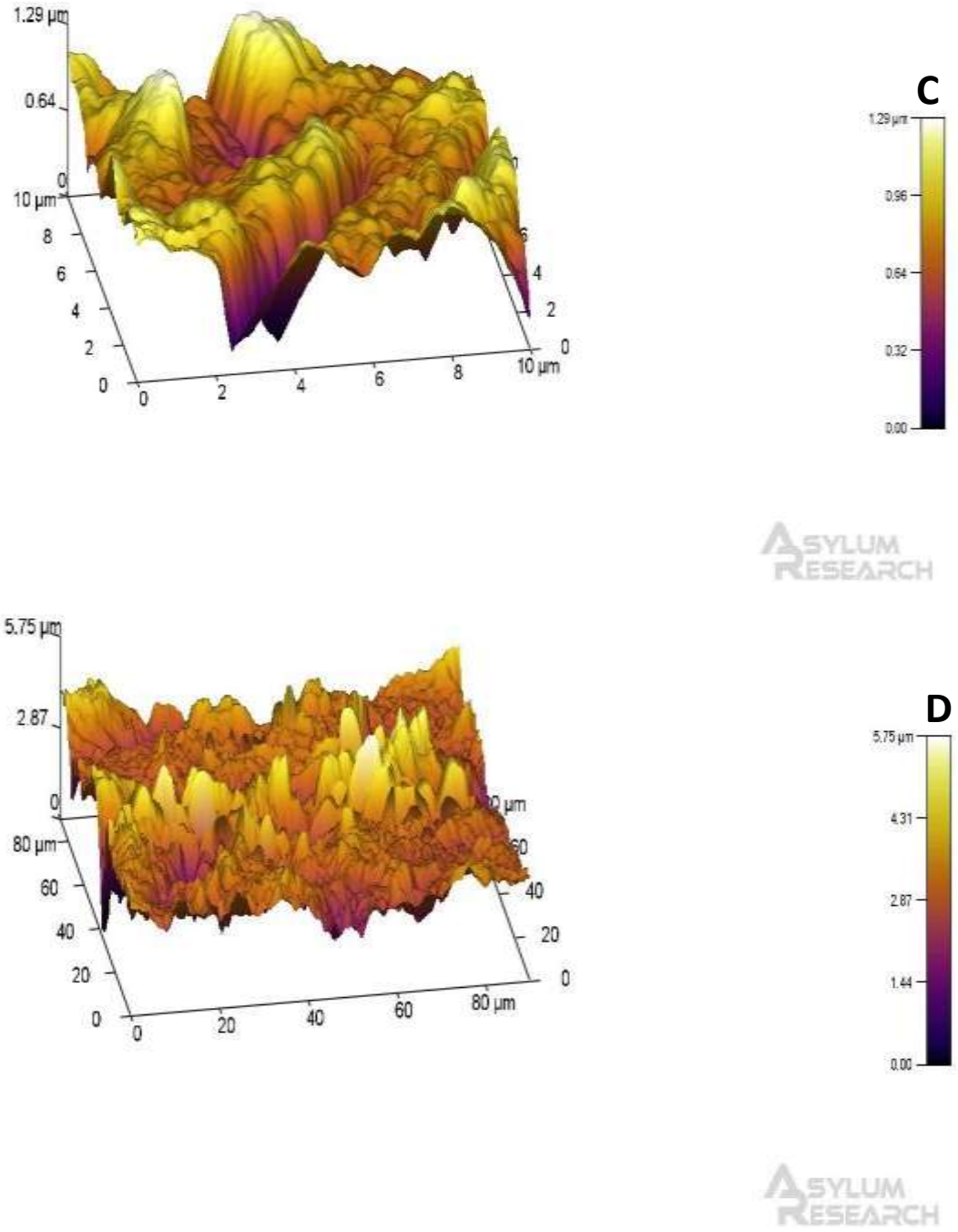

Figure 5.25: Overview of AFM analysis topography showing the external trabecular bone surface after 5 weeks of reseeding process. Scale bars are shown the images: **C)** 10x10 µm^2 and **D)** 80x80 µm^2.

5.3.2.12 Scanning electron microscope (SEM)

The methods for SEM used in this study were adapted from several studies that employed gold and palladium to coat the samples before imaging (Correia et al., 2012; Frohlich et al., 2010; Grayson et al., 2010; Grayson et al., 2008). The bone samples were only coated with gold in our study. Gold coating has a larger particle size which is visible at very high magnification above ~300k or 3 nm resolution. Also during the freeze-drying process, pieces of bone samples of around 1 cm^3 were frozen in liquid isopentane immersed into liquid nitrogen. It was then dried in a sublimation chamber at 5 kPa in order to preserve the microstructural of bone samples.

Representative images of scaffold structures after 21 days of reseeding were shown in **Figure 5.26**. The images taken by SEM indicated that reseeded bone samples cultured both on adherent and non-adherent surfaces have a porous structure comprising of an interconnected network with ideal pore sizes. Based on the previous **Section 5.3.2.10**, pore size range in adherent surface after 21 days of reseeding was 236.46 ± 9.65 μm. Meanwhile in non-adherent surface, pore size range was 267.58 ± 3.56 μm after 21 days of reseeding. Additionally, the cells have migrated to the different areas in the scaffold and had colonised some sites of the scaffold. This activity was also successfully confirmed in the DAPI staining of DNA as explained in **Section 5.3.2.6**. All in all, the SEM results also revealed that the bone samples after being treated with chemicals during decellularization process still have capability to facilitate cell adhesion and proliferation.

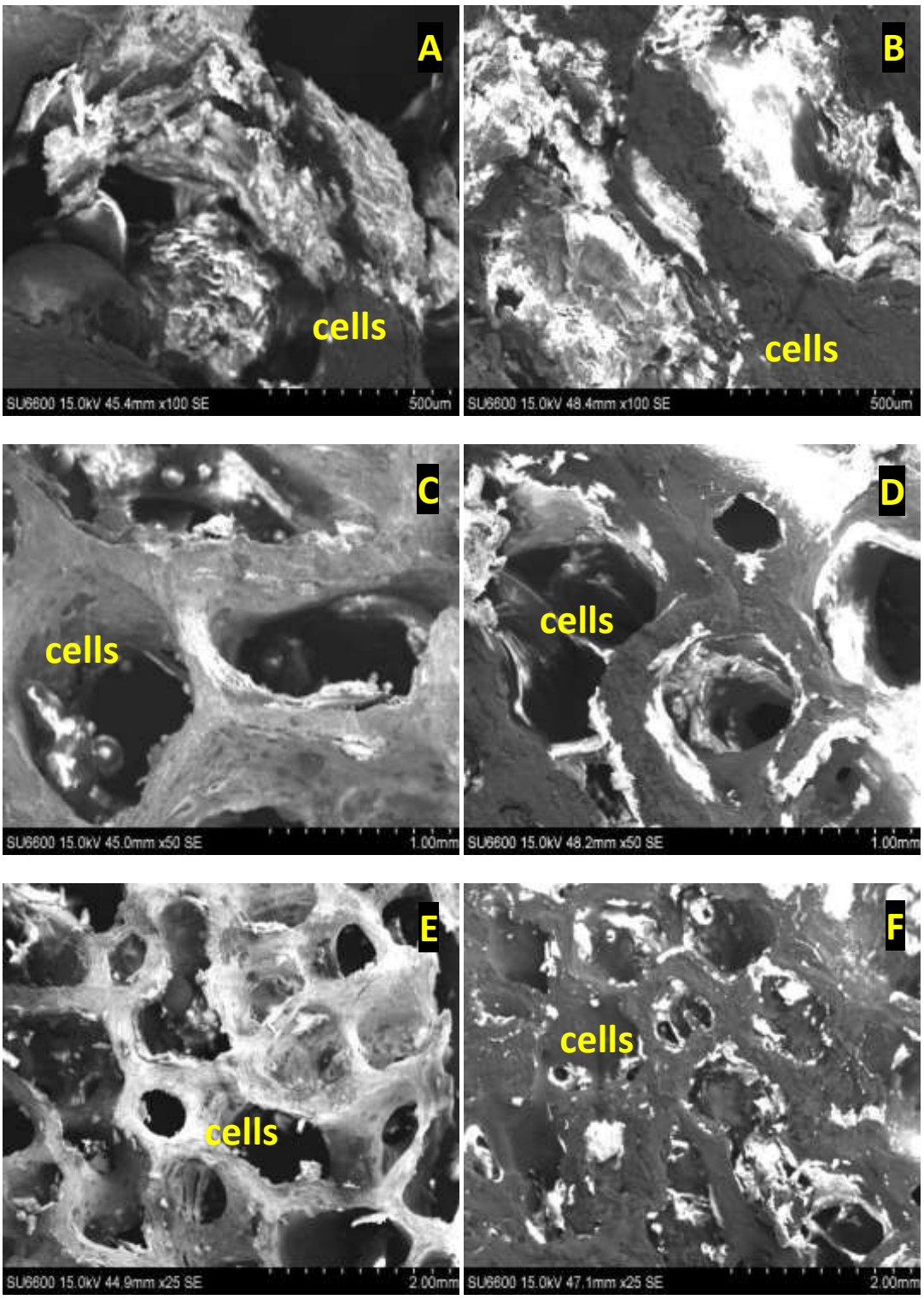

Figure 5.26: Scaffold structures after 3 weeks of recellularisation. SEM images. **A** and **B**, x100, scale bar=500µm, **C** and **D**, x50, scale bar=1.00mm, **E** and **F**, x25, scale bar=2.00mm.

5.4 Conclusion

Overall, recellularisation with human derived cells was efficiently obtained. The studies carried out in this project have proved some important elements in determining the key success of recellularisation processes. Some established test parameters such as the ALP activity, MTT reduction, and osteocalcin secretion were also obtained. The efficiency of cells adherence and proliferation within the scaffolds after recellularisation was successfully confirmed by DAPI staining and SEM. Meanwhile, the mechanical parameters tested and porosity were revealed not to be affected by the cell-recellularisation of bone samples. Furthermore, the attained findings indicated that the decellularized bone scaffolds are capable of supporting the cell adherence and proliferation.

Chapter 6

SUMMARY AND FUTURE WORK

6.1 Introduction

Overall, this study has proposed a method for fabricating a porous bovine bone scaffold as a xenograft, which could be used to repair bone defects in recipient patients for bone tissue engineering. Different aspects such as a sterilised decellularisation protocol, porosity measurement, efficient recellularisation, and functionality of the re-seeded human derived bone cells have been investigated.

6.2 Chapter summaries

6.2.1 Decellularisation approach for the trabecular bovine bone

These studies have addressed a successful decellularisation process in which the concept of decellularisation as the extraction of cellular elements from the tissue is established from chemical and biological treatments in combination with physical treatment. The most efficient method to decellularise the trabecular bovine bone was with digestion buffer (consists of 10 mM Tris, 1 mM EDTA, and 0.1% (v/v) Triton x-100) plus trypsin (0.5% (w/v) Trypsin) incubated at 37°C and 5% CO_2 overnight for six cycles. Elimination of cells in bone specimens was tracked by DAPI staining of DNA while the ECM integrity was preserved. To conclude, the decellularised bones obtained from this optimal protocol could be utilised for bone grafting and meaningful

impacts of biologic scaffolds in the field of tissue engineering and regenerative medicine may be achieved.

6.2.2 The effect of decellularisation protocols on mechanical properties of bone samples

The mechanical testing of the bone samples was carried out in fresh and frozen bones, before and after decellularisation, and before and after autoclaving. The study was extended to determine the effect of repeated measurements on mechanical properties during the mechanical testing and to investigate the present of microdamage due to the mechanical testing. In terms of porosity measurement, comparisons have been highlighted for the fresh and frozen bone samples, and decellularised and recellularised bone samples using the Mercury Porosimetry. There were no significant differences between fresh and frozen bone samples in terms of stiffness, therefore use of frozen bone for this study instead of freshly obtained bone was acceptable and practical. Moreover, the estimated marginal means of stiffness was not influenced by the protocols of the decellularisation process in digestion buffer with or without trypsin, recellularisation or the autoclaving process. However, the stiffness of bone samples during the mechanical testing might be affected by the number of repeated measurements. There was, however, no microdamage detected after the mechanical testing experiments and this was confirmed by SEM. Microdamage development in trabecular bone is associated with both architecture and loading history (Wang & Niebur, 2006), and in this project was not caused by the decellularisation protocol or by mechanical testing. Moreover, no significant differences regarding the pore

diameters were observed in fresh and frozen bone samples, and before and after decellularisation. The mean of pore diameter from this study seemed to be very appropriate for the growth of osteoblast. These outcomes have supported that the decellularised bones created from this study are capable of supporting tissue engineering applications due to their mechanical properties and porosity.

6.2.3 The development of bone scaffolds after reseeding

Recellularisation of the decellularised bovine bone with human derived cells was carried out in this study and main aims in the recellularisation techniques were to achieve a homogeneous cell distribution and also gain adequate cell survival. The chosen seeding density for recellularisation in this study was $5x10^5$cells/ml. This is based on Grayson and co-workers (2008), who reported that greater early cell numbers do not necessarily result in enhanced bone development. To maximise adhesion and distribution of cells, they were grown on scaffolds maintained in both adherent and non-adherent 24-well plates, under both static and dynamic conditions of culture. Many established test parameters were measured in recellularised scaffolds in adherent and non-adherent plates. They were the ALP activity (on day 3, 7, 10, 15, and 21), MTT reduction (on day 21, 28, and 35), and total protein measurement (on day 7, 10, 15, 21, 28, and 35). ALP activity increases gradually with time until days 15 – 21, then shows a large increase between 21 and 28 days. MTT reduction which reflects the number of viable cells increases between days 21 and 35. With both ALP activity and MTT reduction, values are higher when the cells were grown on the decellularised bone on non-adherent surfaces. Values for total protein were subject to

interference derived from soaking the decellularised scaffolds in serum-containing medium. The effect of static and dynamic condition on the ALP activity was observed (on day 3 and 7). Seeding the decellularised scaffolds in static and dynamic conditions did not significantly alter the ALP activity of early cultures up to 7 days. Furthermore, the effect of vitamin D3 on the function of the cells on the bone samples was also measured in terms of the ALP activity on day 7, 10, 15, 21,

28, and 35. A comparison of ALP activities in cells in the presence and absence of $1,25(OH)_2D_3$ treatment showed a significant decrease in activity on day 15 in adherent cultures, and between days 15 and 21 in non-adherent cultures. Further experiments on osteocalcin secretion were carried out only in the presence of the vitamin. Osteocalcin secretion declined with time in culture between 21 and 35 days. The efficiency of cell adherence and proliferation within the scaffolds after recellularisation was confirmed by DAPI staining (on day 3, 7, 10, 15, and 21) and SEM (on day 21). DAPI staining was the most sensitive parameter to measure the number of cells on the decellularised scaffolds, and it was unaffected by cell metabolic rate or differentiation status. Neither, the stiffness nor the porosity of the bone samples was affected after 21 days of cell growth after the recellularisation process. Picric Sirius red staining showed that the decellularised bone samples retained collagen. The application of AFM to see the cells after 21 days of reseeding process onto the bone scaffold was not successful. All in all, the findings obtained in this thesis help the decellularised bone plus cell-based regenerative medicine approach for functional bone replacement. Thus, the possible *in vivo* construction of bone grafts employing decellularised and recellularised bone graft eventually as an *in vivo* model for bone growth and regeneration is envisaged.

6.3 Contributions and novelty

In summary, the bone scaffolds were characterised based on several important parameters such as stiffness (in fresh and frozen bone sample, before and after autoclaving, and before and after decellularisation and recellularisation in adherent and non-adherent plates), presence of collagen (before and after decellularisation), pore size (before and after decellularisation and recellularisation in adherent and non-adherent plates), and microdamage (before and after decellularisation and recellularisation in adherent and non-adherent plates) as summarised in **Table 6.1** below:

Test parameters	**Sample's condition**		**Autoclaving**	
	Fresh	**Frozen**	**Before**	**After**
Stiffness	√	√	√	√
Test parameters	**Decellularisation**		**Recellularisation**	
	Before	**After**	**Before (Adherent and nonadherent)**	**After (Adherent and nonadherent)**
Stiffness	√	√	√	√
Pore size	√	√	√	√
Microdamage	√	√	√	√
Presence of collagen	√	√		

Table 6.1: Test parameters for the characterisation of the bone scaffold.

Moreover, there were a number of novel contributions resulting from this project, including the use of non-adherent well plates to promote greater adhesion to the scaffold, and the use of biocompatible detergent (Triton X-100) that leaves the protein

on the scaffold. This replaces SDS detergents used in most studies (Frohlich et al., 2010; Marcos-Campos et al., 2012; Grayson et al., 2008, 2010; Pathak et al., 2012; Correia et al., 2012), which strip the proteins as well as the cells. Triton X-100 was also used by Correia and colleagues (2011) to decellularise bovine bone but without Trypsin. In this project, we measured the stiffness (Young's modulus) of bone samples after the decellularisation process. There was a study that measured the Young's modulus after culture (Correia et al., 2012). The use of HOS TE85 cells after reseeding in this study was also novel as many of previous studies used different cell types instead, such as hASCs (Frohlich et al., 2010; Correia et al., 2010), hESC (Marcos-Campos et al., 2012; Grayson et al., 2012), hMSCs (Grayson et al., 2010, Correia et al., 2011), rat MSCs (Hashimoto et al., 2011) and HUVECs (Correia et al., 2011; Quan et al., 2014). Other novelties were the use of stored (at 20C) bone samples and, to date, there have been no studies observing the distribution of reseeded cells on scaffolds after the recellularisation process as demonstrated in this project. The contributions from this project have lead to greater understanding and efficiency of this process of generating bone scaffolds suitable for implantation.

6.4 Limitations and future work

As we previously discussed and as various studies have shown the successful decellularisation of most tissues involves a combination of physical, enzymatic, and chemical treatments, and the methods will be dependent on the tissue of interest. In

fact any combination of methods could not eliminate 100% of cell elements from a tissue or organ. But, it appears clearly that approaches which eliminate most or all of the observable cellular material result in biologic scaffold materials that are harmless for implantation (Gilbert et al., 2006). Throughout the study, the elimination of DNA (nucleic material) from the tissues was critical and this is justified because the presence of DNA is directly associated with adverse host responses. Efficient decellularisation is required in this study as the source tissue for the biologic scaffold is derived from a xenogenic origin. The host reaction resulting after *in vivo* implantation of the decellularised bones is reliant upon the effectiveness of decellularisation and elimination of cell residues (Crapo et al., 2011). Macchiarini and coworkers (2008) further proved decellularisation of their tracheal scaffold by staining for the absence of tissue morphology using haematoxylin and eosin, and the absence of MHC antigen expression using specific antibodies. In future studies these parameters should be determined for the decellularised bovine bone. Futhermore, Macchiarini and coworkers (2008), used 25 cycles of incubations with 4% sodium deoxycholate (SDC) and DNase over 6 weeks to eliminate all identities of donor cells and antigens instead of the 6 cycles of overnight incubations in our project. Thus, the cycles of incubations need to be extended in future work, as also recommended by Conconi et al. (2005).

Regarding the decellularisation methods also, these are different in a lot of aspects. For instance, strain and species of animal employed, and decellularization agents to attain the ECM scaffold needed for recellularisation. ECM structures are recognised to be different from batch to batch (also animal to animal), and therefore, standardization of fundamental parameters including species, strain, gender (male/ female), age, phenotype, and weight of the bovine bone need to be clarified and carried

out in order to accomplish useful comparisons in results (He & Callanan, 2013). In this field in general, standardisation of decellularisation protocols for each tissue is urgently required as there are numerous methods in the literature.

The progress of a tissue engineering scaffold needs an estimation of its performance on some preclinical studies before implantation in a human subject. The correct selection of an experimental model is vital to the success of the preclinical studies. Selection of bovine bone for decellularisation was based on the fact that load bearing conditions and bone remodelling processes seem similar between bovine and human bone, and the tissue was readily available (Salgado et al., 2004). However, actually, the utilisation of this model in the literature is infrequent because of the potential high costs (Salgado et al., 2004). It is impossible to achieve 100% similarity with human physiological application, but the use of larger animals like pig, bovine, and sheep could hopefully reduce the error.

Mechanical testing physical properties of similar samples from several animals would also be needed in the future to determine whether the samples used in this project are representative of the wider variability of bovine trabecular bone. During the mechanical testing, the aspect of microdamage in the bone samples was highlighted. Such damage in bone is related to strain, and not to stress. The cutting of bone samples exposed and induced additional damage that could affect the mechanical testing. In order to reduce further damage, the bone samples were suggested to be supported throughout the cutting process (Moore & Gibson, 2003). By supporting the bone samples during cutting, this also enabled us to produce exact dimensions of bone specimens and the surface was flat and uniform. However, it was difficult in this study to get a flat surface of specimen for the compression test, (and also for AFM). This led

to variation in the mechanical testing of the specimen. It was observed that the non-flat nature of the samples affected the stress-strain graphs, in which the stiffness (gradient of the graph) could not be easily interpreted. Thus, appropriate dimensions and surfaces of bone specimens are critical for analysing the mechanical testing. Moreover, the decrease in strength, stiffness and energy dissipation have been known to be related to the microdamage accumulation. However, the impact of microdamage accumulation on the fatigue life of bone is not well explained (Burr, 2003). In this study, we obtained the evaluation of microdamage by section area rather than bone area (Moore & Gibson, 2002). In addition, the axial loading applied to the bone samples is also exposed to local damage, and alterations in geometry, morphology, and microenvironment. The loading process could not be controlled, so that, the loading parameters such as magnitude of load and parameters of frequency, speed, and time must be properly set up.

Bovine trabecular bone used in this study has a denser, on normal, compared to human trabecular bone, particularly osteoporotic human bone. While it is complicated to infer certain results from bovine to human bone, Arthur and Gibson have stated that the series of actions in the accumulation of damage in human trabecular bone will be the same as that in bovine trabecular bone (Moore & Gibson, 2002). The analysis of other local parameters including shear stresses to trabecular microdamage needs future study. By correlating the capability of various local mechanical parameters to anticipate spatial distribution of microdamage inside trabecular bone samples, the local failure criteria for normal (control) and osteoporotic human trabecular bone could be extrapolated.

In most of test parameters, the number of samples used in this study was from three to six samples. In fact a larger number of sample sizes would produce superior representation. The results of study will be improved by increasing the sample sizes. In power analyses determine that more than twenty-five samples would be needed in every group to perform statistical significance at the observed difference (Moore & Gibson, 2002; Singh et al., 2010).

As we discussed in **Chapter 5, Section 5.3.2.3.1** and as various studies have shown the dynamic condition encouraged the growth of cells and increased the ALP activity. However, in this study, we only employed the dynamic condition to the bone samples to compare the ALP activity on day 3 and day 7 in adherent and nonadherent plates due to limited spaces in the incubator. Static conditions do not mimic the dynamics of the *in vivo* circumstance found in the bone, specifically the mechanical stimulation initiated by hydrostatic pressure and shear stress. Moreover as reported by Salgado et al., (2004), the maintenance of the cells in microgravity conditions in static conditions performing a small fluid shear stress prevents cell deposition and all together stimulates cellular communications. Nevertheless, microgravity is destructive for bone; it may often cause losses in total bone mass (Salgado et al., 2004). Once total bone mass is decreased, the osteoblast activity and numbers will also decrease.

Comprehension of the architectural, molecular, and functional biology of bone is required for improved knowledge of this tissue as a multicellular unit and dynamic architecture, a role still not fully understood. Hence, extensive knowledge of the dynamic nature of bone tissue will definitely assist in the development of new therapeutic strategies to bone defects (Florencio-Silva et al., 2015). Particularly useful is the approach by employing perfusion systems during reseeding process in which

very promising findings comprising induction of osteoblastic differentiation and development of cells on the scaffold have been obtained. The scaffolds could then be homogenously cultured and seeded in the conditions that would result in rapid proliferation and osteoblastic differentiation with a continual oxygen content monitoring system and automatic medium change when essential (Yeatts & Fisher, 2011).

Up to now, most of the published papers about decellularisation and recellularisation protocols represent *in vitro* outcomes. However, the most critical challenge is to implant the decellularised and recellularised bovine trabecular bone into patients. Functional evaluation of recellularised scaffolds based on the degree of recellularisation accomplished differs from organ to organ, and also whether the graft is appropriate for implantation *in vivo.* Future studies regarding implantation need to overcome some limitations that occurr in most of the tissue-engineered organ scaffolds. They require functionality and viability *in vivo*, and to attain adequate or equivalent to regular cellular density, complete cellular and tissue differentiation, and long-term viability, functionality, and productive remodelling of organ when implanted *in vivo* (He & Callanan, 2013). The challenge should also be further emphasised whether the remodelling of the ECM construct *in vivo* is good enough to create tissue that is capable of entirely resisting natural mechanical strain and to achieve access to oxygen and blood sources. Furthermore, immunogenecity and transmission of diseases could also limit the use of xeno- or allogenic ECM, however, optimal decellularisation and excellent sterilisation protocols could avoid these limitations (Gundula S-T. et al., 2012). Severe inflammation, cytotoxicity, and graft rejection are the crucial criteria to avoid in *in vivo* transplantation. Ideally, the acellular

bone scaffolds should undergo *in vivo* biocompatibility, histology, and immunohistochemistry test after transplantation (Quan et al., 2014).

The choice of cells for bone tissue engineering is also a challenge. In fact, the optimal cell source should be simply extendible to greater passages, consist of a protein expression pattern alike to the tissue to be redeveloped, and nonimmunogeneic (Salgado et al., 2004). Further, it is important to examine the possibility of organ regeneration from another cell source like a stem cell population. There could be important clinical advantage in solving the immune obstacle and complication of rejection, if ultimately autologous cells, for example, mesenchymal stem cells extracted from the recipient could be employed to produce a functional organ graft. This effort has huge promise in patients with organ failure and brings solutions related to organ engineering in the future (Fu et al., 2014). Other than the provision of a scaffold on which to grow the cells, perhaps the greatest challenge in the field of tissue engineering generally relates to the source of suitable cells.

PUBLICATIONS

1. Mohamad M. R., Riches P. E., & Grant M. H. (2014). Engineering of Artificial Bone tissues. Glasgow Orthopaedic Research Initiative (GLORI) Meeting, Southern General Hospital, Glasgow, UK, January 2014.

2. Mohamad M. R., Riches P. E., & Grant M. H. (2014). The Effects of Decellularisation on the Mechanical Properties of Bone. *European Cells and Materials, 28(Suppl 4)*, 72. Tissue & Cell Engineering Society Conference, Newcastle, UK, April 2014.

3. Mohamad M. R., Riches P. E., & Grant M. H. (2015). The Effects of Decellularisation on the Mechanical Properties of Bone, and Subsequent

Recellularisation of the Samples. *Journal of Bone and Mineral Research, 30(Suppl 1)*, S378-S379. Bone and Mineral Research (ASBMR) Conference, Seattle, Washington, USA, October 2015.

APPENDIX – Some buffers and solutions used

ALP buffer

7.51 g glycine

203 mg $MgCl_2$

136 mg $ZnCl_2$

Dissolve in 900 ml dH_2O. Adjust to pH 10.4 with 5M NaOH.

Bouin's solution:

75 ml picric acid (saturated)

25 ml 40% formaldehyde

5 ml glacial acetic acid

Digestion buffer

121.14 mg Tris

37.224 mg EDTA

100 µl Triton X-100

Dissolve in 100 ml d.H_2O. Adjust to pH 10.4.

Glutaraldehye fixative:

2.5 ml 25% glutaraldehyde

12.5 ml 0.2M PO_4 buffer

10 ml d.H_2O

REFERENCES

Abukawa H., Terai H., Hannouche D., Vacanti J. P., Kaban L. B., & Troulis M. J. (2003). *Journal of Oral and Maxillofacial Surgery, 61,* 94.

Almin S. F., Lu H. H., Khan Y., Burems J., Mitchell J., Tuan R. S., & Laurencin C. T. (2003). *Biomaterials, 24,* 1213.

Alvarez K., & Nakajima H. (2009). Metallic scaffolds for bone regeneration. *Materials, 2,* 790-832. doi: 10.3390/ma2030790.

Arlot M. E., Brigitte B. P., Roux J. P., Vashishth D., Bouxsein M. L., & Delmas P. D. (2008). Microarchitecture influences microdamage accumulation in human vertebral trabecular bone. *Journal of Bone and Mineral Research, 23*(10), 1613-1618. doi: 10.1359/JBMR.080517.

Arvidson K., Abdallah B. M., Applegate L. A., Baldini N., Cenni E., Gomez-Barrena E., . . . Finne-Wistrand A. (2011). Bone regeneration and stem cells. *Journal of Cellular and Molecular Medicine, 15*(4), 718-746. doi: 10.1111/j.15824934.2010.01224.x.

Ashman R. B., Corin J. D., & Turner C. H. (1987). Elastic properties of cancellous bone: measurement by an ultrasonic technique. *J. Biomechanics, 20*(10), 979986.

Ashman R. B., & Rho J. Y. (1988). Elastic modulus of trabecular bone material. *J. Biomechanics, 21*(3), 177-181.

Baptista P. M., & et al. (2009). Whole organ decellularization - a tool for bioscaffold fabrication and organ bioengineering. *Conf Proc IEEE Engineering in Medicine Biology Society 2009*, 6526.

Baptista P. M., Siddiqui M. M., Lozier G., Rodriguez S. R., Atala A., & Soker S. (2011). The use of whole organ decellularization for the generation of a whole liver organoid. *Hepatology, 53*, 604.

Barakat O., Abbasi S., Rodriguez G., Rios J., Wood R. P., Ozaki C., . . . Gauthier P. K. (2012). Use of decellularized porcine liver for engineering humanized liver organ. *Journal of Surgical Research, 173*(e11).

Baran E. T., Tuzlagoklu K., Salgado A. J., & Reis R. L. (2004). *Journal of Materials Science: Materials in Medicine, 15*, 161.

Benders K. E. M., Weeren P. R., Badylak S. F., Daniel B. F. Saris, Wouter J. A. Dhert, & Malda J. (2012). Extracellular matrix scaffolds for cartilage and bone regeneration. *Trends in Biotechnology*, 1–8. doi: http://dx.doi.org/10.1016/j.tibtech.2012.12.004.

Berg J. M., Tymoczko J. L., & Stryer L. (2006). *Biochemistry Sixth Edition*. New York, USA: W. H. Freeman and Company.

Bikle D. D. (2012). Vitamin D and Bone. *Current Osteoporosis Reports, 10*(2), 151–159. doi: 10.1007/s11914-012-0098-z.

Boccaccini A. R., & Blaker J. J. (2005). Bioactive composite materials for tissue engineering scaffolds. *Expert Review of Medical Devices, 2*(3), 303-317.

Booth C., Soker T., Baptista P., Ross C. L., Soker S., Farooq U., . . . Orlando G. (2012). Liver bioengineering: Current status and future perspectives. *World J Gastroenterol, 18*(47), 6926-6934. doi: 10.3748/wjg.v18.i47.6926.

Bouvier S., Alves J. L., Oliveira M. C., & Menezes L. F. (2005). Modelling of anisotropic work-hardening behaviour of metallic materials subjected to strain-path changes. *Computational Materials Science, 32*, 301–315.

Bracey D. N., Seyler T. M., Lively M. O., Willey J. S., Smith T. L., & Whitlock P. W. (2014). *A xenograft-derived bone scaffold to serve as a bone graft substitute in treatment of critical bone defects*. Paper presented at the Orthopaedic Research Society Annual Meeting, New Orleans, Louisiana, USA.

Brekke J. H., & Toth J. M. (1998). *Journal of Biomedical Materials Research, 43*, 380.

Burg J. L., Porter S., & Kellam J. F. (2000). Biomaterial developments for bone tissue engineering. *Biomaterials, 21*, 2347-2359.

Burr D. (2003). Microdamage and bone strength. *Osteoporos Int., 14*(Suppl 5), S67S72. doi: 10.1007/s00198-003-1476-2.

Chen G. Q, & Wu Q. (2005). The application of polyhydroxyalkanoates as tissue engineering materials. *Biomaterials, 26*(33), 6565-6578.

Chen L. J., & Wang M. (2002). *Biomaterials, 23*, 2631.

Chen Q., Zhu C., & Thouas G. A. (2012). Progress and challenges in biomaterials used for bone tissue engineering: Bioactive glasses and elastomeric composites. *Progress in Biomaterials, 1*(2), 1-22. doi: 10.1186/2194-0517-12.

Choi Y. C., Choi J. S., Kim B. S., Kim J. D., Yoon H. I., & Cho Y. W. (2012). Decellularized extracellular matrix derived from porcine adipose tissue as a xenogeneic biomaterial for tissue engineering. *Tissue Engineering: Part C, 18*(11), 1-11. doi: 10.1089/ten.tec.2012.0009.

Choueka J., Charvet J. L., Koval K. J., Alexander H., James K. S., Kooper K. A., & Khon J. (1996). *Journal of Biomedical Materials Research, 31*, 35.

Chung C. H., Golub E. E., Forbes E., Tokuoka T., & Shapiro I. M. (1992). Mechanism of action of beta-glycerophosphate on bone cell mineralization. *Calcified Tissue International 51*, 305-311.

Cigliano A., Gandaglia A., Lepedda A. J., Zinellu E., Naso F., Gastaldello A., . . . Formato M. (2012). Fine structure of glycosaminoglycans from fresh and decellularized porcine cardiac valves and pericardium. *Biochemistry Research International, 2012*, 1-10. doi: 10.1155/2012/979351.

Clarke B. (2008). Normal Bone Anatomy and Physiology. *Clinical Journal of the American Society of Nephrology, 3*, 131-139. doi: 10.2215/CJN.04151206.

Clover J., & Gowen M. (1994). Are MG-63 and HOS TE85 human osteosarcoma cell lines representative models of the osteoblastic phenotype? *Bone, 15*(6), 585–591. doi: 10.1016/8756-3282(94)90305-0.

Conconi M. T., De Coppi P., & Di Liddo R. (2005). Tracheal matrices, obtained by a detergent-enzymatic method, support in vitro the adhesion of chondrocytes and tracheal epithelial cells. *Transplant International, 18*, 727–734.

Correia C., Bhumiratana S., Yan L. P., Oliveira A. L., Gimble J. M., Rockwood D., . . . Gordana V. N. (2012). Development of silk-based scaffolds for tissue engineering of bone from human adipose-derived stem cells. *Acta Biomaterialia, 8*, 2483–2492.

Correia C., Grayson W. L., Park M., Hutton D., Zhou B., Guo X. E., . . . Gordana V. N. (2011). In vitro model of vascularized bone: Snergizing vascular development and osteogenesis. *PLoS One, 6*(12), 1-9.

Cortiella J., & et al. (2010). Influence of acellular natural lung matrix on murine embryonic stem cell differentiation and tissue formation. *Tissue Eng Part A., 16*, 2565.

Crapo P. M., Gilbert T. W., & Badylak S. F. (2011). An overview of tissue and whole organ decellularization processes. *Biomaterials, 32*(12), 3233-3243. doi: 10.1016/j.biomaterials.2011.01.057.

Cruz F. (2010). Fabrication of HA/PLLA composite scaffolds for bone tissue engineering using additive manufacturing technologies. *Biopolymers, Magdy Elnashar (Ed.)*, 227-243.

Czekanska E. M., Stoddart M. J., Richards R. G., & Hayes J. S. (2012). In search of an osteoblast cell model for in vitro research. *European Cells and Materials, 24*, 1-17.

De Kock J., Ceelen L., De Spiegelaere W., Casteleyn C., Claes P., Vanhaecke T., & Rogiers V. (2011). Simple and quick method for whole-liver

decellularization: a novel in vitro three-dimensional bio-engineering tool? *Archives of Toxicology, 85*, 607.

Delmas P. D., Eastell R., Garnero P., Seibel M. J., & Stepan J. (2000). The use of biochemical markers of bone turnover in osteoporosis. *Osteoporos Int., 11*(Suppl. 6), S2-17.

Doi Y., Kitamura S., & Abe H. (1995). Microbial Synthesis and Characterization of Poly(3- Hydroxybutyrate-Co-3-Hydroxyhexanoate). *Macromolecules, 28*(14), 4822-4828.

Doyle C., Tanner E. T., & Bonfield W. (1991). In vitro and In vivo Evaluation of Polyhydroxybutyrate and of Polyhydroxybutyr Reinforced with Hydroxyapatite. *Biomaterials, 12*(9), 841-847.

Draenert G. F., & Delius M. (2007). The mechanically stable steam sterilization of bone grafts. *Biomaterials 28*, 1531–1538. doi: 10.1016/j.biomaterials.2006.11.029.

Duane Knudson. (2006). The Biomechanics of Stretching. *Journal of Exercise Science & Physiotherapy, 2*, 3-12.

Dulekgurgen E. (2004). *Proteins (Lowry) Protocol*. Paper presented at the UIUC'04, University of Illinois at Urbana-Champaign.

Edmondson J. M., Armstrong L. S., & Martinez A. O. (1988). A rapid and simple MTT-based spectrophotometric assay for determining drug sensitivity in monolayer cultures. *Journal of Tissue Culture Methods, 11*(1), 15-17.

Elder B. D., Eleswarapu S. V., & Athanasiou K. A. (2009). Extraction techniques for the decellularization of tissue engineered articular cartilage constructs. *Biomaterials, 30*, 3749–3756. doi: 10.1016/j.biomaterials.2009.03.050.

Elvira C., Mano J. F., San Roman J., & Reis R. L. (2002). *Biomaterials, 23*, 1955.

Endres M., Schantz J. T., Salgado A. J., Kaps C., Ringe J., Lim T. C., . . . Hutmacher D. W. (2003). *Tissue Engineering, 9*, 689.

Ertel S. I., Khon J., Zimmerman M. C., & Passos J. R. (1995). *Journal of Biomedical Materials Research, 29*, 1337.

Fini M., Bondioli E., Castagna A., Torricelli P., Giavaresi G., Rotini R., . . . Melandri D. (2012). Decellularized human dermis to treat massive rotator cuff tears: In vitro evaluations. *Connective Tissue Research, Early Online*, 1-11. doi: 10.3109/03008207.2011.649929.

Florencio-Silva R., Rodrigues da Silva Sasso G., Sasso-Cerri E., Simões M. J., & Cerri P. S. (2015). Review Article Biology of Bone Tissue: Structure, Function, and Factors That Influence Bone Cells. *BioMed Research International*, 1-17.

Flynn L., Semple J. L., & Woodhouse K. A. (2006). Decellularized placental matrices for adipose tissue engineering. *Journal of Biomedical Materials Research Part A*, 359-369. doi: 10.1002/jbm.a.30762.

Fogelman I., Gnanasegaran G., & van der Wall H. (2012). *Radionuclide and Hybrid Bone Imaging* Berlin: Springer.

Frohlich M., Grayson W. L., Marolt D., Gimble J. M., Nevenka K. V., & Gordana V. N. (2010). Bone grafts engineered from human adipose-derived stem cells in perfusion bioreactor culture. *Tissue Engineering: Part A, 16*(1), 179-189. doi: 10.1089/ten.tea.2009.0164

Frost H. M. (1994). Wolff's Law and bone's structural adaptations to mechanical usage: an overview for clinicians. . *The Angle Orthodontist: June 1994, 64*(3), 175-188.

Fu R-H., Wang Y. C., Liu S. P., Shih T. R., Lin H. L., Chen Y. M., . . . Lin S. Z. (2014). Review: Decellularization and recellularization technologies in tissue engineering. *Cell Transplantation, 23*, 621-630. doi: http://dx.doi.org/10.3727/096368914X678382.

Funamoto S., Nama K., Kimura T., Murakoshi A., Hashimoto Y., Niwaya K., . . . Kishida A. (2010). The use of high-hydrostatic pressure treatment to decellularize blood vessels. *Biomaterials, 31*, 3590-3595. doi: 10.1016/j.biomaterials.2010.01.073.

Gerhardt L. C., Widdows K. L., Erol M. M., Nandakumar A., Roqan I. S., Ansari T., & Boccaccini A. R. (2012). Neocellularization and neovascularization of nanosized bioactive glass-coated decellularized trabecular bone scaffolds. *Journal of Biomedical Materials Research A, 00A*(00), 000-000. doi: 10.1002/jbm.a.34373.

Giesche H. (2006). Mercury porosimetry: A general (practical) overview. *Particle and Particle Systems Characterization, 23*, 1-11. doi: 10.1002/ppsc.200601009.

Gilbert T. W., Sellaro T. L., & Badylak S. F. (2006). Decellularization of tissues and organs. *Biomaterials, 27*, 3675–3683. doi: 10.1016/j.biomaterials.2006.02.014.

Gleeson J. P., Plunkett N. A., & O'Brien F. J. (2010). Addition of hydroxyapatite improves stiffness, interconnectivity and osteogenic potential of a highly porous collagen-based scaffold for bone tissue regeneration. *European Cells and Materials, 20*, 218-230.

Goldstein S. A. (1987). The mechanical properties of trabecular bone: Dependence on anatomic location and function. *J. Biomechanics, 20*(11/12), 1055-1061.

Gollwitzer H., Ibrahim K., Meyer H., Mittelmeier W., Busch R., & Stemberger A. (2003). Antibacterial poly(D,L-lactic acid) coating of medical implants using a biodegradable drug delivery technology. *Journal of Antimicrobial Chemotherapy, 51*(3), 585-591.

Grayson W. L., Bhumiratana S., Cannizzaro C., Grace Chao P. H., Lennon D. P., Caplan A. I., & Gordana V. N. (2008). Effects of initial seeding density and fluid perfusion rate on formation of tissue-engineered bone. *Tissue Eng Part A., 14*(11), 1809-1820. doi: 10.1089/ten.tea.2007.0255.

Grayson W. L., Frohlich M., Yeager K., Bhumiratana S., Chan M. E., Cannizzaro C., . . . Gordana V. N. (2010). Engineering anatomically shaped human bone grafts. *PNAS, 107*(8), 3299-3304. doi: www.pnas.org/cgi/doi/10.1073/pnas.0905439106.

Griensven M. van, Zeichen J., Tschernig T., Seekamp A., & Pape H. C. (2002). A modified method to culture human osteoblasts from bone tissue specimens using fibrin glue. *Experimental and Toxicologic Pathology, 54*, 25-29.

Gundula S-T., Onays A. S., Wolfgang Ertel, & Anke Lohan. (2012). Decellularized tendon extracellular matrix - A valuable approach for tendon reconstruction? *Cells, 1*(1010-1028). doi: 10.3390/cells1041010.

Haimi S., Vienonen A., Hirn M., Pelto M., Virtanen V., & Suuronen R. (2008). The effect of chemical cleansing procedures combined with peracetic acideethanol sterilization on biomechanical properties of cortical bone. *Biologicals 36 (2008) 99e104, 36*, 99-104. doi: 10.1016/j.biologicals.2007.06.001.

Hasegawa T., Miwa M., Sakai Y., Niikura T., Lee S. Y., Oe K., . . . Komori T. (2010). Efficient cell-seeding into scaffolds improves bone formation. *Journal of Dental Research, 89*(8), 854-859. doi: 10.1177/0022034510370022.

Hashimoto Y., Funamoto S., Kimura T., Nama K., Fujisato T., & Kishida A. (2011). The effect of decellularized bone/bone marrow produced by high-hydrostatic pressurization on the osteogenic differentiation of mesenchymal stem cells. *Biomaterials, 32*, 7060-7067. doi: 10.1016/j.biomaterials.2011.06.008.

Hashimoto Y., Funamoto S., Sasaki S., Honda T., Hattori S., Nama K., . . . Kishida A. (2010). Preparation and characterization of decellularized cornea using high-hydrostatic pressurization for corneal tissue engineering. *Biomaterials, 31*, 3941-3948. doi: 10.1016/j.biomaterials.2010.01.122.

He M., & Callanan A. (2013). Comparison of methods for whole-organ decellularization in tissue engineering of bioartificial organs. *Tissue Engineering: Part B, 19*(3), 1-15. doi: 10.1089/ten.teb.2012.0340.

Hojo M., Inokuchi S., Kidokoro M., Fukuyama N., Tanaka E., Tsuji C., . . . Nakazawa H. (2003). *Plastic and Reconstructive Surgery, 111*, 1638.

Holtrop M. E. (1975). The ultra-structure of bone. *Annals of Clinical & Laboratory Science, 5*(264).

Holy C. E., Shoichet M. S., & Davies J. E. (2000). Engineering three-dimensional bone tissue in vitro using biodegradable scaffolds: Investigating initial cellseeding density and culture period. *Journal of Biomedical Materials Research, 51*, 376–382.

Hulbert S. F., Young F. A., Mathews R. S., Klawitter J. J. , Talbert C. D., & Stelling F. H. (1970). Potential of ceramic materials as permanently implantable skeletal prostheses. *Journal of Biomedical Materials Research, 4*, 436-456.

Hutmacher D. W., Schantz J. T., Lam C. X., Tan K. C., & Lim T. C. (2007). *Journal of Tissue Engineering and Regenerative Medicine, 1*, 245–260.

Ibim S. E., Uhrich K. E., Attawia M., Shastri V. R., El-Amin S. F., Bronson R., . . . Laurencin C. T. (1998). *Journal of Biomedical Materials Research, 43*, 374.

Itala A. I., Ylanen H. O., Ekholm C., Karlsson K. H., & Aro H. T. (2001). Pore diameter of more than 100 micro meter is not requisite for bone ingrowth in rabbits. *Journal of Biomedical Materials Research (Appl Biomater), 58*, 679–683.

Jaszczyszyn A., & Gasiorowski K. (2008). Limitations of the MTT Assay in Cell Viability Testing. *Advances in Clinical and Experimental Medicine, 17*(5), 525–529.

Jonsson K. B., Frost A., Nilsson O., Ljunghall S., & Ljunggren O. (1999). Three isolation techniques for primary culture of human osteoblast-like cells. *Acta Orthopaedica Scandinavica, 70*(4), 365-373.

Kang Y., Kim S., Khademhosseini A., & Yang Y. (2011). Creation of bony microenvironment with CaP and cell-derived ECM to enhance human

bonemarrow MSC behavior and delivery of BMP-2. *Biomaterials, 32*, 6119-6130. doi: 10.1016/j.biomaterials.2011.05.015.

Kheir E., Stapleton T., Shaw D., Jin Z., Fisher J., & Ingham E. (2011). Development and characterization of an acellular porcine cartilage bone matrix for use in tissue engineering. *Journal of Biomedical Materials Research A, 99A*, 283–294. doi: 10.1002/jbm.a.33171.

Kim H. W., Jonathan C. Knowles, & Kim H. E. (2004). Development of hydroxyapatite bone scaffold for controlled drug release via poly(ecaprolactone) and hydroxyapatite hybrid coatings. *Wiley InterScience*, 240249. doi: 10.1002/jbm.b.30038.

Kim H. W., Lee S. Y., Bae C. J., Noh Y. J., Kim H. E., Kim H. M., & Jea Seung Ko. (2003). Porous ZrO_2 bone scaffold coated with hydroxyapatite with fluorapatite intermediate layer. *Biomaterials, 24*, 3277-3284. doi: 10.1016/S0142-9612(03)00162-5.

Klawitter J. J., Bagwell J. G., Weinstein A. M., & Sauer B. W. (1976). An evaluation of bone growth into porous high density polyethylene. *Journal of Biomedical Materials Research, 10*, 311-323.

Kliment C. R., Englert J. M., Crum L. P., & Oury T. D. (2011). A novel method for accurate collagen and biochemical assessment of pulmonary tissue utilizing one animal. *International Journal of Clinical and Experimental Pathology, 4*(4), 349-355.

Koch H., Graneist C., Emmrich F., Till H., Metzger R., Aupperle H., . . . Boldt A. (2012). Xenogenic esophagus scaffolds fixed with several agents: Comparative in vivo study of rejection and inflammation. *Journal of Biomedicine and Biotechnology, 2012*, 1-11. doi: 10.1155/2012/948320.

Komlev V. S., Mastrogiacomo M., Pereira R. C., Peyrin F., Rustichelli F., & Cancedda R. (2010). Biodegradation of porous calcium phosphate scaffolds in an ectopic bone formation model studied by x-ray computed microtomography. *European Cells and Materials, 19*, 136-146.

Kostenuik P. J., Halloran B. P., Morey-Holton E. R., & Bikle D. D. (1997). Skeletal unloading inhibits the in vitro proliferation and differentiation of rat osteoprogenitor cells. *American Journal of Physiology 273*, E1133–E1139.

Kostopoulos L., & Karring T. (1994). *Clinical Oral Implants Research, 5*, 75.

Kubista M., Akerman B., & Norden B. (1987). Characterization of interaction between DNA and 4',6-Diamidino-2-phenylindole by optical spectroscopy *Biochemistry Research International, 26*(14), 4545-4553.

Kweon H., Yoo M. K., Park I. K., Lim T. H., Lee H. C., Lee H. S., . . . Chi C. S. (2003). *Biomaterials, 24*, 801.

Lambers F. M., Koch K., Kuhn G., Ruffoni D., Weigt C., Schulte F. A., & Muller R. (2013). Trabecular bone adapts to long-term cyclic loading by increasing stiffness and normalization of dynamic morphometric rates. *Bone, 55*, 325334. doi: 10.1016/j.bone.2013.04.016.

Lee T. C., Mohsin S., Taylor D., Parkesh R., Gunnlaugsson T., O'Brien F. J., . . . Gowin W. (2003). Review: Detecting microdamage in bone. *Journal of Anatomy, 203*, 161-172.

Leon C. A. (1998). New perspectives in mercury porosimetry. *Advances in Colloid and Interface Science, 76-77*, 341-372.

Leukers B., Gulkan H., Irsen S. H., Milz S., Tille C., Schieker M., & Seitz H. (2005). Biocompatibility of ceramic scaffolds for bone replacement made by 3D printing. *Werkstofftech., 36*(12), 781-787. doi: 10.1002/mawe.200500968

Leukers B., Gulkan H., Irsen S. H., Milz S., Tille C., Schieker M., & Seitz H. (2005). Hydroxyapatite scaffolds for bone tissue engineering made by 3D printing. *Journal of Materials Science: Materials in Medicine, 16*, 1121-1124.

Lian J. B., & Stein G. S. (1993). Development of the osteoblast phenotype: Molecular mechanisms mediating osteoblast growth and differentiation. *The Iowa Orthopaedic Journal, 15*, 118-140.

Lindsay. L. McManus, Franck. Bonnier, George. A. Burke, Brian. J. Meenan, Adrian. R. Boyd, & Hugh. J. Byrne. (2012). Assessment of an osteoblast-like cell line as a model for human primary osteoblasts using Raman spectroscopy. *Analyst*, 1-49. doi: 10.1039/c2an16209a. 2012.

Liu C. X., & et al. (2009). Preparation of whole-kidney acellular matrix in rats by perfusion. *Nan Fang Yi Ke Da Xue Xue Bao, 29*, 979.

Liu L. S., Thompson A. Y., Heidaran M. A., Poser J. W., & Spiro R. C. (1999). *Biomaterials, 20*, 1097.

Lowry O. H., Rosebrough N. J., Farr A. L., & Randall R. J. (1951). Protein measurement with the Folin Phenol Reagent. *The Journal of Biological Chemistry, 193*, 265-275.

Luu Y. K., Kim K., Hsiao B. S., Chu B., & Hadjiargyrou M. (2003). *Journal of Controlled Release 89*, 341.

Macchiarini P., Jungebluth P., Go T., Asnaghi M. A., Rees L. E., Cogan T. A., . . . Birchall M. A. (2008). Clinical transplantation of a tissue-engineered airway. *Lancet, 372*, 2023–2030.

Malkani A. L., Voor M. J., Hellman E. J., Khalily C., Capello W., Wang M., . . . Crawford C. H. (2005). Histologic and Mechanical Evaluation of Impaction Grafting for Femoral Component Revision in a Goat Model. *Orthopedics, 28*(1), 49-58.

Manolagas S. C., Burton D. W., & Deftos L. J. (1981). 1,25-Dihydroxyvitamin D3 Stimulates the Alkaline Phosphatase Activity of Osteoblast-like Cells*. *The Journal of Biological Chemistry, 256*(14), 7115-7117.

Marcos-Campos I., Marolt D., Petridis P., Bhumiratana S., Schmidt D., & VunjakNovakovic G. (2012). Bone scaffold architecture modulates the development
of mineralized bone matrix by human embryonic stem cells. *Biomaterials, 33*, 8329-8342.

Marques A. P., Reis R. L., & Hunt J. A. (2002). *Biomaterials, 23*, 1471.

Martens M., VanAudekercke R., Delport P., P., D., & Muelier J. C. (1983). The mechanical characteristics of cancellous bone at the upper femoral region. *Journal of Biomechanics 16*, 971-983.

Martin B. R. (1991). Determinants of the mechanical properties of bones. *J. Biomechanics, 24*(Suppl. 1), 79-88.

Marti'nez P., Moreno I., De Miguel F., Vila V., Esbrit P., & Marti´nez M. E. (2001). Changes in osteocalcin response to 1,25-Dihydroxyvitamin D3 stimulation and basal vitamin D receptor expression in human osteoblastic cells according to donor age and skeletal origin. *Bone 29*(1), 35–41.

Martins A. M., Alves C. M., Kasper F. K., Mikos A. G., & Reis R. L. (2010). Responsive and in situ-forming chitosan scaffolds for bone tissue engineering applications: An overview of the last decade. *Journal of Materials Chemistry, 20*, 1638–1645. doi: 10.1039/b916259n.

Mayr-Wohlfart U., Fiedler J., Gu¨nther K. P., Puhl W., & Kessler S. (2001). Proliferation and differentiation rates of a human osteoblast-like cell line (SaOS-2) in contact with different bone substitute materials. *Journal of Biomedical Materials Research, 57*, 132–139.

McAllister R. M., Gardner M. B., Greene A. E., Bradt C., Nichols W. W., & Landing B. H. (1971). Cultivation in vitro of cells from a human osteosarcoma. *Cancer, 27*, 397-402.

Meyer S. R., Chiu B., Churchill T. A., Zhu L., Lakey J. R. T., & Ross D. B. (2006). Comparison of aortic valve allograft decellularization techniques in the rat. *Journal of Biomedical Materials Research Part A, 79A*, 254-262. doi: 10.1002/jbm.a.30777.

Miao, Xigeng & Tan, Dawn Meifang & Li, Jian & Xiao, Yin & Crawford, & Ross W. (2008). Mechanical and biological properties of hydroxyapatite/tricalcium phosphate scaffolds coated with poly(lactic-co-glycolic acid). *Acta Biomaterialia, 4*(3), 638-645.

Middleton J. C., & Tipton A. J. (2000). Synthetic biodegradable polymers as orthopedic devices. *Biomaterials, 21*, 2335-2346.

Milovanovic P., Djuric M., Neskovic O., Djonic D., Potocnik J., Nikolic S., . . . Rakocevic Z. (2013). Atomic Force Microscopy Characterization of the External Cortical Bone Surface in Young and Elderly Women: Potential Nanostructural Traces of Periosteal Bone Apposition During Aging. *Microscopy and Microanalysis, 19*, 1341–1349. doi: 10.1017/S1431927613001761.

Misra S. K., Valappil S. P., Roy I., & Boccaccini A. R. (2006). Polyhydroxyalkanoate (PHA)/inorganic phase composites for tissue engineering applications. *Biomacromolecules, 7*(8), 2249-2258.

Moore T. L., & Gibson L. J. (2003). Fatigue microdamage in bovine trabecular bone. *Journal of Biomechanical Engineering, 125*, 769-776. doi: 10.1115/1.1631584.

Moore T. L., & Gibson L. J. (2002). Microdamage accumulation in bovine trabecular bone in uniaxial compression. *Journal of Biomechanical Engineering, 124*, 63-71. doi: 10.1115/1.1428745.

Mulkins M. A., Manolagas S. C., Deftos L. J., & Sussman H. H. (1983). 1,25Dihydroxyvitamin D3 Increases Bone Alkaline Phosphatase Isoenzyme Levels in Human Osteogenic Sarcoma Cells. *The Journal of Biological Chemistry, 258*(10), 6219-6225.

Murphy C. M., Haugh M. G., & O'Brien F. J. (2010). The effect of mean pore size on cell attachment, proliferation and migration in collagen–glycosaminoglycan scaffolds for bone tissue engineering. *Biomaterials 31*, 461–466. doi: 10.1016/j.biomaterials.2009.09.063.

Murphy C. M., & O'Brien F. J. (2010). Understanding the effect of mean pore size on cell activity in collagen-glycosaminoglycan scaffolds. *Cell Adhesion & Migration 4*(3), 377-381. doi: 10.4161/cam.4.3.11747.

Nakamura H. (2007). Review: Morphology, Function, and Differentiation of Bone Cells. *Journal of Hard Tissue Biology, 16*(1), 15-22.

Narbat M. K., Orang F., Hashtjin M. S., & Goudarzi A. (2006). Fabrication of porous hydroxyapatite-gelatin composite scaffolds for bone tissue engineering. *Iranian Biomedical Journal 10, 10*(4), 215-223.

Nguyen L. H., Annabi N., Nikkhah M., Bae H., Binan L., Park S., . . . Khademhosseini A. (2012). Vascularized bone tissue engineering: Approaches for potential improvement. *Tissue Engineering: Part B, 18*(5), 363-381. doi: 10.1089/ten.teb.2012.0012.

Ning L. J., Yi Zhang, Chen X. H., Luo J. C., Li X. Q., Yang Z. M., & Qin T. W. (2012). Preparation and characterization of decellularized tendon slices for tendon tissue engineering. *J Biomed Mater Res Part A, 100A*, 1448–1456. doi: 10.1002/jbm.a.34083.

Noble B. (2003). Bone microdamage and cell apoptosis. *European Cells and Materials, 6*, 46-56.

Nulend J. K., & Burger E. H. (2003). Osteocyte and Bone Structure. *Current Osteoporosis Reports, 1*, 5-10.

Odgaard A., & Linde F. (1991). The Understimation of Young's Modulus in Compressive Testing of Cancellous Bone Specimens. *Journal of Biomechanics, 24*(8), 691-698.

Ott H.C., & et al. (2008). Perfusion-decellularized matrix: using nature's platform to engineer a bioartificial heart. *Nature Medicine, 14*, 213.

Ott H.C., & et al. (2010). Regeneration and orthotopic transplantation of a bioartificial lung. *Nature Medicine, 16*, 927.

Parkinson I. H., & Fazzalari N. L. (2013). Characterisation of trabecular bone structure. *Stud Mechanobiol Tissue Eng Biomater, 5*, 31–51. doi: 10.1007/8415_2011_113.

Pathak R., Amarpal, Tiwari A. K., Kurade N. P., & Amar Nath. (2012). Decellulariztion of buffalo bone to prepare bone scaffolds for effective bone tissue engineering. *Journal of Cell and Tissue Research, 12*(3), 3291-3295.

Patnaik S. S., Wang B., Weed B., Wertheim J. A., & Liao J. (2013). Decellularized scaffolds: Concepts, methodologies, and applications in cardiac tissue engineering and whole-organ regeneration *Tissue Regeneration: Where Nano-Structure Meets Biology* (pp. 1-48).

Pei M., Li J. T., Shoukry M., & Zhang Y. (2011). A review of decellularized stem cell matrix: A novel cell expansion system for cartilage tissue engineering. *European Cells and Materials, 22*, 333-343.

Perniconi B., Costa A., Aulino P., Teodori L., Adamo S., & Coletti D. (2011). The pro-myogenic environment provided by whole organ scale acellular scaffolds from skeletal muscle. *Biomaterials, 32*, 7870-7882. doi: 10.1016/j.biomaterials.2011.07.016.

Petersen T. H., & et al. (2010). Tissue-engineered lungs for in vivo implantation. *Science, 329*, 538.

Pradel W. , Mai R., Gedrange T., & Lauer G. (2008). Cell passage and composition of culture medium effects proliferation and differentiation of human osteoblastlike cells from facial bone. *Journal of Physiology and Pharmacology, 59*(5), 47-58.

Price A. P., & et al. (2010). Development of a decellularized lung bioreactor system for bioengineering the lung: the matrix reloaded. *Tissue Eng Part A., 16*, 2581.

Quan T. M., Vu D. N., Ngoc My N. T., & Bao Ha T. L. (2014). Decellularization of xenogenic bone grafts for potential use as tissue engineering scaffolds. *International Journal of Life Science and Medical Research, 4* (4), 38-45. doi: 10.5963/LSMR0404001.

Ramay H. R., & Zhang M. (2003). Preparation of porous hydroxyapatite scaffolds by combination of the gel-casting and polymer sponge methods. *Biomaterials, 24*, 3293–3302. doi: 10.1016/S0142-9612(03)00171-6.

Riss T. (2014). Is Your MTT Assay Really the Best Choice? Retrieved 20/08/2015, from Promega Corporation http://www.promega.com/resources/pubhub/isyourmtt-assay-really-the-best-choice.

Ritchie R. O., Koester K. J., Ionova S., Yao W., Lane N. E., & Joel W. Ager III. (2008). Measurement of the toughness of bone: A tutorial with special reference to small animal studies. *Bone, 43*, 798–812. doi: 10.1016/j.bone.2008.04.027.

Ross E. A., & et al. (2009). Embryonic stem cells proliferate and differentiate when seeded into kidney scaffolds. *Journal of the American Society of Nephrology, 20*, 2338.

Sachlos E., Reis N., Ainsley C., Derby B., & Czernuszka J. T. (2003). *Biomaterials, 24*, 1487.

Salgado A. J., Coutinho O. P., & Reis R. L. (2004). Bone tissue engineering: State of the art and future trends. *Macromolecular Bioscience, 4*, 743-765. doi: 10.1002/mabi.200400026.

Salgado A. J., Coutinho O. P., & Reis R. L. (2004). *Tissue Engineering, 10*, 465.

Salgado A. J., Gomes M. E., Chou A., Coutinho O. P., Reis R. L., & Hutmacher D. W. (2002). *Materials Science and Engineering: C, 20*, 27.

Sandmann G. H., & Tischer T. (2010). *Tissue engineering of the anterior cruciate ligament and meniscus using acellularized scaffolds*.

Sasaki S., Funamoto S., Hashimoto Y., Kimura T., Honda T., Hattori S., . . . Mochizuki M. (2009). In vivo evaluation of a novel scaffold for artificial corneas prepared by using ultrahigh hydrostatic pressure to decellularize porcine corneas. *Molecular Vision, 15*, 2022-2028.

Schantz J. T., Hutmacher D. W., Chim H., Ng K. W., Lim T. C., & Teoh S. H. (2002). *Cell Transplantation, 11*, 125.

Schliephake H., Zghoul N., Ja¨ger V., van Griensven M., Zeichen J., Gelinsky M., & Wu¨lfing T. (2009). Effect of seeding technique and scaffold material on bone formation in tissue-engineered constructs. *Journal of Biomedical Materials Research, 90A*, 429–437. doi: 10.1002/jbm.a.32104.

Schmidmaier G., Wildemann B., Bail H., Lucke M., Fuchs T., & Stemberger A. (2001). Local application of growth factors (insulin-like growth factor-1 and transforming growth factor beta1) from a biodegradable poly(D,L-lactide) coating of osteosynthetic implants accelerates fracture healing in rats. *Bone, 28*(4), 341-350.

Schoenfeld C. M., Lautenschlager E. P., & Meyer P. R. (1974). Mechanical properties of human cancellous bone in the femoral head. *Journal of Medical and Biological Engineering, 12*, 313-317.

Seal B. L., Otero T. C, & Panitch A. (2001). Polymeric biomaterials for tissue and organ regeneration. *Materials Science & Engineering R-Reports 34*(4-5), 147-230.

Sharir A., Barak M. M., & Shahar R. (2008). Whole bone mechanics and mechanical testing. *The Veterinary Journal, 177*, 8-17.

Shuai C., Nie Y., Gao C., Lu H., Hu H., Wen X., & Peng S. (2012). Poly (l-lactide acid) improves complete nano-hydroxyapatite bone scaffolds through the microstructure rearrangement. *Electronic Journal of Biotechnology, 15*(6), 113. doi: 10.2225/vol15-issue6-fulltext-3.

Shun A. K., Timmer M. D., Jo S., Engel P. S., & Mikos A. G. (2002). *Journal of Biomaterials Science, Polymer Edition, 13*, 95.

Shung A. K., Behravesh E., Jo S., & Mikos A. G. (2003). *Tissue Engineering, 9*, 243.

Shupe T., & et al. (2010). Method for the decellularization of intact rat liver. *Organogenesis, 6*, 134.

Sila-Asna M., Bunyaratvej A., Maeda S., Kitaguchi H., & Bunyaratavej N. (2007). Osteoblast Differentiation and Bone Formation Gene Expression in Strontium-inducing Bone Marrow Mesenchymal Stem Cell. *Kobe Journal of Medical Sciences, 53*(1), 25-35.

Sim H., Temenoff J. S., & Mikos A. G. (2003). *Biomacromolecules, 4*, 552.

Sin H., Quinten Ruhe P., Mikos A. G., & Jansen J. A. (2003). *Biomaterials, 24*, 3201.

Singh V. A., Nagalingam J., Saad M., & Pailoor J. (2010). Which is the best method of sterilization of tumour bone for reimplantation? a biomechanical and histopathological study. *BioMedical Engineering OnLine 9*(48), 1-15.

Sladkova M., & de Peppo G. M. (2014). Review: Bioreactor systems for human bone tissue engineering. *Open Access Processes, 2*, 494-525. doi: 10.3390/pr2020494.

Solchaga L. A., Dennis J. E., Goldberg V. M., & Caplan A. I. (1999). *Journal of Orthopaedic Research, 17*, 205.

Song J. J., Guyette J. P., Gilpin S. E., Gonzalez G., Vacanti J. P., & Ott H. C. (2013). Regeneration and Experimental Orthotopic Transplantation of a Bioengineered Kidney. *Nature Medicine, 19*(5), 646–651.

Song J. J., Kim S. S., Liu Z., Madsen J. C., Mathisen D. J., Vacanti J. P., & Ott H. C. (2011). Enhanced in vivo function of bioartificial lungs in rats. *The Annals of Thoracic Surgery, 92*(3), 998-1005. doi: 10.1016/j.athoracsur.2011.05.018. Soto-Gutierrez A., Zhang L., Medberry C., Fukumitsu K., Faulk D., Jiang H., . . . Badylak S. F. (2011). A whole organ regenerative medicine approach for liver replacement. *Tissue Engineering Part C Methods, 17*, 677.

Sun L. Y., Lin S. Z., Li Y. S., Harn H. J., & Chiou T. W. (2011). Functional cells cultured on microcarriers for use in regenerative medicine research. *Cell Transplantation, 20*, 49-62.

Syahrom A., Abdul Kadir M. R., & Muslim D. A-J. (2010). *Relationship between morphological parameters of cancellous bone and its mechanical properties*. Paper presented at the IEEE EMBS Conference on Biomedical Engineering & Sciences (IECBES 2010), Kuala Lumpur, Malaysia.

Taboas J. M., Maddox R. D., Krebsbach P. H., & Hollister S. J. (2003). *Biomaterials, 24*, 181.

Takahashi K., Tanabe K., Ohnuki M., Narita M., Ichisaka T., Tomoda K., & Yamanaka S. (2007). Induction of pluripotent stem cells from adult human fibroblasts by defined factors. *Cell, 131*, 861–872.

Taskiran D., Taskiran E., Yercan H., & Kutay F. Z. (1999). Quantification of Total Collagen in Rabbit Tendon by the Sirius Red Method. *Turkish Journal of Medical Sciences, 29*, 7-9.

Teixeira S., Rodriguez M. A., Pena P., De Aza A. H., De Aza S., Ferraz M. P., & Monteiro F. J. (2008). Physical characterization of hydroxyapatite porous scaffolds for tissue engineering. *Materials Science and Engineering C*, 1-5. doi: 10.1016/j.msec.2008.09.052.

Thurner P. J., Oroudjev E., Jungmann R., Kreutz C., Kindt J. H., Schitter G., . . . Hansma P. K. (2007). Imaging of Bone Ultrastructure using Atomic Force Microscopy. *Modern Research and Educational Topics in Microscopy*, 3748.

Tolaimate A., Desbrieres J., Rhazi M., & Alagui A. (2003). *Polymer, 44*, 7939.

Totonelli G., Maghsoudlou P., Garriboli, M., Riegler J., Orlando G., Burns A. J., . . . De Coppi P. (2012). A rat decellularized small bowel scaffold that preserves villus crypt architecture for intestinal regeneration. *Biomaterials, 33*, 3401.

Turner C. H. (2006). Bone strength: Current concepts. *Annals New York Academy of Sciences, 1068*, 429-446. doi: 10.1196/annals.1346.039.

Ueda H., Hong L., Yamamoto M., Shigeno K., Inoue M., Toba T., . . . Shimizu Y. (2002). *Biomaterials, 23*, 1003.

Uhrich K. E., Ibim S. E., Larrier D. R., Langer R., & Laurencin C. T. (1998). *Biomaterials, 19*, 2045.

University of Michigan Health Services. Pathology Handbook Review. Available at http://www.pathology.med.umich.edu/apps/handbook/details.php?testID=1128&print=1. Accessed: 9/7/2012.

Uygun B. E., & et al. (2010). Organ reengineering through development of transplantable recellularized liver graft using decellularized liver matrix. *Nature Medicine, 16*, 814.

Vacanti C. A., Bonassar L. J., & Vacanti J. P. (2000). *Structure tissue engineering*. California: Academic Press.

Vaccaro A. R. (2002). The role of the osteoconductive scaffold in synthetic bone graft. *Orthopedics, 25*(5/Supplement), 571-578.

Vavken P., Joshi S., & Murray M. M. (2009). TRITON-X Is Most Effective among Three Decellularization Agents for ACL Tissue Engineering. *Journal of Orthopaedic Research*, 1612-1618. doi: 10.1002/jor.20932.

Vissers C. A. B., Harvestine J. N., & Leach J. K. (2015). Pore size regulates mesenchymal stem cell response to Bioglass-loaded composite scaffolds. *Journal of Materials Chemistry B, 3*, 8650--8658.

Wahl D. A., & Czernuszka J. T. (2006). Collagen-hydroxyapatite composites for hard tissue repair. *European Cells and Materials, 11*, 43-56.

Wainwright J. M., & et al. (2010). Preparation of cardiac extracellular matrix from an intact porcine heart. *Tissue Eng Part C Methods, 16*, 525.

Wallace J. M. (2012). Review: Applications of atomic force microscopy for the asessment of nanoscale morphological and mechanical properties of bone. *Bone, 50*, 420-427. doi: 10.1016/j.bone.2011.11.008.

Walsh B. J., Thornton S. C., Penny R., & Breit S. N. (1992). Microplate reader-based quantitation of collagens. *Analytical Biochemistry, 203*, 187-190.

Wang B., Borazjani A., Tahai M., Jongh Curry A. L. de , Simionescu D. T., Guan J., . . . Liao J. (2010). Fabrication of cardiac patch with decellularized porcine myocardial scaffold and bone marrow mononuclear cells. *Journal of Biomedical Materials Research A, 94A*(4), 1100-1110. doi: 10.1002/jbm.a.32781.

Wang X., Cui J., Zhang B. Q., Zhang H., Bi Y., Kang Q., . . . He T. C. (2013). Decellularized liver scaffolds effectively support the proliferation and differentiation of mouse fetal hepatic progenitors. *Journal of Biomedical Materials Research Part A, 00*, 000-000. doi: 10.1002/jbm.a.34764.

Wang X., & Niebur G. L. (2006). Microdamage propagation in trabecular bone due to changes in loading mode. *Journal of Biomechanics, 39*, 781–790. doi: 10.1016/j.jbiomech.2005.02.007.

Wang Y., Huang Y. C., Arthur A. Gertzman, Xie L., Nizkorodov A., Sharon L. Hyzy, . . . Barbara D. Boyan. (2012). Endogenous regeneration of criticalsize chondral defects in immunocompromised rat xiphoid cartilage using decellularized human bone matrix scaffolds. *Tissue Engineering: Part A, 18*(21/22), 2332-2342. doi: 10.1089/ten.tea.2011.0688.

Washburn N. R., Simon C. G., Jr., Tona A., Elgendy H. M., Karim A., & Amis E. J. (2002). *Journal of Biomedical Materials Research, 60*, 20.

Wei G., & Ma P. X. (2004). Structure and properties of nanohydroxyapatite/polymer composite scaffolds for bone tissue engineering. *Biomaterials, 25*, 4749–4757. doi: 10.1016/j.biomaterials.2003.12.005.

Wen Y., Yuan J. M., Dang R. S., Yang X. Q., Xiong S. H., Shen M. R., . . . Zhang C. S. (2012). Construction of tissue-engineered venous valves in vitro using two types of progenitor cells and decellularized scaffolds category: original article. *The Open Tissue Engineering and Regenerative Medicine Journal, 5*, 9-16.

Wendlova J. (2008). Bone quality. Elasticity and strength. *Bratisl Lek Listy, 109*(9), 383-386.

Woodard J. R., Hilldore A. J., Lan S. K., Park C. J., Morgan A. W., Eurell Jo Ann C., . . . Wagoner Johnson A. J. (2007). The mechanical properties and osteoconductivity of hydroxyapatite bone scaffolds with multi-scale porosity. *Biomaterials, 28*, 45–54. doi: 10.1016/j.biomaterials.2006.08.021.

Xu J., Rho J. Y., Mishra S. R., & Fan Z. (2003). Atomic force microscopy and nanoindentation characterization of human lamellar bone prepared by microtome sectioning and mechanical polishing technique. *Wiley Periodicals, Inc*, 719-726.

Yamanouchi K., Gotoh Y., & Nagayama M. (1997). Dexamethasone enhances differentiation of human osteoblastic cells in vitro. *Journal of Bone and Mineral Metabolism, 15*, 23-29.

Yang S., Kah-Fai L., Du Z., & Chee-Kai C. (2001). Review: The design of scaffolds for use in tissue engineering. Part I. Traditional factors. *Tissue Engineering, 7*(6), 679-689.

Yang S., Kah-Fai L, Du Z., & Chee-Kai C. (2002). Review: The design of scaffolds for use in tissue engineering. Part II. Rapid prototyping techniques. *Tissue Engineering, 8*(1), 1-11.

Yeatts A. B., & Fisher J. P. (2011). Bone tissue engineering bioreactors: Dynamic culture and the influence of shear stress. *Bone, 48*, 171–181. doi: 10.1016/j.bone.2010.09.138.

Zhang Y., Ni M., Zhang M., & Ratner B. (2003). *Tissue Engineering, 9*, 337

Zhao F., Yin Y., Lu W. W., Leong J. C., Zhang W., Zhang J., . . . Yao K. (2002). *Biomaterials, 23*, 3227.

Internet References

Brooklyn College. (2015). Long bones. Retrieved 06/12/2015, 2015, from http://academic.brooklyn.cuny.edu/physed/yingling/bone/Structure/Cortical/graphics/long-bones.gif

Cambridge Bioscience. (2015). β-Glycerophosphate (sodium salt hydrate). *Product*

Information. Retrieved 06/12/2015, 2015, from https://www.caymanchem.com/pdfs/14405.pdf

Cell Migration Consortium. (2014). Adhesion. Retrieved 22/03/2016, from https://www.cellmigration.org/topics/adhesion.shtml

Farm Sanctuary. (2016). Cattle Care. Retrieved 06/12/2015, from http://www.farmsanctuary.org/wp-content/uploads/2012/06/Animal-CareCattle.pdf

Heiner A. D. (2002). Impaction Grafting. Retrieved 22/03/2016, from http://user.engineering.uiowa.edu/~bme_158/lecture/Impaction%20Grafting%20Lecture%20Slides%2010-25-03.pdf

Kramer D. K. (2015, 12/06/2013). Radioimmunoassay (RIA). Retrieved 10/12/2015, 2015, from http://www.antibodies online.com/resources/17/1215/Radioimmunoassay+RIA/

Microbiology and Immunology Mobile. (2015). Immunology Chapter Seven. *Radioimmunoassay (RIA)/Enzyme Linked Immunosorbent Assay (ELISA)*. Retrieved 10/12/2015, 2015, from http://www.microbiologybook.org/mobile/m.index.htm.

Public Health England. (2014, 31/07/2014). Culture collections. *General Cell Collection: HOS*. Retrieved 25/02/2014, 2014, from http://www.phe culturecollections.org.uk/

Quilty-Harper C. (2012). The world's fattest countries: how do you compare?. Retrieved 06/12/2015, from http://www.telegraph.co.uk/news/earth/earthnews/9345086/The-worldsfattest-countries-how-do-you-compare.html

Thermo Fisher Scientific Inc. (2015). DAPI (4',6-Diamidino-2-Phenylindole, Dilactate). Retrieved 06/12/2015, from https://www.thermofisher.com/order/catalog/product/D3571

Thermo Fisher Scientific Inc. (2015). Osteocalcin ELISA Kit, Human. Retrieved 06/12/2015, 2015, from http://www.thermofisher.com/order/catalog/product/KAQ1381?ICID=searc product

University of Washington Engineered Biomaterials. (2016). Biomaterials Tutorial: *Mechanical Properties of Biomaterials*. Retrieved 22/03/2016, from http://www.uweb.engr.washington.edu/research/tutorials/mechproperties.html